

From Nuclei to Compact Stars

Contents

1. Topics	587
2. Participants	589
2.1. ICRA Net participants	589
2.2. Past collaborators	589
2.3. On going collaborations	589
2.4. Ph.D. Students	589
3. Brief description	591
3.1. From heavy nuclei and superheavy nuclei to nuclear matter cores of stellar dimensions	591
3.2. The equation of state of nuclear matter under high pressures .	594
3.3. Electrodynamics of compact stars in general relativity	596
4. Publications (before 2009)	599
4.1. Refereed Journals	599
4.2. Conference Proceedings	600
5. Publications (2009-2010)	603
5.1. Refereed Journals	603
5.2. Conference Proceedings	606
6. Invited talks in international conferences	611
7. APPENDICES	613
A. The Thomas-Fermi model: from nuclei to nuclear matter cores of stellar dimensions	615
A.1. On gravitationally and electro dy nami cally bound massive nu- clear density cores	615
A.1.1. Introduction	615
A.1.2. The relativistic Thomas-Fermi equation and the beta equi- librium condition	617
A.1.3. The ultra-relativistic analytic solutions	619
A.1.4. New results derived from the analytic solutions	623
A.1.5. Estimates of gravitational effects in a Newtonian ap- proximation	624

A.1.6.	Possible applications to neutron stars	626
A.1.7.	Conclusions	627
A.2.	On the relativistic Thomas-Fermi treatment of compressed atoms and compressed nuclear matter cores of stellar dimensions . . .	629
A.2.1.	Introduction	629
A.2.2.	The Thomas-Fermi model for compressed atoms: the Feynman-Metropolis-Teller treatment	631
A.2.3.	The relativistic generalization of the Feynman-Metropolis- Teller treatment	635
A.2.4.	Comparison and contrast with approximate treatments	641
A.2.5.	Application to nuclear matter cores of stellar dimensions	649
A.2.6.	Compressional energy of nuclear matter cores of stellar dimensions	657
A.2.7.	Conclusions	658
A.3.	Electrodynamics for Nuclear Matter in Bulk	662
A.4.	On the Charge to Mass Ratio of Neutron Cores and Heavy Nuclei	672
A.4.1.	Introduction	672
A.4.2.	The theoretical model	672
A.4.3.	N_p versus A relation	674
A.4.4.	Conclusions	677
A.5.	Supercritical fields on the surface of massive nuclear cores: neutral core v.s. charged core	680
A.5.1.	Equilibrium of electron distribution in neutral cores. . .	680
A.5.2.	Equilibrium of electron distribution in super charged cores	681
A.5.3.	Ultra-relativistic solution	682
A.6.	The Extended Nuclear Matter Model with Smooth Transition Surface	684
A.6.1.	The Relativistic Thomas-Fermi Equation	684
A.6.2.	The Woods-Saxon-like Proton Distribution Function . . .	684
A.6.3.	Results of the Numerical Integration.	685
A.7.	Electron-positron pairs production in an electric potential of massive cores	688
A.7.1.	Introduction	688
A.7.2.	Classical description of electrons in potential of cores . .	690
A.7.3.	Semi-Classical description	693
A.7.4.	Production of electron-positron pair	696
A.7.5.	Summary and remarks	699
A.8.	On Magnetic Fields in Rotating Nuclear Matter Cores of Stellar Dimensions	702
A.8.1.	Introduction	702
A.8.2.	The Relativistic Thomas-Fermi equation	703
A.8.3.	The ultra-relativistic analytic solutions	705

A.8.4.	Rotating Nuclear Matter Cores of Stellar Dimensions in Classical Electrodynamics	705
A.8.5.	Conclusions	708
B.	The Thomas-Fermi model in general relativistic systems	711
B.1.	The general relativistic Thomas-Fermi theory of white-dwarfs	711
B.1.1.	Introduction	711
B.1.2.	The Equation of State	716
B.1.3.	The uniform approximation	716
B.1.4.	Uniform approximation with point-like nucleus	717
B.1.5.	Salpeter's approach	719
B.1.6.	The Feynman-Metropolis-Teller treatment	721
B.1.7.	The relativistic Feynman-Metropolis-Teller treatment	724
B.1.8.	General relativistic equations of equilibrium	730
B.1.9.	The weak-field non-relativistic limit	732
B.1.10.	The Post-Newtonian limit	733
B.1.11.	Mass and radius of general relativistic stable white-dwarfs	734
B.1.12.	Conclusions	737
B.2.	On the self-consistent general relativistic equilibrium equations of neutron stars	744
B.3.	The Outer Crust of Neutron Stars	750
B.3.1.	The General Relativistic Model	750
B.3.2.	The mass and the thickness of the crust	751
B.3.3.	The Fireshell Model of GRBs	752
B.3.4.	The mass of the crust and M_B	753
B.4.	The Role of Thomas-Fermi approach in Neutron Star Matter	755
B.4.1.	Introduction	755
B.4.2.	Thomas-Fermi model	758
B.4.3.	White dwarfs and Neutron Stars as Thomas-Fermi systems	758
B.4.4.	The relativistic Thomas-Fermi equation	759
B.4.5.	The essential role of the non point-like nucleus	761
B.4.6.	Nuclear matter in bulk: $A \approx 300$ or $A \approx (m_{Planck}/m_n)^3$	761
B.4.7.	The energetically favorable configurations	764
B.4.8.	Conclusions	767
B.5.	A Self-consistent Approach to Neutron Stars	768
B.5.1.	Introduction	768
B.5.2.	The Equilibrium Equations	769
B.5.3.	Some Specific Solutions	770
B.5.4.	Conclusions	771
B.6.	On the electrostatic structure of neutron stars	772
B.6.1.	Introduction	772
B.6.2.	Structure Equations	773
B.6.3.	The Equation of State	774

B.6.4. Numerical Integration	777
B.7. A New Family of Neutron Star Models: Global Neutrality vs. Local Neutrality	784
B.7.1. Introduction	784
B.7.2. The equilibrium equations	784
B.7.3. Discussion	785
B.8. A general relativistic Thomas Fermi treatment of neutron star cores II. Generalized Fermi energies and beta equilibrium. . .	787
B.8.1. Introduction	787
B.8.2. General formulation	788
B.8.3. Generalized Fermi energies and beta equilibrium . . .	790
B.8.4. Constancy of the generalized Fermi energies	791
B.8.5. Conclusions	791
B.9. A self-consistent general relativistic solution for a self-gravitating system of degenerate neutrons, protons and electrons in beta equilibrium	792
B.9.1. Introduction	792
B.9.2. Einstein-Maxwell, general relativistic Thomas-Fermi equa- tions and boundary conditions	794
B.9.3. Numerical integration of the equilibrium equations . .	797
B.9.4. Conclusions	799
Bibliography	801

1. Topics

- From heavy nuclei and superheavy nuclei to nuclear matter cores of stellar dimensions.
- The equation of state of nuclear matter under high pressures.
- Electrodynamics of compact stars in general relativity.

2. Participants

2.1. ICRAANet participants

- D. Arnett (Steward Observatory, University of Arizona, USA)
- H. Kleinert (Free University of Berlin , Germany)
- V. Popov (ITEP, Moscow, Russia)
- M. Rotondo (ICRAANet, University of Rome, Italy)
- Jorge A. Rueda (ICRAANet, University of Rome, Italy)
- R. Ruffini (ICRAANet, University of Rome, Italy)
- G.'t Hooft (Institute for Theoretical Physic Universiteit Utrecht)
- S.-S. Xue (ICRAANet, University of Rome, Italy)

2.2. Past collaborators

- L. Stella (Rome Astronomical Observatory, Italy)
- W. Greiner (Institut für Theoretical Physics Johann Wolfgang Goethe-Universität, Frankfurt am Main)

2.3. On going collaborations

- M. Malheiro (Instituto Tecnológico de Aeronáutica, Brazil)

2.4. Ph.D. Students

- R. Belvedere (ICRAANet, University of Rome, Italy)
- K. Boshkayev (ICRAANet, University of Rome, Italy)
- M. Haney (ICRAANet, University of Rome, Italy)
- S. Martins de Carvalho (ICRAANet, University of Rome, Italy)

2. *Participants*

- D. Pugliese (ICRANet, University of Rome, Italy)

3. Brief description

3.1. From heavy nuclei and superheavy nuclei to nuclear matter cores of stellar dimensions

One of the most active field of research has been to analyze a general approach to Compact Stars like White-Dwarfs and Neutron Stars, based on the Thomas-Fermi ultrarelativistic equations amply adopted in the study of superheavy nuclei. The aim is to have a unified approach for nuclei, for superheavy nuclei up to atomic numbers of the order of 10^5 – 10^6 , and for what we have called “nuclear matter cores of stellar dimensions”. These massive nuclear cores are

- characterized by atomic number of the order of 10^{57} ;
- composed by a degenerate fluid of neutrons, protons and electrons in beta equilibrium;
- globally neutral configurations;
- expected to be kept at nuclear density by self gravity.

The analysis of superheavy nuclei has historically represented a major field of research, developed by Prof. V. Popov and Prof. W. Greiner and their schools. This same problem was studied in the context of the relativistic Thomas-Fermi equation also by R. Ruffini and L. Stella, already in the '80s. The recent approach was started with the Ph.D. Thesis of M. Rotonondo and has shown the possibility to extrapolate this treatment of superheavy nuclei to the case of nuclear matter cores of stellar dimensions (see App. A.3). The very unexpected result has been that also around these massive cores there is the distinct possibility of having an electromagnetic field close to the critical value

$$E_c = \frac{m_e^2 c^3}{e \hbar},$$

although localized in a very narrow shell of the order of the electron Compton wavelength (see Figs. 3.1, 3.2).

The welcome result has been that all the analytic work developed by Prof. V. Popov and the Russian school can be applied using scaling laws satisfied by the relativistic Thomas-Fermi equation to the case of nuclear matter cores

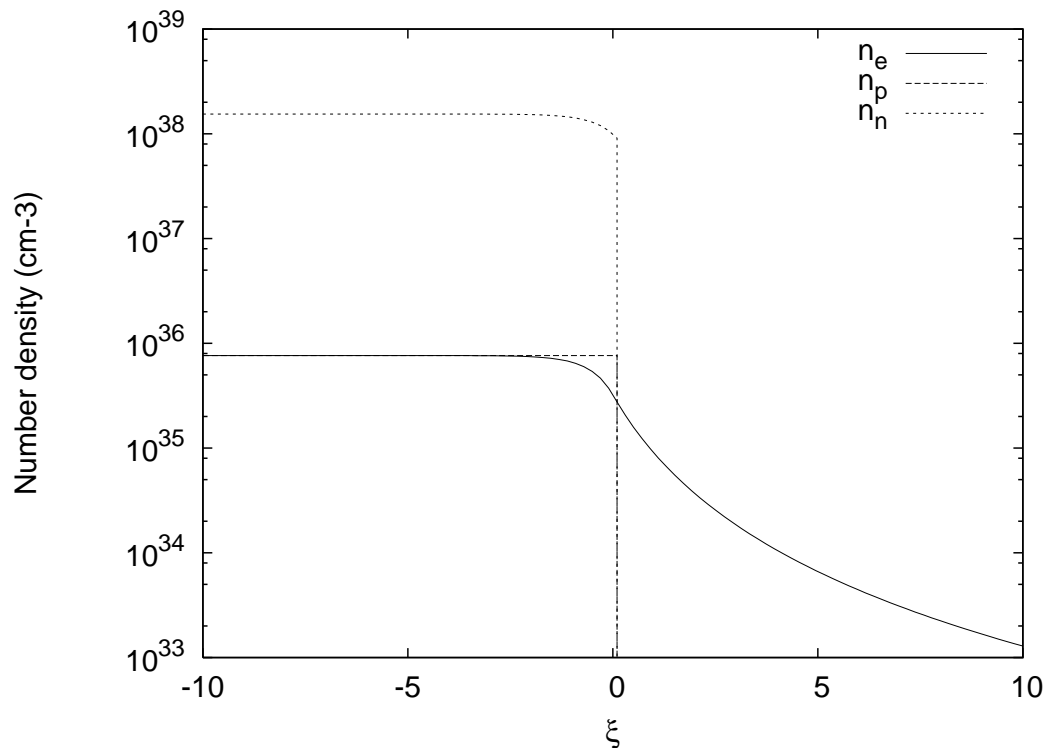


Figure 3.1.: Number density of electrons, protons and neutrons.

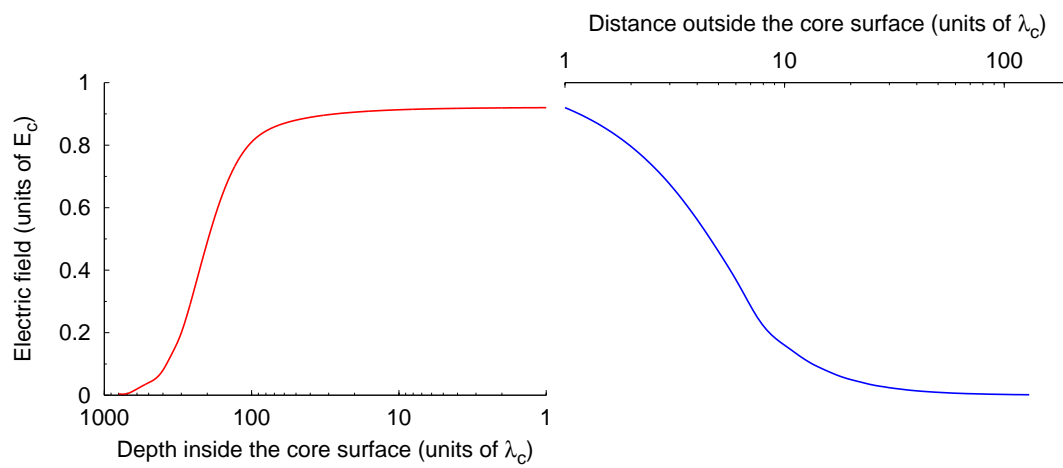


Figure 3.2.: Electric Field in units of the critical field E_c .

of stellar dimensions, if the beta equilibrium condition is properly taken into account (see App. A.1 and A.3). This has been the result obtained and published by Ruffini, Rotondo and Xue already in 2007. Since then, a large variety of problems has emerged, which have seen the direct participation at ICRANet of Prof. Greiner, Prof. Popov, and Prof. 't Hooft.

One of the crucial issues to be debated is the stability of such cores under the competing effects of self gravity and Coulomb repulsion. In App. A.1 it has been demonstrated their stability against nuclear fission, as opposed to the case of heavy nuclei. In particular, on the basis of Newtonian gravitational energy considerations it has been found the existence of a possible new island of stability for mass numbers $A > A_R = 0.039 \left(\frac{N_p}{A}\right)^{1/2} \left(\frac{m_{\text{Planck}}}{m_n}\right)^3$, where N_p is the number of protons, A is the total number of baryons, m_n is the neutron mass and $m_{\text{Planck}} = (\hbar c/G)^{1/2}$ is the Planck mass. The equilibrium against Coulomb repulsion originates now from the combined effect of the screening of the relativistic electrons, of the surface tension due to strong interactions and of the gravitational interaction of these massive cores.

By enforcing the condition of beta equilibrium, it has been also obtained a generalization to the relation between the mass number A and atomic number N_p which encompasses phenomenological expressions (see App. A.1 and A.4 for details).

All these considerations have been made for an isolated core with constant proton density whose boundary has been sharply defined by a step function. No external forces are exerted. Consequently, the Fermi energy of the electrons has been assumed to be equal to zero.

Different aspects concerning these macroscopic systems are also considered. For instance, the analysis of the electron distribution around such cores in both the case of global charge neutrality and the case of not global charge neutrality has been presented (see App. A.5).

For instance, the assumption of a sharp proton density profile has been relaxed and, consequently, a smooth surface modeled by a Woods-Saxon-like proton distribution has been introduced (see App. A.6 for details). The presence of overcritical electric fields close to their surface has been confirmed also in this more general case.

The classical and semi-classical energy states of relativistic electrons bounded by a massive and charged core with the charge-mass-ratio Q/M and macroscopic radius R_c are discussed (see App. A.7). It is shown that the energies of semi-classical (bound) states can be much smaller than the negative electron mass-energy ($-mc^2$), and thus energy-level crossing to negative energy continuum occurs. It has been then advanced the possibility that in neutral cores with equal proton and electron number, the configuration of relativistic electrons in these semi-classical (bound) states should be stabilized by photon emission.

Another topic of current interest concerns the case of rotating nuclear matter cores of stellar dimensions. Preliminary results on the induced magnetic field by electric field rotation has been recently obtained (see App. A.8). Such analysis has been done in the framework of classical electrodynamics under the assumption of uniform rigid rotation of the macroscopic nuclear cores in the non-compressed case. For a period of rotation ~ 10 ms, overcritical magnetic fields has been obtained near the surface of the configuration.

3.2. The equation of state of nuclear matter under high pressures

It has been the existence of the scaling laws of the ultrarelativistic Thomas-Fermi equation (see App. A.1), which has led to the very exciting possibility of having macroscopic configurations of nuclear matter in beta equilibrium exhibiting strong electric fields on their surfaces. In order to go one step further towards a more realistic description of macroscopic configurations like white-dwarfs and/or neutron stars, further improvements and extensions must be applied to the starting model.

In the earliest description of neutron stars in the work of Oppenheimer and Volkoff (1939) only a gas of neutrons was considered and the equation of equilibrium was written in the Schwarzschild metric. They considered the model of a degenerate gas of neutrons to hold from the center to the border, with the density monotonically decreasing away from the center.

In the intervening years, a more realistic model has been presented challenging the original considerations of Tolman (1939) and Oppenheimer and Volkoff (1939) (TOV). The TOV equations considered the existence of neutrons all the way to the surface of the star. The presence of neutrons, protons and electrons in beta equilibrium were instead introduced by Harrison et al. (1965). Still more important, the neutron stars have been shown to be composed of two sharply different components: the core at nuclear and supra-nuclear densities consisting of degenerate neutrons, protons and electrons in beta equilibrium and a crust of white dwarf like material, namely a nuclei lattice in a background of degenerate electrons (see Harrison et al. (1965); Baym et al. (1971a) for details). Further works describing the nuclear interactions were later introduced. Clearly all these considerations departed profoundly from the TOV approximation.

The matching between the core and the crust is still today an open issue in neutron star physics. In order to handle with this interesting problem, a step-by-step procedure is needed. In such a case, the neutron, proton, and electron fluid is confined within the core radius due to the compression exerted by the crust component of the neutron star.

It is well known that the Thomas-Fermi model has been extensively ap-

plied in atomic physics, also has been applied extensively in atomic physics in its relativistic form as well as in the study of atoms with heavy nuclei (see Gombás (1949) for instance). Similarly there have been considerations of relativistic Thomas-Fermi model for quark stars pointing out the existence of critical electric fields on their surfaces Alcock et al. (1986). Similar results have also been obtained in the transition at very high densities, from the normal nuclear matter phase in the core to the color-flavor-locked phase of quark matter in the inner core of hybrid stars Alford et al. (2001). However, no example exists to the application of the electromagnetic Thomas-Fermi model for neutron stars.

It is therefore interesting, in order to approach both the complex problem of a neutron star core and its interface with the neutron star crust and the problem of the equilibrium of gas in a white dwarf taking into account all possible global electromagnetic interactions between the nucleus and the relativistic electrons, to extend the model to the compressed case in which the Fermi energy of electrons turns to be positive.

The analysis of globally neutral and compressed configurations composed by a relativistic fluid of degenerate neutrons, protons, and electrons in beta equilibrium has been recently accomplished. It has been generalized the Feynman-Metropolis-Teller treatment of compressed atoms to relativistic regimes, and the concept of compressed nuclear matter cores of stellar dimensions has been introduced (see App. A.2 for details).

In the relativistic generalization of the Feynman-Metropolis-Teller approach, the equation to be integrated is the relativistic Thomas-Fermi equation, also called the Vallarta-Rosen equation. The integration of this equation does not admit any regular solution for a point-like nucleus and both the nuclear radius and the nuclear composition have necessarily to be taken into account. This introduces a fundamental difference from the non-relativistic Thomas-Fermi model where a point-like nucleus was adopted.

Due to the introduction of the concept of Wigner-Seitz cells, the study of degenerate compressed matter in white dwarfs can be addressed. This problem presents, still today, open issues of great interest such as the equilibrium of the electron gas and the associated nuclear component, taking into account the electromagnetic, the gravitational and the weak interactions formulated in a correct special and general relativistic framework.

A complete analysis of the properties of such configurations as a function of the compression can be duly done through the relativistic generalization of the Feynman-Metropolis-Teller approach (see App. A.2 for details). It is then possible to derive a consistent equation of state for compressed matter which generalizes both the uniform free-electron fluid approximation, adopted for instance by Chandrasekhar (1931b) in his famous treatment of white-dwarfs, and the well-known work of Salpeter (1961) which describes the electro-dynamical and relativistic effects by a sequence of approximations.

Apart from taking into account all possible electromagnetic and special rel-

ativistic corrections to the equation of state of white-dwarf matter, the new equation of state, which incorporates the beta equilibrium condition, leads to a self-consistent calculation of the onset for inverse beta-decay of a given nuclear composition as function of the Fermi energy of electrons or equivalently, as a function of the density of the system. This important achievement, leads to a self-consistent calculation of the critical mass of white-dwarfs with heavy nuclear composition (see App. B.1 for details).

In addition, the numerical value of the mass, of the radius, and of the critical mass of white-dwarfs turn to be smaller with respect to the ones obtained with approximate equations of state (see e.g. Hamada and Salpeter (1961)). Therefore, the analysis of compressed atoms following the relativistic Feynman-Metropolis-Teller treatment has important consequences in the determination of the mass-radius relation of white dwarfs, leading to the possibility of a direct confrontation of these results with observations, in view of the current great interest for the cosmological implications of the type Ia supernovae.

In neutron star cores, nuclear matter is under very extreme conditions of density and pressure. The importance of the strong interactions between nucleons at such extreme pressures it has been known for years (see e.g. Cameron (1970)). However, due to the absence of a complete theory of the strong interactions, and due to the impossibility of performing terrestrial experiments with similar extreme pressure-density conditions, the equation of state of nuclear matter at densities larger than the so-called nuclear saturation density $\sim 2.7 \times 10^{14} \text{ g/cm}^3$, is still today unknown.

The construction of nuclear equations of state within a fully consistent formulation of the equations of equilibrium in general relativity is an active topic of research, which is being covered currently in the Ph. D. thesis of D. Pugliese (see App. B.8 for instance), R. Belvedere and S. Martins de Carvalho.

3.3. Electrodynamics of compact stars in general relativity

A branch of research which is currently under continuous evolution corresponds to the extension to the case of general relativity, all the previous theory about the Thomas-Fermi model and the relativistic Thomas-Fermi model, applied initially to the study of heavy nuclei, superheavy nuclei as well as to the theoretical hypothesis of nuclear matter cores of stellar dimensions. The aim is to construct a self-consistent theory of self-gravitating systems relativistic quantum statistics, electromagnetic, weak and strong interactions in the framework of general relativity, from which it is possible to study the properties of compact objects like white-dwarfs and neutron stars.

The recent generalization of the Feynman-Metropolis-Teller treatment to

relativistic regimes, which led to a new equation of state of white-dwarf matter (see App. A.2), has been recently used to construct equilibrium configurations of white-dwarfs in general relativity (see App. B.1). Thus, a fully consistent special and general relativistic theory of white-dwarfs has been formulated leading to a new mass-radius relation of white-dwarfs.

Concerning to neutron stars, most of effort have been given to the construction of self-consistent solutions of the equations of equilibrium for neutron stars in general relativity taking into account the traditionally neglected electromagnetic interaction. In nearly all the scientific literature on neutron stars, a “local approach”, where the equation of state of neutron star matter is constructed ignoring global gravitational and Coulombian effects by assuming not only flat space but also local charge neutrality, has been traditionally used. A barotropic relation $P = P(\mathcal{E})$ between the energy-density \mathcal{E} and pressure P is then obtained. The gravitational effects are then taken into account by embedding such an equation of state into the so-called TOV equations of hydrostatic equilibrium.

Then, the first step has been to obtain the first self-consistent globally but not locally neutral solution of the Einstein-Maxwell equations for a self-gravitating system of degenerate neutrons, protons and electrons in beta equilibrium (see App. B.9). The impossibility of imposing the condition of local charge neutrality on such systems has been proved in complete generality and the crucial role of the constancy of the generalized Fermi energy has been emphasized. Such a solution, although does not represent a realistic model for a neutron star, contains all the essential physics with respect to the Coulomb interactions between protons and electrons in neutron star interiors.

Subsequently, the generalization to the case of realistic neutron stars with core and crust has been examined (see App. B.2). The role of the constancy of the general relativistic Thomas-Fermi energy of particles is there evidenced by demonstrating that they lead to the neutron star equilibrium configurations with a core-crust transition interface which shows similar electro-dynamical properties to the ones predicted by the nuclear matter cores of stellar dimensions.

The next step is to introduce self-consistently the strong interaction in the construction of the equilibrium configurations. Neutron star equilibrium configurations satisfying global but not local charge neutrality can be found in App. B.6 where the nuclear interaction was derived from phenomenological models. A fully consistent formulation of the equations of equilibrium taking into account relativistic quantum statistics, electromagnetic, weak and strong interactions in the framework of general relativity has been one of the research topics of the Ph. D. of D. Pugliese (see App. B.8).

The many interesting aspects of the physics and the structure of the crust of neutron stars are the research topic of the Ph. D. thesis of R. Belvedere. The entire formulation of the equilibrium equations of rotating neutron stars

as well as their numerical integration are part of the K. Boshkayev's Ph. D. thesis. M. Haney is studying the problem of the pulsational modes of these neutron star configurations with strong electric fields in the core-crust boundary and, S. Martins de Carvalho, is starting to analyze the influence of the temperature on the properties of these new neutron star equilibrium configurations.

4. Publications (before 2009)

4.1. Refereed Journals

1. R. Ruffini, M. Rotondo and S.-S. Xue, "Electrodynamics for Nuclear Matter in Bulk", *Int. J. Mod. Phys. D* Vol. 16, No. 1 (2007) 1-9.

A general approach to analyze the electrodynamics of nuclear matter in bulk is presented using the relativistic Thomas-Fermi equation generalizing to the case of $N \simeq (m_{\text{Planck}}/m_n)^3$ nucleons of mass m_n the approach well tested in very heavy nuclei ($Z \simeq 10^6$). Particular attention is given to implement the condition of charge neutrality globally on the entire configuration, versus the one usually adopted on a microscopic scale. As the limit $N \simeq (m_{\text{Planck}}/m_n)^3$ is approached the penetration of electrons inside the core increases and a relatively small tail of electrons persists leading to a significant electron density outside the core. Within a region of 10^2 electron Compton wavelength near the core surface electric fields close to the critical value for pair creation by vacuum polarization effect develop. These results can have important consequences on the understanding of physical process in neutron stars structures as well as on the initial conditions leading to the process of gravitational collapse to a black hole.

2. R. Ruffini and L. Stella, "Some comments on the relativistic Thomas-Fermi model and the Vallarta-Rosen equation", *Phys. Lett. B* 102 (1981) 442.

Some basic differences between the screening of the nuclear charge due to a relativistic cloud of electrons in a neutral atom and the screening due to vacuum polarization effects induced by a superheavy ion are discussed.

3. J. Ferreira, R. Ruffini and L. Stella, "On the relativistic Thomas-Fermi model", *Phys. Lett. B* 91, (1980) 314. The relativistic generalization of the Thomas-Fermi model of the atom is derived. It approaches the usual nonrelativistic equation in the limit $Z \ll Z_{\text{crit}}$, where Z is the total number of electrons of the atom and $Z_{\text{crit}} = (3\pi/4)^{1/2} \alpha^{-3/2}$ and α is the fine structure constant. The new equation leads to the breakdown of scaling laws and to the appearance of a critical charge, purely as a consequence of relativistic effects. These results are compared and contrasted with those corresponding to N self-gravitating degenerate relativistic fermions, which for $N \approx N_{\text{crit}} = (3\pi/4)^{1/2} (m/m_p)^3$ give rise to the concept of a critical mass against gravitational collapse. Here m is the mass of the fermion and $m_p = (\hbar c/G)^{1/2}$ is the Planck mass.

4.2. Conference Proceedings

1. R. Ruffini, M. Rotondo and S.-S. Xue, "Neutral nuclear core vs super charged one ", in Proceedings of the Eleventh Marcel Grossmann Meeting, R. Jantzen, H. Kleinert, R. Ruffini (eds.), (World Scientific, Singapore, 2008).

Based on the Thomas-Fermi approach, we describe and distinguish the electron distributions around extended nuclear cores: (i) in the case that cores are neutral for electrons bound by protons inside cores and proton and electron numbers are the same; (ii) in the case that super charged cores are bare, electrons (positrons) produced by vacuum polarization are bound by (fly into) cores (infinity).

2. B. Patricelli, M. Rotondo and R. Ruffini, "On the Charge to Mass Ratio of Neutron Cores and Heavy Nuclei", AIP Conference Proceedings, Vol. 966 (2008), pp. 143-146.

We determine theoretically the relation between the total number of protons N_p and the mass number A (the charge to mass ratio) of nuclei and neutron cores with the model recently proposed by Ruffini et al. (2007) and we compare it with other N_p versus A relations: the empirical one, related to the Periodic Table, and the semi-empirical relation, obtained by minimizing the Weizsäcker mass formula. We find that there is a very good agreement between all the relations for values of A typical of nuclei, with differences of the order of percent. Our relation and the semi-empirical one are in agreement up to $A \approx 10^4$ for higher values, we find that the two relations differ. We interpret the different behavior of our theoretical relation as a result of the penetration of electrons (initially confined in an external shell) inside the core, that becomes more and more important by increasing A ; these effects are not taken into account in the semi-empirical mass-formula.

3. M. Rotondo, R. Ruffini and S.-S Xue, "On the Electrodynamical properties of Nuclear matter in bulk", AIP Conference Proceedings, Vol. 966 (2008), pp. 147-152.

We analyze the properties of solutions of the relativistic Thomas-Fermi equation for globally neutral cores with radius of the order of $R \approx 10$ Km, at constant densities around the nuclear density. By using numerical techniques as well as well tested analytic procedures developed in the study of heavy ions, we confirm the existence of an electric field close to the critical value $E_c = m_e^2 c^3 / e \hbar$ in a shell $\Delta R \approx 10^4 \hbar / m_\pi c$ near the core surface. For a core of ≈ 10 Km the difference in binding energy reaches 10^{49} ergs. These results can be of interest for the understanding of very heavy nuclei as well as physics of neutron stars, their formation processes and further gravitational collapse to a black hole.

4. B. Patricelli, M. Rotondo, J. A. Rueda H. and R. Ruffini, "The Electrodynamics of the Core and the Crust components in Neutron Stars", AIP Conference Proceedings, Vol. 1059 (2008), pp. 68–71.

We study the possibility of having a strong electric field (E) in Neutron Stars. We consider a system composed by a core of degenerate relativistic electrons, protons and neutrons, surrounded by an oppositely charged leptonic component and show that at the core surface it is possible to have values of E of the order of the critical value for electron-positron pair creation, depending on the mass density of the system. We also describe Neutron Stars in general relativity, considering a system composed by the core and an additional component: a crust of white dwarf - like material. We study the characteristics of the crust, in particular we calculate its mass M_{crust} . We propose that, when the mass density of the star increases, the core undergoes the process of gravitational collapse to a black hole, leaving the crust as a remnant; we compare M_{crust} with the mass of the baryonic remnant considered in the fireshell model of GRBs and find that their values are compatible.

5. R. Ruffini, "The Role of Thomas-Fermi approach in Neutron Star Matter", Proceedings of the 9th International Conference "Path Integrals-New trends and perspectives", Max Planck Institute for the Physics of Complex Systems, Dresden, Germany, September 23–28 2007, World Scientific 207–218 (2008), eds. W. Janke and A. Pelster

The role of the Thomas-Fermi approach in Neutron Star matter cores is presented and discussed with special attention to solutions globally neutral and not fulfilling the traditional condition of local charge neutrality. A new stable and energetically favorable configuration is found. This new solution can be of relevance in understanding unsolved issues of the gravitational collapse processes and their energetics.

5. Publications (2009-2010)

5.1. Refereed Journals

1. Jorge A. Rueda, M. Rotondo, R. Ruffini, and S.-S. Xue, "A self-consistent approach to neutron stars", J. Korean Phys. Soc. 57, 560 (2010).

We present a set of equilibrium equations for a self-gravitating system of degenerate neutrons, protons and electrons in beta equilibrium in the framework of relativistic quantum statistics and the Einstein-Maxwell equations. Special emphasis is given to the crucial role of the constancy of the generalized Fermi energy of particles, from which we formulate the general relativistic version of the Thomas-Fermi equation. We discuss briefly the consequences of this approach in the general case of neutron star configurations with a core and a crust.

2. Jorge A. Rueda, M. Rotondo, R. Ruffini, and S.-S. Xue, "A self-consistent general relativistic solution for a self-gravitating system of degenerate neutrons, protons and electrons in beta equilibrium", submitted to Phys. Rev. Lett.

A self-consistent treatment of the simplest, nontrivial, self-gravitating system of degenerate neutrons, protons and electrons in beta equilibrium is presented in the framework of relativistic quantum statistics and the Einstein-Maxwell equations. The impossibility of imposing the condition of local charge neutrality on such systems is proved in complete generality. The crucial role of the constancy of the generalized Fermi energy is emphasized and consequently the coupled system of the general relativistic Thomas-Fermi equations and the Einstein-Maxwell equations is solved. We then give an explicit solution corresponding to a violation of the local charge neutrality condition over the entire star, still fulfilling the global charge neutrality, which is obtained by solving a sophisticated eigenvalue problem. The complete electro-dynamical and gravitational potentials for such a system are given, from the center all the way to the surface boundary layers. The value of the Coulomb potential at the center of the configuration is $eV(0) \simeq m_\pi c^2$ and the system is intrinsically stable against Coulomb repulsion in the proton component. Also, the more general systems, including nuclear interactions, must have a constant electron Fermi energy and fulfill the associated general relativistic Thomas-Fermi equations here introduced with the proper boundary conditions. Such require-

ments have been neglected in the current literature, based on the Tolman-Oppenheimer-Volkoff equilibrium equations.

3. Jorge A. Rueda, R. Ruffini, and S.-S. Xue, "On the self-consistent general relativistic equilibrium equations of neutron stars", submitted to Phys. Rev. Lett.

We address the existence of globally neutral neutron star configurations in contrast with the traditional ones constructed by imposing local neutrality. The equilibrium equations describing this system are the Einstein-Maxwell equations which must be solved self-consistently with the general relativistic Thomas-Fermi equation and β -equilibrium condition. To illustrate the application of this novel approach we adopt the Baym, Bethe, and Pethick (1971) strong interaction model of the baryonic matter in the core and of the white-dwarf-like material of the crust. We illustrate the crucial role played by the boundary conditions satisfied by the leptonic component of the matter at the interface between the core and the crust. For every central density an entire new family of equilibrium configurations exists for selected values of the Fermi energy of the electrons at the surface of the core. Each such configuration fulfills global charge neutrality and is characterized by a non-trivial electro-dynamical structure. The electric field extends over a thin shell of thickness $\sim \hbar/(m_e c)$ between the core and the crust and becomes largely overcritical in the limit of decreasing values of the crust mass.

4. Jorge A. Rueda, M. Rotondo, R. Ruffini, and S.-S. Xue, "The relativistic Feynman-Metropolis-Teller theory for white-dwarfs in general relativity", submitted to Phys. Rev. D.

The recently formulation of the relativistic Thomas-Fermi model within the Feynman-Metropolis-Teller theory for compressed atoms is applied to the study of general relativistic white-dwarf equilibrium configurations. The equation of state, which takes into account the beta equilibrium of the nuclei with the surrounding electrons, is obtained as a function of the compression by considering each atom constrained in a Wigner-Seitz cell and leading to the estimate of the Coulomb interaction. The general relativistic equilibrium of white-dwarf matter can be expressed by the simple formula $\sqrt{g_{00}}\mu_{ws} = \text{constant}$, which links the chemical potential of the Wigner-Seitz cell μ_{ws} with the general relativistic gravitational potential at each point of the configuration. The configuration outside each Wigner-Seitz cell is strictly neutral and therefore no global electric field is necessary to warranty the equilibrium of the white-dwarf. These equations correct the ones used by Chandrasekhar by taking into due account the Coulomb interaction between the nuclei and the electrons. They also generalize the work of Salpeter by considering a unified self-consistent approach to the Coulomb interaction in each Wigner-Seitz cell. The consequences on the numerical value of the Chandrasekhar-Landau mass limit are presented. The modifications of the mass-radius relation for ${}^4\text{He}$ and

^{56}Fe white-dwarf equilibrium configurations are also presented. These effects become observable in processes requiring a precision knowledge of the white-dwarf parameters.

5. M. Rotondo, Jorge A. Rueda, R. Ruffini, and S.-S. Xue, "On the relativistic Thomas-Fermi treatment of compressed atoms and compressed nuclear matter cores of stellar dimensions", submitted to Phys. Rev. C.

The Feynman, Metropolis and Teller treatment of compressed atoms is extended to the relativistic regimes. Each atomic configuration is confined by a Wigner-Seitz cell and is characterized by a positive electron Fermi energy. The non-relativistic treatment assumes a point-like nucleus and infinite values of the electron Fermi energy can be attained. In the relativistic treatment there exists a limiting configuration, reached when the Wigner-Seitz cell radius equals the radius of the nucleus, with a maximum value of the electron Fermi energy $(E_e^F)_{max}$, here expressed analytically in the ultra-relativistic approximation. The corrections given by the relativistic Thomas-Fermi-Dirac exchange term are also evaluated and shown to be generally small and negligible in the relativistic high density regime. The dependence of the relativistic electron Fermi energies by compression for selected nuclei are compared and contrasted to the non-relativistic ones and to the ones obtained in the uniform approximation. The relativistic Feynman, Metropolis, Teller approach here presented overcomes some difficulties in the Salpeter approximation generally adopted for compressed matter in physics and astrophysics. The treatment is then extrapolated to compressed nuclear matter cores of stellar dimensions with $A \simeq (m_{\text{Planck}}/m_n)^3 \sim 10^{57}$ or $M_{core} \sim M_{\odot}$. A new family of equilibrium configurations exists for selected values of the electron Fermi energy varying in the range $0 < E_e^F \leq (E_e^F)_{max}$. Such configurations fulfill global but not local charge neutrality. They have electric fields on the core surface, increasing for decreasing values of the electron Fermi energy reaching values much larger than the critical value $E_c = m_e^2 c^3 / (e\hbar)$, for $E_e^F = 0$. We compare and contrast our results with the ones of Thomas-Fermi model in strange stars.

6. V. Popov, M. Rotondo, R. Ruffini, and S.-S. Xue, "On gravitationally and electrostatically bound massive nuclear density cores", submitted to Phys. Rev. C.

In a unified treatment we extrapolate results for neutral atoms with heavy nuclei to massive nuclear density cores with mass number $A \approx (m_{\text{Planck}}/m_n)^3 \sim 10^{57}$. We give explicit analytic solutions for the relativistic Thomas-Fermi equation of N_n neutrons, N_p protons and N_e electrons in beta equilibrium, fulfilling global charge neutrality, with $N_p = N_e$. We give explicit expressions for the physical parameters including the Coulomb and the surface energies and we study as well the stability of such configurations. Analogous to heavy nuclei these macroscopic cores exhibit an overcritical electric field near their surface.

7. R. Ruffini and S.-S. Xue, "Electron-positron pairs production in an electric potential of massive cores ", to be submitted to Phys. Lett. B

Classical and semi-classical energy states of relativistic electrons bounded by a massive and charged core with the charge-mass-radius Q/M and macroscopic radius R_c are discussed. We show that the energies of semi-classical (bound) states can be much smaller than the negative electron mass-energy ($-mc^2$), and energy-level crossing to negative energy continuum occurs. Electron-positron pair production takes place by quantum tunneling, if these bound states are not occupied. Electrons fill into these bound states and positrons go to infinity. We explicitly calculate the rate of pair-production, and compare it with the rates of electron-positron production by the Sauter-Euler-Heisenberg-Schwinger in a constant electric field. In addition, the pair-production rate for the electro-gravitational balance ratio $Q/M = 10^{-19}$ is much larger than the pair-production rate due to the Hawking processes. We point out that in neutral cores with equal proton and electron numbers, the configuration of relativistic electrons in these semi-classical (bound) states should be stabilized by photon emissions.

5.2. Conference Proceedings

1. Jorge A. Rueda, R. Ruffini, and S.-S. Xue, "On the electrostatic structure of neutron stars", AIP Conf. Proc. 1205, 143 (2010).

We consider neutron stars composed by, (1) a core of degenerate neutrons, protons, and electrons above nuclear density; (2) an inner crust of nuclei in a gas of neutrons and electrons; and (3) an outer crust of nuclei in a gas of electrons. We use for the strong interaction model for the baryonic matter in the core an equation of state based on the phenomenological Weizsacker mass formula, and to determine the properties of the inner and the outer crust below nuclear saturation density we adopt the well-known equation of state of Baym-Bethe-Pethick. The integration of the Einstein-Maxwell equations is carried out under the constraints of β -equilibrium and global charge neutrality. We obtain baryon densities that sharply go to zero at nuclear density and electron densities matching smoothly the electron component of the crust. We show that a family of equilibrium configurations exists fulfilling overall neutrality and characterized by a non-trivial electro-dynamical structure at the interface between the core and the crust. We find that the electric field is overcritical and that the thickness of the transition surface-shell separating core and crust is of the order of the electron Compton wavelength.

2. D. Pugliese, Jorge A. Rueda, R. Ruffini, and S.-S. Xue, "A general relativistic Thomas Fermi treatment of neutron star cores II. Generalized Fermi energies and beta equilibrium ", to be published by Int. J. Mod.

Phys. D as a contribution for the Proceedings of the 2nd Galileo-Xu Guangqi Meeting, Ventimiglia-Italy (2010).

We formulate the set of self-consistent ground-state equilibrium equations of a system of degenerate neutrons, protons and electrons in beta equilibrium taking into account quantum statistics, electro-weak, and strong interactions, within the framework of general relativity. The strong interaction between nucleons is modeled through sigma-omega-rho meson exchange in the context of the extended Walecka model, all duly expressed in general relativity. We demonstrate that, as in the non-interacting case, the thermodynamic equilibrium condition given by the constancy of the Fermi energy of each particle-specie can be properly generalized to include the contribution of all fields.

3. K. Boshkayev, M. Rotondo, and R. Ruffini, "On Magnetic Fields in Rotating Nuclear Matter Cores of Stellar Dimensions ", to be published by Int. J. Mod. Phys. D as a contribution for the Proceedings of the 2nd Galileo-Xu Guangqi Meeting, Ventimiglia-Italy (2010).

We consider a globally neutral system of a stellar dimension consisting of degenerate and mostly non-interacting N_n neutrons, N_p protons and N_e electrons in beta equilibrium. Such a system at nuclear density having mass numbers $A \approx 10^{57}$ can exhibit a charge distribution different from zero. We present the analysis in the framework of classical electrodynamics to investigate the magnetic field induced by this charge distribution when the system is allowed to rotate as a whole rigid body with constant angular velocity around the axis of symmetry.

4. R. Mohammadi, Jorge A. Rueda, R. Ruffini, and S.-S. Xue, "The solution of the Thomas-Fermi equation in the presence of strong magnetic fields ", to be published by Int. J. Mod. Phys. D as a contribution for the Proceedings of the 2nd Galileo-Xu Guangqi Meeting, Ventimiglia-Italy (2010).

We study the influence of strong constant magnetic fields on a globally but not locally neutral compressed system of degenerate neutrons, protons and electrons in beta equilibrium. The ultrarelativistic Thomas-Fermi equation for such a compressed magnetized system is obtained and solved analytic closed form. We analyze the effects of the magnetic field on the properties of the configuration such as the Coulomb potential, the electric field, and the proton fraction.

5. Jorge A. Rueda H., B. Patricelli, M. Rotondo, R. Ruffini, and S. S. Xue, "The Extended Nuclear Matter Model with Smooth Transition Surface", Proceedings of the 3rd Stueckelberg Workshop on Relativistic Field Theories, Pescara-Italy (2008). In press.

The existence of electric fields close to their critical value $E_c = m_e^2 c^3 / (e\hbar)$ has been proved for massive cores of 10^7 up to 10^{57} nucleons using a proton dis-

tribution of constant density and a sharp step function at its boundary. We explore the modifications of this effect by considering a smoother density profile with a proton distribution fulfilling a Woods-Saxon dependence. The occurrence of a critical field has been confirmed. We discuss how the location of the maximum of the electric field as well as its magnitude is modified by the smoother distribution.

6. Jorge A. Rueda, M. Rotondo, R. Ruffini, and S.-S. Xue, "On compressed nuclear matter: from nuclei to neutron stars", to be published in the Proceedings of the 1st Galileo-Xu Guangqi Meeting, Shanghai-China (2009).

We address the description of neutron-proton-electron degenerate matter in beta equilibrium subjected to compression both in the case of confined nucleons into a nucleus as well as in the case of deconfined nucleons. We follow a step-by-step generalization of the classical Thomas-Fermi model to special and general relativistic regimes, which leads to a unified treatment of beta equilibrated neutron-proton-electron degenerate matter applicable from the case of nuclei all the way up to the case of white-dwarfs and neutron stars. New gravito-electrodynamical effects, missed in the traditional approach for the description of neutron star configurations, are found as a consequence of the new set of general relativistic equilibrium equations.

7. Jorge A. Rueda, M. Rotondo, R. Ruffini, and S.-S. Xue, "A New Family of Neutron Star Models: Global Neutrality vs. Local Neutrality", to be published in the Proceedings of the 12th Marcel Grossmann Meeting On General Relativity, Paris-France (2009).

We formulate the set of self-consistent ground-state equilibrium equations of a system of degenerate neutrons, protons and electrons in beta equilibrium taking into account quantum statistics and electro-weak interactions within the framework of general relativity. We point out the existence of globally neutral neutron star configurations in contrast with the traditional locally neutral ones. We discuss new gravito-electrodynamic effects present in such globally neutral neutron star equilibrium configurations.

8. R. Ruffini, A. G. Aksenov, M. G. Bernardini, C. Bianco, L. Caito, P. Charbonnet, M. G. Dainotti, G. De Barros, R. Guida, L. Izzo, B. Patricelli, L. J. Rangel Lemos, M. Rotondo, Jorge A. Rueda, G. Vereshchagin, and S.-S. Xue, "The Blackholic energy and the canonical Gamma-Ray Burst IV: the "long", "genuine short" and "fake - disguised short" GRBs", AIP Conf. Proc. 1132, 199 (2009).

We report some recent developments in the understanding of GRBs based on the theoretical framework of the "fireshell" model, already presented in the last three editions of the "Brazilian School of Cosmology and Gravitation". After recalling the basic features of the "fireshell model", we emphasize the fol-

lowing novel results: 1) the interpretation of the X-ray flares in GRB afterglows as due to the interaction of the optically thin fireshell with isolated clouds in the CircumBurst Medium (CBM); 2) an interpretation as “fake - disguised” short GRBs of the GRBs belonging to the class identified by Norris & Bonnell; we present two prototypes, GRB 970228 and GRB 060614; both these cases are consistent with an origin from the final coalescence of a binary system in the halo of their host galaxies with particularly low CBM density $n_{cbm} \sim 10^{-3}$ particles/cm³; 3) the first attempt to study a genuine short GRB with the analysis of GRB 050509B, that reveals indeed still an open question; 4) the interpretation of the GRB-SN association in the case of GRB 060218 via the “induced gravitational collapse” process; 5) a first attempt to understand the nature of the “Amati relation”, a phenomenological correlation between the isotropic-equivalent radiated energy of the prompt emission E_{iso} with the cosmological rest-frame νF_ν spectrum peak energy $E_{p,i}$. In addition, recent progress on the thermalization of the electron-positron plasma close to their formation phase, as well as the structure of the electrodynamics of Kerr-Newman Black Holes are presented. An outlook for possible explanation of high-energy phenomena in GRBs to be expected from the AGILE and the Fermi satellites are discussed. As an example of high energy process, the work by Enrico Fermi dealing with ultrarelativistic collisions is examined. It is clear that all the GRB physics points to the existence of overcritical electro-dynamical fields. In this sense we present some progresses on a unified approach to heavy nuclei and neutron stars cores, which leads to the existence of overcritical fields under the neutron star crust.

6. Invited talks in international conferences

1. 2nd Galileo-Xu Guangqi Meeting, July 12–18 2010, Ventimiglia (Italy).
2. 11th Italian-Korean Symposium on Relativistic Astrophysics, November 2–4 2009, Seoul (Korea).
3. 1st Galileo-Xu Guangqi Meeting, October 26–30 2009, Shanghai (China).
4. 12th Marcel Grossmann Meeting On General Relativity, July 12–18 2009, Paris (France).
5. 6th Italian-Sino Workshop on Relativistic Astrophysics, June 29–July 1 2009, Pescara (Italy).
6. 1st Sobral Meeting, May 26–29 2009, Fortaleza (Brazil).
7. Probing stellar populations out to the distant universe, September 7–19 2008, Cefalù (Italy).
8. XIII Brazilian School of Cosmology and Gravitation, July 20–August 2 2008, Rio de Janeiro (Brazil).
9. 3rd Stueckelberg Workshop, July 8–18 2008, Pescara (Italy).
10. 5th Italian-Sino Workshop, May 28–June 1 2008, Taipei (Taiwan).
11. APS April meeting, April 12–15 2008, Saint Louis (USA).
12. Path Integrals - New Trends and Perspectives, September 23–28 2007, Dresden (Germany).
13. APS April meeting, April 14–17 2007, Jacksonville (USA).
14. XIth Marcel Grossmann Meeting on General Relativity, July 23–29 2006, Berlin (Germany).

7. APPENDICES

A. The Thomas-Fermi model: from nuclei to nuclear matter cores of stellar dimensions

A.1. On gravitationally and electrodynamically bound massive nuclear density cores

A.1.1. Introduction

Models involving e^+e^- plasmas of total energy $\leq 10^{55}$ ergs originating from a vacuum polarization process during the formation of a black hole are being studied to explain a variety of ultra-relativistic astrophysics events Ruffini et al. (2010); Cherubini et al. (2009); Aksenov et al. (2007). The formation of such a Kerr-Newman black hole with overcritical electromagnetic fields can only occur during the process of gravitational collapse, e.g., of two coalescing neutron stars. Accordingly in this article we consider new electrodynamical properties of massive nuclear density cores which have been neglected in the astrophysics literature. This issue has been overlooked in the traditional description of neutron stars by considering only neutrons Oppenheimer and Volkoff (1939) or by imposing *ab initio* local charge neutrality, i.e., local identity of the densities of protons and electrons $n_p = n_e$, thus bypassing the description of any possible electrodynamical effect Harrison et al. (1965); Baym et al. (1971a).

The model we consider here generalizes the relativistic Thomas-Fermi treatment for neutral atoms with heavy nuclei Pieper and Greiner (1969); Müller et al. (1972); Greenberg and Greiner (1982); Popov (1971b); Zeldovich and Popov (1972); Migdal et al. (1976). The study of neutral atoms with nuclei of mass number $A \sim 10^2-10^6$ is a classic problem of theoretical physics Zeldovich and Popov (1972); Ruffini et al. (2010). Special attention has been given to a possible vacuum polarization process and the creation of e^+e^- pairs Pieper and Greiner (1969); Zeldovich and Popov (1972); Ruffini et al. (2010) as well as to the study of nuclear stability against Coulomb repulsion Greenberg and Greiner (1982). The existence of electric fields larger than the critical value $E_c = m_e^2 c^3 / (e\hbar)$ near their surfaces Popov (1971b) has also been shown. We have generalized these models by enforcing the beta equilibrium conditions Ruffini et al. (2007b).

We have then extrapolated those results by numerical integration to the case of massive nuclear density cores of mass $\approx 1M_{\odot}$ and radius $R_c \approx 10$ km Ruffini et al. (2007b). Such a massive nuclear density core is a globally neutral system of N_n neutrons, N_p protons and N_e electrons in beta equilibrium at nuclear density having mass numbers $A \sim (m_{\text{Planck}}/m_n)^3$ where m_n (m_e) is the neutron (electron) mass and $m_{\text{Planck}} = (\hbar c/G)^{1/2}$ Ruffini et al. (2007b). As in the nuclear model Migdal et al. (1976), the proton distribution is here assumed to be constant up to the core radius R_c . We have obtained configurations with global charge neutrality $N_p = N_e$ but $n_p \neq n_e$, in contrast with the local condition $n_p = n_e$ traditionally assumed in astrophysics. As a result electric fields of critical value are confirmed to exist, near the surface, also in the case of massive nuclear density cores in analogy to the case of heavy nuclei.

Recently a new dimensionless form of the relativistic Thomas-Fermi treatment for a nuclear density core has been obtained which reveals the existence of new scaling laws for this model.

In this article we present a unified treatment extending from heavy nuclei to massive nuclear density cores by using an explicit analytic solitonic solution of the new dimensionless form of the relativistic Thomas-Fermi equation. We confirm the existence of and give an analytic expression for the overcritical electric field near the surface of massive nuclear density cores already obtained in Ruffini et al. (2007b) by numerical integration. Furthermore there are a variety of new results made possible by the new analytic formulation. First we give an explicit expression for the Coulomb energy of such cores, demonstrating their stability against nuclear fission, as opposed to the case of heavy nuclei. Secondly on the basis of Newtonian gravitational energy considerations we propose the existence of a possible new island of stability for mass numbers $A > A_R = 0.039 \left(\frac{N_p}{A}\right)^{1/2} \left(\frac{m_{\text{Planck}}}{m_n}\right)^3$. The equilibrium against Coulomb repulsion originates now from the combined effect of the screening of the relativistic electrons, of the surface tension due to strong interactions and of the gravitational interaction of the massive dense cores. By enforcing the condition of beta equilibrium, we also obtain a generalized relation between the mass number A and atomic number N_p which encompasses previous phenomenological expressions.

All the above solutions have been obtained assuming the electron Fermi energy to be equal to zero. The necessity and the methodology of extending these results to the case of compressed atoms along the lines of the Feynman-Metropolis-Teller treatment Feynman et al. (1949), corresponding to positive values of the Fermi energy of electrons, are outlined here. We also motivate the clear necessity and the general methodology of justifying the above results using a self-consistent general relativistic treatment of the system. These ideas will be pursued in detail elsewhere.

A.1.2. The relativistic Thomas-Fermi equation and the beta equilibrium condition

It has been known since the classic work of Fermi Fermi (1950) that the phenomenological drop model of the nucleus gives excellent results for a variety of properties including the isobaric behavior and nuclear fission. In addition to the masses of the baryonic components and the asymmetry energy and pairing term, the mass formula contains terms estimating the surface tension energy of the nucleus Fermi (1950)

$$\varepsilon_s = 17.5 \cdot A^{2/3} \text{ MeV}, \quad (\text{A.1.1})$$

and the Coulomb energy Fermi (1950)

$$\varepsilon_c = \frac{3\alpha N_p^2}{5R_c}, \quad (\text{A.1.2})$$

where $R_c = r_0 A^{1/3}$, $r_0 = 1.5 \cdot 10^{-13}$ cm and the numerical factors are derived by fitting the observational data. From the extremization of the mass formula the following relation between A and N_p is obtained Fermi (1950)

$$N_p \simeq \left[\frac{2}{A} + \frac{3}{200} \frac{1}{A^{1/3}} \right]^{-1}, \quad (\text{A.1.3})$$

which in the limit of small A gives

$$N_p \simeq \frac{A}{2}. \quad (\text{A.1.4})$$

The analysis of the stability of the nucleus against finite deformation leads to a stability condition against fission given by the equality of the surface energy term to the Coulomb energy. This leads to the condition Fermi (1950)

$$\frac{N_p^2}{A} < 45. \quad (\text{A.1.5})$$

A novel situation occurs when super-heavy nuclei ($A > \tilde{A} \sim 10^4$) are examined Ferreirinho et al. (1980); Ruffini et al. (2007b). The distribution of electrons penetrates inside the nucleus: a much smaller effective net charge of the nucleus occurs due to the screening of relativistic electrons Migdal et al. (1976); Ferreirinho et al. (1980). In Ruffini and Stella (1981) a definition of an effective nuclear charge due to the penetration of the electrons was presented. A treatment based on the relativistic Thomas-Fermi model has been developed in order to describe the penetration of the electrons and their effective screening of the positive nuclear charge. In particular, by assuming

$N_p \simeq A/2$, Greiner *et al.* Pieper and Greiner (1969); Müller *et al.* (1972); Greenberg and Greiner (1982) and Popov *et al.* Popov (1971b); Zeldovich and Popov (1972); Migdal *et al.* (1976) in a series of papers were able to solve the non-linear Thomas-Fermi equation. It was demonstrated in Migdal *et al.* (1976) that the effective positive nuclear charge is confined to a small layer of thickness $\sim \hbar/\sqrt{\alpha}m_\pi c$ where m_π is the pion mass and as usual $\alpha = e^2/\hbar c$. Correspondingly electric fields of strength much larger than the critical value E_c for vacuum polarization at the surface of the core are created. However, the creation of electron-positron pairs due to the vacuum polarization process does not occur because of the Pauli blocking by the degenerate electrons Ruffini *et al.* (2010).

Here we generalize the work of Greiner Pieper and Greiner (1969); Müller *et al.* (1972); Greenberg and Greiner (1982) and Popov Popov (1971b); Zeldovich and Popov (1972); Migdal *et al.* (1976). We have relaxed the condition $N_p \simeq A/2$ adopted by Popov and Greiner as well as the condition $N_p \simeq [2/A + 3/200A^{1/3}]^{-1}$ adopted by Ferreira, Ruffini and Stella Ferreira *et al.* (1980). Instead we explicitly impose the beta decay equilibrium between neutrons, protons and electrons. We then extrapolate such model to the case $A \approx (m_{\text{Planck}}/m_n)^3 \sim 10^{57}$. A supercritical field still exists in a shell of thickness $\sim \hbar/\sqrt{\alpha}m_\pi c$ at the core surface, and a charged lepton-baryonic core is surrounded by an oppositely charged leptonic component. Such massive nuclear density cores, including the leptonic component, are globally neutral.

As usual we assume that the protons are distributed at constant density n_p within a radius

$$R_c = \Delta \frac{\hbar}{m_\pi c} N_p^{1/3}, \quad (\text{A.1.6})$$

where Δ is a parameter such that $\Delta \approx 1$ ($\Delta < 1$) corresponds to nuclear (supranuclear) densities when applied to ordinary nuclei. The overall Coulomb potential satisfies the Poisson equation

$$\nabla^2 V(r) = -4\pi e [n_p(r) - n_e(r)], \quad (\text{A.1.7})$$

with the boundary conditions $V(\infty) = 0$ (due to the global charge neutrality of the system) and finiteness of $V(0)$. The density $n_e(r)$ of the electrons of charge $-e$ is determined by the Fermi energy condition on their Fermi momentum P_e^F ; we assume here

$$E_e^F = [(P_e^F c)^2 + m_e^2 c^4]^{1/2} - m_e c^2 - eV(r) = 0, \quad (\text{A.1.8})$$

which leads to

$$n_e(r) = \frac{(P_e^F)^3}{3\pi^2\hbar^3} = \frac{1}{3\pi^2\hbar^3 c^3} \left[e^2 V^2(r) + 2m_e c^2 eV(r) \right]^{3/2}. \quad (\text{A.1.9})$$

By introducing $x = r/[\hbar/m_\pi c]$, $x_c = R_c/[\hbar/m_\pi c]$ and $\chi/r = eV(r)/c\hbar$, the relativistic Thomas-Fermi equation takes the form

$$\frac{1}{3x} \frac{d^2\chi(x)}{dx^2} = -\frac{\alpha}{\Delta^3} \theta(x_c - x) + \frac{4\alpha}{9\pi} \left[\frac{\chi^2(x)}{x^2} + 2\frac{m_e}{m_\pi} \frac{\chi}{x} \right]^{3/2}, \quad (\text{A.1.10})$$

where $\chi(0) = 0, \chi(\infty) = 0$. The neutron density $n_n(r)$ is determined by the Fermi energy condition on their Fermi momentum P_n^F imposed by beta decay equilibrium

$$\begin{aligned} E_n^F &= [(P_n^F c)^2 + m_n^2 c^4]^{1/2} - m_n c^2 \\ &= [(P_p^F c)^2 + m_p^2 c^4]^{1/2} - m_p c^2 + eV(r), \end{aligned} \quad (\text{A.1.11})$$

which in turn is related to the proton and electron densities by Eqs. (A.1.7), (A.1.9) and (A.1.10). These equations have been integrated numerically (see Ruffini et al. (2007b)).

A.1.3. The ultra-relativistic analytic solutions

In the ultrarelativistic limit, the relativistic Thomas-Fermi equation admits an analytic solution. Introducing the new function ϕ defined by $\phi = \frac{4^{1/3}}{(9\pi)^{1/3}} \Delta \frac{\chi}{x}$ and the new variables $\hat{x} = (12/\pi)^{1/6} \sqrt{\alpha} \Delta^{-1} x$, $\xi = \hat{x} - \hat{x}_c$, where $\hat{x}_c = (12/\pi)^{1/6} \sqrt{\alpha} \Delta^{-1} x_c$, then Eq. (A.1.10) becomes

$$\frac{d^2\hat{\phi}(\xi)}{d\xi^2} = -\theta(-\xi) + \hat{\phi}(\xi)^3, \quad (\text{A.1.12})$$

where $\hat{\phi}(\xi) = \phi(\xi + \hat{x}_c)$. The boundary conditions on $\hat{\phi}$ are: $\hat{\phi}(\xi) \rightarrow 1$ as $\xi \rightarrow -\hat{x}_c \ll 0$ (at the massive nuclear density core center) and $\hat{\phi}(\xi) \rightarrow 0$ as $\xi \rightarrow \infty$. The function $\hat{\phi}$ and its first derivative $\hat{\phi}'$ must be continuous at the surface $\xi = 0$ of the massive nuclear density core. Equation (A.1.12) admits an exact solution

$$\hat{\phi}(\xi) = \begin{cases} 1 - 3 \left[1 + 2^{-1/2} \sinh(a - \sqrt{3}\xi) \right]^{-1}, & \xi < 0, \\ \frac{\sqrt{2}}{(\xi + b)}, & \xi > 0, \end{cases} \quad (\text{A.1.13})$$

A. The Thomas-Fermi model: from nuclei to nuclear matter cores of stellar dimensions

where the integration constants a and b have the values $a = \operatorname{arcsinh}(11\sqrt{2}) \approx 3.439$, $b = (4/3)\sqrt{2} \approx 1.886$. Next we evaluate the Coulomb potential energy function

$$eV(\xi) = \left(\frac{9\pi}{4}\right)^{1/3} \frac{1}{\Delta} m_\pi c^2 \hat{\phi}(\xi), \quad (\text{A.1.14})$$

and by differentiation, the electric field

$$E(\xi) = - \left(\frac{3^5\pi}{4}\right)^{1/6} \frac{\sqrt{\alpha} m_\pi^2 c^3}{\Delta^2 e\hbar} \hat{\phi}'(\xi). \quad (\text{A.1.15})$$

Details are given in Figs. A.1 and A.2.

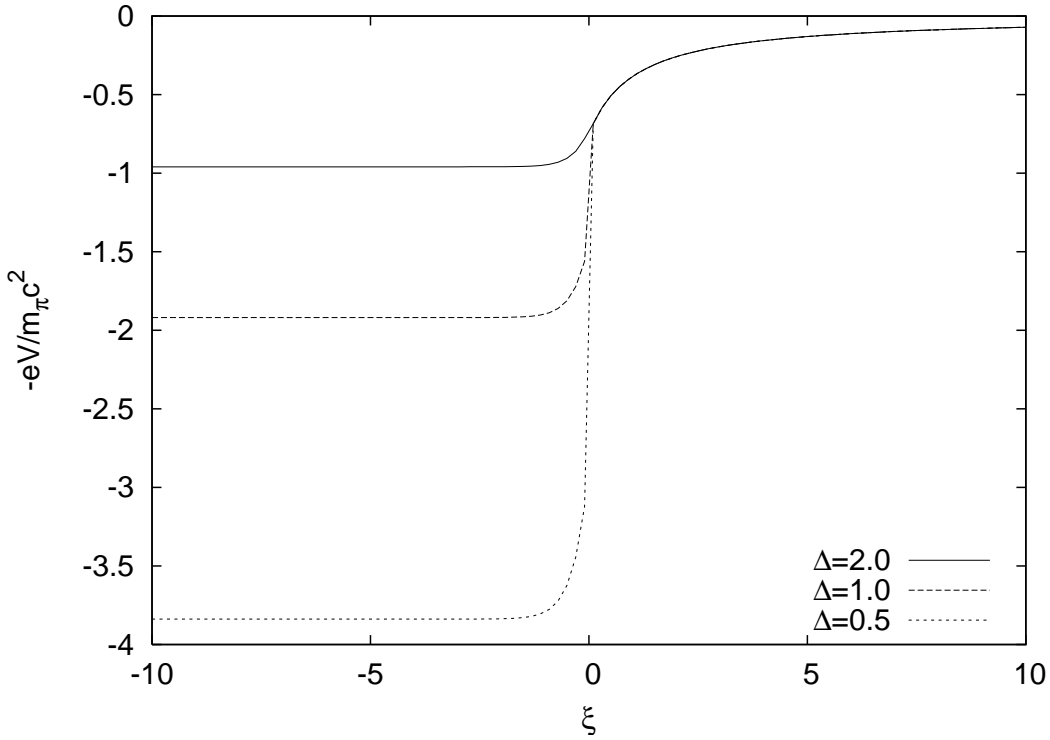


Figure A.1.: The electron Coulomb potential energy $-eV$, in units of pion mass m_π is plotted as a function of the radial coordinate $\xi = \hat{x} - \hat{x}_c$, for selected values of the density parameter Δ .

We now estimate three crucial quantities:

1) the Coulomb potential at the center of the configuration,

$$eV(0) \approx \left(\frac{9\pi}{4}\right)^{1/3} \frac{1}{\Delta} m_\pi c^2, \quad (\text{A.1.16})$$

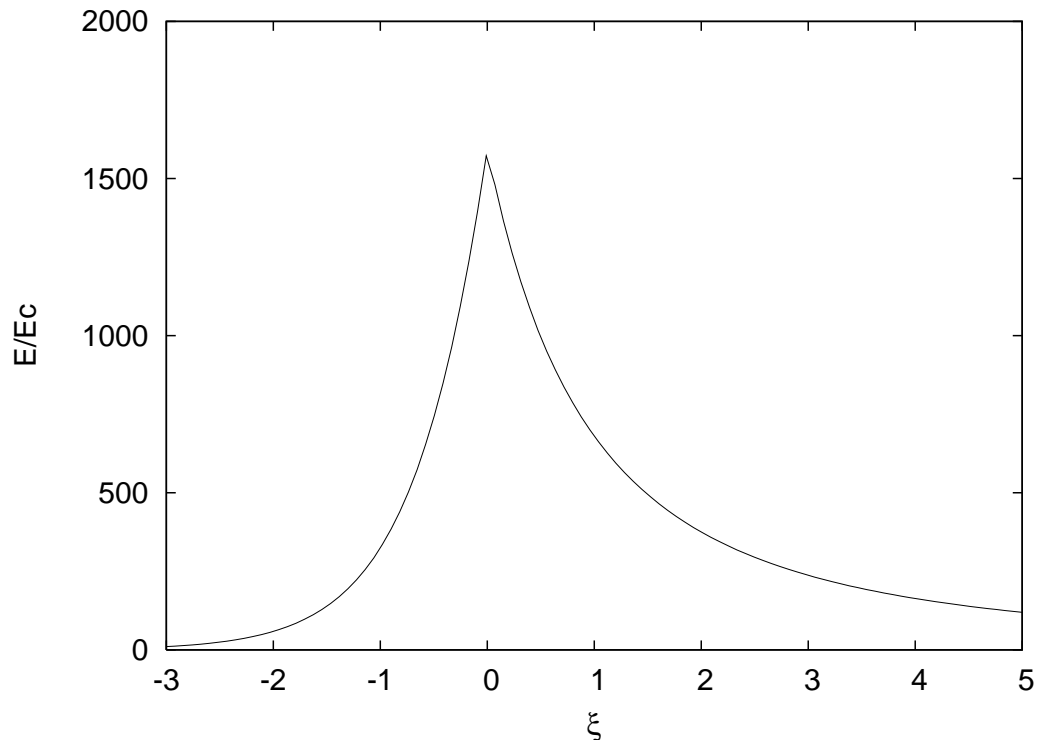


Figure A.2.: The electric field is plotted in units of the critical field E_c as a function of the radial coordinate ξ for $\Delta=2$, showing a sharp peak at the core radius.

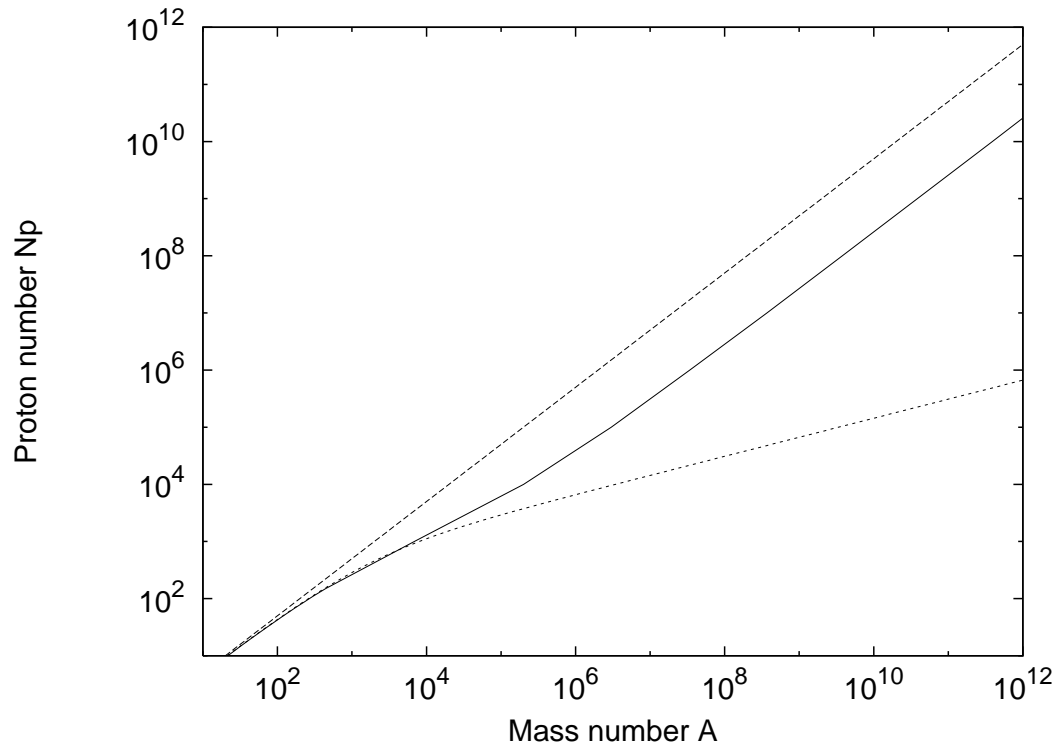


Figure A.3.: The A - N_p relation at nuclear density (solid line) obtained from first principles compared with the phenomenological expressions given by $N_p \simeq A/2$ (dashed line) and Eq. (A.1.3) (dotted line). The asymptotic value, for $A \rightarrow (m_{\text{Planck}}/m_n)^3$, is $N_p \approx 0.0046A$.

2) the electric field at the surface of the core

$$E_{\max} \approx 0.95\sqrt{\alpha}\frac{1}{\Delta^2}\frac{m_\pi^2 c^3}{e\hbar} = 0.95\frac{\sqrt{\alpha}}{\Delta^2}\left(\frac{m_\pi}{m_e}\right)^2 E_c. \quad (\text{A.1.17})$$

3) the Coulomb electrostatic energy of the core

$$\mathcal{E}_{\text{em}} = \int \frac{E^2}{8\pi} d^3r \approx 0.15\frac{3\hbar c(3\pi)^{1/2}}{4\Delta\sqrt{\alpha}}A^{2/3}\frac{m_\pi c}{\hbar}\left(\frac{N_p}{A}\right)^{2/3}. \quad (\text{A.1.18})$$

These three quantities are functions only of the pion mass m_π , the density parameter Δ and of the fine structure constant α . Their formulas apply over the entire range from superheavy nuclei with $N_p \sim 10^3$ all the way up to massive cores with $N_p \approx (m_{\text{Planck}}/m_n)^3$.

A.1.4. New results derived from the analytic solutions

Starting from the analytic solutions of the previous section we obtain the following new results.

a) Using the solution (A.1.13), we have obtained a new generalized relation between A and N_p for any value of A . In the limit of small A this result agrees well with the phenomenological relations given by Eqs. (A.1.3) and (A.1.4), as is clearly shown in Fig. A.3. It appears that the explicit evaluation of the beta equilibrium, in contrast with the previously adopted Eqs.(3,4), leads to an effect comparable in magnitude and qualitatively similar to the asymmetry energy in the phenomenological liquid drop model.

b) The charge-to-mass ratio of the effective charge Q at the core surface to the core mass M is given by

$$\frac{Q}{\sqrt{GM}} \approx \frac{E_{\max}R_c^2}{\sqrt{G}m_n A} \approx \frac{m_{\text{Planck}}}{m_n}\left(\frac{1}{N_p}\right)^{1/3}\frac{N_p}{A}. \quad (\text{A.1.19})$$

For superheavy nuclei with $N_p \approx 10^3$, the charge-to-mass ratio for the nucleus is

$$\frac{Q}{\sqrt{GM}} > \frac{1}{20}\frac{m_{\text{Planck}}}{m_n} \sim 10^{18}. \quad (\text{A.1.20})$$

Gravitation obviously plays no role in the stabilization of these nuclei.

Instead for massive nuclear density cores where $N_p \approx (m_{\text{Planck}}/m_n)^3$, the ratio Q/\sqrt{GM} given by Eq. (A.1.19) is simply

$$\frac{Q}{\sqrt{GM}} \approx \frac{N_p}{A}, \quad (\text{A.1.21})$$

which is approximatively 0.0046 (see Fig. A.3). It is well-known that the charge-to-mass ratio (A.1.21) smaller than 1 evidences the equilibrium of self-gravitating mass-charge system both in Newtonian gravity and general relativity (see, e.g., Chandrasekhar (1992)).

c) For a massive core at nuclear density the criterion of stability against fission ($\mathcal{E}_{em} < 2\mathcal{E}_s$) is satisfied. In order to see this we use Eqs. (A.1.1) and (A.1.18)

$$\frac{\mathcal{E}_{em}}{2\mathcal{E}_s} \approx 0.15 \frac{3}{8} \sqrt{\frac{3\pi}{\alpha}} \frac{1}{\Delta} \left(\frac{N_p}{A} \right)^{2/3} \frac{m_\pi c^2}{17.5 \text{ MeV}} \sim 0.1 < 1. \quad (\text{A.1.22})$$

A.1.5. Estimates of gravitational effects in a Newtonian approximation

In order to investigate the possible effects of gravitation on these massive neutron density cores we proceed to some qualitative and quantitative estimates based on the Newtonian approximation.

a) The *maximum* Coulomb energy per proton is given by Eq. (A.1.16) where the potential is evaluated at the center of the core. The Newtonian gravitational potential energy per proton (of mass m_p) in the field of a massive nuclear density core with $A \approx (m_{\text{Planck}}/m_n)^3$ is given by

$$\mathcal{E}_g = -G \frac{M m_p}{R_c} = -\frac{1}{\Delta} \frac{m_{\text{Planck}}}{m_n} \frac{m_\pi c^2}{N_p^{1/3}} \simeq -\frac{m_\pi c^2}{\Delta} \left(\frac{A}{N_p} \right)^{1/3}. \quad (\text{A.1.23})$$

Since $A/N_p \sim 0.0046$ (see Fig. A.3) for any value of Δ , the gravitational energy is larger in magnitude than and opposite in sign to the Coulomb potential energy per proton of Eq. (A.1.16) so the system should be gravitationally stable.

b) There is yet a more accurate derivation of the gravitational stability based on the analytic solution of the Thomas-Fermi equation Eq. (A.1.12). The Coulomb energy \mathcal{E}_{em} given by (A.1.18) is mainly distributed within a thin shell of width $\delta R_c \approx \hbar \Delta / (\sqrt{\alpha} m_\pi c)$ and proton number $\delta N_p = n_p 4\pi R_c^2 \delta R_c$ at the surface. To ensure the stability of the system, the attractive gravitational energy of the thin proton shell

$$\mathcal{E}_{gr} \approx -3 \frac{G}{\Delta} \frac{A^{4/3}}{\sqrt{\alpha}} \left(\frac{N_p}{A} \right)^{1/3} m_n^2 \frac{m_\pi c}{\hbar} \quad (\text{A.1.24})$$

must be larger than the repulsive Coulomb energy (A.1.18). For small A , the gravitational energy is always negligible. However, since the gravitational energy increases proportionally to $A^{4/3}$ while the Coulomb energy only increases proportionally to $A^{2/3}$, the two must eventually cross, which occurs at

$$A_R = 0.039 \left(\frac{N_p}{A} \right)^{1/2} \left(\frac{m_{\text{Planck}}}{m_n} \right)^3. \quad (\text{A.1.25})$$

This establishes a *lower* limit for the mass number A_R necessary for the existence of an island of stability for massive nuclear density cores. The *upper* limit of the island of stability will be determined by general relativistic effects Rueda et al. (2010c).

c) Having established the role of gravity in stabilizing the Coulomb interaction of the massive nuclear density core, we outline the importance of the strong interactions in determining its surface. We find for the neutron pressure at the surface:

$$P_n = \frac{9}{40} \left(\frac{3}{2\pi} \right)^{1/3} \left(\frac{m_\pi}{m_n} \right) \frac{m_\pi c^2}{(\hbar/m_\pi c)^3} \left(\frac{A}{N_p} \right)^{5/3} \frac{1}{\Delta^5}, \quad (\text{A.1.26})$$

and for the surface tension, as extrapolated from nuclear scattering experiments,

$$P_s = - \left(\frac{0.13}{4\pi} \right) \frac{m_\pi c^2}{(\hbar/m_\pi c)^3} \left(\frac{A}{N_p} \right)^{2/3} \frac{1}{\Delta^2}. \quad (\text{A.1.27})$$

We then obtain

$$\frac{|P_s|}{P_n} = 0.39 \cdot \Delta^3 \left(\frac{N_p}{A} \right) = 0.24 \cdot \frac{\rho_{\text{nucl}}}{\rho_{\text{surf}}}, \quad (\text{A.1.28})$$

where $\rho_{\text{nucl}} = 3m_n A / 4\pi R_c^3$. The relative importance of the nuclear pressure and nuclear tension is a very sensitive function of the density ρ_{surf} at the surface.

It is important to emphasize a major difference between nuclei and the massive nuclear density cores treated in this article: the gravitational binding energy in these massive nuclear density cores is instead $\varepsilon_{\text{gr}} \approx GM_\odot m_n / R_c \approx 0.1 m_n c^2 \approx 93.8 \text{ MeV}$. In other words it is much bigger than the nuclear energy in ordinary nuclei $\varepsilon_{\text{nuclear}} \approx \hbar^2 / m_n r_0^2 \approx 28.8 \text{ MeV}$.

A.1.6. Possible applications to neutron stars

All the above considerations have been made for an isolated massive core at constant density whose boundary has been sharply defined by a step function. No external forces are exerted. Consequently due to the global charge neutrality, the Fermi energy of the electrons has been assumed to be equal to zero. In the earliest description of neutron stars in the work of Oppenheimer and Volkoff (1939) only a gas of neutrons was considered and the equation of equilibrium was written in the Schwarzschild metric. They considered the model of a degenerate gas of neutrons to hold from the center to the border, with the density monotonically decreasing away from the center.

In the intervening years a more realistic model has been presented challenging the original considerations of Tolman, Oppenheimer and Volkoff, Tolman (1939); Oppenheimer and Volkoff (1939). Their TOV equations considered the existence of neutrons all the way to the surface of the star. The presence of neutrons, protons and electrons in beta equilibrium were instead introduced in Harrison et al. (1965). Still more important the neutron stars have been shown to be composed of two sharply different components: the core at nuclear and/or supra-nuclear density consisting of neutrons, protons and electrons and a crust of white dwarf like material, namely of degenerate electrons in a nuclei lattice Harrison et al. (1965); Baym et al. (1971a). The pressure and the density of the core are mainly due to the baryons while the pressure of the crust is mainly due to the electrons with the density due to the nuclei and possibly with some free neutrons due to neutron drip (see e.g. Baym et al. (1971a)). Further works describing the nuclear interactions were later introduced (see e.g. Haensel et al. (2007)). Clearly all these considerations departed profoundly from the TOV approximation. The matching between the core component and the crust is the major unsolved problem. To this issue this article introduces some preliminary results in a simplified model which has the advantage to present explicit analytic solutions.

In all the above treatments in order to close the system of equations the condition of local charge neutrality $n_e = n_p$ was adopted without a proof. The considerations of massive neutron density cores presented in this article offer an alternative to the local charge neutrality condition $n_e = n_p$. In a specific example which can be solved also analytically such condition is substituted by the Thomas-Fermi relativistic equations implying $n_e \neq n_p$ and an overall charge neutral system ($N_e = N_p$). The condition of global charge neutrality as opposed to the local one, leads to the existence of overcritical electric fields at the core surface which may be relevant in the description of neutron stars.

Two important generalizations of the results here presented have been done :

- 1) we have studied the solution for massive neutron density cores with positive values of their Fermi energy of electrons, as contrasted to the one here

studied with zero Fermi energy of electrons. This is a necessary step in order to take into due account the compressional effects of the neutron star crusts on the core. Such a treatment leads, as a by-product, to the generalization of the classic work of Feynman, Metropolis and Teller considering compressed atoms in a Thomas-Fermi model Feynman et al. (1949).

2) the condition of the proton constant density adopted in this article has been relaxed by considering consistently also the gravitational self-interaction of the core. To this scope the Thomas-Fermi equations here considered has been formulated within general relativity: a covariant formulation with the metric and the electrodynamic potential fulfilling the system of the Einstein-Maxwell equations Rueda et al. (2010c). The results presented in this article have been confirmed by this more general treatment.

A.1.7. Conclusions

We have first generalized the treatment of heavy nuclei by enforcing the condition of beta equilibrium in the relativistic Thomas-Fermi equation, avoiding the imposition of $N_p \simeq A/2$ between N_p and A traditionally assumed in the literature. In doing so we have obtained (see Fig. A.3) an $A - N_p$ relation which extends the ones adopted in the literature. Using the existence of scaling laws for the system of equations considered, we extend the results obtained for heavy nuclei to the case of massive nuclear density cores. The novelty in this article is to show how both the considerations of heavy nuclei and of systems of macroscopic astrophysical dimensions can take advantage from a rigorous and analytic solution of the Thomas-Fermi relativistic equations and the beta equilibrium conditions. This task is achieved by obtaining explicit analytic solutions fulfilling precise boundary conditions and using the scaling laws introduced in this article.

Indeed the Thomas-Fermi treatment has been considered also in the context of quark stars with a charge and a density distribution analogous to the one of massive nuclear density cores we consider in this article Itoh (1970); Witten (1984); Alcock et al. (1986); Kettner et al. (1995); Usov (1998). There are however a variety of differences both in the boundary conditions adopted and in the solution obtained. In the present article we show that we can indeed obtain overcritical electric fields at nuclear density on macroscopic scales of $R_c \approx 10$ Km and $M \approx 1M_\odot$ for existing field theories involving only neutrons, protons and electrons and their fundamental interactions and no quarks present. We obtain explicit analytic solutions of the relativistic Thomas-Fermi equations, self-consistently solved with the condition of beta equilibrium. Such analytic solutions allow to give explicit expressions for the Coulomb energy, surface energy and Newtonian gravitational energy of such massive nuclear density cores.

These cores are stable against fission (see Eq. (A.1.22)), the surface tension

determines the sharpness of their boundary (see Eq. (A.1.28)) and the gravitational interaction, at Newtonian level, balances the Coulomb repulsion for mass numbers larger than the critical value given by Eq. (A.1.25).

As a by-product of these results, we also conclude that the arguments often quoted concerning limits on the electric fields of an astrophysical system based on a free test particle (the dust approximation) considering only the gravitational and electric interactions

$$(E_{\max})_{\text{dust}} \approx \frac{m_e m_n c^3}{e \hbar} \frac{m_n}{m_{\text{Planck}}}, \quad (\text{A.1.29})$$

$$\left(\frac{Q}{\sqrt{GM}}\right)_{\text{dust}} \approx \sqrt{G} \frac{m_e}{e} = \frac{1}{\sqrt{\alpha}} \frac{m_e}{m_{\text{Planck}}}, \quad (\text{A.1.30})$$

appear to be inapplicable for $A \sim (m_{\text{Planck}}/m_n)^3$. Here nuclear densities are reached and the roles of *all* fundamental interactions, including weak and strong interactions in addition to the electromagnetic and gravitational ones and including as well quantum statistics, have to be taken into account through the relativistic Thomas-Fermi model. Eqs. (A.1.29) and (A.1.30) are replaced by Eqs. (A.1.17) and (A.1.21),

$$E_{\max} \approx \frac{0.95\sqrt{\alpha} m_{\text{Planck}}}{\Delta^2} \frac{m_{\text{Planck}}}{m_e} \left(\frac{m_\pi}{m_n}\right)^2 (E_{\max})_{\text{dust}}, \quad (\text{A.1.31})$$

$$\frac{Q}{\sqrt{GM}} \approx \frac{N_p}{A} \sqrt{\alpha} \frac{m_{\text{Planck}}}{m_e} \left(\frac{Q}{\sqrt{GM}}\right)_{\text{dust}}. \quad (\text{A.1.32})$$

Details are presented in Rueda et al. (2010c).

A.2. On the relativistic Thomas-Fermi treatment of compressed atoms and compressed nuclear matter cores of stellar dimensions

A.2.1. Introduction

In a classic article Baym, Bethe and Pethick Baym et al. (1971a) presented the problem of matching, in a neutron star, a liquid core, composed of N_n neutrons, N_p protons and N_e electrons, to the crust taking into account the electro-dynamical and surface tension effects. After discussing the different aspects of the problem they concluded: *The details of this picture requires further elaboration; this is a situation for which the Thomas-Fermi method is useful.* This statement, in first instance, may appear surprising: the Thomas-Fermi model has been extensively applied in atomic physics (see e.g Gombás Gombás (1949), March March (1957), Lundqvist and March Lundqvist and March (1983)), also has been applied extensively in atomic physics in its relativistic form (see e.g Ferreirinho, Ruffini and Stella Ferreirinho et al. (1980), Ruffini and Stella Ruffini and Stella (1981)) as well as in the study of atoms with heavy nuclei in the classic works of Migdal, Popov and Voskresenskii Migdal et al. (1976, 1977). Similarly there have been considerations of relativistic Thomas-Fermi model for quark stars pointing out the existence of critical electric fields on their surfaces (see e.g. Alcock, Farhi, Olinto Alcock et al. (1986), Usov Usov (1998)). Similar results have also been obtained by Alford et al. Alford et al. (2001) in the transition at very high densities, from the normal nuclear matter phase in the core to the color-flavor-locked phase of quark matter in the inner core of hybrid stars. No example exists to the application of the electromagnetic Thomas-Fermi model for neutron stars. This problem can indeed be approached with merit by studying the simplified but rigorous concept of a nuclear matter core of stellar dimensions which fulfills the relativistic Thomas-Fermi equation as discussed in Ruffini et al. (2007b); Popov et al. (2010). As we will see this work leads to the prediction of the existence of a critical electric field at the interface between the core and the crust of a neutron star.

In Ruffini et al. (2007b); Popov et al. (2010) we have first generalized the treatment of heavy nuclei by enforcing self-consistently the condition of beta equilibrium in the relativistic Thomas-Fermi equation. Using then the existence of scaling laws we have extended the results from heavy nuclei to the case of nuclear matter cores of stellar dimensions. In both these treatments we had there assumed the Fermi energy of the electrons $E_e^F = 0$. The aim of this article is to proceed with this dual approach and to consider first the case of compressed atoms and then, using the existence of scaling laws, the compressed nuclear matter cores of stellar dimensions with a positive value of their electron Fermi energies.

It is well known that Salpeter has been among the first to study the behavior of matter under extremely high pressures by considering a Wigner-Seitz cell of radius R_{WS} Salpeter (1961). Salpeter assumed as a starting point the nucleus point-like and a uniform distribution of electrons within a Wigner-Seitz cell. He then considered corrections to the above model due to the inhomogeneity of electron distribution. The first correction corresponds to the inclusion of the lattice energy $E_C = -(9N_p^2\alpha)/(10R_{WS})$, which results from the point-like nucleus-electron interaction and, from the electron-electron interaction inside the cell of radius R_{WS} . The second correction is given by a series-expansion of the electron Fermi energy about the average electron density n_e given by the uniform approximation. The electron density is then assumed equals to $n_e[1 + \epsilon(r)]$ with $\epsilon(r)$ considered as infinitesimal. The Coulomb potential energy is assumed to be the one of the point-like nucleus with the uniform distribution of electrons of density n_e thus the correction given by $\epsilon(r)$ is neglected on the Coulomb potential. The electron distribution is then calculated at first-order by expanding the relativistic electron kinetic energy about its value given by the uniform approximation considering as infinitesimal the ratio eV/E_e^F between the Coulomb potential energy eV and the electron Fermi energy $E_e^F = \sqrt{[cP_e^F(r)]^2 + m_e^2c^4} - m_e c^2 - eV$. The inclusion of each additional Coulomb correction results in a decreasing of the pressure of the cell P_S by comparison to the uniform one.

It is quite difficult to assess the self-consistency of all the recalled different approximations adopted by Salpeter. In order to validate and also to see the possible limits of the Salpeter approach, we consider the relativistic generalization of the Feynman, Metropolis, Teller treatment Feynman et al. (1949) which takes automatically and globally into account all electromagnetic and special relativistic contributions. We show explicitly how this new treatment leads in the case of atoms to electron distributions markedly different from the ones often adopted in the literature of constant electron density distributions. At the same time it allows to overcome some of the difficulties in current treatments.

Similarly the point-like description of the nucleus often adopted in literature is confirmed to be unacceptable in the framework of a relativistic treatment.

In Sec. A.2.2 we first recall the non-relativistic treatment of the compressed atom by Feynman, Metropolis and Teller. In Sec. A.2.3 we generalize that treatment to the relativistic regime by integrating the relativistic Thomas-Fermi equation, imposing also the condition of beta equilibrium. In Sec. A.2.4 we first compare the new treatment with the one corresponding to a uniform electron distribution often used in the literature and to the Salpeter treatment. We also compare and contrast the results of the relativistic and the non-relativistic treatment.

We then proceed to analyze the case of compressed nuclear matter cores of

stellar dimensions.

In Sec. A.2.5, using the same scaling laws adopted in Ruffini et al. (2007b); Popov et al. (2010) we turn to the case of nuclear matter cores of stellar dimensions with mass numbers $A \approx (m_{\text{Planck}}/m_n)^3 \sim 10^{57}$ or $M_{\text{core}} \sim M_{\odot}$ where m_n is the neutron mass and $m_{\text{Planck}} = (\hbar c/G)^{1/2}$ is the Planck mass. Such a configuration present global but not local charge neutrality. Analytic solutions for the ultra-relativistic limit are obtained. In particular we find:

- 1) explicit analytic expressions for the electrostatic field and the Coulomb potential energy,
- 2) an entire range of possible Fermi energy for the electrons between zero and a maximum value $(E_e^F)_{\text{max}}$, reached when $R_{\text{WS}} = R_c$, which can be expressed analytically,
- 3) the explicit analytic expression of the ratio between the proton number N_p and the mass number A when $R_{\text{WS}} = R_c$.

We turn then in Sec. A.2.6 to the study of the compressional energy of the nuclear matter cores of stellar dimensions for selected values of the electron Fermi energy. We show that the solution with $E_e^F = 0$ presents the largest value of the electro-dynamical structure.

We finally summarize the conclusions in Sec. A.2.7.

A.2.2. The Thomas-Fermi model for compressed atoms: the Feynman-Metropolis-Teller treatment

The classical Thomas-Fermi model

The Thomas-Fermi model assumes that the electrons of an atom constitute a fully degenerate gas of fermions confined in a spherical region by the Coulomb potential of a point-like nucleus of charge $+eN_p$ Thomas (1927); Fermi (1927). Feynman, Metropolis and Teller have shown that this model can be used to derive the equation of state of matter at high pressures by considering a Thomas-Fermi model confined in a Wigner-Seitz cell of radius R_{WS} Feynman et al. (1949).

We recall that the condition of equilibrium of the electrons in an atom, in the non-relativistic limit, is expressed by

$$\frac{(p_e^F)^2}{2m_e} - eV = E_e^F, \quad (\text{A.2.1})$$

where m_e is the electron mass, V is the electrostatic potential and E_e^F is their Fermi energy.

The electrostatic potential fulfills, for $r > 0$, the Poisson equation

$$\nabla^2 V = 4\pi e n_e, \quad (\text{A.2.2})$$

where the electron number density n_e is related to the Fermi momentum P_e^F by

$$n_e = \frac{(P_e^F)^3}{3\pi^2\hbar^3}. \quad (\text{A.2.3})$$

For neutral atoms and ions n_e vanishes at the boundary so the electron Fermi energy is, respectively, zero or negative. In the case of compressed atoms n_e does not vanish at the boundary while the Coulomb potential energy eV is zero. Consequently E_e^F is positive.

Assuming

$$eV(r) + E_e^F = e^2 N_p \frac{\phi(r)}{r}, \quad (\text{A.2.4})$$

we obtain the following expression for the electron number density

$$n_e(\eta) = \frac{N_p}{4\pi b^3} \left(\frac{\phi(\eta)}{\eta} \right)^{3/2}, \quad (\text{A.2.5})$$

where the new dimensionless radial coordinate η is given by $r = b\eta$, where

$$b = (3\pi)^{2/3} \frac{\hbar^2}{m_e e^2} \frac{1}{2^{7/3}} \frac{1}{N_p^{1/3}}. \quad (\text{A.2.6})$$

Eq. (A.2.2) can be then written in the form

$$\frac{d^2\phi(\eta)}{d\eta^2} = \frac{\phi(\eta)^{3/2}}{\eta^{1/2}}, \quad (\text{A.2.7})$$

which is the classic Thomas-Fermi equation Fermi (1927). A first boundary condition for this equation follows from the point-like structure of the nucleus

$$\phi(0) = 1. \quad (\text{A.2.8})$$

A second boundary condition comes from the conservation of the number of electrons $N_e = \int_0^{R_{WS}} 4\pi n_e(r) r^2 dr$

$$1 - \frac{N_e}{N_p} = \phi(\eta_0) - \eta_0 \phi'(\eta_0), \quad (\text{A.2.9})$$

where $\eta_0 = R_{WS}/b$ defines the radius R_{WS} of the Wigner-Seitz cell. In the case of compressed atoms $N_e = N_p$ so the Coulomb potential energy eV vanishes at the boundary R_{WS} . As a result, using Eqs. (A.2.1) and (A.2.3), the Fermi

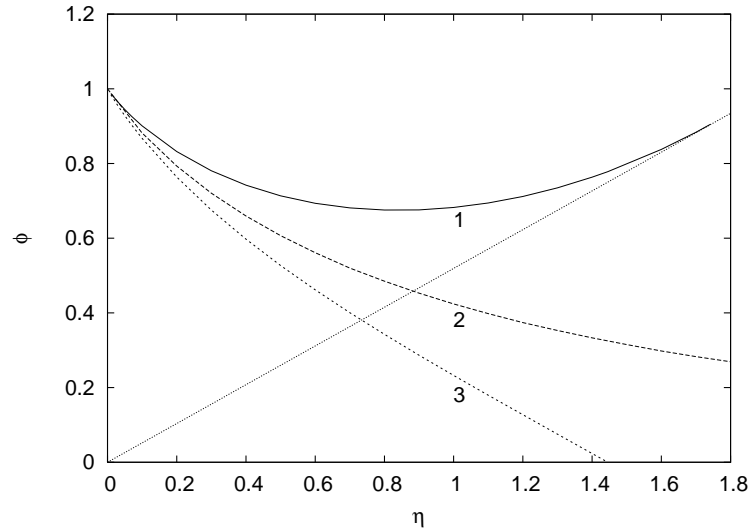


Figure A.4.: Physically relevant solutions of the Thomas-Fermi Equation (A.2.7) with the boundary conditions (A.2.8) and (A.2.9). The curve 1 refers to a neutral compressed atom. The curve 2 refers to a neutral free atom. The curve 3 refers to a positive ion. The dotted straight line is the tangent to the curve 1 at the point $(\eta_0, \phi(\eta_0))$ corresponding to overall charge neutrality (see Eq. (A.2.9)).

energy of electrons is given by

$$E_e^F = \frac{N_p e^2}{b} \frac{\phi(\eta_0)}{\eta_0}. \quad (\text{A.2.10})$$

Therefore in the classic treatment η_0 can approach zero and consequently the range of the possible values of the Fermi energy extends from zero to infinity.

The results are summarized in Figs. A.4 and A.5.

The Thomas-Fermi-Dirac model

Dirac has introduced modifications to the original Thomas-Fermi theory to include effects of exchange Dirac (1930). In this case the condition of equilibrium of the electrons in the atom is generalized as follows

$$\frac{(P_e^F)^2}{2m_e} - eV - \frac{\alpha}{\pi} c P_e^F = E_e^F, \quad (\text{A.2.11})$$

where as usual $\alpha = e^2/\hbar c$ denotes the fine structure constant.

The electron number density is now connected to the Coulomb potential energy by

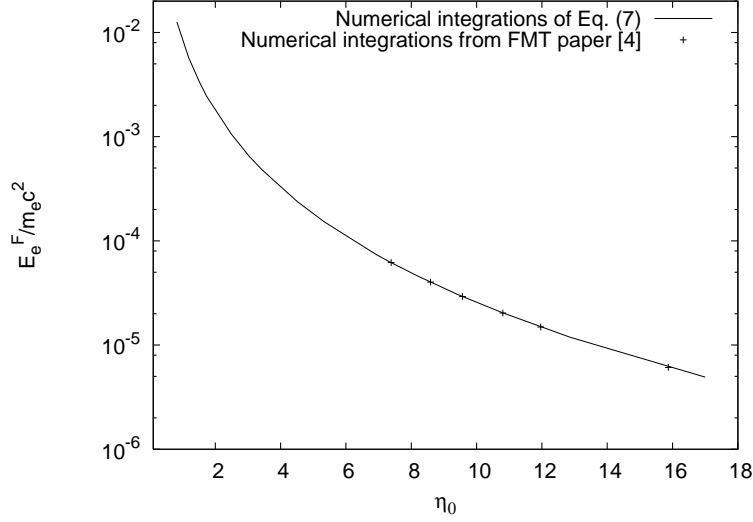


Figure A.5.: The electron Fermi energies for iron, in units of the electron mass, are plotted as a function of the dimensionless compression parameter η_0 . Points refer to the numerical integrations of the Thomas-Fermi equation (A.2.7) performed originally by Feynman, Metropolis and Teller in Feynman et al. (1949).

$$n_e = \frac{1}{3\pi^2 \hbar^3 c^3} \left[\frac{\alpha}{\pi} m_e c^2 + \sqrt{\left(\frac{\alpha}{\pi} m_e c^2 \right)^2 + 2m_e c^2 (eV + E_e^F)} \right]^3. \quad (\text{A.2.12})$$

Assuming

$$\frac{1}{2} \left(\frac{\alpha}{\pi} \right)^2 m_e c^2 + eV(r) + E_e^F = e^2 N_p \frac{\phi(r)}{r}, \quad (\text{A.2.13})$$

and $r = b\eta$, the Poisson equation can be written as

$$\frac{d^2 \phi(\eta)}{d\eta^2} = \eta \left[d + \left(\frac{\phi(\eta)}{\eta} \right)^{1/2} \right]^3, \quad (\text{A.2.14})$$

where b is given by Eq.(A.2.6) and $d = (3/(32\pi^2))^{1/3} (1/N_p)^{2/3}$. The boundary condition for Eq. (A.2.14) are $\phi(0) = 1$ and $\eta_0 \phi'(\eta_0) = \phi(\eta_0)$.

A.2.3. The relativistic generalization of the Feynman-Metropolis-Teller treatment

The relativistic Thomas-Fermi model for atoms

In the relativistic generalization of the Thomas-Fermi equation the point-like approximation of the nucleus must be abandoned Ferreira et al. (1980); Ruffini and Stella (1981) since the relativistic equilibrium condition

$$E_e^F = \sqrt{(P_e^F c)^2 + m_e^2 c^4} - m_e c^2 - eV(r), \quad (\text{A.2.15})$$

which generalizes the Eq. (A.2.1), would lead to a non-integrable expression for the electron density near the origin. Consequently we adopt a finite extended-nucleus. Traditionally the radius of an extended-nucleus is given by the phenomenological relation $R_c = r_0 A^{1/3}$ where A is the number of nucleons and $r_0 = 1.2 \times 10^{-13} \text{cm}$. Further it is possible to show from the extremization of the semi-empirical Weizsacker mass-formula that the relation between A and N_p is given by

$$N_p = \left[\frac{2}{A} + \frac{3}{200} \frac{1}{A^{1/3}} \right]^{-1}, \quad (\text{A.2.16})$$

which in the limit of small A gives

$$N_p \approx \frac{A}{2}, \quad (\text{A.2.17})$$

In Popov et al. (2010) we have relaxed, for $E_e^F = 0$, the condition $N_p \approx A/2$ (adopted, for example, in Migdal, Popov and Voskresenski Migdal et al. (1977)) as well as the condition $N_p = [2/A + 3/(200A^{1/3})]^{-1}$ (adopted for example in Ferreira, Ruffini and Stella Ferreira et al. (1980); Ruffini and Stella (1981)) imposing explicitly the beta decay equilibrium between neutron, protons and electrons.

In particular, following the previous treatments (see e.g. Popov et al. (2010)), we have assumed a constant distribution of protons confined in a radius R_c defined by

$$R_c = \Delta \frac{\hbar}{m_\pi c} N_p^{1/3}, \quad (\text{A.2.18})$$

where m_π is the pion mass and Δ is a parameter such that $\Delta \approx 1$ ($\Delta < 1$) corresponds to nuclear (supranuclear) densities when applied to ordinary nuclei.

Consequently, the proton density can be written as

$$n_p(r) = \frac{N_p}{\frac{4}{3}\pi R_c^3} \theta(R_c - r) = \frac{3}{4\pi} \frac{m_\pi^3 c^3}{\hbar^3} \frac{1}{\Delta^3} \theta(R_c - r), \quad (\text{A.2.19})$$

where $\theta(x)$ is the Heaviside function which by definition is given by

$$\theta(x) = \begin{cases} 0, & x < 0, \\ 1, & x > 0. \end{cases} \quad (\text{A.2.20})$$

The electron density is given by

$$n_e(r) = \frac{(P_e^F)^3}{3\pi^2 \hbar^3} = \frac{1}{3\pi^2 \hbar^3 c^3} \left[e^2 V^2(r) + 2m_e c^2 eV(r) \right]^{3/2}, \quad (\text{A.2.21})$$

where V is the Coulomb potential.

The overall Coulomb potential satisfies the Poisson equation

$$\nabla^2 V(r) = -4\pi e [n_p(r) - n_e(r)], \quad (\text{A.2.22})$$

with the boundary conditions $V'(\infty) = 0$ (due to global charge neutrality).

By introducing the dimensionless quantities $x = r/\lambda_\pi$, $x_c = R_c/\lambda_\pi$ and $\chi(r)/r = eV(r)/(c\hbar)$ with $\lambda_\pi = \hbar/(m_\pi c)$, and replacing the particle densities (A.2.19) and (A.2.26) into the Poisson equation (A.2.22) we obtain the relativistic Thomas-Fermi equation

$$\frac{1}{3x} \frac{d^2 \chi(x)}{dx^2} = -\frac{\alpha}{\Delta^3} \theta(x_c - x) + \frac{4\alpha}{9\pi} \left[\frac{\chi^2(x)}{x^2} + 2 \frac{m_e}{m_\pi} \frac{\chi(x)}{x} \right]^{3/2}, \quad (\text{A.2.23})$$

where $\chi(0) = 0$, $\chi(x_\infty) = 0$. The neutron density $n_n(r)$, related to the neutron Fermi momentum $P_n^F = (3\pi^2 \hbar^3 n_n)^{1/3}$, is determined, as in the previous case Popov et al. (2010), by imposing the condition of beta equilibrium

$$\begin{aligned} E_n^F &= \sqrt{(P_n^F c)^2 + m_n^2 c^4} - m_n c^2 \\ &= \sqrt{(P_p^F c)^2 + m_p^2 c^4} - m_p c^2 + eV(r), \end{aligned} \quad (\text{A.2.24})$$

which in turn is related to the proton density n_p and the electron density by Eqs. (A.2.21), (A.2.22). Integrating numerically these equations we have obtained a new generalized relation between A and N_p for any value of A . In the limit of small A this result agrees with the phenomenological relations given by Eqs. (A.2.16, A.2.17), as is clearly shown in Fig. (A.6)

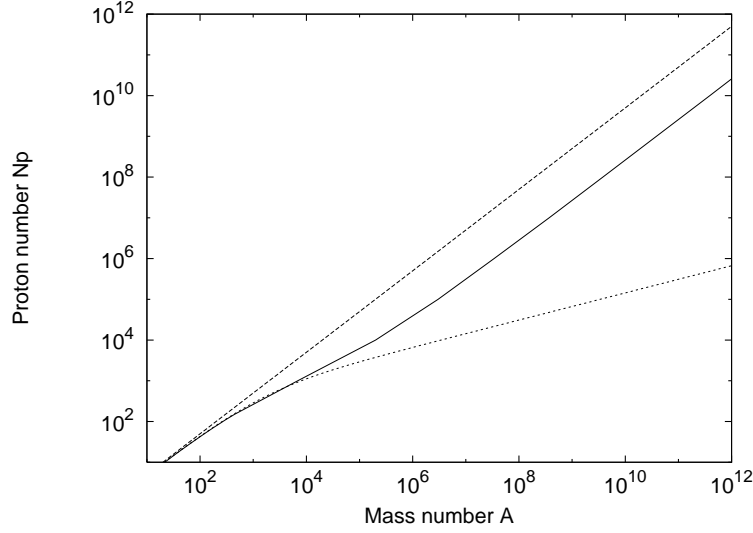


Figure A.6.: The A - N_p relation at nuclear density (solid line) obtained from first principles compared with the phenomenological expressions given by $N_p \simeq A/2$ (dashed line) and Eq. (A.2.16) (dotted line). The asymptotic value, for $A \rightarrow (m_{\text{Planck}}/m_n)^3$, is $N_p \approx 0.0046A$.

The relativistic Thomas-Fermi model for compressed atoms

We turn now to the case of compressed atoms in which the electron Fermi energy is positive. The relativistic generalization of the equilibrium condition (A.2.1) now reads

$$E_e^F = \sqrt{(P_e^F c)^2 + m_e^2 c^4} - m_e c^2 - eV(r) > 0, \quad (\text{A.2.25})$$

Adopting an extended-nucleus with a radius given by Eq. (A.2.18) and a proton density given by Eq. (A.2.19) the Poisson equation (A.2.22), with the following electron density

$$n_e(r) = \frac{(P_e^F)^3}{3\pi^2 \hbar^3} = \frac{1}{3\pi^2 \hbar^3 c^3} \left[e^2 \hat{V}^2(r) + 2m_e c^2 e \hat{V}(r) \right]^{3/2}, \quad (\text{A.2.26})$$

can be written as

$$\frac{1}{3x} \frac{d^2 \chi(x)}{dx^2} = -\frac{\alpha}{\Delta^3} \theta(x_c - x) + \frac{4\alpha}{9\pi} \left[\frac{\chi^2(x)}{x^2} + 2 \frac{m_e}{m_\pi} \frac{\chi(x)}{x} \right]^{3/2}, \quad (\text{A.2.27})$$

where $x = r/\lambda_\pi$, $x_c = R_c/\lambda_\pi$, $\chi(r)/r = e\hat{V}(r)/(c\hbar)$, $\lambda_\pi = \hbar/(m_\pi c)$ and $e\hat{V} = eV + E_e^F$. The equation (A.2.27) has to be integrated with the boundary

conditions $\chi(0) = 0, \chi(x_{WS}) = x_{WS}\chi'(x_{WS}), x_{WS} = R_{WS}/\lambda_\pi$.

The neutron density $n_n(r)$, related to the neutron Fermi momentum $P_n^F = (3\pi^2\hbar^3 n_n)^{1/3}$, is determined by imposing the condition of beta equilibrium

$$\begin{aligned} E_n^F &= \sqrt{(P_n^F c)^2 + m_n^2 c^4} - m_n c^2 \\ &= \sqrt{(P_p^F c)^2 + m_p^2 c^4} - m_p c^2 + eV(r) + E_e^F. \end{aligned} \quad (\text{A.2.28})$$

Using this approach, it is then possible to determine the beta equilibrium nuclide as a function of the density of the system. Infact, as suggested by Hund (1936) and Landau (1938), when the electron Fermi energy is sufficiently high, electrons can be absorbed by protons and converted to neutrons in inverse beta decay $p + e^- \rightarrow n + \nu_e$ because the condition $E_n^F < \sqrt{(P_p^F c)^2 + m_p^2 c^4} - m_p c^2 + eV(r) + E_e^F$ holds. The condition of equilibrium (A.2.28) is crucial, for example, in the construction of a self-consistent equation of state of high energy density matter present in white dwarfs and neutron star crusts Rueda et al. (2010d). In the case of zero electron Fermi energy the generalized $A - N_p$ relation of Fig. (A.6) is obtained.

The relativistic Thomas-Fermi-Dirac model for compressed atoms

We now take into account the exchange corrections to the relativistic Thomas-Fermi equation (A.2.27). In this case we have (see Migdal et al. (1977) for instance)

$$E_e^F = \sqrt{(cP_e^F)^2 + m_e^2 c^4} - m_e c^2 - eV - \frac{\alpha}{\pi} cP_e^F = \text{constant}. \quad (\text{A.2.29})$$

Introducing the function $\chi(r)$ as before

$$E_e^F + eV = e\hat{V} = \hbar c \frac{\chi}{r}, \quad (\text{A.2.30})$$

we obtain the electron number density

$$\begin{aligned} n_e &= \frac{1}{3\pi^2\hbar^3 c^3} \left\{ \gamma (m_e c^2 + e\hat{V}) + [(e\hat{V})^2 + 2m_e c^2 e\hat{V}]^{1/2} \times \right. \\ &\quad \left. \times \left[\frac{(1 + \gamma^2)(m_e c^2 + e\hat{V})^2 - m_e^2 c^4}{(m_e c^2 + e\hat{V})^2 - m_e^2 c^4} \right]^{1/2} \right\}^3, \end{aligned} \quad (\text{A.2.31})$$

where $\gamma = (\alpha/\pi)/(1 - \alpha^2/\pi^2)$.

If we take the approximation $1 + \gamma^2 \approx 1$ the above equation becomes

$$n_e = \frac{1}{3\pi^2\hbar^3c^3} \left\{ \gamma \left(m_e c^2 + e\hat{V} \right) + \left[(e\hat{V})^2 + 2m_e c^2 e\hat{V} \right]^{1/2} \right\}^3. \quad (\text{A.2.32})$$

The second term on the right-hand-side of Eq. (A.2.32) has the same form of the electron density given by the relativistic Thomas-Fermi approach without the exchange correction (A.2.26) and therefore the first term shows the explicit contribution of the exchange term to the electron density.

Using the full expression of the electron density given by Eq. (A.2.31) we obtain the relativistic Thomas-Fermi-Dirac equation

$$\begin{aligned} \frac{1}{3x} \frac{d^2\chi(x)}{dx^2} = & -\frac{\alpha}{\Delta^3} \theta(x_c - x) + \frac{4\alpha}{9\pi} \left\{ \gamma \left(\frac{m_e}{m_\pi} + \frac{\chi(x)}{x} \right) + \left[\left(\frac{\chi(x)}{x} \right)^2 \right. \right. \\ & \left. \left. + 2 \frac{m_e}{m_\pi} \frac{\chi(x)}{x} \right]^{1/2} \left[\frac{(1 + \gamma^2) \left(\frac{m_e}{m_\pi} + \frac{\chi(x)}{x} \right)^2 - \left(\frac{m_e}{m_\pi} \right)^2}{\left(\frac{m_e}{m_\pi} + \frac{\chi(x)}{x} \right)^2 - \left(\frac{m_e}{m_\pi} \right)^2} \right]^{1/2} \right\}^3, \end{aligned} \quad (\text{A.2.33})$$

which by applying the approximation $1 + \gamma^2 \approx 1$ becomes

$$\begin{aligned} \frac{1}{3x} \frac{d^2\chi(x)}{dx^2} = & -\frac{\alpha}{\Delta^3} \theta(x_c - x) + \frac{4\alpha}{9\pi} \left\{ \gamma \left(\frac{m_e}{m_\pi} + \frac{\chi(x)}{x} \right) \right. \\ & \left. + \left[\left(\frac{\chi(x)}{x} \right)^2 + 2 \frac{m_e}{m_\pi} \frac{\chi(x)}{x} \right]^{1/2} \right\}^3. \end{aligned} \quad (\text{A.2.34})$$

The boundary conditions for Eq. (A.2.33) are $\chi(0) = 0$ and $\chi(x_{WS}) = x_{WS}\chi'(x_{WS})$. The neutron density can be obtained as before by using the beta equilibrium condition (A.2.28) with the electron Fermi energy given by Eq. (A.2.29).

In Fig. A.7 we show the results of the numerical integration of the relativistic Thomas-Fermi equation (A.2.27) and of the relativistic Thomas-Fermi-Dirac equation (A.2.33) for helium, carbon and iron. In particular, we show the electron Fermi energy multiplied by $N_p^{-4/3}$ as a function of the ratio R_{WS}/R_c between the Wigner-Seitz cell radius R_{WS} and the nucleus radius R_c given by Eq. (A.2.18).

The effects of the exchange term are appreciable only in the low density (low compression) region, i.e. when $R_{WS} \gg R_c$ (see Fig. A.7). We can then conclude in total generality that the correction given by the Thomas-Fermi-Dirac exchange term is, small in the non-relativistic low compression (low density) regime, and negligible in the relativistic high compression (high density) regime.

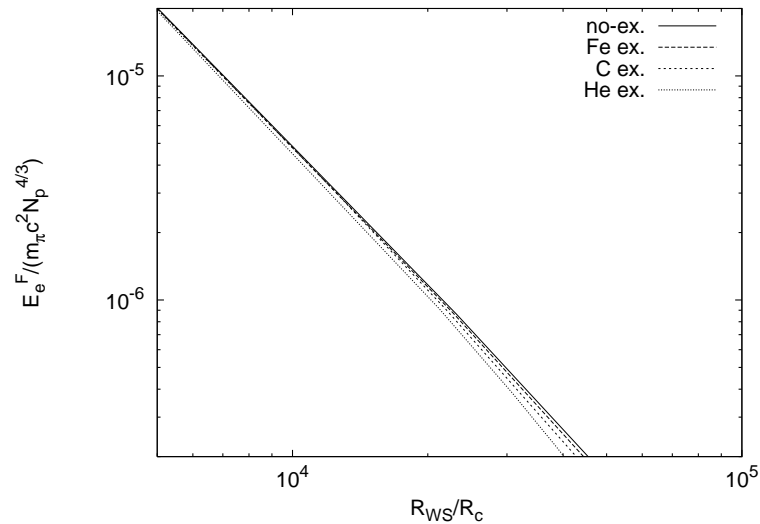


Figure A.7.: The electron Fermi energies in units of $m_\pi c^2 N_p^{4/3}$ is plotted for helium, for carbon and for iron, as a function of the ratio R_{WS}/R_c in the relativistic Feynman-Metropolis-Teller (FMT) treatment with and without the Thomas-Fermi-Dirac exchange effects. Here R_{WS} denotes the Wigner-Seitz cell radius and R_c is the nucleus radius as given by Eq. (A.2.18). It is clear that the exchange terms are appreciable only in the low density region and are negligible as $R_{WS} \rightarrow R_c$.

A.2.4. Comparison and contrast with approximate treatments

There exists in the literature a variety of semi-qualitative approximations adopted in order to describe the electron component of a compressed atom (see e.g. Bürvenich et al. (2007) for applications of the uniform approximation and e.g Chabrier and Potekhin (1998); Potekhin et al. (2009); Haensel and Zdunik (1990a,b, 2008); Douchin and Haensel (2001) for applications of the Salpeter approximate treatment).

We shall see how the relativistic treatment of the Thomas-Fermi equation affects the current analysis of compressed atoms in the literature by introducing qualitative and quantitative differences which deserve attention.

Relativistic FMT treatment vs. relativistic uniform approximation

One of the most used approximations in the treatment of the electron distribution in compressed atoms is the one in which, for a given nuclear charge $+eN_p$, the Wigner-Seitz cell radius R_{WS} is defined by

$$N_p = \frac{4\pi}{3} R_{WS}^3 n_e, \quad (\text{A.2.35})$$

where $n_e = (P_e^F)^3 / (3\pi^2 \hbar^3)$. The Eq. (A.2.35) ensures the global neutrality of the Wigner-Seitz cell of radius R_{WS} assuming a uniform distribution of electrons inside the cell.

We shall first compare the Feynman-Metropolis-Teller treatment, previously introduced, with the uniform approximation for the electron distribution. In view of the results of the preceding section, hereafter we shall consider the non-relativistic and the relativistic formulation of the Feynman-Metropolis-Teller treatment with no Thomas-Fermi-Dirac exchange correction.

In Fig. A.8 we have plotted the electron number density obtained from Eq. (A.2.26) where the Coulomb potential is related to the function χ , which is obtained from numerical integration of the relativistic Thomas-Fermi equation (A.2.27) for different compressions for helium and iron. We have normalized the electron density to the average electron number density $n_0 = 3N_e / (4\pi R_{WS}^3) = 3N_p / (4\pi R_{WS}^3)$ as given by Eq. (A.2.35).

We can see in Fig. A.8 how our treatment, based on the numerical integration of the relativistic Thomas-Fermi equation (A.2.27) and imposing the condition of beta equilibrium (A.2.28), leads to electron density distributions markedly different from the constant electron density approximation.

From Eqs. (A.2.15), (A.2.35) and taking into account the global neutrality condition of the Wigner-Seitz cell $eV(R_{WS}) = 0$, the electron Fermi energy in

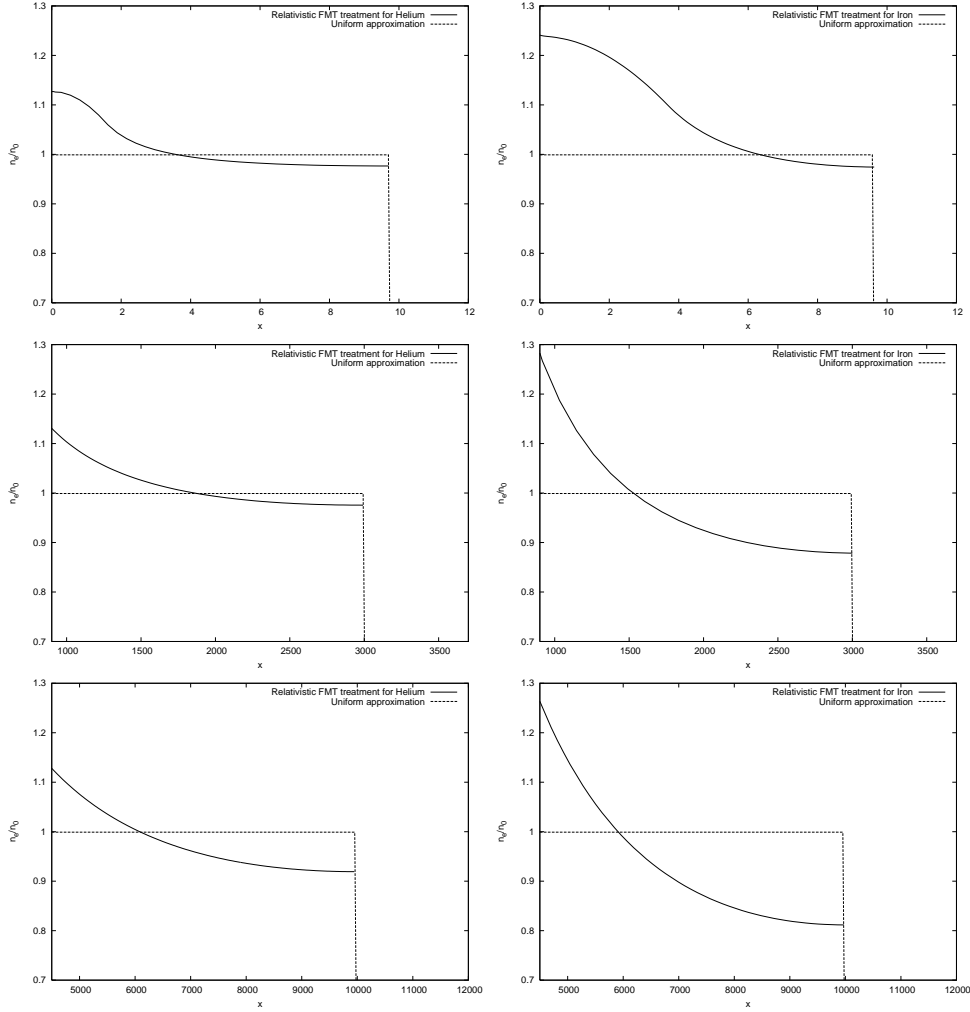


Figure A.8.: The electron number density n_e in units of the average electron number density $n_0 = 3N_e/(4\pi R_{WS}^3)$ is plotted as a function of the dimensionless radial coordinate $x = r/\lambda_\pi$ for the selected compressions $x_{WS} = 9.7$ (upper panels), $x_{WS} = 3 \times 10^3$ (middle panels) and $x_{WS} = 10^4$ (bottom panels), in both the relativistic Feynman, Metropolis, Teller approach and the uniform approximation respectively for Helium (panels on the left) and Iron (panels on the right).

the uniform approximation can be written as

$$E_e^F \simeq \left[-\frac{m_e}{m_\pi} + \sqrt{\left(\frac{m_e}{m_\pi}\right)^2 + \left(\frac{9\pi}{4}\right)^{2/3} \frac{N_p^{2/3}}{x_{WS}^2}} \right] m_\pi c^2. \quad (\text{A.2.36})$$

We show in Fig. A.9 the electron Fermi energy as a function of the average electron density $n_0 = 3N_e/(4\pi R_{WS}^3) = 3N_p/(4\pi R_{WS}^3)$ in units of the Bohr density $n_{\text{Bohr}} = 3/(4\pi R_{\text{Bohr}}^3)$ where $R_{\text{Bohr}} = \hbar^2/(e^2 m_e)$ is the Bohr radius. For selected compositions we show the results for the relativistic Feynman-Metropolis-Teller treatment, based on the numerical integration of the relativistic Thomas-Fermi equation (A.2.27), and for the relativistic uniform approximation.

As clearly shown in Fig. A.8 and summarized in Fig. A.9 the relativistic treatment leads to results strongly dependent at low compression from the nuclear composition. The corresponding value of the electron Fermi energy derived from a uniform approximation overevaluates the true electron Fermi energy (see Fig. A.9). In the limit of high compression the relativistic curves asymptotically approach the uniform one (see also Fig. A.8).

The uniform approximation becomes exact in the limit when the electron Fermi energy acquires its maximum value as given by

$$(E_e^F)_{\text{max}} \simeq \left[-\frac{m_e}{m_\pi} + \sqrt{\left(\frac{m_e}{m_\pi}\right)^2 + \left(\frac{3\pi^2}{2}\right)^{2/3} \left(\frac{N_p}{A}\right)^{2/3}} \right] m_\pi c^2, \quad (\text{A.2.37})$$

which is attained when R_{WS} coincides with the nuclear radius R_c . Here, the maximum electron Fermi energy (A.2.37) is obtained replacing in Eq. (A.2.36) the value of the normalized Wigner-Seitz cell radius $x_{WS} = x_c = R_c/\lambda_\pi \approx [(3/2)\pi]^{1/3} A^{1/3}$, where we have approximated the nuclear density as $n_{\text{nuc}} \approx (1/2)\lambda_\pi^{-3}$.

Relativistic FMT treatment vs. Salpeter approximate treatment

Corrections to the uniform distribution were also studied by Salpeter Salpeter (1961) and his approximations are largely applied in physics Chabrier and Potekhin (1998); Potekhin et al. (2009) and astrophysics Haensel and Zdunik (1990a,b); Douchin and Haensel (2001); Haensel and Zdunik (2008).

Keeping the point-like nucleus assumption, Salpeter Salpeter (1961) studied the corrections to the above models due to the inhomogeneity of the electron distribution inside the Wigner-Seitz cell. He expressed an analytic formula for the total energy of a Wigner-Seitz cell based on Coulomb corrections to the uniform distribution of electrons. The first correction corresponds to the inclusion of the lattice energy $E_C = -(9N_p^2\alpha)/(10R_{WS})$, which re-

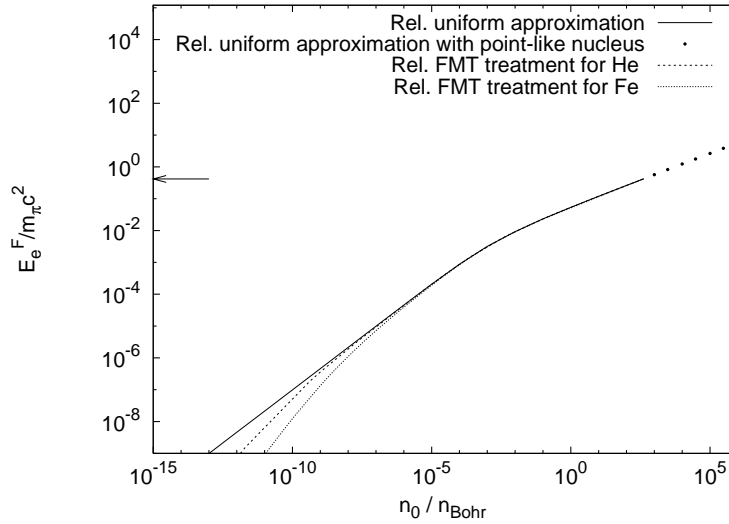


Figure A.9.: The electron Fermi energies E_e^F in the relativistic Feynman-Metropolis-Teller (FMT) treatment and in the uniform approximation in units of the pion rest mass, are plotted as a function of the average electron density $n_0 = 3N_e/(4\pi R_{WS}^3) = 3N_e/(4\pi R_{WS}^3)$ in units of the Bohr density $n_{\text{Bohr}} = 3/(4\pi R_{\text{Bohr}}^3)$ where $R_{\text{Bohr}} = \hbar^2/(e^2 m_e)$ is the Bohr radius. The filled circles correspond to the case of a relativistic uniform approximation with a point-like nucleus. In such a case the electron Fermi energy can reach arbitrary large values as $R_{WS} \rightarrow 0$. The arrow indicates the value of the maximum electron Fermi energy as given by Eq. (A.2.37).

sults from the point-like nucleus-electron interaction and, from the electron-electron interaction inside the cell of radius R_{ws} . The second correction is given by a series-expansion of the Thomas-Fermi energy about the average electron density n_e given by the uniform approximation $n_e = 3Z/(4\pi R_{\text{ws}}^3)$. The electron density is then assumed equals to $n_e[1 + \epsilon(r)]$ with $\epsilon(r)$ considered as infinitesimal. The Coulomb potential energy is assumed to be the one of the point-like nucleus with the uniform distribution of electrons of density n_e given by, thus the correction given by $\epsilon(r)$ is neglected on the Coulomb potential. The electron distribution is then calculated at first-order by expanding the relativistic electron kinetic energy

$$\begin{aligned}\epsilon_k &= \sqrt{[cP_e^F(r)]^2 + m_e^2c^4} - m_e c^2 \\ &= \sqrt{(3\pi^2 n_e)^{2/3}[1 + \epsilon(r)]^{2/3} + m_e^2c^4} - m_e c^2,\end{aligned}\quad (\text{A.2.38})$$

about its value given by the uniform approximation

$$\epsilon_k^{\text{unif}} = \sqrt{(3\pi^2 n_e)^{2/3} + m_e^2c^4} - m_e c^2,\quad (\text{A.2.39})$$

considering as infinitesimal the ratio eV/E_e^F between the Coulomb potential energy eV and the electron Fermi energy $E_e^F = \sqrt{[cP_e^F(r)]^2 + m_e^2c^4} - m_e c^2 - eV$.

The effect of the Dirac electron-exchange correction Dirac (1930) on the equation of state was also considered by Salpeter Salpeter (1961). However, adopting the general approach of Migdal et al. Migdal et al. (1977), these effects are negligible in the relativistic regime (see Subsec. A.2.3).

The inclusion of each additional Coulomb correction results in a decreasing of the pressure of the cell P_S . However, despite to be very interesting in identifying piecewise contributions to the total pressure, the validity of the Salpeter approach needs a verification by a more general treatment. For instance, the failure of the Salpeter formulas can be seen at densities of the order of $\sim 10^2 - 10^3 \text{ g cm}^{-3}$ for nuclei with large N_p as in the case of iron where the pressure becomes negative (see Table A.1). Therefore, the problem of solving the relativistic Thomas-Fermi equation within the Feynman, Metropolis, Teller approach becomes a necessity since this approach gives all the possible Coulomb and relativistic contributions automatically and correctly.

Relativistic FMT treatment vs. non-relativistic FMT treatment

In order to compare and contrast the Fermi energy of a compressed atom in the non-relativistic and the relativistic limit we first express the non-relativistic equations in terms of the dimensionless variables used for the relativistic

ρ (g/cm ³)	x_S	x_{FMTrel}	P (bar)	P_S (bar)	P_{FMTrel} (bar)
2.63×10^2	0.05	0.0400	2.9907×10^{10}	-1.8800×10^8	9.9100×10^9
2.10×10^3	0.10	0.0857	9.5458×10^{11}	4.4590×10^{11}	5.4840×10^{11}
1.68×10^4	0.20	0.1893	3.0227×10^{13}	2.2090×10^{13}	2.2971×10^{13}
5.66×10^4	0.30	0.2888	2.2568×10^{14}	1.8456×10^{14}	1.8710×10^{14}
1.35×10^5	0.40	0.3887	9.2964×10^{14}	8.0010×10^{14}	8.0790×10^{14}
2.63×10^5	0.50	0.4876	2.7598×10^{15}	2.4400×10^{15}	2.4400×10^{15}
4.53×10^5	0.60	0.5921	6.6536×10^{15}	6.0040×10^{15}	6.0678×10^{15}
7.19×10^5	0.70	0.6820	1.3890×10^{16}	1.2693×10^{16}	1.2810×10^{16}
1.08×10^6	0.80	0.7888	2.6097×10^{16}	2.4060×10^{16}	2.4442×10^{16}
2.10×10^6	1.00	0.9853	7.3639×10^{16}	6.8647×10^{16}	6.8786×10^{16}
3.63×10^6	1.20	1.1833	1.6902×10^{17}	1.5900×10^{17}	1.5900×10^{17}
5.77×10^6	1.40	1.3827	3.3708×10^{17}	3.1844×10^{17}	3.1898×10^{17}
8.62×10^6	1.60	1.5810	6.0754×10^{17}	5.7588×10^{17}	5.7620×10^{17}
1.23×10^7	1.80	1.7790	1.0148×10^{18}	9.6522×10^{17}	9.6592×10^{17}
1.68×10^7	2.00	1.9770	1.5981×10^{18}	1.5213×10^{18}	1.5182×10^{18}
3.27×10^7	2.50	2.4670	4.1247×10^{18}	3.9375×10^{18}	3.9101×10^{18}
5.66×10^7	3.00	2.965	8.8468×10^{18}	8.4593×10^{18}	8.4262×10^{18}
1.35×10^8	4.00	3.956	2.9013×10^{19}	2.7829×10^{19}	2.7764×10^{19}
2.63×10^8	5.00	4.939	7.2160×10^{19}	6.9166×10^{19}	6.9062×10^{19}
8.85×10^8	7.50	7.423	3.7254×10^{20}	3.5700×10^{20}	3.5700×10^{20}

Table A.1.: Pressure for Iron as a function of the density ρ in the uniform approximation (P), in the Salpeter approximation (P_S) and in the relativistic Feynman-Metropolis-Teller approach (P_{FMTrel}). Here $x_S = P_{eS}^F/(m_e c)$, $x_{FMTrel} = P_e^F/(m_e c)$ are respectively the normalized Salpeter Fermi momentum and the relativistic Feynmann-Metropolis-Teller Fermi momentum.

treatment. We then have

$$x = \frac{r}{\lambda_\pi}, \quad \frac{\chi}{r} = \frac{e\hat{V}}{c\hbar}, \quad (\text{A.2.40})$$

and the non-relativistic limit of Eq. (A.2.27) becomes

$$\frac{d^2\chi(x)}{dx^2} = \frac{2^{7/2}}{3\pi} \alpha \left(\frac{m_e}{m_\pi} \right)^{3/2} \frac{\chi^{3/2}}{x^{1/2}}, \quad (\text{A.2.41})$$

with the boundary conditions

$$\chi(0) = \alpha N_p, \quad x_{WS}\chi(x_{WS})' = \chi(x_{WS}), \quad (\text{A.2.42})$$

and dimensionless variable $x_{WS} = R_{WS}/\lambda_\pi$.

In these new variables the electron Fermi energy is given by

$$E_e^F = \frac{\chi(x_{WS})}{x_{WS}} m_\pi c^2. \quad (\text{A.2.43})$$

The two treatment, the relativistic and the non-relativistic one, can be now directly compared and contrasted by using the same units (see Fig. A.10).

There are major differences:

- 1) The electron Fermi energy in the relativistic treatment is strongly dependent on the nuclear composition, while the non-relativistic treatment presents a universal behavior in the units of Figs. A.10. In the limit of low densities the relativistic curves approach the universal non-relativistic curve.
- 2) The relativistic treatment leads to values of the electron Fermi energy consistently smaller than the ones of the non-relativistic treatment.
- 3) While in the non-relativistic treatment the electron Fermi energy can reach, by compression, infinite values as $R_{WS} \rightarrow 0$, in the relativistic treatment it reaches a perfectly finite value given by Eq. (A.2.37) attained when R_{WS} coincides with the nuclear radius R_c .

The universality of the electron Fermi energy with respect to the number of protons N_p has been obtained by expressing the Coulomb potential energy eV in terms of the function ϕ given by Eq. (A.2.4), and by introducing the scale factor b given by (A.2.6). Accordingly, the radius of the Wigner-Seitz cell has been expressed in terms of the nucleus radius (A.2.18) which is proportional to $N_p^{1/3}$.

It is clear then, from above considerations, the relativistic treatment of the Thomas-Fermi equation introduces significant differences from the current approximations in the literature: a) the uniform electron distribution Bürvenich et al. (2007), b) the approximate perturbative solutions departing from the uniform distribution Salpeter (1961) and c) the non-relativistic treatment Feynman et al. (1949). We have recently applied these results of the

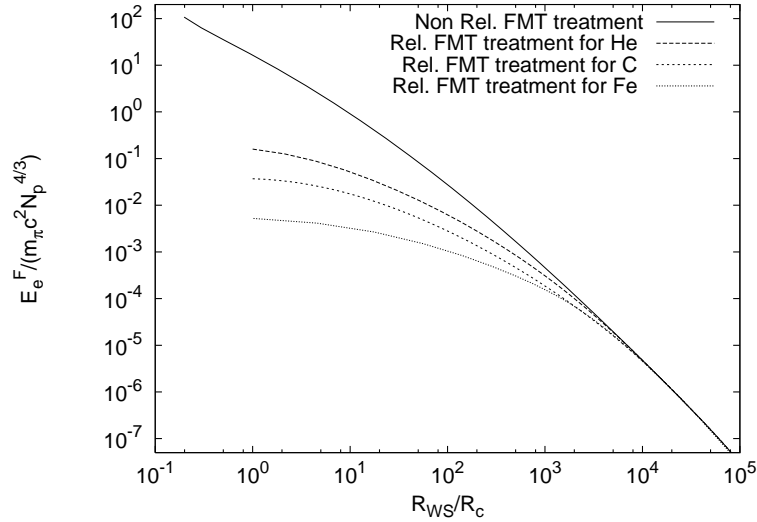


Figure A.10.: The electron Fermi energies in units of $m_{\pi}c^2N_p^{4/3}$ for helium, for carbon and for iron are plotted as a function of the ratio R_{WS}/R_c respectively in the non-relativistic and in the relativistic Feynman-Metropolis-Teller (FMT) treatment without the Thomas-Fermi-Dirac exchange effects. Here R_{WS} is the radius of the Wigner-Seitz cell and R_c is the radius of the nucleus given by Eq. (A.2.18). The relativistic treatment leads to results of the electron Fermi energy strongly dependent on the nuclear composition and systematically smaller than the non-relativistic ones, which can attain arbitrary large values as the point-like nucleus is approached.

relativistic Feynman, Metropolis, Teller treatment of a compressed atom to the study of white dwarfs and their consequences on the determination of their masses, radii and critical mass Rueda et al. (2010d).

A.2.5. Application to nuclear matter cores of stellar dimensions

We turn to nuclear matter cores of stellar dimensions of $A \simeq (m_{\text{Planck}}/m_n)^3 \sim 10^{57}$ or $M_{\text{core}} \sim M_{\odot}$. Following the treatment presented in Popov et al. (2010), we use the existence of scaling laws and proceed to the ultra-relativistic limit of Eqs. (A.2.19), (A.2.26), (A.2.27), (A.2.28). For positive values of the electron Fermi energy E_e^F , we introduce the new function $\phi = 4^{1/3}(9\pi)^{-1/3}\chi\Delta/x$ and the new variable $\hat{x} = kx$ where $k = (12/\pi)^{1/6}\sqrt{\alpha}\Delta^{-1}$, as well as the variable $\xi = \hat{x} - \hat{x}_c$ in order to describe better the region around the core radius.

Eq. (A.2.27) becomes

$$\frac{d^2\hat{\phi}(\xi)}{d\xi^2} = -\theta(-\xi) + \hat{\phi}(\xi)^3, \quad (\text{A.2.44})$$

where $\hat{\phi}(\xi) = \phi(\xi + \hat{x}_c)$ and the curvature term $2\hat{\phi}'(\xi)/(\xi + \hat{x}_c)$ has been neglected.

The Coulomb potential energy is given by

$$eV(\xi) = \left(\frac{9\pi}{4}\right)^{1/3} \frac{1}{\Delta} m_{\pi} c^2 \hat{\phi}(\xi) - E_e^F, \quad (\text{A.2.45})$$

corresponding to the electric field

$$E(\xi) = - \left(\frac{3^5\pi}{4}\right)^{1/6} \frac{\sqrt{\alpha} m_{\pi}^2 c^3}{\Delta^2 e\hbar} \hat{\phi}'(\xi), \quad (\text{A.2.46})$$

and the electron number-density

$$n_e(r) = \frac{1}{3\pi^2\hbar^3 c^3} \left(\frac{9\pi}{4}\right) \frac{1}{\Delta^3} (m_{\pi} c^2)^3 \hat{\phi}^3(\xi). \quad (\text{A.2.47})$$

In the core center we must have $n_e = n_p$. From Eqs. (A.2.19) and (A.2.47) we then have that, for $\xi = -\hat{x}_c$, $\hat{\phi}(-\hat{x}_c) = 1$.

In order to consider a compressed nuclear density core of stellar dimensions, we then introduce a Wigner-Seitz cell determining the outer boundary of the electron distribution which, in the new radial coordinate ξ is characterized by ξ^{WS} . In view of the global charge neutrality of the system the electric field goes to zero at $\xi = \xi^{WS}$. This implies, from Eq. (A.2.46), $\hat{\phi}'(\xi^{WS}) = 0$.

We now turn to the determination of the Fermi energy of the electrons in this compressed core. The function $\hat{\phi}$ and its first derivative $\hat{\phi}'$ must be continuous at the surface $\xi = 0$ of the nuclear density core.

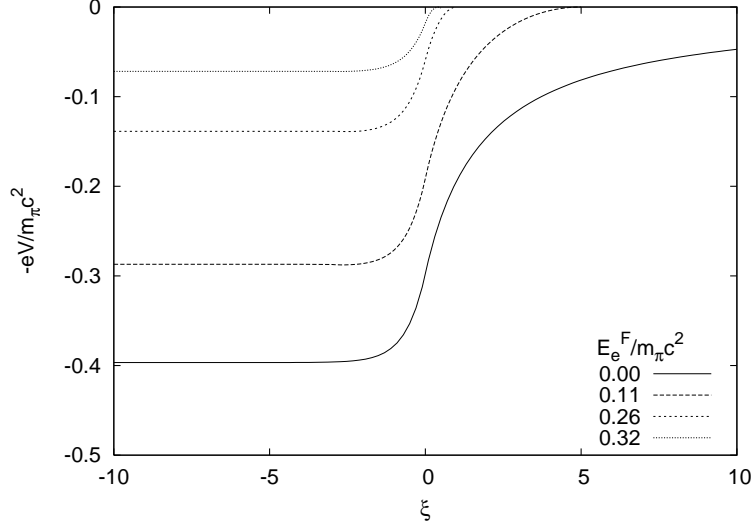


Figure A.11.: The electron Coulomb potential energies in units of the pion rest mass in a nuclear matter core of stellar dimensions with $A \simeq 10^{57}$ or $M_{core} \sim M_{\odot}$ and $R_c \approx 10^6$ cm, are plotted as a function of the dimensionless variable ξ , for different values of the electron Fermi energy also in units of the pion rest mass. The solid line corresponds to the case of null electron Fermi energy. By increasing the value of the electron Fermi energy the electron Coulomb potential energy depth is reduced.

This boundary-value problem can be solved analytically and Eq. (A.2.44) has the first integral,

$$2[\hat{\phi}'(\xi)]^2 = \begin{cases} \hat{\phi}^4(\xi) - 4\hat{\phi}(\xi) + 3, & \xi < 0, \\ \hat{\phi}^4(\xi) - \hat{\phi}^4(\xi^{WS}), & \xi > 0, \end{cases} \quad (\text{A.2.48})$$

with boundary conditions at $\xi = 0$:

$$\begin{aligned} \hat{\phi}(0) &= \frac{\hat{\phi}^4(\xi^{WS}) + 3}{4}, \\ \hat{\phi}'(0) &= -\sqrt{\frac{\hat{\phi}^4(0) - \hat{\phi}^4(\xi^{WS})}{2}}. \end{aligned} \quad (\text{A.2.49})$$

Having fulfilled the continuity condition we integrate Eq. (A.2.48) obtaining

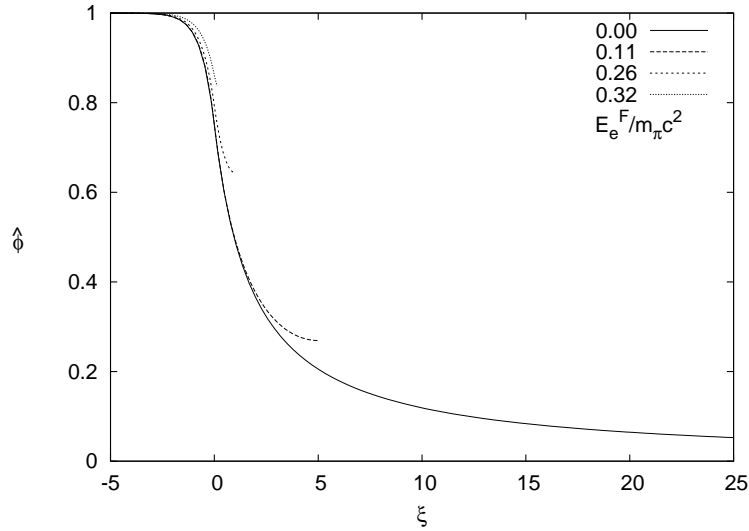


Figure A.12.: Solutions of the ultra-relativistic Thomas-Fermi equation (A.2.44) for different values of the Wigner-Seitz cell radius R_{WS} and correspondingly of the electron Fermi energy in units of the pion rest mass as in Fig. A.11, near the core surface. The solid line corresponds to the case of null electron Fermi energy.

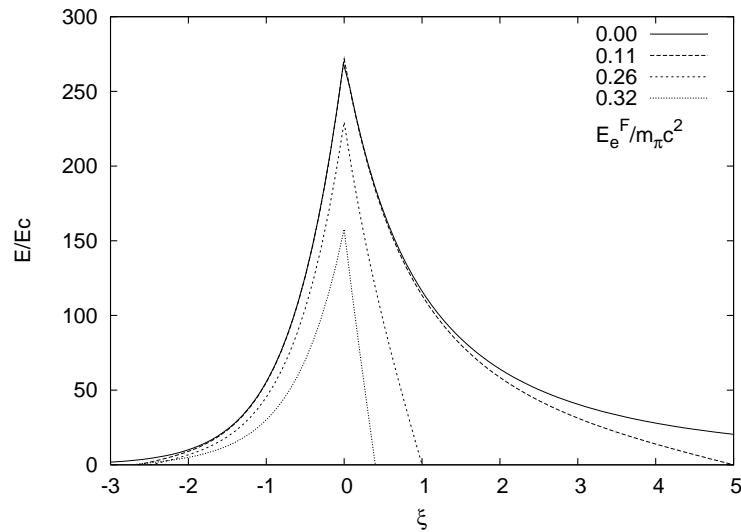


Figure A.13.: The electric field in units of the critical field for vacuum polarization $E_c = m_e^2 c^3 / (e\hbar)$ is plotted as a function of the coordinate ξ , for different values of the electron Fermi energy in units of the pion mass. The solid line corresponds to the case of null electron Fermi energy. To an increase of the value of the electron Fermi energy it is found a reduction of the peak of the electric field.

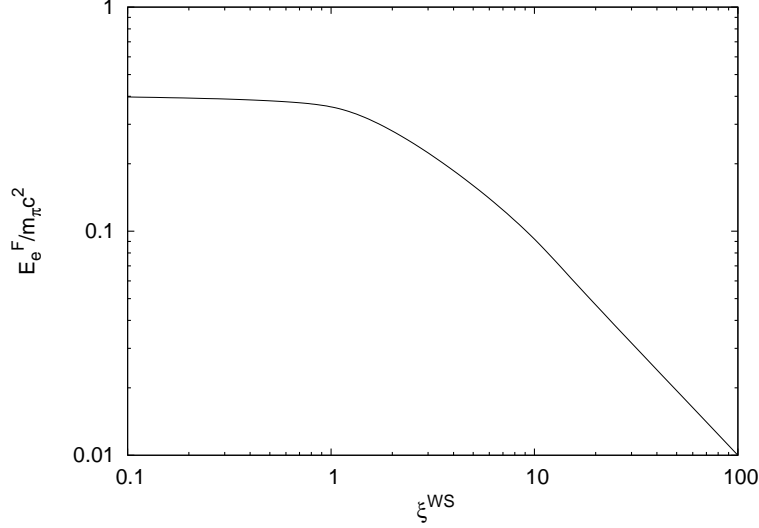


Figure A.14.: The Fermi energy of electrons in units of the pion rest mass is plotted for different Wigner-Seitz cell dimensions (i.e for different compressions) ξ^{WS} in the ultra-relativistic approximation . In the limit $\xi^{WS} \rightarrow 0$ the electron Fermi energy approaches asymptotically the value $(E_e^F)_{max}$ given by Eq. (A.2.63).

for $\xi \leq 0$

$$\hat{\phi}(\xi) = 1 - 3 \left[1 + 2^{-1/2} \sinh(a - \sqrt{3}\xi) \right]^{-1}, \quad (\text{A.2.50})$$

where the integration constant a has the value

$$\sinh(a) = \sqrt{2} \left(\frac{11 + \hat{\phi}^4(\xi^{WS})}{1 - \hat{\phi}^4(\xi^{WS})} \right). \quad (\text{A.2.51})$$

In the interval $0 \leq \xi \leq \xi^{WS}$, the field $\hat{\phi}(\xi)$ is implicitly given by

$$F \left(\arccos \frac{\hat{\phi}(\xi^{WS})}{\hat{\phi}(\xi)}, \frac{1}{\sqrt{2}} \right) = \hat{\phi}(\xi^{WS})(\xi - \xi^{WS}), \quad (\text{A.2.52})$$

where $F(\varphi, k)$ is the elliptic function of the first kind, and $F(0, k) \equiv 0$. For $F(\varphi, k) = u$, the inverse function $\varphi = F^{-1}(u, k) = \text{am}(u, k)$ is the well known Jacobi amplitude. In terms of it, we can express the solution (A.2.52) for $\xi > 0$ as,

$$\hat{\phi}(\xi) = \hat{\phi}(\xi^{WS}) \left\{ \cos \left[\text{am} \left(\hat{\phi}(\xi^{WS})(\xi - \xi^{WS}), \frac{1}{\sqrt{2}} \right) \right] \right\}^{-1}. \quad (\text{A.2.53})$$

In the present case of $E_e^F > 0$ the ultra-relativistic approximation is indeed always valid up to $\xi = \xi^{WS}$ for high compression factors, i.e. for $R_{WS} \simeq R_c$. In the case $E_e^F = 0$, $\xi^{WS} \rightarrow \infty$, there is a breakdown of the ultra-relativistic approximation when $\xi \rightarrow \xi^{WS}$.

Details are given in Figs. A.11, A.12, A.13.

We can now estimate two crucial quantities of the solutions: the Coulomb potential at the center of the configuration and the electric field at the surface of the core

$$eV(0) \simeq \left(\frac{9\pi}{4}\right)^{1/3} \frac{1}{\Delta} m_\pi c^2 - E_e^F, \quad (\text{A.2.54})$$

$$E_{\max} \simeq 2.4 \frac{\sqrt{\alpha}}{\Delta^2} \left(\frac{m_\pi}{m_e}\right)^2 E_c |\hat{\phi}'(0)|, \quad (\text{A.2.55})$$

where $E_c = m_e^2 c^3 / (e\hbar)$ is the critical electric field for vacuum polarization. These functions depend on the value $\hat{\phi}(\xi^{WS})$ via Eqs. (A.2.48)–(A.2.52). At the boundary $\xi = \xi^{WS}$, due to the global charge neutrality, both the electric field $E(\xi^{WS})$ and the Coulomb potential $eV(\xi^{WS})$ vanish. From Eq. (A.2.45), we determine the value of $\hat{\phi}(\xi)$ at $\xi = \xi^{WS}$

$$\hat{\phi}(\xi^{WS}) = \Delta \left(\frac{4}{9\pi}\right)^{1/3} \frac{E_e^F}{m_\pi c^2}, \quad (\text{A.2.56})$$

as a function of the electron Fermi energies E_e^F . From the above Eq. (A.2.56), one can see that there exists a solution, characterized by the value of electron Fermi energy

$$\frac{(E_e^F)_{\max}}{m_\pi c^2} = \frac{1}{\Delta} \left(\frac{9\pi}{4}\right)^{1/3}, \quad (\text{A.2.57})$$

such that $\hat{\phi}(\xi^{WS}) = 1$. From Eq. (A.2.52) and $\xi = 0$, we also have

$$\xi^{WS}(\hat{\phi}(\xi^{WS})) = \left\{ \frac{1}{\hat{\phi}(0)} F \left[\arccos \left(4 - \frac{3}{\hat{\phi}(0)} \right), \frac{1}{\sqrt{2}} \right] \right\}. \quad (\text{A.2.58})$$

For $\hat{\phi}(\xi^{WS}) = 1$, from Eq. (A.2.49) follows $\hat{\phi}(0) = 1$ hence Eq. (A.2.58) becomes

$$\xi^{WS}(\hat{\phi}(0)) = F \left[0, \frac{1}{\sqrt{2}} \right]. \quad (\text{A.2.59})$$

It is well known that if the inverse Jacobi amplitude $F[0, 1/\sqrt{2}]$ is zero, then

$$\xi^{WS}(\hat{\phi}(\xi^{WS}) = \hat{\phi}(0) = 1) = 0. \quad (\text{A.2.60})$$

Indeed from $\hat{\phi}(\xi^{WS}) = 1$ follows $\hat{\phi}(0) = 1$ and $\xi^{WS} = 0$. When $\xi^{WS} = 0$ from Eq. (A.2.49) follows $\hat{\phi}'(0) = 0$ and, using Eq. (A.2.55), $E_{\max} = 0$. In other words for the value of E_e^F fulfilling Eq. (A.2.56) no electric field exists on the boundary of the core and from Eq. (A.2.47) and Eqs. (A.2.18, A.2.19) it follows that indeed this is the solution fulfilling both global $N_e = N_p$ and local $n_e = n_p$ charge neutrality. In this special case, starting from Eq. (A.2.28) and $A = N_p + N_n$, we obtain

$$(E_e^F)_{\max}^{3/2} = \frac{\frac{9\pi}{4}(\hbar c)^3 \frac{A}{R_c^3} - (E_e^F)_{\max}^3}{2^{3/2} \left[\left(\frac{9\pi}{4}(\hbar c)^3 \frac{A}{R_c^3} - (E_e^F)_{\max}^3 \right)^{2/3} + m_n^2 c^4 \right]^{3/4}}. \quad (\text{A.2.61})$$

In the ultra-relativistic approximation we have

$$(E_e^F)_{\max}^3 / \frac{9\pi}{4}(\hbar c)^3 \frac{A}{R_c^3} \ll 1, \quad (\text{A.2.62})$$

then Eq. (A.2.61) can be approximated to

$$(E_e^F)_{\max} = 2^{1/3} \frac{m_n}{m_\pi} \gamma \left[-1 + \sqrt{1 + \frac{\beta}{2\gamma^3}} \right]^{2/3} m_\pi c^2, \quad (\text{A.2.63})$$

where

$$\beta = \frac{9\pi}{4} \left(\frac{\hbar}{m_n c} \right)^3 \frac{A}{R_c^3}, \quad \gamma = \sqrt{1 + \beta^{2/3}}. \quad (\text{A.2.64})$$

The corresponding limiting value to the N_p/A ratio is obtained as follows

$$\frac{N_p}{A} = \frac{2\gamma^3}{\beta} \left[-1 + \sqrt{1 + \frac{\beta}{2\gamma^3}} \right]^2. \quad (\text{A.2.65})$$

Inserting Eqs. (A.2.63), (A.2.64) in Eq. (A.2.65) one obtains the ultra-relativistic limit of Eq. (A.2.37), since the electron Fermi energy, in view of the scaling laws introduced in Popov et al. (2010), is independent of the value of A and depends only on the density of the core.

The N_p -independence in the limiting case of maximum electron Fermi energy attained when $R_{WS} = R_c$, in which the ultra-relativistic treatment approaches the uniform one, and the N_p -dependence for smaller compressions

$R_{WS} > R_c$ can be understood as follows. Let see the solution to the ultra-relativistic equation (A.2.44) for small $\zeta > 0$. Analogously to the Feynman-Metropolis-Teller approach to the non-relativistic Thomas-Fermi equation, we solve the ultra-relativistic equation (A.2.44) for small ζ . Expanding $\hat{\phi}(\zeta)$ about $\zeta = 0$ in a semi convergent power series,

$$\frac{\hat{\phi}(\zeta)}{\hat{\phi}(0)} = 1 + \sum_{n=2}^{\infty} a_n \zeta^{n/2} \quad (\text{A.2.66})$$

and substituting it into the ultra-relativistic equation (A.2.44), we have

$$\sum_{k=3}^{\infty} a_k \frac{k(k-2)}{4} \zeta^{(k-4)/2} = \phi^2(0) \exp \left[3 \ln \left(1 + \sum_{n=2}^{\infty} a_n \zeta^{n/2} \right) \right]. \quad (\text{A.2.67})$$

This leads to a recursive determination of the coefficients:

$$\begin{aligned} a_3 = 0, a_4 = \frac{\phi^2(0)}{2}, a_5 = 0, a_6 = \frac{\phi^2(0)a_2}{2}, a_7 = 0, \\ a_8 = \frac{\phi^2(0)(1-a_2^2)}{8}, \dots, \end{aligned} \quad (\text{A.2.68})$$

with $a_2 = \hat{\phi}'(0)/\hat{\phi}(0)$ determined by the initial slop, namely, the boundary condition $\hat{\phi}'(0)$ and $\hat{\phi}(0)$ in Eq. (A.2.49):

$$\hat{\phi}(0) = \frac{\hat{\phi}^4(\zeta^{WS}) + 3}{4}, \quad \hat{\phi}'(0) = -\sqrt{\frac{\hat{\phi}^4(0) - \hat{\phi}^4(\zeta^{WS})}{2}} \quad (\text{A.2.69})$$

Thus the series solution (A.2.66) is uniquely determined by the boundary value $\hat{\phi}(\zeta^{WS})$ at the Wigner-Seitz cell radius.

Now we consider the solution up to the leading orders

$$\begin{aligned} \hat{\phi}(\zeta) &= \hat{\phi}(0) + \hat{\phi}'(0)\zeta + \frac{1}{2}\hat{\phi}^3(0)\zeta^2 + \frac{1}{2}\hat{\phi}^3(0)a_2\zeta^3 \\ &+ \frac{1}{8}\hat{\phi}^3(0)(1-a_2^2)\zeta^4 + \dots. \end{aligned} \quad (\text{A.2.70})$$

Using Eq. (A.2.70), the electron Fermi energy (A.2.56) becomes

$$\begin{aligned} E_e^F &= (E_e^F)_{max} \left[1 + a_2 \zeta^{WS} + \frac{1}{2} \hat{\phi}^2(0) (\zeta^{WS})^2 + \frac{1}{2} \hat{\phi}^2(0) a_2 (\zeta^{WS})^3 \right. \\ &\left. + \frac{1}{8} \hat{\phi}^2(0) (1 - a_2^2) (\zeta^{WS})^4 + \dots \right] \hat{\phi}(0), \end{aligned} \quad (\text{A.2.71})$$

where $(E_e^F)_{max} = (9\pi/4)^{1/3} \Delta^{-1}$ is the maximum Fermi energy which is at-

tained when the Wigner-Seitz cell radius equals the nucleus radius R_c (see Eq. A.2.57). For $\hat{\phi}(\xi^{WS}) < 1$, we approximately have $\hat{\phi}(0) = 3/4$, $\hat{\phi}'(0) = -(3/4)^2/\sqrt{2}$ and the initial slope $a_2 = \hat{\phi}'(0)/\hat{\phi}(0) = -(3/4)/\sqrt{2}$. Therefore Eq. (A.2.71) becomes

$$E_e^F \approx (E_e^F)_{max} \left[1 - \frac{3}{4\sqrt{2}} \xi^{WS} + \frac{1}{2} \left(\frac{3}{4}\right)^2 (\xi^{WS})^2 - \frac{1}{2^{3/2}} \left(\frac{3}{4}\right)^3 (\xi^{WS})^3 + \frac{1}{8} \left(\frac{3}{4}\right)^2 \left(\frac{41}{32}\right) (\xi^{WS})^4 + \dots \right]. \quad (\text{A.2.72})$$

By the definition of the coordinate ξ , we know all terms except the first term in the square bracket depend on the values of N_p . In the limit of maximum compression when the electron Fermi energy acquires its maximum value, namely when $\xi^{WS} = 0$, the electron Fermi energy (A.2.72) is the same as the one obtained from the uniform approximation which is independent of N_p . For smaller compressions, namely for $\xi^{WS} > 0$ the electron Fermi energy deviates from the one given by the uniform approximation becoming N_p -dependent.

In Fig. A.14 we plot the Fermi energy of electrons, in units of the pion rest mass, as a function of the dimensionless parameter ξ^{WS} and, as $\xi^{WS} \rightarrow 0$, the limiting value given by Eq. (A.2.63) is clearly displayed.

In ref. Alcock et al. (1986), in order to study the electro-dynamical properties of strange stars, the ultra-relativistic Thomas-Fermi equation was numerically solved in the case of bare strange stars as well as in the case of strange stars with a crust (see e.g. curves (a) and (b) in Fig. 6 of ref. Alcock et al. (1986)). In Fig. 6 of Alcock et al. (1986) was plotted what they called the Coulomb potential energy, which we will denote as V_{Alcock} . The potential V_{Alcock} was plotted for different values of the electron Fermi momentum at the edge of the crust. Actually, such potential V_{Alcock} is not the Coulomb potential eV but it coincides with our function $e\hat{V} = eV + E_e^F$. Namely, the potential V_{Alcock} corresponds to the Coulomb potential shifted by the Fermi energy of the electrons. We then have from Eq. (A.2.45)

$$e\hat{V}(\xi) = \left(\frac{9\pi}{4}\right)^{1/3} \frac{1}{\Delta} m_\pi c^2 \hat{\phi}(\xi) = V_{\text{Alcock}}. \quad (\text{A.2.73})$$

This explains why in Alcock et al. (1986), for different values of the Fermi momentum at the crust the depth of the potential V_{Alcock} remains unchanged. Instead, the correct behaviour of the Coulomb potential is quite different and, indeed, its depth decreases with increasing of compression as can be seen in Fig. A.11.

A.2.6. Compressional energy of nuclear matter cores of stellar dimensions

We turn now to the compressional energy of these family of compressed nuclear matter cores of stellar dimensions each characterized by a different Fermi energy of the electrons. The kinematic energy-spectra of complete degenerate electrons, protons and neutrons are

$$\epsilon^i(p) = \sqrt{(pc)^2 + m_i^2 c^4}, \quad p \leq P_i^F, \quad i = e, p, n. \quad (\text{A.2.74})$$

So the compressional energy of the system is given by

$$\mathcal{E} = \mathcal{E}_B + \mathcal{E}_e + \mathcal{E}_{\text{em}}, \quad \mathcal{E}_B = \mathcal{E}_p + \mathcal{E}_n, \quad (\text{A.2.75})$$

$$\mathcal{E}_i = 2 \int_i \frac{d^3 r d^3 p}{(2\pi\hbar)^3} \epsilon^i(p), \quad i = e, p, n, \quad \mathcal{E}_{\text{em}} = \int \frac{E^2}{8\pi} d^3 r. \quad (\text{A.2.76})$$

Using the analytic solution (A.2.53) we calculate the energy difference between two systems, *I* and *II*,

$$\Delta\mathcal{E} = \mathcal{E}(E_e^F(\text{II})) - \mathcal{E}(E_e^F(\text{I})), \quad (\text{A.2.77})$$

with $E_e^F(\text{II}) > E_e^F(\text{I}) \geq 0$, at fixed A and R_c .

We first consider the infinitesimal variation of the total energy $\delta\mathcal{E}_{\text{tot}}$ with respect to the infinitesimal variation of the electron Fermi energy δE_e^F

$$\delta\mathcal{E} = \left[\frac{\partial\mathcal{E}}{\partial N_p} \right]_{VWS} \left[\frac{\partial N_p}{\partial E_e^F} \right] \delta E_e^F + \left[\frac{\partial\mathcal{E}}{\partial VWS} \right]_{N_p} \left[\frac{\partial VWS}{\partial E_e^F} \right] \delta E_e^F. \quad (\text{A.2.78})$$

For the first term of this relation we have

$$\begin{aligned} \left[\frac{\partial\mathcal{E}}{\partial N_p} \right]_{VWS} &= \left[\frac{\partial\mathcal{E}_p}{\partial N_p} + \frac{\partial\mathcal{E}_n}{\partial N_p} + \frac{\partial\mathcal{E}_e}{\partial N_p} + \frac{\partial\mathcal{E}_{\text{em}}}{\partial N_p} \right]_{VWS} \\ &\simeq \left[E_p^F - E_n^F + E_e^F + \frac{\partial\mathcal{E}_{\text{em}}}{\partial N_p} \right]_{VWS}, \end{aligned} \quad (\text{A.2.79})$$

where the general definition of chemical potential $\partial\epsilon_i/\partial n_i = \partial\mathcal{E}_i/\partial N_i$ is used ($i = e, p, n$) neglecting the mass defect $m_n - m_p - m_e$. Further using the condition of the beta-equilibrium (A.2.28) we have

$$\left[\frac{\partial\mathcal{E}}{\partial N_p} \right]_{VWS} = \left[\frac{\partial\mathcal{E}_{\text{em}}}{\partial N_p} \right]_{VWS}. \quad (\text{A.2.80})$$

For the second term of the Eq. (A.2.78) we have

$$\begin{aligned} \left[\frac{\partial \mathcal{E}}{\partial V^{WS}} \right]_{N_p} &= \left[\frac{\partial \mathcal{E}_p}{\partial V^{WS}} + \frac{\partial \mathcal{E}_n}{\partial V^{WS}} + \frac{\partial \mathcal{E}_e}{\partial V^{WS}} + \frac{\partial \mathcal{E}_{em}}{\partial V^{WS}} \right]_{N_p} \\ &= \left[\frac{\partial \mathcal{E}_e}{\partial V^{WS}} \right]_{N_p} + \left[\frac{\partial \mathcal{E}_{em}}{\partial V^{WS}} \right]_{N_p}, \end{aligned} \quad (\text{A.2.81})$$

since in the process of increasing the electron Fermi energy namely, by decreasing the radius of the Wigner-Seitz cell, the system by definition maintains the same number of baryons A and the same core radius R_c .

Now $\delta \mathcal{E}$ reads

$$\delta \mathcal{E} = \left\{ \left[\frac{\partial \mathcal{E}_e}{\partial V^{WS}} \right]_{N_p} \frac{\partial V^{WS}}{\partial E_e^F} + \left[\frac{\partial \mathcal{E}_{em}}{\partial V^{WS}} \right]_{N_p} \frac{\partial V^{WS}}{\partial E_e^F} + \left[\frac{\partial \mathcal{E}_{em}}{\partial N_p} \right]_{V^{WS}} \frac{\partial N_p}{\partial E_e^F} \right\} \delta E_e^F, \quad (\text{A.2.82})$$

so only the electromagnetic energy and the electron energy give non-null contributions.

From this equation it follows that

$$\Delta \mathcal{E} = \Delta \mathcal{E}_{em} + \Delta \mathcal{E}_e, \quad (\text{A.2.83})$$

where $\Delta \mathcal{E}_{em} = \mathcal{E}_{em}(E_e^F(II)) - \mathcal{E}_{em}(E_e^F(I))$ and $\Delta \mathcal{E}_e = \mathcal{E}_e(E_e^F(II)) - \mathcal{E}_e(E_e^F(I))$.

In the particular case in which $E_e^F(II) = (E_e^F)_{max}$ and $E_e^F(I) = 0$ we obtain

$$\Delta \mathcal{E} \simeq 0.75 \frac{3^{5/3}}{2} \left(\frac{\pi}{4} \right)^{1/3} \frac{1}{\Delta \sqrt{\alpha}} \left(\frac{\pi}{12} \right)^{1/6} N_p^{2/3} m_\pi c^2, \quad (\text{A.2.84})$$

which is positive.

The compressional energy of a nuclear matter core of stellar dimensions increases with its electron Fermi energy as expected.

A.2.7. Conclusions

We have generalized to the relativistic regime the classic work of Feynman, Metropolis and Teller, solving a compressed atom by the Thomas-Fermi equation in a Wigner-Seitz cell.

In the relativistic generalization the equation to be integrated is the relativistic Thomas-Fermi equation, also called the Vallarta-Rosen equation Vallarta and Rosen (1932). The integration of this equation does not admit any regular solution for a point-like nucleus and both the nuclear radius and the nuclear composition have necessarily to be taken into account Ferreira et al. (1980); Ruffini and Stella (1981). This introduces a fundamental difference from the non-relativistic Thomas-Fermi model where a point-like nucleus was adopted.

As in previous works Ferreira et al. (1980); Ruffini and Stella (1981); Ruffini et al. (2007b) the protons in the nuclei have been assumed to be at constant density, the electron distribution has been derived by the Thomas-Fermi relativistic equation and the neutron component has been derived by the beta equilibrium between neutrons, protons and electrons.

We have also examined for completeness the relativistic generalization of the Thomas-Fermi-Dirac equation by taking into due account the exchange terms Dirac (1930), adopting the general approach of Migdal, Popov and Voskresenskii Migdal et al. (1977), and shown that these effects, generally small, can be neglected in the relativistic treatment.

There are marked differences between the relativistic and the non-relativistic treatments.

The first and the most general one is that the existence of a finite size nucleus introduces necessarily a limit to the compressibility: the dimension of the Wigner-Seitz cell can never be smaller than the nuclear size. Consequently the electron Fermi energy which in the non-relativistic approach can reach arbitrarily large values, reaches in the present case a perfectly finite value whose expression has been given in analytic form. There are in the literature many papers adopting a relativistic treatment for the electrons together with a point-like approximation for the nucleus, which is clearly inconsistent (see e.g. Chabrier and Potekhin (1998); Potekhin et al. (2009)).

The second is the clear difference of the electron distribution as a function of the radius and of the nuclear composition as contrasted to the uniform approximation often adopted in the literature (see e.g. Bürvenich et al. (2007)) which we have explicitly shown in the Fig. A.8 of Sec. A.2.4. Inferences based on the uniform approximation are not appropriate both in the relativistic and in the non-relativistic regime.

The third, one of the most relevant, is that the relativistic Feynman-Metropolis-Teller treatment allows to treat globally and in generality the electro-dynamical interaction within the atom and the relativistic corrections leading to a softening of the dependence of the electron Fermi energy on the compression factor, as well as a gradual decrease of the exchange terms in proceeding from the non-relativistic to the fully relativistic regimes. It is then possible to derive, as shown in Table A.1 of Sec. A.2.4 a consistent equation of state for compressed matter which overcomes some of the difficulties of existing treatments describing the electro-dynamical effect by a sequence of approximations which have led to the occurrence of unphysical regimes e.g. the existence of negative pressure as in the Salpeter approach. As a direct application of this treatment we have reconsidered the study of white dwarfs within the relativistic Feynman, Metropolis, Teller approach and evaluate their effects on the value of the radii, of the masses of the equilibrium configurations as well as on the numerical value of the critical mass Rueda et al. (2010d). We have there compared and contrasted the results obtained by Chandrasekhar with a uniform approximation with the ones obtained by the equation of state

of Salpeter and the ones following from the treatment presented in this article.

We have then extrapolated these results to the case of nuclear matter cores of stellar dimensions for $A \approx (m_{\text{Planck}}/m_n)^3 \sim 10^{57}$ or $M_{\text{core}} \sim M_{\odot}$. The aim here is to explore the possibility of obtaining for these systems a self-consistent solution presenting global and not local charge neutrality. The results generalize the considerations presented in the previous article corresponding to a nuclear matter core of stellar dimensions with null Fermi energy of the electrons Popov et al. (2010). The ultra-relativistic approximation allows to obtain analytic expressions for the fields. The exchange terms can in this approximation be safely neglected. An entire family of configurations exist with values of the Fermi energy of the electrons ranging from zero to a maximum value $(E_e^F)_{\text{max}}$ which is reached when the Wigner-Seitz cell coincides with the core radius. The configuration with $E_e^F = (E_e^F)_{\text{max}}$ corresponds to the configuration with $N_p = N_e$ and $n_p = n_e$. For this limiting value of the Fermi energy the system fulfills both the global and the local charge neutrality and correspondingly no electrodynamical structure is present in the core. All the other configurations presents overcritical electric fields close to their surface. The configuration with $E_e^F = 0$ has the maximum value of the electric field at the core surface, well above the critical value E_c (see Fig. A.11, Fig. A.12 and Fig. A.13 of Section A.2.5). All these cores with overcritical electric fields are stable against the vacuum polarization process due to the Pauli blocking by the degenerate electrons Ruffini et al. (2010). We have also compared and contrasted our treatment of the relativistic Thomas-Fermi solutions to the corresponding one addressed in the framework of strange stars Alcock et al. (1986) pointing out in these treatments some inconsistency in the definition of the Coulomb potential.

We have finally compared the compressional energy of configurations with selected values of the electron Fermi energy. In both systems of the compressed atoms and of the nuclear matter cores of stellar dimensions a maximum value of the Fermi energy has been reached corresponding to the case of Wigner-Seitz cell radius R_{WS} coincident with the core radius R_c .

In conclusion the analysis of compressed atoms following the relativistic Feynman, Metropolis, Teller treatment presented in the first part of this article has important consequences in the determination of the mass-radius relation of white dwarfs leading to the possibility of a direct confrontation of these results with observations, in view of the current great interest for the cosmological implications of the type Ia supernovae Phillips (1993); Riess et al. (1998); Perlmutter et al. (1999); Riess et al. (2004). The results presented in the second part of this article on nuclear matter cores of stellar dimensions evidence the possibility of having the existence of critical electromagnetic fields in the interface of the core and the neutron star crust. The results here obtained in a simplified but rigorous approach of the application of the relativistic Feynman, Metropolis, Teller treatment to the constant density cores in

beta equilibrium conform to the prediction of Baym, Bethe and Pethick Baym et al. (1971a). This treatment has been further extended to the case in which a self-gravitating system of degenerate neutrons, protons and electrons is considered within the framework of relativistic quantum statistics and Einstein-Maxwell equations Rueda et al. (2010c) and to the case in which also strong interactions are present Pugliese et al. (2010).

A.3. Electrodynamics for Nuclear Matter in Bulk

It is well known that the Thomas-Fermi equation is the exact theory for atoms, molecules and solids as $Z \rightarrow \infty$ Lieb and Simon (1973). We show in this letter that the relativistic Thomas-Fermi theory developed for the study of atoms for heavy nuclei with $Z \simeq 10^6$ Pieper and Greiner (1969), Greenberg and Greiner (1982), Müller et al. (1972), Popov (1971b), Zeldovich and Popov (1972), Ferreira et al. (1980), Ruffini and Stella (1981), Müller and Rafelski (1975), Migdal et al. (1976) gives important basic new information on the study of nuclear matter in bulk in the limit of $N \simeq (m_{\text{Planck}}/m_n)^3$ nucleons of mass m_n and on its electrodynamic properties. The analysis of nuclear matter bulk in neutron stars composed of degenerate gas of neutrons, protons and electrons, has traditionally been approached by implementing microscopically the charge neutrality condition by requiring the electron density $n_e(x)$ to coincide with the proton density $n_p(x)$,

$$n_e(x) = n_p(x). \quad (\text{A.3.1})$$

It is clear however that especially when conditions close to the gravitational collapse occur, there is an ultra-relativistic component of degenerate electrons whose confinement requires the existence of very strong electromagnetic fields, in order to guarantee the overall charge neutrality of the neutron star. Under these conditions equation (A.3.1) will be necessarily violated. We are going to show in this letter that they will develop electric fields close to the critical value E_c introduced by Sauter Sauter (1931), Heisenberg and Euler Heisenberg and Euler (1936), and by Schwinger Schwinger (1951, 1954a,b)

$$E_c = \frac{m^2 c^3}{e \hbar}. \quad (\text{A.3.2})$$

Special attention for the existence of critical electric fields and the possible condition for electron-positron (e^+e^-) pair creation out of the vacuum in the case of heavy bare nuclei, with the atomic number $Z \geq 173$, has been given by Popov Popov (1971b), Popov and Zel'dovich Zeldovich and Popov (1972), Greenberg and Greiner Greenberg and Greiner (1982), Müller, Peitz, Rafelski and Greiner Müller et al. (1972). They analyzed the specific pair creation process of an electron-positron pair around both a point-like and extended bare nucleus by direct integration of Dirac equation. These considerations have been extrapolated to much heavier nuclei $Z \gg 1600$, implying the creation of a large number of e^+e^- pairs, by using a statistical approach based on the relativistic Thomas-Fermi equation by Müller and Rafelski Müller and Rafelski (1975), Migdal, Voskresenskii and Popov Migdal et al. (1976). Using substantially the same statistical approach based on the relativistic Thomas-Fermi equation, Ferreira et al. Ferreira et al. (1980), Ruffini and Stella Ruffini

and Stella (1981) have analyzed the electron densities around an extended nucleus in a neutral atom all the way up to $Z \simeq 6000$. They have shown the effect of penetration of the electron orbitals well inside the nucleus, leading to a screening of the nuclei positive charge and to the concept of an “effective” nuclear charge distribution. All the above works assumed for the radius of the extended nucleus the semi-empirical formulae Segré (1977),

$$R_c \approx r_0 A^{1/3}, \quad r_0 = 1.2 \cdot 10^{-13} \text{cm}, \quad (\text{A.3.3})$$

where the mass number $A = N_n + N_p$, N_n and N_p are the neutron and proton numbers. The approximate relation between A and the atomic number $Z = N_p$,

$$Z \simeq \frac{A}{2}, \quad (\text{A.3.4})$$

was adopted in Refs. Müller and Rafelski (1975); Migdal et al. (1976), or the empirical formulae

$$Z \simeq \left[\frac{2}{A} + \frac{3}{200} \frac{1}{A^{1/3}} \right]^{-1}, \quad (\text{A.3.5})$$

was adopted in Refs. Ferreira et al. (1980); Ruffini and Stella (1981).

The aim of this letter is to outline an alternative approach of the description of nuclear matter in bulk: it generalizes, to the case of $N \simeq (m_{\text{Planck}}/m_n)^3$ nucleons, the above treatments, already developed and tested for the study of heavy nuclei. This more general approach differs in many aspects from the ones in the current literature and recovers, in the limiting case of A smaller than 10^6 , the above treatments. We shall look for a solution implementing the condition of overall charge neutrality of the star as given by

$$N_e = N_p, \quad (\text{A.3.6})$$

which significantly modifies Eq. (A.3.1), since now $N_e(N_p)$ is the total number of electrons (protons) of the equilibrium configuration. Here we present only a simplified prototype of this approach. We outline the essential relative role of the four fundamental interactions present in the neutron star physics: the gravitational, weak, strong and electromagnetic interactions. In addition, we also implement the fundamental role of Fermi-Dirac statistics and the phase space blocking due to the Pauli principle in the degenerate configuration. The new results essentially depend from the coordinated action of the five above theoretical components and cannot be obtained if any one of them is neglected. Let us first recall the role of gravity. In the case of neutron stars, unlike in the case of nuclei where its effects can be neglected, gravitation has the fundamental role of defining the basic parameters of the equilibrium con-

figuration. As pointed out by Gamow (1931), at a Newtonian level and by Oppenheimer and Volkoff (1939) in general relativity, configurations of equilibrium exist at approximately one solar mass and at an average density around the nuclear density. This result is obtainable considering only the gravitational interaction of a system of Fermi degenerate self-gravitating neutrons, neglecting all other particles and interactions. It can be formulated within a Thomas-Fermi self-gravitating model (see e.g. Ruffini and Bonazzola (1969)). In the present case of our simplified prototype model directed at evidencing new electrodynamic properties, the role of gravity is simply taken into account by considering, in line with the generalization of the above results, a mass-radius relation for the baryonic core

$$R^{NS} = R_c \approx \frac{\hbar}{m_\pi c} \frac{m_{\text{Planck}}}{m_n}. \quad (\text{A.3.7})$$

This formula generalizes the one given by Eq. (A.3.3) extending its validity to $N \approx (m_{\text{Planck}}/m_n)^3$, leading to a baryonic core radius $R_c \approx 10\text{km}$. We also recall that a more detailed analysis of nuclear matter in bulk in neutron stars (see e.g. Bethe et al. (1970) and Cameron (1970)) shows that at mass densities larger than the "melting" density of

$$\rho_c = 4.34 \cdot 10^{13} \text{g/cm}^3, \quad (\text{A.3.8})$$

all nuclei disappear. In the description of nuclear matter in bulk we have to consider then the three Fermi degenerate gas of neutrons, protons and electrons. In turn this naturally leads to consider the role of strong and weak interactions among the nucleons. In the nucleus, the role of the strong and weak interaction, with a short range of one Fermi, is to bind the nucleons, with a binding energy of 8 MeV, in order to balance the Coulomb repulsion of the protons. In the neutron star case we have seen that the neutrons confinement is due to gravity. We still assume that an essential role of the strong interactions is to balance the effective Coulomb repulsion due to the protons, partly screened by the electrons distribution inside the neutron star core. We shall verify, for self-consistency, the validity of this assumption on the final equilibrium solution we are going to obtain. We now turn to the essential weak interaction role in establishing the relative balance between neutrons, protons and electrons via the direct and inverse β -decay



Since neutrinos escape from the star and the Fermi energy of the electrons is null, as we will show below, the only non-vanishing terms in the equilibrium

condition given by the weak interactions are:

$$\sqrt{(P_n^F c)^2 + M_n^2 c^4} - M_n c^2 = \sqrt{(P_p^F c)^2 + M_p^2 c^4} - M_p c^2 + eV_{\text{coul}}^p, \quad (\text{A.3.11})$$

where P_n^F and P_p^F are respectively, the neutron and proton Fermi momenta, and V_{coul}^p is the Coulomb potential of protons. At this point, having fixed all these physical constraints, the main task is to find the electrons distributions fulfilling in addition to the Dirac-Fermi statistics also the Maxwell equations for the electrostatic. The condition of equilibrium of the Fermi degenerate electrons implies the null value of the Fermi energy:

$$\sqrt{(P_e^F c)^2 + m^2 c^4} - mc^2 + eV_{\text{coul}}(r) = 0, \quad (\text{A.3.12})$$

where P_e^F is the electron Fermi momentum and $V_{\text{coul}}(r)$ the Coulomb potential. In line with the procedure already followed for the heavy atoms Ferreira et al. (1980), Ruffini and Stella (1981) we here adopt the relativistic Thomas-Fermi Equation:

$$\frac{1}{x} \frac{d^2 \chi(x)}{dx^2} = -4\pi\alpha \left\{ \theta(x - x_c) - \frac{1}{3\pi^2} \left[\left(\frac{\chi(x)}{x} + \beta \right)^2 - \beta^2 \right]^{3/2} \right\}, \quad (\text{A.3.13})$$

where $\alpha = e^2 / (\hbar c)$, $\theta(x - x_c)$ represents the normalized proton density distribution, the variables x and χ are related to the radial coordinate and the electron Coulomb potential V_{coul} by

$$x = \frac{r}{R_c} \left(\frac{3N_p}{4\pi} \right)^{1/3}; \quad eV_{\text{coul}}(r) \equiv \frac{\chi(r)}{r}, \quad (\text{A.3.14})$$

and the constants $x_c(r = R_c)$ and β are respectively

$$x_c \equiv \left(\frac{3N_p}{4\pi} \right)^{1/3}; \quad \beta \equiv \frac{mcR_c}{\hbar} \left(\frac{4\pi}{3N_p} \right)^{1/3}. \quad (\text{A.3.15})$$

The solution has the boundary conditions

$$\chi(0) = 0; \quad \chi(\infty) = 0, \quad (\text{A.3.16})$$

with the continuity of the function χ and its first derivative χ' at the boundary of the core R_c . The crucial point is the determination of the eigenvalue of the first derivative at the center

$$\chi'(0) = \text{const.}, \quad (\text{A.3.17})$$

which has to be determined by fulfilling the above boundary conditions (A.3.16) and constraints given by Eq. (A.3.11) and Eq. (A.3.6). The difficulty of the integration of the Thomas-Fermi Equations is certainly one of the most celebrated chapters in theoretical physics and mathematical physics, still challenging a proof of the existence and uniqueness of the solution and strenuously avoiding the occurrence of exact analytic solutions. We recall after the original papers of Thomas Thomas (1927) and Fermi Fermi (1927), the works of Sommerfeld Sommerfeld (1932), all the way to the many hundredth papers reviewed in the classical articles of Lieb and Simon Lieb and Simon (1973), Lieb Lieb (1981) and Spruch Spruch (1991). The situation here is more difficult since we are working on the special relativistic generalization of the Thomas-Fermi Equation. Also in this case, therefore, we have to proceed by numerical integration. The difficulty of this numerical task is further enhanced by a consistency check in order to fulfill all different constraints. It is so that we start the computations by assuming a total number of protons and a value of the core radius R_c . We integrate the Thomas-Fermi Equation and we determine the number of neutrons from the Eq. (A.3.11). We iterate the procedure until a value of A is reached consistent with our choice of the core radius. The paramount difficulty of the problem is the numerical determination of the eigenvalue in Eq. (A.3.17) which already for $A \approx 10^4$ had presented remarkable numerical difficulties Ferreira et al. (1980). In the present context we have been faced for a few months by an apparently unsurmountable numerical task: the determination of the eigenvalue seemed to necessitate a significant number of decimals in the first derivative (A.3.17) comparable to the number of the electrons in the problem! The solution is given in Fig. (A.15) and Fig. (A.16).

A relevant quantity for exploring the physical significance of the solution is given by the number of electrons within a given radius r :

$$N_e(r) = \int_0^r 4\pi(r')^2 n_e(r') dr'. \quad (\text{A.3.18})$$

This allows to determine, for selected values of the A parameter, the distribution of the electrons within and outside the core and follow the progressive penetration of the electrons in the core at increasing values of A [see Fig. (A.17)]. We can then evaluate, generalizing the results in Ferreira et al. (1980), Ruffini and Stella (1981), the net charge inside the core

$$N_{\text{net}} = N_p - N_e(R_c) < N_p, \quad (\text{A.3.19})$$

and consequently determine the electric field at the core surface, as well as within and outside the core [see Fig. (A.18)] and evaluate as well the Fermi degenerate electron distribution outside the core [see Fig. (A.19)]. It is interesting to explore the solution of the problem under the same conditions and

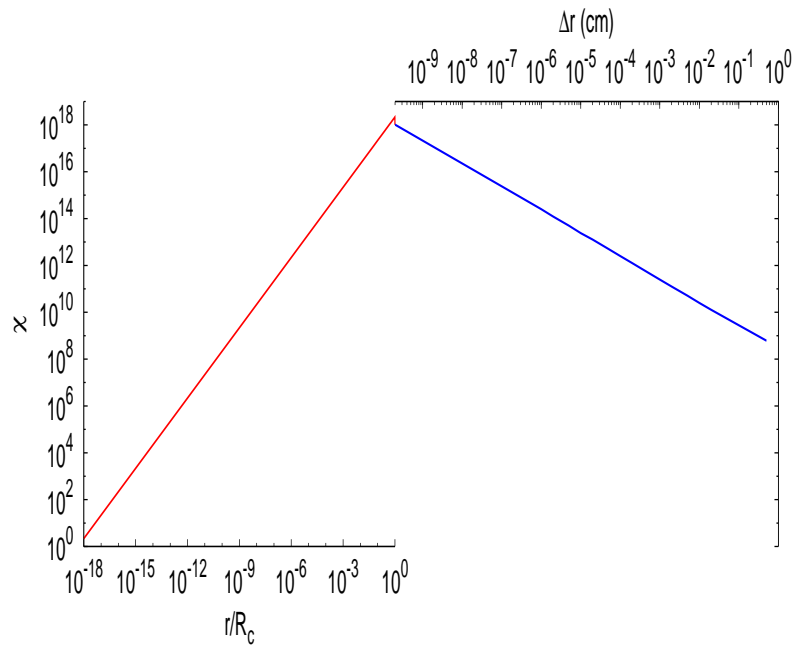


Figure A.15.: The solution χ of the relativistic Thomas-Fermi Equation for $A = 10^{57}$ and core radius $R_c = 10\text{km}$, is plotted as a function of radial coordinate. The left red line corresponds to the internal solution and it is plotted as a function of radial coordinate in unit of R_c in logarithmic scale. The right blue line corresponds to the solution external to the core and it is plotted as function of the distance Δr from the surface in the logarithmic scale in centimeter.

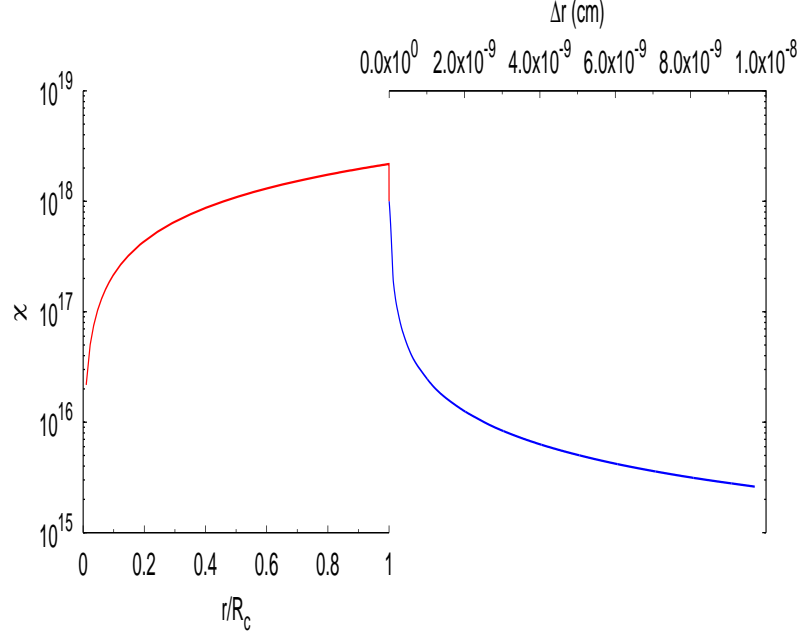


Figure A.16.: The same as Fig. (A.15): enlargement around the core radius R_c showing explicitly the continuity of function χ and its derivative χ' from the internal to the external solution.

constraints imposed by the fundamental interactions and the quantum statistics and imposing instead of Eq. (A.3.1) the corresponding Eq. (A.3.6). Indeed a solution exist and is much simpler

$$n_n(x) = n_p(x) = n_e(x) = 0, \quad \chi = 0. \quad (\text{A.3.20})$$

Before concluding as we announce we like to check on the theoretical consistency of the solution. We obtain an overall neutral configuration for the nuclear matter in bulk, with a positively charged baryonic core with

$$N_{\text{net}} = 0.92 \left(\frac{m}{m_\pi} \right)^2 \left(\frac{e}{m_n \sqrt{G}} \right)^2 \left(\frac{1}{\alpha} \right)^2, \quad (\text{A.3.21})$$

and an electric field on the baryonic core surface (see Fig. (A.18))

$$\frac{E}{E_c} = 0.92. \quad (\text{A.3.22})$$

The corresponding Coulomb repulsive energy per nucleon is given by

$$U_{\text{coul}}^{\text{max}} = \frac{1}{2\alpha} \left(\frac{m}{m_\pi} \right)^3 mc^2 \approx 1.78 \cdot 10^{-6} (\text{MeV}), \quad (\text{A.3.23})$$

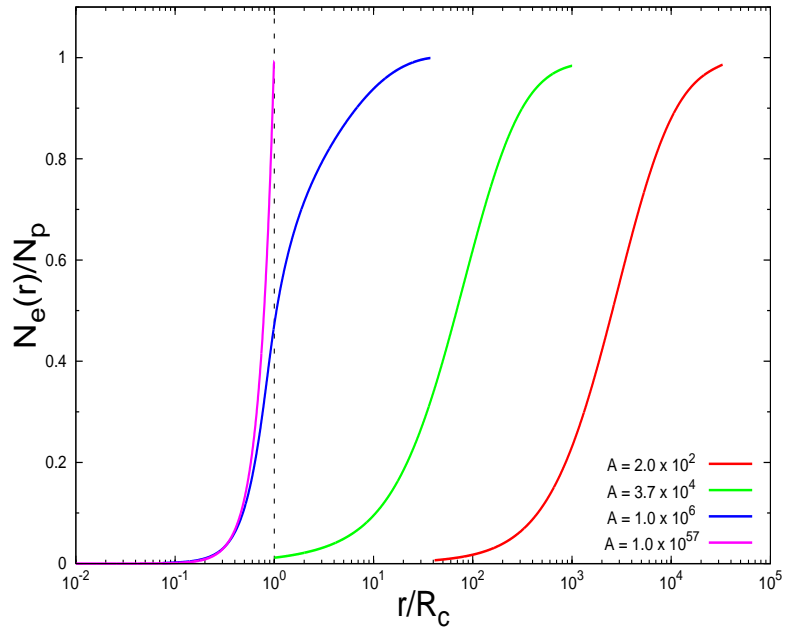


Figure A.17.: The electron number (A.3.18) in the unit of the total proton number N_p , for selected values of A , is given as function of radial distance in the unit of the core radius R_c , again in logarithmic scale. It is clear how by increasing the value of A the penetration of electrons inside the core increases. The detail shown in Fig. (A.18) and Fig. (A.19) demonstrates how for $N \simeq (m_{\text{Planck}}/m_n)^3$ a relatively small tail of electron outside the core exists and generates on the baryonic core surface an electric field close to the critical value. A significant electron density outside the core is found.

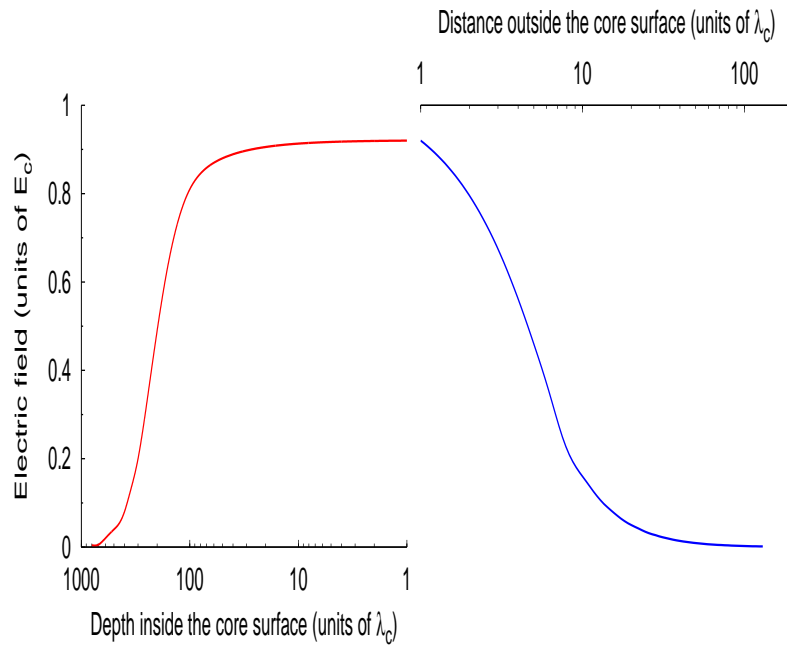


Figure A.18.: The electric field in the unit of the critical field E_c is plotted around the core radius R_c . The left (right) diagram in the red (blue) refers the region just inside (outside) the core radius plotted logarithmically. By increasing the density of the star the field approaches the critical field.

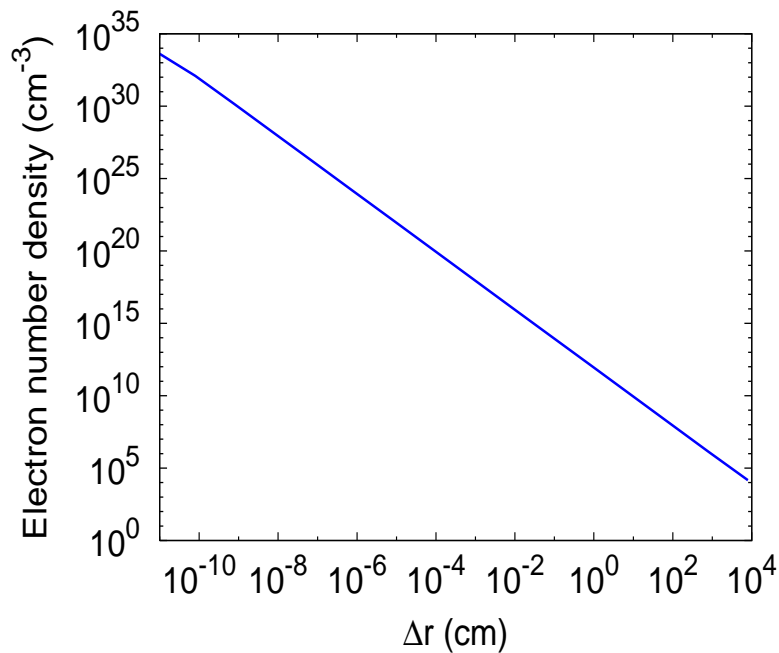


Figure A.19.: The density of electrons for $A = 10^{57}$ in the region outside the core; both scale are logarithmically.

well below the nucleon binding energy per nucleon. It is also important to verify that this charge core is gravitationally stable. We have in fact

$$\frac{Q}{\sqrt{GM}} = \alpha^{-1/2} \left(\frac{m}{m_\pi} \right)^2 \approx 1.56 \cdot 10^{-4}. \quad (\text{A.3.24})$$

The electric field of the baryonic core is screened to infinity by an electron distribution given in Fig. (A.19). As usual any new solution of Thomas-Fermi systems has relevance and finds its justification in the theoretical physics and mathematical physics domain. We expect that as in the other solutions previously obtained in the literature of the relativistic Thomas-Fermi equations also this one we present in this letter will find important applications in physics and astrophysics. There are a variety of new effects that such a generalized approach naturally leads to: (1) the mass-radius relation of neutron star may be affected; (2) the electrodynamic aspects of neutron stars and pulsars will be different; (3) we expect also important consequence in the initial conditions in the physics of gravitational collapse of the baryonic core as soon as the critical mass for gravitational collapse to a black hole is reached. The consequent collapse to a black hole will have very different energetics properties.

A.4. On the Charge to Mass Ratio of Neutron Cores and Heavy Nuclei

A.4.1. Introduction

It is well known that stable nuclei are located, in the N_n - N_p plane (where N_n and N_p are the total number of neutrons and protons respectively), in a region that, for small values of N_p , is almost a line well described by the relation $N_n = N_p$.

In the past, several efforts have been made to explain theoretically this property, for example with the liquid drop model of atoms, that is based on two properties common to all nuclei: their mass densities and their binding energies for nucleons are almost independent from the mass number $A = N_n + N_p$ (Segré (1977)). This model takes into account the strong nuclear force and the Coulombian repulsion between protons and explains different properties of nuclei, for example the relation between N_p and A (the charge to mass ratio).

In this work Patricelli et al. (2008) we derive theoretically the charge to mass ratio of nuclei and extend it to neutron cores (characterized by higher values of A) with the model of Ruffini et al. (2007b). We consider systems composed of degenerate neutrons, protons and electrons and we use the relativistic Thomas-Fermi equation and the equation of β -equilibrium to determine the number density and the total number of these particles, from which we obtain the relation between N_p and A .

A.4.2. The theoretical model

Following the work of Ruffini et al. (2007b), we describe nuclei and neutron cores as spherically symmetric systems composed of degenerate protons, electrons and neutrons and impose the condition of global charge neutrality.

We assume that the proton's number density $n_p(r)$ is constant inside the core ($r \leq R_C$) and vanishes outside the core ($r > R_C$):

$$n_p(r) = \left(\frac{3N_p}{4\pi R_C^3} \right) \theta(R_C - r), \quad (\text{A.4.1})$$

where N_p is the total number of protons and R_C is the core-radius, parametrized as:

$$R_C = \Delta \frac{\hbar}{m_\pi c} N_p^{1/3}. \quad (\text{A.4.2})$$

We choose Δ in order to have $\rho \sim \rho_N$, where ρ and ρ_N are the mass density of the system and the nuclear density respectively ($\rho_N = 2.314 \cdot 10^{14} \text{ g cm}^{-3}$).

The electron number density $n_e(r)$ is given by:

$$n_e(r) = \frac{1}{3\pi^2\hbar^3} \left[p_e^F(r) \right]^3, \quad (\text{A.4.3})$$

where $p_e^F(r)$ is the electron Fermi momentum. It can be calculated from the condition of equilibrium of Fermi degenerate electrons, that implies the null value of their Fermi energy $\epsilon_e^F(r)$:

$$\epsilon_e^F(r) = \sqrt{[p_e^F(r)c]^2 + m_e^2c^4} - m_e c^2 + V_c(r) = 0, \quad (\text{A.4.4})$$

where $V_c(r)$ is the Coulomb potential energy of electrons.

From this condition we obtain:

$$p_e^F(r) = \frac{1}{c} \sqrt{V_c^2(r) - 2m_e c^2 V_c(r)}, \quad (\text{A.4.5})$$

hence the electron number density is:

$$n_e(r) = \frac{1}{3\pi^2\hbar^3 c^3} \left[V_c^2(r) - 2m_e c^2 V_c(r) \right]^{3/2}. \quad (\text{A.4.6})$$

The Coulomb potential energy of electrons, necessary to derive $n_e(r)$, can be determined as follows. Based on the Gauss law, $V_c(r)$ obeys the following Poisson equation:

$$\nabla^2 V_c(r) = -4\pi e^2 [n_e(r) - n_p(r)], \quad (\text{A.4.7})$$

with the boundary conditions $V_c(\infty) = 0$, $V_c(0) = \text{finite}$. Introducing the dimensionless function $\chi(r)$, defined by the relation:

$$V_c(r) = -\hbar c \frac{\chi(r)}{r}, \quad (\text{A.4.8})$$

and the new variable $x = rb^{-1} = r \left(\frac{\hbar}{m\pi c} \right)^{-1}$, from Eq. (A.4.7) we obtain the relativistic Thomas-Fermi equation:

$$\frac{1}{3x} \frac{d^2 \chi(x)}{dx^2} = -\alpha \left\{ \frac{1}{\Delta^3} \theta(x_c - x) - \frac{4}{9\pi} \left[\frac{\chi^2(x)}{x^2} + 2 \frac{m_e}{m\pi} \frac{\chi(x)}{x} \right]^{3/2} \right\}. \quad (\text{A.4.9})$$

The boundary conditions for the function $\chi(x)$ are:

$$\chi(0) = 0, \quad \chi(\infty) = 0, \quad (\text{A.4.10})$$

as well as the continuity of $\chi(x)$ and its first derivative $\chi'(x)$ at the boundary

of the core.

The number density of neutrons $n_n(r)$ is:

$$n_n(r) = \frac{1}{3\pi^2\hbar^3} \left[p_n^F(r) \right]^3, \quad (\text{A.4.11})$$

where $p_n^F(r)$ is the neutron Fermi momentum. It can be calculated with the condition of equilibrium between the processes

$$e^- + p \rightarrow n + \nu_e; \quad (\text{A.4.12})$$

$$n \rightarrow p + e^- + \bar{\nu}_e, \quad (\text{A.4.13})$$

Assuming that neutrinos escape from the core as soon as they are produced, this condition (condition of β -equilibrium) is

$$\epsilon_e^F(r) + \epsilon_p^F(r) = \epsilon_n^F(r). \quad (\text{A.4.14})$$

Eq. (A.4.14) can be explicitly written as:

$$\sqrt{[p_p^F(r)c]^2 + m_p^2c^4} - m_p c^2 - V_c(r) = \sqrt{[p_n^F(r)c]^2 + m_n^2c^4} - m_n c^2. \quad (\text{A.4.15})$$

A.4.3. N_p versus A relation

Using the previous equations, we derive $n_e(r)$, $n_n(r)$ and $n_p(r)$ and, by integrating these, we obtain the N_e , N_n and N_p . We also derive a theoretical relation between N_p and A and we compare it with the data of the Periodic Table and with the semi-empirical relation:

$$N_p = \left(\frac{A}{2} \right) \cdot \frac{1}{1 + \left(\frac{3}{400} \right) \cdot A^{2/3}} \quad (\text{A.4.16})$$

that, in the limit of low A , gives the well known relation $N_p = A/2$ Segré (1977).

Eq. (A.4.16) can be obtained by minimizing the semi-empirical mass formula, that was first formulated by Weizsäcker in 1935 and is based on empirical measurements and on theory (the liquid drop model of atoms).

The liquid drop model approximates the nucleus as a sphere composed of protons and neutrons (and not electrons) and takes into account the Coulombian repulsion between protons and the strong nuclear force. Another important characteristic of this model is that it is based on the property that the mass densities of nuclei are approximately the same, independently from A . In fact, from scattering experiments it was found the following expression for the nuclear radius R_N :

$$R_N = r_0 A^{1/3}, \quad (\text{A.4.17})$$

with $r_0 = 1.2$ fm. Using eq. (A.4.17) the nuclear density can be write as follows:

$$\rho_N = \frac{Am_N}{V} = \frac{3Am_N}{4\pi r_0^3 A} = \frac{3m_N}{4\pi r_0^3}, \quad (\text{A.4.18})$$

where m_N is the nucleon mass. From eq. (A.4.18) it is clear that nuclear density is independent from A , so it is constant for all nuclei.

The property of constant density for all nuclei is a common point with our model: in fact, we choose Δ in order to have the same mass density for every value of A ; in particular we consider the case $\rho \sim \rho_N$, as previously said.

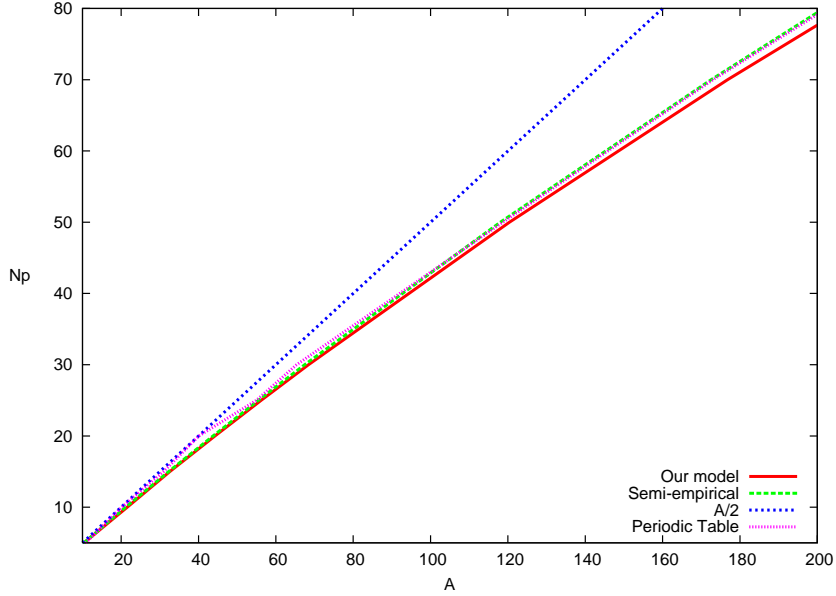


Figure A.20.: The $N_p - A$ relation obtained with our model and with the semi-empirical mass formula, the $N_p = A/2$ relation and the data of the Periodic Table; relations are plotted for values of A from 0 to 200.

In table (A.2) are listed some values of A obtained with our model and the semi-empirical mass formula, as well as the data of the Periodic Table; in fig. (A.20) and (A.21) it is shown the comparison between the various $N_p - A$ relations.

It is clear that there is a good agreement between all the relations for values of A typical of nuclei, with differences of the order of per cent. Our relation and the semi-empirical one are in agreement up to $A \sim 10^4$; for higher values, we find that the two relations differ. We interpret these differences as due to the effects of penetration of electrons inside the core [see fig. (A.22)]: in our model we consider a system composed of degenerate protons, neutrons and electrons. For the smallest values of A , all the electrons are in a shell outside the core; by increasing A , they progressively penetrate into the core Ruffini et al. (2007b). These effects, which need the relativistic approach introduced in Ruffini et al. (2007b), are not taken into account in the semi-empirical mass

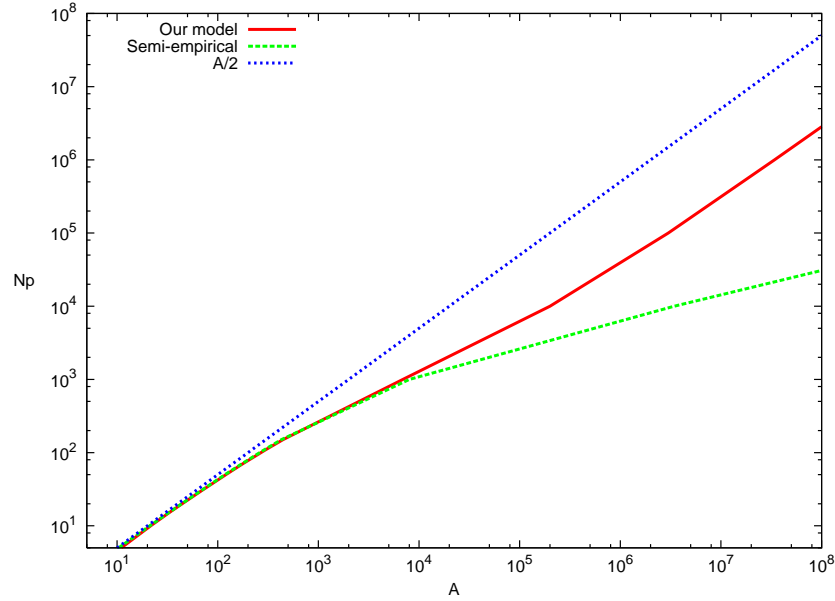


Figure A.21.: The $N_p - A$ relation obtained with our model and with the semi-empirical mass formula and the $N_p = A/2$ relation; relations are plotted for values of A from 0 to 10^8 . It is clear how the semi-empirical relation and the one obtained with our model are in good agreement up to values of A of the order of 10^4 ; for greater values of A the two relation differ because our model takes into account the penetration of electrons inside the core, which is not considered in the semi-empirical mass formula.

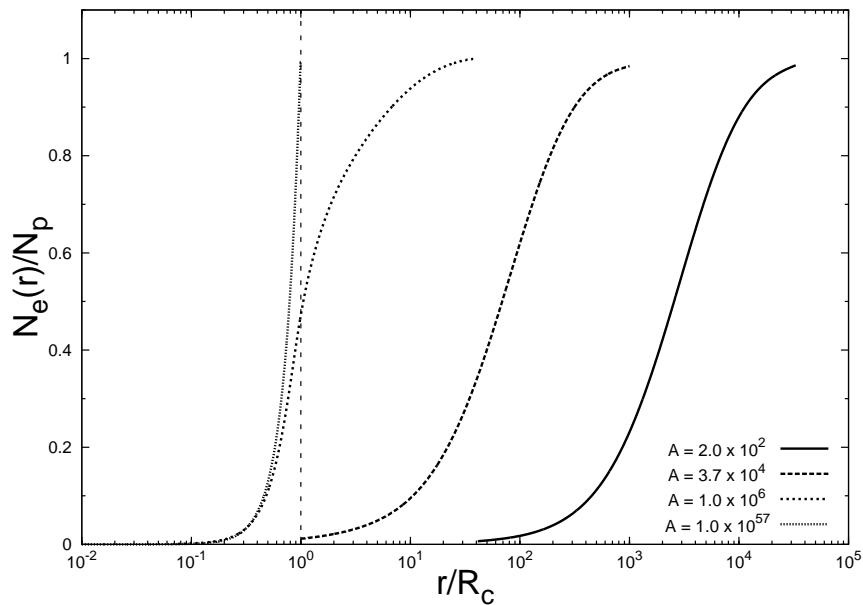


Figure A.22.: The electron number in units of the total proton number N_p as function of the radial distance in units of the core radius R_C , for different values of A . It is clear that, by increasing the value of A , the penetration of electrons inside the core increases. Figure from R. Ruffini, M. Rotondo and S. S. Xue Ruffini et al. (2007b).

formula.

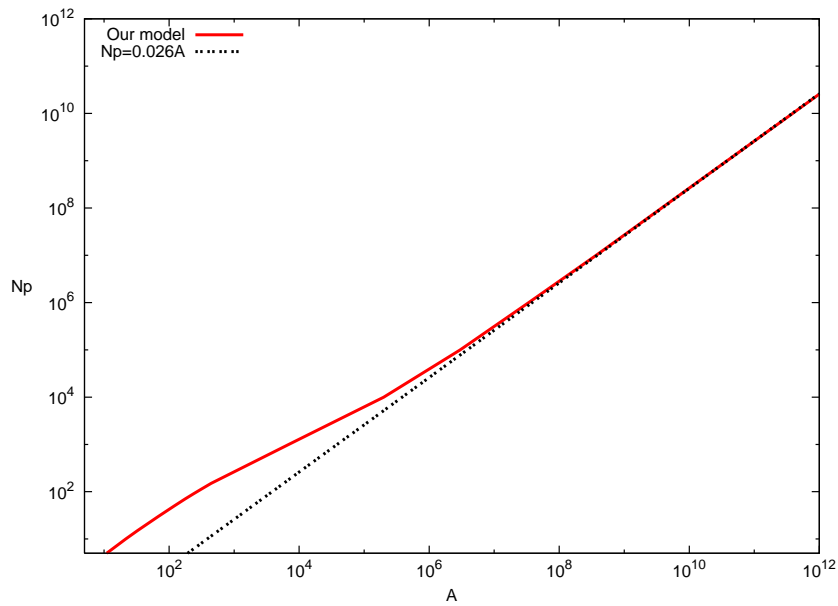


Figure A.23.: The $N_p - A$ relation obtained with our model and the asymptotic limit $N_p = 0.026A$

We also note that the charge to mass ratio become constant for A greater than 10^7 ; in particular, it is well approximated by the relation $N_p = 0.026A$ [see fig. (A.23)].

A.4.4. Conclusions

In this work we have derived theoretically a relation between the total number of protons N_p and the mass number A for nuclei and neutron cores with the model recently proposed by Ruffini et al. (2007b)).

We have considered spherically symmetric systems composed of degenerate electrons, protons and neutrons having global charge neutrality and the same mass densities ($\rho \sim \rho_N$). By integrating the relativistic Thomas-Fermi equation and using the equation of β -equilibrium, we have determined the total number of protons, electrons and neutrons in the system and hence a theoretical relation between N_p and A .

We have compared this relation with the empirical data of the Periodic Table and with the semi-empirical relation, obtained by minimizing the Weizsäcker mass formula by considering systems with the same mass densities. We have shown that there's a good agreement between all the relations for values of A typical of nuclei, with differences of the order of per cent. Our relation and the semi-empirical one are in agreement up to $A \sim 10^4$; for higher values, we find that the two relations differ. We interpret the different behaviour of our

N_p	A_M	A_{PT}	A_{SE}
5	10.40	10.811	10.36
10	21.59	20.183	21.15
15	32.58	30.9738	32.28
20	44.24	40.08	43.72
25	56.17	54.938	55.45
30	68.43	65.37	67.46
50	120.40	118.69	118.05
70	176.78	173.04	172.54
90	237.41	232.038	230.79
110	302.18	271	292.75
150	443.98		427.73
200	644.03		617.56
250	869.32		831.63
300	1119.71		1071.08
350	1395.12		1337.23
450	2019.48		1955.57
500	2367.77		2310.96
550	2739.60		2699.45
600	3134.28		3122.83
10^3	$6.9 \cdot 10^3$		$8 \cdot 10^3$
10^4	$2.0 \cdot 10^5$		$3.45 \cdot 10^6$
10^5	$3.0 \cdot 10^6$		$3.38 \cdot 10^9$
10^6	$3.4 \cdot 10^7$		$3.37 \cdot 10^{12}$
10^7	$3.7 \cdot 10^8$		$3.37 \cdot 10^{15}$
10^{10}	$3.9 \cdot 10^{11}$		$3.37 \cdot 10^{24}$

Table A.2.: Different values of N_p (column 1) and corresponding values of A from our model (A_M , column 2), the Periodic Table (A_{PT} , column 3) and the semi-empirical mass formula (A_{SE} , column 4).

theoretical relation as a result of the penetration of electrons (initially confined in an external shell) inside the core [see fig.(A.22)], that becomes more and more important by increasing A ; these effects, which need the relativistic approach introduced in Ruffini et al. (2007b), are not taken into account in the semi-empirical mass-formula.

A.5. Supercritical fields on the surface of massive nuclear cores: neutral core v.s. charged core

A.5.1. Equilibrium of electron distribution in neutral cores.

In Refs. Ruffini et al. (2007b); Ferreira et al. (1980); Ruffini and Stella (1981), the Thomas-Fermi approach was used to study the electrostatic equilibrium of electron distributions $n_e(r)$ around extended nuclear cores, where total proton and electron numbers are the same $N_p = N_e$. Proton's density $n_p(r)$ is constant inside core $r \leq R_c$ and vanishes outside the core $r > R_c$,

$$n_p(r) = n_p \theta(R_c - r), \quad (\text{A.5.1})$$

where R_c is the core radius and n_p proton density. Degenerate electron density,

$$n_e(r) = \frac{1}{3\pi^2 \hbar^3} (P_e^F)^3, \quad (\text{A.5.2})$$

where electron Fermi momentum P_e^F , Fermi-energy $\mathcal{E}_e(P_e^F)$ and Coulomb potential energy $V_{\text{coul}}(r)$ are related by,

$$\mathcal{E}_e(P_e^F) = [(P_e^F c)^2 + m_e^2 c^4]^{1/2} - m_e c^2 - V_{\text{coul}}(r). \quad (\text{A.5.3})$$

The electrostatic equilibrium of electron distributions is determined by

$$\mathcal{E}_e(P_e^F) = 0, \quad (\text{A.5.4})$$

which means the balance of electron's kinetic and potential energies in Eq. (A.5.3) and degenerate electrons occupy energy-levels up to $+m_e c^2$. Eqs. (A.5.2), (A.5.3), and (A.5.4) give the relationships:

$$P_e^F = \frac{1}{c} \left[V_{\text{coul}}^2(r) + 2m_e c^2 V_{\text{coul}}(r) \right]^{1/2}; \quad (\text{A.5.5})$$

$$n_e(r) = \frac{1}{3\pi^2 (c\hbar)^3} \left[V_{\text{coul}}^2(r) + 2m_e c^2 V_{\text{coul}}(r) \right]^{3/2}. \quad (\text{A.5.6})$$

The Gauss law leads the following Poisson equation and boundary conditions,

$$\Delta V_{\text{coul}}(r) = 4\pi\alpha [n_p(r) - n_e(r)]; \quad V_{\text{coul}}(\infty) = 0, \quad V_{\text{coul}}(0) = \text{finite} \quad (\text{A.5.7})$$

These equations describe a Thomas-Fermi model for neutral nuclear cores, and have numerically solved together with the empirical formula Ferreira et al. (1980); Ruffini and Stella (1981) and β -equilibrium equation Ruffini et al.

(2007b) for the proton number N_p and mass number $A = N_p + N_n$, where N_n is the neutron number.

A.5.2. Equilibrium of electron distribution in super charged cores

In Ref. Müller and Rafelski (1975); Migdal et al. (1976), assuming that super charged cores of proton density (A.5.1) are bare, electrons (positrons) produced by vacuum polarization fall (fly) into cores (infinity), one studied the equilibrium of electron distribution when vacuum polarization process stop. When the proton density is about nuclear density, super charged core creates a negative Coulomb potential well $-V_{\text{coul}}(r)$, whose depth is much more profound than $-m_e c^2$ (see Fig. [A.24]), production of electron-positron pairs take places, and electrons bound by the core and screen down its charge. Since the phase space of negative energy-levels $\epsilon(p)$

$$\epsilon(p) = [(pc)^2 + m_e^2 c^4]^{1/2} - V_{\text{coul}}(r), \quad (\text{A.5.8})$$

below $-m_e c^2$ for accommodating electrons is limited, vacuum polarization process completely stops when electrons fully occupy all negative energy-levels up to $-m_e c^2$, even electric field is still critical. Therefore an equilibrium of degenerate electron distribution is expected when the following condition is satisfied,

$$\epsilon(p) = [(pc)^2 + m_e^2 c^4]^{1/2} - V_{\text{coul}}(r) = -m_e c^2, \quad p = P_e^F, \quad (\text{A.5.9})$$

and Fermi-energy

$$\mathcal{E}_e(P_e^F) = \epsilon(P_e^F) - m_e c^2 = -2m_e c^2, \quad (\text{A.5.10})$$

which is rather different from Eq. (A.5.4). This equilibrium condition (A.5.10) leads to electron's Fermi-momentum and number-density (A.5.2),

$$P_e^F = \frac{1}{c} \left[V_{\text{coul}}^2(r) - 2m_e c^2 V_{\text{coul}}(r) \right]^{1/2}; \quad (\text{A.5.11})$$

$$n_e(r) = \frac{1}{3\pi^2 (c\hbar)^3} \left[V_{\text{coul}}^2(r) - 2m_e c^2 V_{\text{coul}}(r) \right]^{3/2}. \quad (\text{A.5.12})$$

which have a different sign contracting to Eqs. (A.5.5,A.5.6). Eq. (A.5.7) remains the same. However, contracting to the neutrality condition $N_e = N_p$ and $n_e(r)|_{r \rightarrow \infty} \rightarrow 0$ in the case of neutral cores, the total number of electrons is given by

$$N_e^{\text{ion}} = \int_0^{r_0} 4\pi r^2 dr n_e(r) < N_p, \quad (\text{A.5.13})$$

where r_0 is the finite radius at which electron distribution $n_e(r)$ (A.5.12) vanishes: $n_e(r_0) = 0$, i.e., $V_{\text{coul}}(r_0) = 2m_e c^2$, and $n_e(r) \equiv 0$ for the range $r > r_0$. $N^{\text{ion}} < N_p$ indicates that such configuration is not neutral. These equations describe a Thomas-Fermi model for super charged cores, and have numerically Müller and Rafelski (1975) and analytically Migdal et al. (1976) solved with assumption $N_p = A/2$.

A.5.3. Ultra-relativistic solution

In analytical approach Migdal et al. (1976), the ultra-relativistic approximation is adopted for $V_{\text{coul}}(r) \gg 2m_e c^2$, the term $2m_e c^2 V_{\text{coul}}(r)$ in Eqs. (A.5.5), (A.5.6), (A.5.11), and (A.5.12) is neglected. It turns out that approximated Thomas-Fermi equations are the same for both cases of neutral and charged cores, and solution $V_{\text{coul}}(r) = \hbar c (3\pi^2 n_p)^{1/3} \phi(x)$,

$$\phi(x) = \left\{ \begin{array}{ll} 1 - 3 \left[1 + 2^{-1/2} \sinh(3.44 - \sqrt{3}x) \right]^{-1}, & \text{for } x < 0, \\ \frac{\sqrt{2}}{(x+1.89)}, & \text{for } x > 0, \end{array} \right\}, \quad (\text{A.5.14})$$

where $x = 2(\pi/3)^{1/6} \alpha^{1/2} n_p^{1/3} (r - R_c) \sim 0.1(r - R_c)/\lambda_\pi$ and the pion Compton length $\lambda_\pi = \hbar/(m_\pi c)$. At the core center $r = 0$ ($x \rightarrow -\infty$), $V_{\text{coul}}(0) = \hbar c (3\pi^2 n_p)^{1/3} \sim m_\pi c^2$. On the surface of the core $r = R_c$, namely $x = 0$, and $V_{\text{coul}}(R_c) = (3/4)V_{\text{coul}}(0) \gg m_e c^2$, indicating that the ultra-relativistic approximation is applicable for $r \lesssim R_c$. This approximation breaks down at $r \gtrsim r_0$. Clearly, it is impossible to determine the value r_0 out of ultra-relativistically approximated equation, and full Thomas-Fermi equation (A.5.7) with source terms Eq. (A.5.6) for the neutral case, and Eq. (A.5.12) for the charged case have to be solved.

For $r < r_0$ where $V_{\text{coul}}(r) > 2m_e c^2$, we treat the term $2m_e c^2 V_{\text{coul}}(r)$ in Eqs. (A.5.6, A.5.12) as a small correction term, and find the following inequality is always true

$$n_e^{\text{neutral}}(r) > n_e^{\text{charged}}(r), \quad r < r_0, \quad (\text{A.5.15})$$

where $n_e^{\text{neutral}}(r)$ and $n_e^{\text{charged}}(r)$ stand for electron densities of neutral and super charged cores. For the range $r > r_0$, $n_e^{\text{charged}}(r) \equiv 0$ in the case of super charged core, while $n_e^{\text{neutral}}(r) \rightarrow 0$ in the case of neutral core, which should be calculated in non-relativistic approximation: the term $V_{\text{coul}}^2(r)$ in Eq. (A.5.6) is neglected.

In conclusion, the physical scenarios and Thomas-Fermi equations of neutral and super charged cores are slightly different. When the proton density n_p of cores is about nuclear density, ultra-relativistic approximation applies for the Coulomb potential energy $V_{\text{coul}}(r) \gg m_e c^2$ in $0 < r < r_0$ and $r_0 > R_c$, and approximate equations and solutions for electron distributions

A.5. Supercritical fields on the surface of massive nuclear cores: neutral core
v.s. charged core

inside and around cores are the same. As relativistic regime $r \sim r_0$ and non-relativistic regime $r > r_0$ (only applied to neutral case) are approached, solutions in two cases are somewhat different, and need direct integrations.

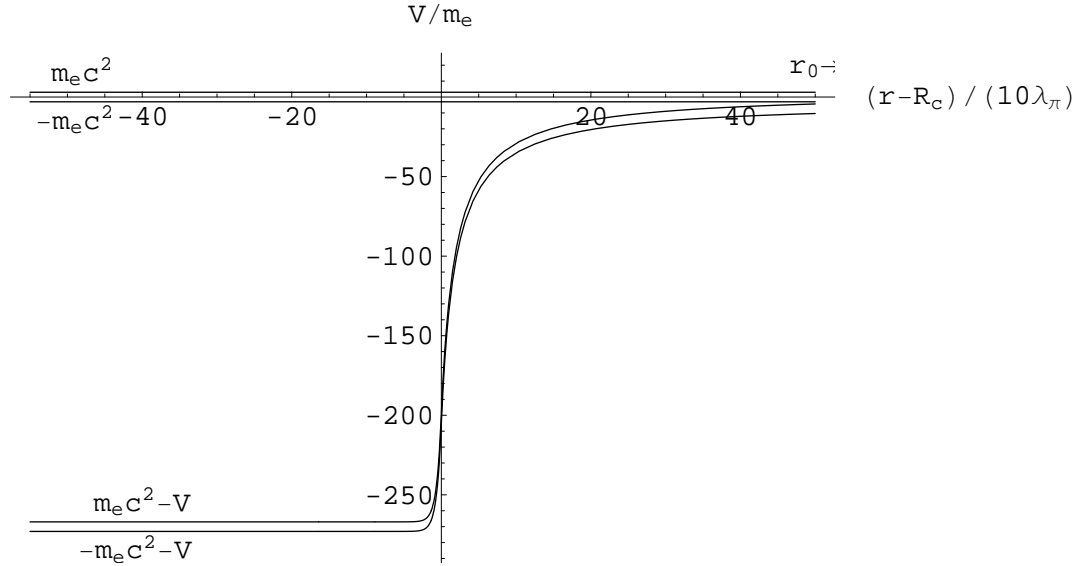


Figure A.24.: Potential energy-gap $\pm m_e c^2 - V_{\text{coul}}(r)$ and electron mass-gap $\pm m_e c^2$ in the unit of $m_e c^2$ are plotted as a function of $(r - R_c)/(10\lambda_\pi)$. The potential depth inside core ($r < R_c$) is about pion mass $m_\pi c^2 \gg m_e c^2$ and potential energy-gap and electron mass-gap are indicated. The radius r_0 where electron distribution $n_e(r_0)$ vanishes in super charged core case is indicated as r_0- , since it is out of plotting range.

A.6. The Extended Nuclear Matter Model with Smooth Transition Surface

A.6.1. The Relativistic Thomas-Fermi Equation

Let us to introduce the proton distribution function $f_p(x)$ by mean of $n_p(x) = n_p^c f_p(x)$, where n_p^c is the central number density of protons. We use the dimensionless unit $x = (r - b)/a$, with $a^{-1} = \sqrt{4\pi\alpha\lambda_e n_p^c}$, λ_e is the electron Compton wavelength, b the length where initial conditions are given ($x = 0$) and α is the fine structure constant.

Using the Poisson's equation and the equilibrium condition for the gas of electrons

$$E_F^e = m_e c^2 \sqrt{1 + x_e^2} - m_e c^2 - eV = 0, \quad (\text{A.6.1})$$

where e is the fundamental charge, x_e the normalized electron Fermi momentum and V the electrostatic potential, we obtain the relativistic Thomas-Fermi equation

$$\zeta_e''(x) + \left(\frac{2}{x + b/a} \right) \zeta_e'(x) - \frac{[\zeta_e^2(x) - 1]^{3/2}}{\mu} + f_p(x) = 0, \quad (\text{A.6.2})$$

where $\mu = 3\pi^2 \lambda_e^3 n_p^c$ and we have introduced the normalized electron chemical potential in absence of any field $\zeta_e = \sqrt{1 + x_e^2}$. For a given distribution function $f_p(x)$ and a central number density of protons n_p^c , the above equation can be integrated numerically with the boundary conditions

$$\zeta_e(0) = \sqrt{1 + [\mu \delta f_p(0)]^{2/3}}, \quad \zeta_e'(0) < 0, \quad (\text{A.6.3})$$

where $\delta \equiv n_e(0)/n_p(0)$.

A.6.2. The Woods-Saxon-like Proton Distribution Function

We simulate a monotonically decreasing proton distribution function fulfilling a Woods-Saxon dependence

$$f_p(x) = \frac{\gamma}{\gamma + e^{\beta x}}, \quad (\text{A.6.4})$$

where $\gamma > 0$ and $\beta > 0$. In Fig. A.25 we show the proton distribution function for a particular set of parameters.

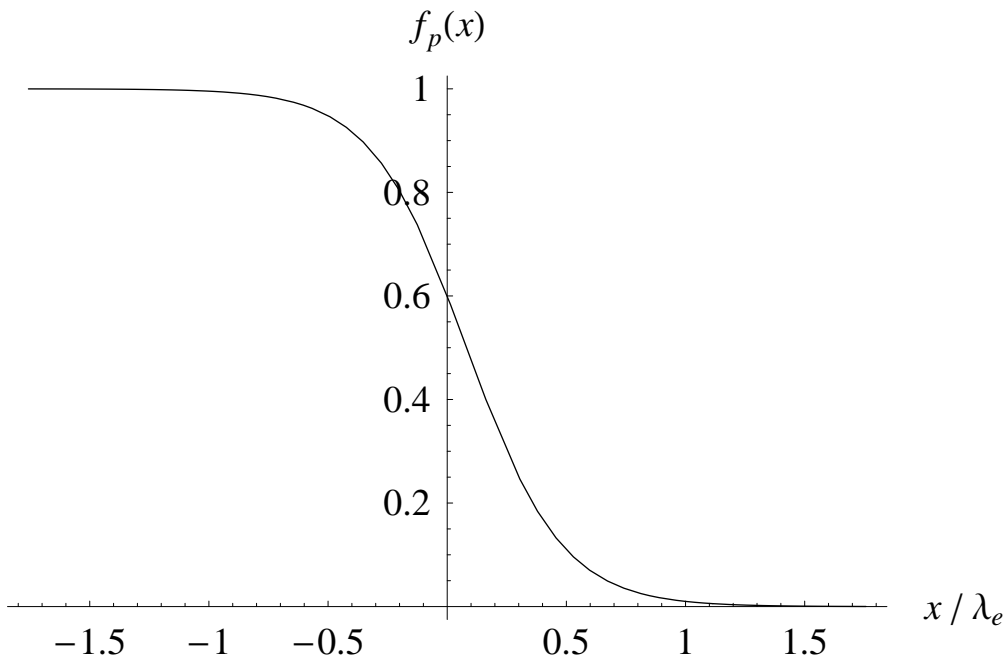


Figure A.25.: Proton distribution function for $\gamma = 1.5$, $\beta \approx 0.0585749$.

A.6.3. Results of the Numerical Integration.

We have integrated numerically the Eq. (A.6.2) for several sets of parameters and initial conditions. As an example, we show the results for the proton distribution function shown in Fig. A.25, with $n_p^c = 1.38 \times 10^{36} (\text{cm}^{-3})$. This system was integrated with $N_e = N_p = 10^{54}$, mass number $A = 1.61 \times 10^{56}$ and $\delta \approx 0.967$.

We summarize the principal features of our model in Figs. A.26 and A.27, where we have plotted the electric field in units of the critical field $E_c = \frac{m_e^2 c^3}{e \hbar}$, (m_e and e are the electron mass and charge), and the normalized charge separation function

$$\Delta(x) = \frac{n_p(x) - n_e(x)}{n_p(0)}. \quad (\text{A.6.5})$$

We see that the electric field is overcritical but smaller respect to the case of a sharp step proton distribution used in Ruffini et al. (2007b); Migdal et al. (1976). We have performed several numerical integrations expanding the transition surface and confirm the existence of overcritical fields but it is worth to mention that it could be subcritical expanding the width of the transition surface several orders of magnitude in electron Compton wavelength units.

We also see a displacement of the location of the maximum of intensity. This effect is due to the displacement of the point where $n_e = n_p$. After this point, the charge density becomes negative producing an effect of screening

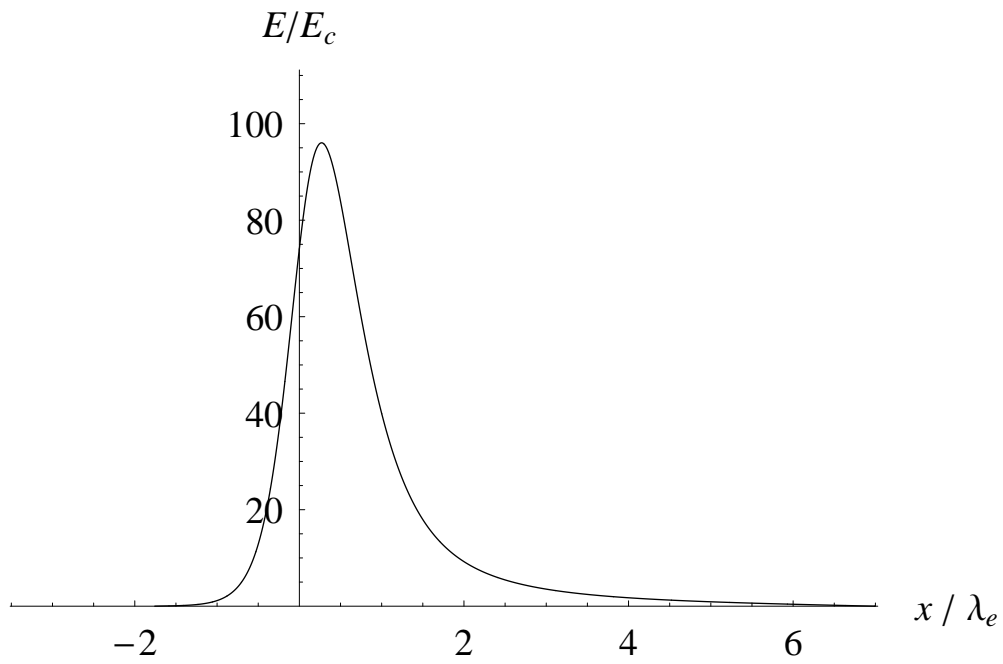


Figure A.26.: Electric field in units of the critical field E_c .

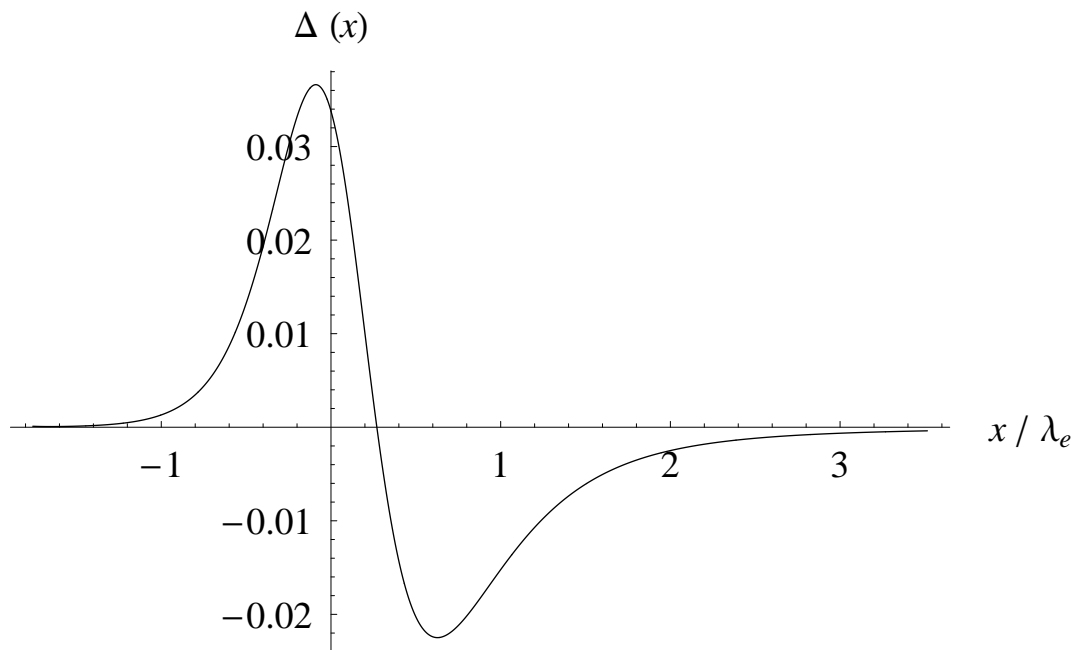


Figure A.27.: Charge separation function.

of the charged core up to global charged neutrality is achieved.

A.7. Electron-positron pairs production in an electric potential of massive cores

A.7.1. Introduction

Very soon after the Dirac equation for a relativistic electron was discovered Dirac (1928a,b, 1958), Gordon Gordon (1928) (for all $Z < 137$) and Darwin Darwin (1928) (for $Z = 1$) found its solution in the point-like Coulomb potential $V(r) = -Z\alpha/r$, they obtained the well-known Sommerfeld's formula for energy-spectrum,

$$\varepsilon(n, j) = mc^2 \left[1 + \left(\frac{Z\alpha}{n - |K| + (K^2 - Z^2\alpha^2)^{1/2}} \right)^2 \right]^{-1/2}, \quad (\text{A.7.1})$$

where the fine-structure constant $\alpha = e^2/\hbar c$, the principle quantum number $n = 1, 2, 3, \dots$ and

$$K = \begin{cases} -(j + 1/2) = -(l + 1), & \text{if } j = l + \frac{1}{2}, \quad l \geq 0 \\ (j + 1/2) = l, & \text{if } j = l - \frac{1}{2}, \quad l \geq 1 \end{cases} \quad (\text{A.7.2})$$

$l = 0, 1, 2, \dots$ is the orbital angular momentum corresponding to the upper component of Dirac bi-spinor, j is the total angular momentum. The integer values n and j label bound states whose energies are $\varepsilon(n, j) \in (0, mc^2)$. For the example, in the case of the lowest energy states, one has

$$\varepsilon(1S_{\frac{1}{2}}) = mc^2 \sqrt{1 - (Z\alpha)^2}, \quad (\text{A.7.3})$$

$$\varepsilon(2S_{\frac{1}{2}}) = \varepsilon(2P_{\frac{1}{2}}) = mc^2 \sqrt{\frac{1 + \sqrt{1 - (Z\alpha)^2}}{2}}, \quad (\text{A.7.4})$$

$$\varepsilon(2P_{\frac{3}{2}}) = mc^2 \sqrt{1 - \frac{1}{4}(Z\alpha)^2}. \quad (\text{A.7.5})$$

For all states of the discrete spectrum, the binding energy $mc^2 - \varepsilon(n, j)$ increases as the nuclear charge Z increases. No regular solution with $n = 1, l = 0, j = 1/2$ and $K = -1$ (the $1S_{1/2}$ ground state) is found for $Z > 137$, this was first noticed by Gordon in his pioneer paper Gordon (1928). This is the problem so-called “ $Z = 137$ catastrophe”.

The problem was solved Case (1950); Werner and Wheeler (1958); Popov (1970, 1971b,a) by considering the fact that the nucleus is not point-like and has an extended charge distribution, and the potential $V(r)$ is not divergent when $r \rightarrow 0$. The $Z = 137$ catastrophe disappears and the energy-levels $\varepsilon(n, j)$ of the bound states $1S, 2P$ and $2S, \dots$ smoothly continue to drop toward the negative energy continuum ($E_- < -mc^2$), as Z increases to values

larger than 137. The critical values Z_{cr} for $\mathcal{E}(n, j) = -mc^2$ were found Werner and Wheeler (1958); Popov (1970, 1971b,a); Rafelski et al. (1978); Kleinert et al. (2008): $Z_{cr} \simeq 173$ is a critical value at which the lowest energy-level of the bound state $1S_{1/2}$ encounters the negative energy continuum, while other bound states $2P_{1/2}, 2S_{3/2}, \dots$ encounter the negative energy continuum at $Z_{cr} > 173$, thus energy-level-crossings and productions of electron and positron pair takes place, provided these bound states are unoccupied. We refer the readers to Popov (1970, 1971b,a); Rafelski et al. (1978); Kleinert et al. (2008) for mathematical and numerical details.

The energetics of this phenomenon can be understood as follow. The energy-level of the bound state $1S_{1/2}$ can be estimated as follow,

$$\mathcal{E}(1S_{1/2}) = mc^2 - \frac{Ze^2}{\bar{r}} < -mc^2, \quad (\text{A.7.6})$$

where \bar{r} is the average radius of the $1S_{1/2}$ state's orbit, and the binding energy of this state $Ze^2/\bar{r} > 2mc^2$. If this bound state is unoccupied, the bare nucleus gains a binding energy Ze^2/\bar{r} larger than $2mc^2$, and becomes unstable against the production of an electron-positron pair. Assuming this pair-production occur around the radius \bar{r} , we have energies of electron (ϵ_-) and positron (ϵ_+):

$$\epsilon_- = \sqrt{(c|\mathbf{p}_-|)^2 + m^2c^4} - \frac{Ze^2}{\bar{r}}; \quad \epsilon_+ = \sqrt{(c|\mathbf{p}_+|)^2 + m^2c^4} + \frac{Ze^2}{\bar{r}}, \quad (\text{A.7.7})$$

where \mathbf{p}_\pm are electron and positron momenta, and $\mathbf{p}_- = -\mathbf{p}_+$. The total energy required for a pair production is,

$$\epsilon_{-+} = \epsilon_- + \epsilon_+ = 2\sqrt{(c|\mathbf{p}_-|)^2 + m^2c^4}, \quad (\text{A.7.8})$$

which is independent of the potential $V(\bar{r})$. The potential energies $\pm eV(\bar{r})$ of electron and positron cancel each other and do not contribute to the total energy (A.7.8) required for pair production. This energy (A.7.8) is acquired from the binding energy ($Ze^2/\bar{r} > 2mc^2$) by the electron filling into the bound state $1S_{1/2}$. A part of the binding energy becomes the kinetic energy of positron that goes out. This is analogous to the familiar case that a proton ($Z = 1$) catches an electron into the ground state $1S_{1/2}$, and a photon is emitted with the energy not less than 13.6 eV.

In this article, we study classical and semi-classical states of electrons, electron-positron pair production in an electric potential of macroscopic cores with charge $Q = Z|e|$, mass M and macroscopic radius R_c .

A.7.2. Classical description of electrons in potential of cores

Effective potentials for particle's radial motion

Setting the origin of spherical coordinates (r, θ, ϕ) at the center of such cores, we write the vectorial potential $A_\mu = (\mathbf{A}, A_0)$, where $\mathbf{A} = 0$ and A_0 is the Coulomb potential. The motion of a relativistic electron with mass m and charge e is described by its radial momentum p_r , total angular momenta p_ϕ and the Hamiltonian,

$$H_\pm = \pm mc^2 \sqrt{1 + \left(\frac{p_r}{mc}\right)^2 + \left(\frac{p_\phi}{mcr}\right)^2} - V(r), \quad (\text{A.7.9})$$

where the potential energy $V(r) = eA_0$, and \pm corresponds for positive and negative energies. The states corresponding to negative energy solutions are fully occupied. The total angular momentum p_ϕ is conserved, for the potential $V(r)$ is spherically symmetric. For a given angular momentum $p_\phi = mv_\perp r$, where v_\perp is the transverse velocity, the effective potential energy for electron's radial motion is

$$E_\pm(r) = \pm mc^2 \sqrt{1 + \left(\frac{p_\phi}{mcr}\right)^2} - V(r). \quad (\text{A.7.10})$$

Outside the core ($r \geq R_c$), the Coulomb potential energy $V(r)$ is given by

$$V_{\text{out}}(r) = \frac{Ze^2}{r}, \quad (\text{A.7.11})$$

where \pm indicates positive and negative effective energies. Inside the core ($r \leq R_c$), the Coulomb potential energy is given by

$$V_{\text{in}}(r) = \frac{Ze^2}{2R_c} \left[3 - \left(\frac{r}{R_c}\right)^2 \right], \quad (\text{A.7.12})$$

where we postulate the charged core has a uniform charge distribution with constant charge density $\rho = Ze/V_c$, and the core volume $V_c = 4\pi R_c^3/3$. Coulomb potential energies outside the core (A.7.11) and inside the core (A.7.12) is continuous at $r = R_c$. The electric field on the surface of the core,

$$E_s = \frac{Q}{R_c^2} = \frac{\lambda_e}{R_c} E_c, \quad \beta \equiv \frac{Ze^2}{mc^2 R_c} \quad (\text{A.7.13})$$

where the electron Compton wavelength $\lambda_e = \hbar/(mc)$, the critical electric field $E_c = m^2 c^3 / (e\hbar)$ and the parameter β is the electric potential-energy on the surface of the core in unit of the electron mass-energy.

Stable classical orbits (states) outside the core.

Given different values of total angular momenta p_ϕ , the stable circulating orbits R_L (states) are determined by the minimum of the effective potential $E_+(r)$ (A.7.10) (see Fig. A.28), at which $dE_+(r)/dr = 0$. We obtain stable orbits locate at the radii R_L ,

$$R_L = \left(\frac{p_\phi^2}{Ze^2 m} \right) \sqrt{1 - \left(\frac{Ze^2}{cp_\phi} \right)^2}, \quad R_L \geq R_c, \quad (\text{A.7.14})$$

for different p_ϕ -values. Substituting Eq. (A.7.14) into Eq. (A.7.10), we find the energy of electron at each stable orbit,

$$\varepsilon \equiv \min(E_+) = mc^2 \sqrt{1 - \left(\frac{Ze^2}{cp_\phi} \right)^2}. \quad (\text{A.7.15})$$

For the condition $R_L \gtrsim R_c$, we have

$$\left(\frac{Ze^2}{cp_\phi} \right)^2 \lesssim \frac{1}{2} [\beta(4 + \beta^2)^{1/2} - \beta^2], \quad (\text{A.7.16})$$

where the semi-equality holds for the last stable orbits outside the core $R_L \rightarrow R_c + 0^+$. In the point-like case $R_c \rightarrow 0$, the last stable orbits are

$$cp_\phi \rightarrow Ze^2 + 0^+, \quad R_L \rightarrow 0^+, \quad \varepsilon \rightarrow 0^+. \quad (\text{A.7.17})$$

Eq. (A.7.15) shows that only positive or null energy solutions (states) to exists in the case of a point-like charge, which is the same as the energy-spectrum Eqs. (A.7.3,A.7.4,A.7.5) in quantum mechanic scenario. While for $p_\phi \gg 1$, radii of stable orbits $R_L \gg 1$ and energies $\varepsilon \rightarrow mc^2 + 0^-$, classical electrons in these orbits are critically bound for their banding energy goes to zero. We conclude that the energies (A.7.15) of stable orbits outside the core must be smaller than mc^2 , but larger than zero, $\varepsilon > 0$. Therefore, no energy-level crossing with the negative energy spectrum occurs.

Stable classical orbits inside the core.

We turn to the stable orbits of electrons inside the core. Analogously, using Eqs. (A.7.10,A.7.12) and $dE_+(r)/dr = 0$, we obtain the stable orbit radius $R_L \leq 1$ in the unit of R_c , obeying the following equation,

$$\beta^2(R_L^8 + \kappa^2 R_L^6) = \kappa^4; \quad \kappa = \frac{p_\phi}{mcR_c}. \quad (\text{A.7.18})$$

and corresponding to the minimal energy (binding energy) of these states

$$\varepsilon = \frac{Ze^2}{R_c} \left[\left(\frac{cp_\phi}{Ze^2} \right)^2 \frac{1}{R_L^4} - \frac{1}{2}(3 - R_L^2) \right]. \quad (\text{A.7.19})$$

There are 8 solutions to this polynomial equation (A.7.18), only one is physical solution R_L that has to be real, positive and smaller than one. As example, the numerical solution to Eq. (A.7.18) is $R_L = 0.793701$ for $\beta = 4.4 \cdot 10^{16}$ and $\kappa = 2.2 \cdot 10^{16}$. In following, we respectively adopt non-relativistic and ultra-relativistic approximations to obtain analytical solutions.

First considering the non-relativistic case for those stable orbit states whose the kinetic energy term characterized by angular momentum term p_ϕ , see Eq. (A.7.10), is much smaller than the rest mass term mc^2 , we obtain the following approximate equation,

$$\beta^2 R_L^8 \simeq \kappa^4, \quad (\text{A.7.20})$$

and the solutions for stable orbit radii are,

$$R_L \simeq \frac{\kappa^{1/2}}{\beta^{1/4}} = \left(\frac{cp_\phi}{Ze^2} \right)^{1/2} \beta^{1/4} < 1, \quad (\text{A.7.21})$$

and energies,

$$\varepsilon \simeq \left(1 - \frac{3}{2}\beta + \frac{1}{2}\kappa\beta^{1/2} \right) mc^2. \quad (\text{A.7.22})$$

The consistent conditions for this solution are $\beta^{1/2} > \kappa$ for $R_L < 1$, and $\beta \ll 1$ for non-relativistic limit $v_\perp \ll c$. As a result, the binding energies (A.7.22) of these states are $mc^2 > \varepsilon > 0$, are never less than zero. These in fact correspond to the stable states which have large radii closing to the radius R_c of cores and $v_\perp \ll c$.

Second considering the ultra-relativistic case for those stable orbit states whose the kinetic energy term characterized by angular momentum term p_ϕ , see Eq. (A.7.10), is much larger than the rest mass term mc^2 , we obtain the following approximate equation,

$$\beta^2 R_L^6 \simeq \kappa^2, \quad (\text{A.7.23})$$

and the solutions for stable orbit radii are,

$$R_L \simeq \left(\frac{\kappa}{\beta} \right)^{1/3} = \left(\frac{p_\phi c}{Ze^2} \right)^{1/3} < 1, \quad (\text{A.7.24})$$

which gives $R_L \simeq 0.7937007$ for the same values of parameters β and κ in above. The consistent condition for this solution is $\beta > \kappa \gg 1$ for $R_L < 1$.

The energy levels of these ultra-relativistic states are,

$$\varepsilon \simeq \frac{3}{2}\beta \left[\left(\frac{p_\phi c}{Ze^2} \right)^{2/3} - 1 \right] mc^2, \quad (\text{A.7.25})$$

and $mc^2 > \varepsilon > -1.5\beta mc^2$. The particular solutions $\varepsilon = 0$ and $\varepsilon \simeq -mc^2$ are respectively given by

$$\left(\frac{p_\phi c}{Ze^2} \right) \simeq 1; \quad \left(\frac{p_\phi c}{Ze^2} \right) \simeq \left(1 - \frac{2}{3\beta} \right)^{3/2}. \quad (\text{A.7.26})$$

These in fact correspond to the stable states which have small radii closing to the center of cores and $v_\perp \lesssim c$.

To have the energy-level crossing to the negative energy continuum, we are interested in the values $\beta > \kappa \gg 1$ for which the energy-levels (A.7.25) of stable orbit states are equal to or less than $-mc^2$,

$$\varepsilon \simeq \frac{3}{2}\beta \left[\left(\frac{p_\phi c}{Ze^2} \right)^{2/3} - 1 \right] mc^2 \leq -mc^2. \quad (\text{A.7.27})$$

As example, with $\beta = 10$ and $\kappa = 2$, $R_L \simeq 0.585$, $\varepsilon_{\min} \simeq -9.87mc^2$. The lowest energy-level of electron state is $p_\phi/(Ze^2) = \kappa/\beta \rightarrow 0$ with the binding energy,

$$\varepsilon_{\min} = -\frac{3}{2}\beta mc^2, \quad (\text{A.7.28})$$

locating at $R_L \simeq (p_\phi c/Ze^2)^{1/3} \rightarrow 0$, the bottom of the potential energy $V_{\text{in}}(0)$ (A.7.12).

A.7.3. Semi-Classical description

Bohr-Sommerfeld quantization

In order to have further understanding, we consider the semi-classical scenario. Introducing the Planck constant $\hbar = h/(2\pi)$, we adopt the semi-classical Bohr-Sommerfeld quantization rule

$$\int p_\phi d\phi \simeq h\left(l + \frac{1}{2}\right), \quad \Rightarrow \quad p_\phi(l) \simeq \hbar\left(l + \frac{1}{2}\right), \quad l = 0, 1, 2, 3, \dots, \quad (\text{A.7.29})$$

which are discrete values selected from continuous total angular momentum p_ϕ in the classical scenario. The variation of total angular momentum $\Delta p_\phi = \pm\hbar$ in th unit of the Planck constant \hbar . Substitution

$$\left(\frac{p_\phi c}{Ze^2} \right) \Rightarrow \left(\frac{2l + 1}{2Z\alpha} \right), \quad (\text{A.7.30})$$

where the fine-structure constant $\alpha = e^2/(\hbar c)$, must be performed in classical solutions that we obtained in section (A.7.2).

1. The radii and energies of stable states outside the core (A.7.14) and (A.7.15) become:

$$R_L = \lambda \left(\frac{2l+1}{Z\alpha} \right) \sqrt{1 - \left(\frac{2Z\alpha}{2l+1} \right)^2}, \quad (\text{A.7.31})$$

$$\varepsilon = mc^2 \sqrt{1 - \left(\frac{2Z\alpha}{2l+1} \right)^2}, \quad (\text{A.7.32})$$

where λ is the electron Compton length.

2. The radii and energies of non-relativistic stable states inside the core (A.7.21) and (A.7.22) become:

$$R_L \simeq \left(\frac{2l+1}{2Z\alpha} \right)^{1/2} \beta^{1/4}, \quad (\text{A.7.33})$$

$$\varepsilon \simeq \left(1 - \frac{3}{2}\beta + \frac{\lambda(2l+1)}{4R_c} \beta^{1/2} \right) mc^2. \quad (\text{A.7.34})$$

3. The radii and energies of ultra-relativistic stable states inside the core (A.7.24) and (A.7.25) become:

$$R_L \simeq \left(\frac{2l+1}{2Z\alpha} \right)^{1/3}, \quad (\text{A.7.35})$$

$$\varepsilon \simeq \frac{3}{2}\beta \left[\left(\frac{2l+1}{2Z\alpha} \right)^{2/3} - 1 \right] mc^2. \quad (\text{A.7.36})$$

Note that radii R_L in the second and third cases are in unit of R_c .

Stability of semi-classical states

When these semi-classical states are not occupied as required by the Pauli Principle, the transition from one state to another with different discrete values of total angular momentum l (l_1, l_2 and $\Delta l = l_2 - l_1 = \pm 1$) undergoes by emission or absorption of a spin-1 (\hbar) photon. Following the energy and angular-momentum conservations, photon emitted or absorbed in the transition have angular momenta $p_\phi(l_2) - p_\phi(l_1) = \hbar(l_2 - l_1) = \pm\hbar$ and energy $\varepsilon(l_2) - \varepsilon(l_1)$. In this transition of stable states, the variation of radius is $\Delta R_L = R_L(l_2) - R_L(l_1)$.

We first consider the stability of semi-classical states against such transition in the case of point-like charge, i.e., Eqs. (A.7.31,A.7.32) with $l = 0, 1, 2, \dots$. As

required by the Heisenberg indeterminacy principle $\Delta\phi\Delta p_\phi \simeq 4\pi p_\phi(l) \gtrsim \hbar$, the absolute ground state for minimal energy and angular momentum is given by the $l = 0$ state, $p_\phi \sim \hbar/2$, $R_L \sim \lambda(Z\alpha)^{-1} \sqrt{1 - (2Z\alpha)^2} > 0$ and $\mathcal{E} \sim mc^2 \sqrt{1 - (2Z\alpha)^2} > 0$, which corresponds to the last stable orbit (A.7.17) in the classical scenario. Thus the stability of all semi-classical states $l > 0$ is guaranteed by the Pauli principle. This is only case for $Z\alpha \leq 1/2$. While for $Z\alpha > 1/2$, there is not an absolute ground state in the semi-classical scenario. This can be understood by examining how the lowest energy states are selected by the quantization rule in the semi-classical scenario out of the last stable orbits (A.7.17) in the classical scenario. For the case of $Z\alpha \leq 1/2$, equating p_ϕ in Eq. (A.7.17) to $p_\phi = \hbar(l + 1/2)$ (A.7.29), we find the selected state $l = 0$ is only possible solution so that the ground state $l = 0$ in the semi-classical scenario corresponds to the last stable orbits (A.7.17) in the classical scenario. While for the case of $Z\alpha > 1/2$, equating p_ϕ in Eq. (A.7.17) to $p_\phi = \hbar(l + 1/2)$ (A.7.29), we find the selected semi-classical state

$$\tilde{l} = \frac{Z\alpha - 1}{2} > 0, \quad (\text{A.7.37})$$

in the semi-classical scenario corresponds to the last stable orbits (A.7.17) in the classical scenario. This state $l = \tilde{l} > 0$ is not protected by the Heisenberg indeterminacy principle from quantum-mechanically decaying in \hbar -steps to the states with lower angular momenta and energies (correspondingly smaller radius R_L (A.7.31)) via photon emissions. This clearly shows that the “Z = 137-catastrophe” corresponds to $R_L \rightarrow 0$, falling to the center of the Coulomb potential and all semi-classical states (l) are unstable.

Then we consider the stability of semi-classical states against such transition in the case of charged cores $R_c \neq 0$. Substituting p_ϕ in Eq. (A.7.29) into Eq. (A.7.16), we obtain the selected semi-classical state \tilde{l} corresponding to the last stable orbit outside the core,

$$\tilde{l} = \sqrt{2} \left(\frac{R_c}{\lambda} \right) \left[\left(\frac{4R_c}{Z\alpha\lambda} + 1 \right)^{1/2} - 1 \right]^{-1/2} \approx (Z\alpha)^{1/4} \left(\frac{R_c}{\lambda} \right)^{3/4} > 0. \quad (\text{A.7.38})$$

Analogously to Eq. (A.7.37), the same argument concludes the instability of this semi-classical state, which must quantum-mechanically decay to states with angular momentum $l < \tilde{l}$ inside the core, provided these semi-classical states are not occupied. This conclusion is independent of $Z\alpha$ -value.

We go on to examine the stability of semi-classical states inside the core. In the non-relativistic case ($1 \gg \beta > \kappa^2$), the last classical stable orbits locate at $R_L \rightarrow 0$ and $p_\phi \rightarrow 0$ given by Eqs. (A.7.21,A.7.22), corresponding to the lowest semi-classical state (A.7.33,A.7.34) with $l = 0$ and energy $mc^2 > \mathcal{E} > 0$. In the ultra-relativistic case ($\beta > \kappa \gg 1$), the last classical stable orbits locate

at $R_L \rightarrow 0$ and $p_\phi \rightarrow 0$ given by Eqs. (A.7.24,A.7.25), corresponding to the lowest semi-classical state (A.7.35,A.7.36) with $l = 0$ and minimal energy,

$$\varepsilon \simeq \frac{3}{2}\beta \left[\left(\frac{1}{2Z\alpha} \right)^{2/3} - 1 \right] mc^2 \approx -\frac{3}{2}\beta mc^2. \quad (\text{A.7.39})$$

This concludes that the $l = 0$ semi-classical state inside the core is an absolute ground state in both non- and ultra-relativistic cases. The Pauli principle assure that all semi-classical states $l > 0$ are stable, provided all these states accommodate electrons. The electrons can be either present inside the neutral core or produced from the vacuum polarization, later will be discussed in details.

We are particular interested in the ultra-relativistic case $\beta > \kappa \gg 1$, i.e., $Z\alpha \gg 1$, the energy-levels of semi-classical states can be profound than $-mc^2$ ($\varepsilon < -mc^2$), energy-level crossings and pair-productions occur if these states are unoccupied, as discussed in introductory section. It is even more important to mention that neutral cores like neutron stars of proton number $Z \sim 10^{52}$, the Thomas-Fermi approach has to be adopted to find the configuration of electrons in these semi-classical states, which has the depth of energy-levels $\varepsilon \sim -m_\pi c^2$ to accommodate electrons and a supercritical electric field ($E > E_c$) on the surface of the core Ruffini et al. (2007b).

A.7.4. Production of electron-positron pair

When the energy-levels of semi-classical (bound) states $\varepsilon \leq -mc^2$ (A.7.27), energy-level crossings between these energy-levels (A.7.25) and negative energy continuum (A.7.10) for $p_r = 0$, as shown in Fig. A.29. The energy-level-crossing indicates that ε (A.7.25) and E_- (A.7.10) are equal,

$$\varepsilon = E_-, \quad (\text{A.7.40})$$

where angular momenta p_ϕ in ε (A.7.36) and E_- (A.7.10) are the same for angular-momentum conservation. The production of electron-positron pairs must takes place, provided these semi-classical (bound) states are unoccupied. The phenomenon of pair production can be understood as a quantum-mechanical tunneling process of relativistic electrons. The energy-levels ε of semi-classical (bound) states are given by Eq. (A.7.36) or (A.7.27). The probability amplitude for this process can be evaluated by a semi-classical calculation using WKB method Kleinert et al. (2008):

$$W_{\text{WKB}}(|\mathbf{p}_\perp|) \equiv \exp \left\{ -\frac{2}{\hbar} \int_{R_b}^{R_n} p_r dr \right\}, \quad (\text{A.7.41})$$

where $|\mathbf{p}_\perp| = p_\phi/r$ is transverse momenta and the radial momentum,

$$p_r(r) = \sqrt{(c|\mathbf{p}_\perp|)^2 + m^2c^4 - [\mathcal{E} + V(r)]^2}. \quad (\text{A.7.42})$$

The energy potential $V(r)$ is either given by $V_{\text{out}}(r)$ (A.7.11) for $r > R_c$, or $V_{\text{in}}(r)$ (A.7.12) for $r < R_c$. The limits of integration (A.7.41): $R_b = R_L < R_c$ (A.7.24) or (A.7.35) indicating the location of the classical orbit (classical turning point) of semi-classical (bound) state; while another classical turning point R_n is determined by setting $p_r(r) = 0$ in Eq. (A.7.42). There are two cases: $R_n < R_c$ and $R_n > R_c$, depending on β and κ values.

To obtain a maximal WKB-probability amplitude (A.7.41) of pair production, we only consider the case that the charge core is bare and

- the lowest energy-levels of semi-classical (bound) states: $p_\phi/(Ze^2) = \kappa/\beta \rightarrow 0$, the location of classical orbit(A.7.24) $R_L = R_b \rightarrow 0$ and energy (A.7.25) $\mathcal{E} \rightarrow \mathcal{E}_{\text{min}} = -3\beta mc^2/2$ (A.7.28);
- another classical turning point $R_n \leq R_c$, since the probability is exponentially suppressed by a large tunneling length $\Delta = R_n - R_b$.

In this case ($R_n \leq R_c$), Eq. (A.7.42) becomes

$$p_r = \sqrt{(c|\mathbf{p}_\perp|)^2 + m^2c^4} \sqrt{1 - \frac{\beta^2 m^2 c^4}{4[(c|\mathbf{p}_\perp|)^2 + m^2c^4]} \left(\frac{r}{R_c}\right)^4}, \quad (\text{A.7.43})$$

and $p_r = 0$ leads to

$$\frac{R_n}{R_c} = \left(\frac{2}{\beta mc^2}\right)^{1/2} [(c|\mathbf{p}_\perp|)^2 + m^2c^4]^{1/4}. \quad (\text{A.7.44})$$

Using Eqs. (A.7.41,A.7.43,A.7.44), we have

$$\begin{aligned} W_{\text{WKB}}(|\mathbf{p}_\perp|) &= \exp \left\{ -\frac{2^{3/2}[(c|\mathbf{p}_\perp|)^2 + m^2c^4]^{3/4} R_c}{c\hbar(mc^2\beta)^{1/2}} \int_0^1 \sqrt{1-x^4} dx \right\} \\ &= \exp \left\{ -0.87 \frac{2^{3/2}[(c|\mathbf{p}_\perp|)^2 + m^2c^4]^{3/4} R_c}{c\hbar(mc^2\beta)^{1/2}} \right\}. \end{aligned} \quad (\text{A.7.45})$$

Dividing this probability amplitude by the tunneling length $\Delta \simeq R_n$ and time interval $\Delta t \simeq 2\hbar\pi/(2mc^2)$ in which the quantum tunneling occurs, and integrating over two spin states and the transverse phase-space $2 \int d\mathbf{r}_\perp d\mathbf{p}_\perp / (2\pi\hbar)^2$, we approximately obtain the rate of pair-production per the unit of time and

volume,

$$\Gamma_{\text{NS}} \equiv \frac{d^4 N}{dt d^3 x} \simeq \frac{1.15}{6\pi^2} \left(\frac{Z\alpha}{\tau R_c^3} \right) \exp \left\{ -\frac{2.46}{(Z\alpha)^{1/2}} \left(\frac{R_c}{\lambda} \right)^{3/2} \right\}, \quad (\text{A.7.46})$$

$$= \frac{1.15}{6\pi^2} \left(\frac{\beta}{\tau \lambda R_c^2} \right) \exp \left\{ -\frac{2.46 R_c}{\beta^{1/2} \lambda} \right\}, \quad (\text{A.7.47})$$

$$= \frac{1.15}{6\pi^2} \left(\frac{1}{\tau \lambda^2 R_c} \right) \left(\frac{E_s}{E_c} \right) \exp \left\{ -2.46 \left(\frac{R_c}{\lambda} \right)^{1/2} \left(\frac{E_c}{E_s} \right)^{1/2} \right\}, \quad (\text{A.7.48})$$

where $E_s = Ze/R_c^2$ being the electric field on the surface of the core and the Compton time $\tau = \hbar/mc^2$.

To have the size of this pair-production rate, we compare it with the Sauter-Euler-Heisenberg-Schwinger rate of pair-production in a constant field E Heisenberg and Euler (1936); Sauter (1931); Schwinger (1951, 1954a,b),

$$\Gamma_S \equiv \frac{d^4 N}{dt d^3 x} \simeq \frac{1}{4\pi^3 \tau \lambda^3} \left(\frac{E}{E_c} \right)^2 \exp \left\{ -\pi \frac{E_c}{E} \right\}. \quad (\text{A.7.49})$$

When the parameter $\beta \simeq (R_c/\lambda)^2$, Eq. (A.7.47) becomes

$$\Gamma_{\text{NS}} \equiv \frac{d^4 N}{dt d^3 x} \simeq \frac{1.15}{6\pi^2} \left(\frac{1}{\tau \lambda^3} \right) \exp \{-2.46\} = 1.66 \cdot 10^{-3}/(\tau \lambda^3), \quad (\text{A.7.50})$$

which is close to the Sauter-Euler-Heisenberg-Schwinger rate (A.7.49) $\Gamma_S \simeq 3.5 \cdot 10^{-4}/(\tau \lambda^3)$ at $E \simeq E_c$. Taking a neutron star with core mass $M = M_\odot$ and radius $R_c = 10\text{km}$, we have $R_c/\lambda = 2.59 \cdot 10^{16}$ and $\beta = 3.86 \cdot 10^{-17} Z\alpha$, leading to $Z \simeq 2.4 \cdot 10^{51}$ and the electric field on the core surface $E_s/E_c = Z\alpha(\lambda/R_c)^2 \simeq 2.6 \cdot 10^{16}$. In this case, the charge-mass ratio $Q/(G^{1/2}M) = 2 \cdot 10^{-6}|e|/(G^{1/2}m_p) = 2.2 \cdot 10^{12}$, where where G is the Newton constant and proton's charge-mass ratio $|e|/(G^{1/2}m_p) = 1.1 \cdot 10^{18}$.

Let us consider another case that the electric field on the core surface E_s (A.7.13) is about the critical field ($E_s \simeq E_c$). In this case, $Z = \alpha^{-1}(R_c/\lambda)^2 \simeq 9.2 \cdot 10^{34}$, $\beta = Z\alpha\lambda/R_c = R_c/\lambda \simeq 2.59 \cdot 10^{16}$, and the rate (A.7.47) becomes

$$\Gamma_{\text{NS}} \equiv \frac{d^4 N}{dt d^3 x} \simeq \frac{1.15}{6\pi^2} \left(\frac{1}{\tau \lambda^3} \right) \left(\frac{\lambda}{R_c} \right) \exp \left\{ -2.46 \left(\frac{R_c}{\lambda} \right) \right\}, \quad (\text{A.7.51})$$

which is exponentially smaller than Eq. (A.7.50) for $R_c \gg \lambda$. In this case, the charge-mass ratio $Q/(G^{1/2}M) = 8.46 \cdot 10^{-5}$.

It is interesting to compare this rate of electron-positron pair-production with the rate given by the Hawking effect. We take $R_c = 2GM/c^2$ and the charge-mass ratio $Q/(G^{1/2}M) \simeq 10^{-19}$ for a naive balance between gravita-

tional and electric forces. In this case $\beta = \frac{1}{2}(Q/G^{1/2}M)(|e|/G^{1/2}m) \simeq 10^2$, the rate (A.7.47) becomes,

$$\Gamma_{\text{NS}} = \frac{1.15}{6\pi^2} \left(\frac{25}{\tau\lambda^3} \right) \left(\frac{1}{mM} \right) \exp \{-0.492(mM)\}, \quad (\text{A.7.52})$$

where $mM = R_c/(2\lambda)$. This is much larger than the rate of electron-positron emission by the Hawking effect Hawking (1974, 1975); Gibbons and Hawking (1977),

$$\Gamma_{\text{H}} \sim \exp \{-8\pi(mM)\}, \quad (\text{A.7.53})$$

since the exponential factor $e^{-0.492mM}$ is much larger than $e^{-8\pi mM}$, where $2mM = R_c/\lambda \gg 1$.

A.7.5. Summary and remarks

In this letter, analogously to the study in atomic physics with large atomic number Z , we study the classical and semi-classical (bound) states of electrons in the electric potential of a massive and charged core, which has a uniform charge distribution and macroscopic radius. We have found negative energy states of electrons inside the core, whose energies can be smaller than $-mc^2$, and the appearance of energy-level crossing to the negative energy spectrum. As results, quantum tunneling takes place, leading to electron-positron pairs production, electrons then occupy these semi-classical (bound) states and positrons are repelled to infinity. Assuming that massive charged cores are bare and non of these semi-classical (bound) states are occupied, we analytically obtain the maximal rate of electron-positron pair production in terms of core's radius, charge and mass, and we compare it with the Sauter-Euler-Heisenberg-Schwinger rate of pair-production in a constant field. We have seen that even for very small charge-mass ratio of the core that is given by the the naive balance between gravitational and electric forces, this rate is much larger than the rate of electron-positron pair-production by the Hawking effect.

Any electron occupations of these semi-classical (bound) states must screen core's charge and the massive core is no longer bare. The electric potential inside the core is changed. For the core consists of a large number of electrons, the Thomas-Fermi approach has to be adopted. We recently study Ruffini et al. (2007b) the electron distribution inside and outside the massive core, i.e., the distribution of electrons occupying stable states of the massive core, and find the electric field on the surface of the massive core is overcritical.

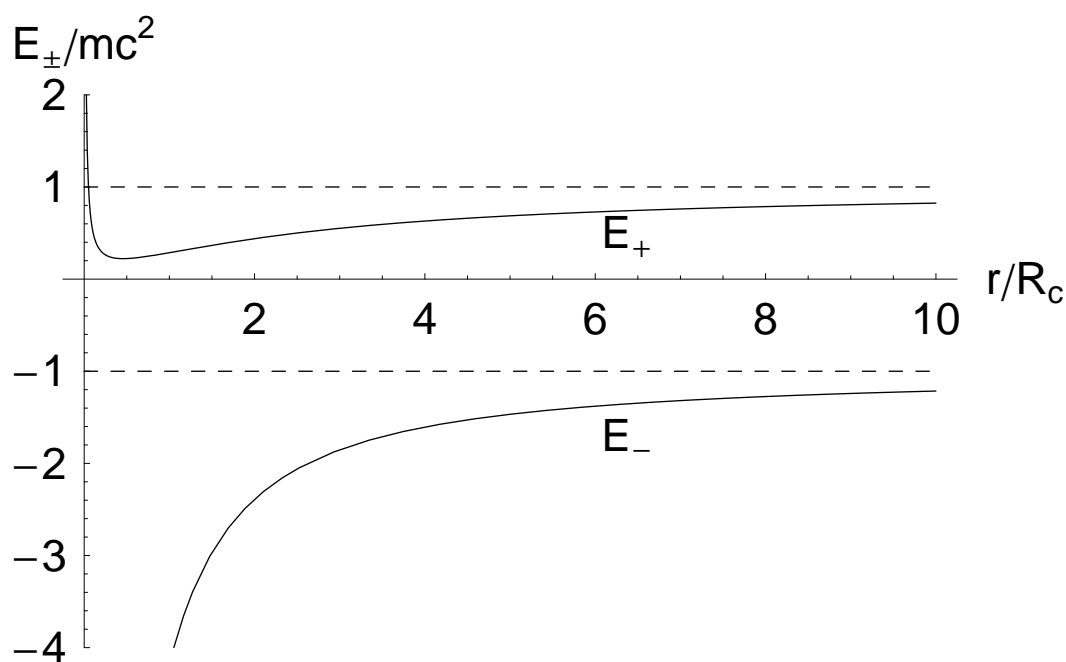


Figure A.28.: In the case of point-like charge distribution, we plot the positive and negative effective potential energies E_{\pm} (A.7.10), $p_{\phi}/(mcR_c) = 2$ and $Ze^2 = 1.95mc^2R_c$, to illustrate the radial location R_L (A.7.14) of stable orbits where E_+ has a minimum (A.7.15). All stable orbits are described by $cp_{\phi} > Ze^2$. The last stable orbits are given by $cp_{\phi} \rightarrow Ze^2 + 0^+$, whose radial location $R_L \rightarrow 0$ and energy $\mathcal{E} \rightarrow 0^+$. There is no any stable orbit with energy $\mathcal{E} < 0$ and the energy-level crossing with the negative energy spectrum E_- is impossible.

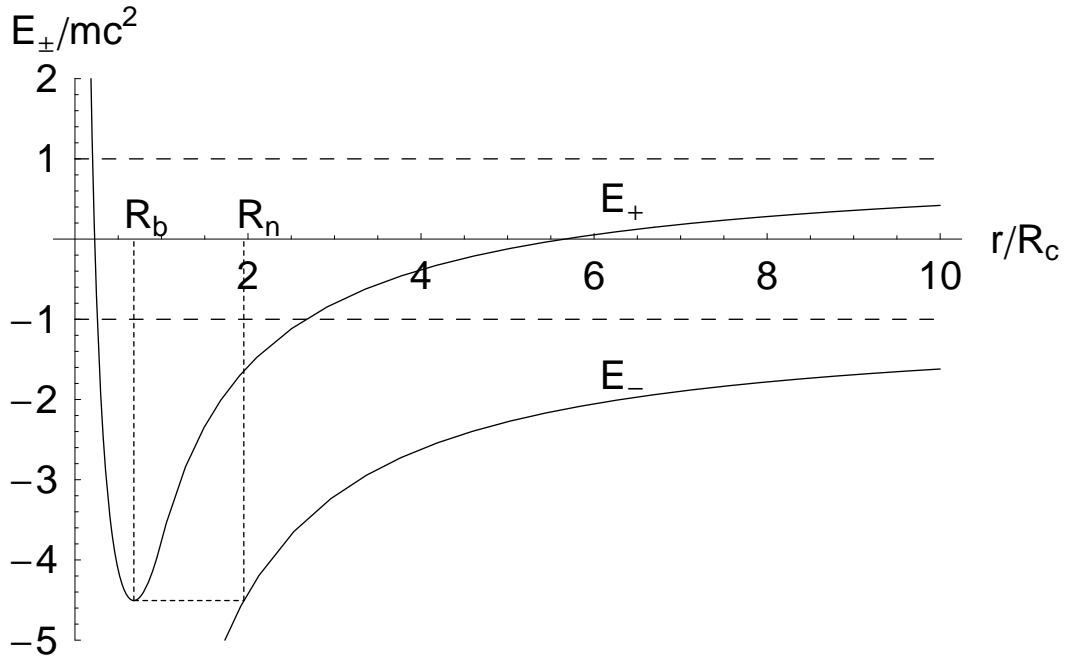


Figure A.29.: For the core $\kappa = 2$ and $\beta = 6$, we plot the positive and negative effective potentials E_{\pm} (A.7.10), in order to illustrate the radial location (A.7.24) $R_L < R_c$ of stable orbit, where E_+ 's minimum (A.7.25) $\mathcal{E} < mc^2$ is. All stable orbits inside the core are described by $\beta > \kappa > 1$. The last stable orbit is given by $\kappa/\beta \rightarrow 0$, whose radial location $R_L \rightarrow 0$ and energy $\mathcal{E} \rightarrow \mathcal{E}_{\min}$ (A.7.28). We indicate that the energy-level crossing between bound state (stable orbit) energy at $R_L = R_b$ and negative energy spectrum E_- (A.7.25) at the turning point R_n .

A.8. On Magnetic Fields in Rotating Nuclear Matter Cores of Stellar Dimensions

A.8.1. Introduction

Neutron stars are mainly detected as pulsars, whose regular pulsations in the radio, X-ray, and optical bands are produced by constant, ordered magnetic fields that are the strongest known in the Universe. However the origin of the magnetic field in the neutron stars is not fully understood, so far. Nevertheless in the literature one may find various hypotheses explaining the formation of the magnetic field Ginzburg (1964); Woltjer (1964); Ruderman (1972, 1995); Reisenegger (2001, 2007); Reisenegger et al. (2007). The simplest hypothesis to explain the presence of the strong fields observed in neutron stars is the conservation of the magnetic flux already present in the progenitor stars during the gravitational collapse. This idea is based on the assumption that all stars at all stages of their evolution have some magnetic field, due to electronic currents circulating in their interiors. Thus this argument led to the prediction of the fields $B \approx 10^{12}$ G in neutron stars a few years before the discovery of pulsars Ginzburg (1964); Woltjer (1964). However, there is no detailed physical picture of such a flux conserving collapse. Thompson and Duncan Thompson and Duncan (1993) put forward the hypothesis that newborn neutron stars are likely to combine vigorous convection and differential rotation making a dynamo process operate in them. They predicted fields up to $10^{15} - 10^{16}$ G in neutron stars with few millisecond initial periods, and suggested that such fields could explain much of the phenomenology associated with Soft Gamma Repeaters and Anomalous X-ray Pulsars Thompson and Duncan (1995, 1996).

Probably, these processes are not mutually exclusive. A strong field might be present in the collapsing star, but later be deformed and perhaps amplified by some combination of convection, differential rotation, and magnetic instabilities Tayler (1973); Spruit (2002). The relative importance of these ingredients depends on the initial field strength and rotation rate of the star. For both mechanisms, the field and its supporting currents are not likely to be confined to the solid crust of the star, but distributed in most of the stellar interior, which is mostly a fluid mixture of neutrons, protons, electrons, and other, more exotic particles.

Unlike aforementioned hypotheses which are based on the assumptions that all stars are magnetized or charged with some net charge different from zero, we explore the system recently considered by Ruffini et al. Ruffini et al. (2007b). According to that work the system consisting of degenerate neutrons, protons and electrons in beta equilibrium is globally neutral and expected to be kept at nuclear density by self gravity. In what follows these systems are termed as Nuclear Matter Cores of Stellar Dimensions. Despite

the global neutrality the charge distribution turned out to be different from zero inside and outside (near the surface) the star. The magnitude of the net charge inside and outside the core is equal, but the sign is opposite. Such an effect takes place as a consequence of the beta equilibrium, the penetration of electrons into the core, hence the screening of the core charge and global charge neutrality. As a result of this effect, one may show the presence of an electric field close to the critical value $E_c = m_e^2 c^3 / e \hbar$ near the surface of the massive cores, although localized in a very narrow shell. Thus in this case the magnetic field of the neutron star may be generated only if it spins like pulsars, even though the progenitor star has not been magnetized or electrically charged.

A.8.2. The Relativistic Thomas-Fermi equation

The Thomas-Fermi equation is the exact theory for atoms, molecules and solids as $Z \rightarrow \infty$ Lieb and Simon (1973). The relativistic Thomas-Fermi theory developed for the study of atoms for heavy nuclei with $Z = 10^6$ Ferreira et al. (1980); Ruffini and Stella (1981) gives important basic new information on the study of nuclear matter in bulk in the limit of $A = (m_{Planck}/m_n)^3$ nucleons of mass m_n and on its electrodynamic properties. The analysis of nuclear matter bulk in neutron stars composed of degenerate gas of neutrons, protons and electrons, has traditionally been approached by implementing microscopically the charge neutrality condition by requiring the electron density $n_e(r)$ to coincide with the proton density $n_p(r)$,

$$n_e(r) = n_p(r). \quad (\text{A.8.1})$$

It is clear however that especially when conditions close to the gravitational collapse occur, there is an ultra-relativistic component of degenerate electrons whose confinement requires the existence of very strong electromagnetic fields, in order to guarantee the overall charge neutrality of the neutron star. Under these conditions equation (A.8.1) will be necessarily violated.

Using substantially a statistical approach based on the relativistic Thomas-Fermi equation, Ferreira et al. Ferreira et al. (1980), Ruffini and Stella Ruffini and Stella (1981) have analyzed the electron densities around an extended nucleus in a neutral atom all the way up to $Z = 6000$. They have shown the effect of penetration of the electron orbital well inside the nucleus, leading to a screening of the nuclei positive charge and to the concept of an "effective" nuclear charge distribution.

In the work of Ruffini et. al. Ruffini et al. (2007b) and Popov et. al. Popov et al. (2010) the relativistic Thomas-Fermi equation has been used to extrapolate the treatment of super heavy nuclei to the case of nuclear matter cores of stellar dimensions. These cores represent the inner part of neutron stars and are characterized by an atomic number of order of $A = (m_{Planck}/m_n)^3 \approx 10^{57}$,

composed of degenerate N_n neutrons, N_p protons and N_e electrons in beta equilibrium and expected to be kept at nuclear density by self gravity. It has been shown that near the surface of the massive cores it is possible to have an electric field close to the critical value E_c , although localized in a very narrow shell of the order of the λ_e electron Compton wavelength. Now let us review the main assumptions and results of those works.

According to Ruffini et al. (2007b) and Popov et al. (2010) the protons are distributed at constant density n_p within a radius

$$R_c = \Delta \frac{\hbar}{m_\pi c} N_p^{1/3}, \quad (\text{A.8.2})$$

where Δ is a parameter such that $\Delta \approx 1$ ($\Delta < 1$) corresponds to nuclear (supranuclear) densities when applied to ordinary nuclei. The overall Coulomb potential satisfies the Poisson equation

$$\nabla^2 V(r) = -4\pi e [n_p(r) - n_e(r)], \quad (\text{A.8.3})$$

with the boundary conditions $V(\infty) = 0$ (due to the global charge neutrality of the system) and finiteness of $V(0)$. The density $n_e(r)$ of the electrons of charge $-e$ is determined by the Fermi energy condition on their Fermi momentum P_e^F ; we assume here

$$E_e^F = [(P_e^F c)^2 + m_e^2 c^4]^{1/2} - m_e c^2 - eV(r) = 0, \quad (\text{A.8.4})$$

which leads to

$$n_e(r) = \frac{(P_e^F)^3}{3\pi^2 \hbar^3} = \frac{1}{3\pi^2 \hbar^3 c^3} [e^2 V^2(r) + 2m_e c^2 eV(r)]^{3/2}. \quad (\text{A.8.5})$$

Introducing the dimensionless quantities $x = r/[\hbar/m_\pi c]$, $x_c = R_c/[\hbar/m_\pi c]$ and $\chi/r = eV(r)/c\hbar$, the relativistic Thomas-Fermi equation takes the form

$$\frac{1}{3x} \frac{d^2 \chi(x)}{dx^2} = -\frac{\alpha}{\Delta^3} H(x_c - x) + \frac{4\alpha}{9\pi} \left[\frac{\chi^2(x)}{x^2} + 2 \frac{m_e}{m_\pi} \frac{\chi}{x} \right]^{3/2}, \quad (\text{A.8.6})$$

where $\alpha = e^2/(\hbar c)$ is the fine structure constant, $H(x_c - x)$ is the Heaviside step function and the boundary conditions for $\chi(x)$ are $\chi(0) = 0, \chi(\infty) = 0$. The neutron density $n_n(r)$ is determined by the Fermi energy condition on their Fermi momentum P_n^F imposed by beta decay equilibrium

$$E_n^F = [(P_n^F c)^2 + m_n^2 c^4]^{1/2} - m_n c^2 = [(P_p^F c)^2 + m_p^2 c^4]^{1/2} - m_p c^2 + eV, \quad (\text{A.8.7})$$

which in turn is related to the proton and electron densities by Eqs. (A.8.3), (A.8.5) and (A.8.6).

A.8.3. The ultra-relativistic analytic solutions

In the ultrarelativistic limit with the planar approximation the relativistic Thomas-Fermi equation admits an analytic solution. Introducing the new function ϕ defined by $\phi = 4^{1/3}(9\pi)^{-1/3}\Delta\chi/x$ and the new variables $\hat{x} = (12/\pi)^{1/6}\sqrt{\alpha}\Delta^{-1}x$, $\xi = \hat{x} - \hat{x}_c$, where $\hat{x}_c = (12/\pi)^{1/6}\sqrt{\alpha}\Delta^{-1}x_c$, Eq. (A.8.6) becomes

$$\frac{d^2\hat{\phi}(\xi)}{d\xi^2} = -H(-\xi) + \hat{\phi}(\xi)^3, \quad (\text{A.8.8})$$

where $\hat{\phi}(\xi) = \phi(\xi + \hat{x}_c)$. The boundary conditions on $\hat{\phi}$ are: $\hat{\phi}(\xi) \rightarrow 1$ as $\xi \rightarrow -\hat{x}_c \ll 0$ (at the nuclear matter core center) and $\hat{\phi}(\xi) \rightarrow 0$ as $\xi \rightarrow \infty$. The function $\hat{\phi}$ and its first derivative $\hat{\phi}'$ must be continuous at the surface $\xi = 0$ of the nuclear matter core of stellar dimensions. Hence equation (A.8.8) admits an exact solution

$$\hat{\phi}(\xi) = \begin{cases} 1 - 3 \left[1 + 2^{-1/2} \sinh(a - \sqrt{3}\xi) \right]^{-1}, & \xi < 0, \\ \frac{\sqrt{2}}{(\xi + b)}, & \xi > 0, \end{cases} \quad (\text{A.8.9})$$

where the integration constants a and b have the values $a = \text{arccosh}(9\sqrt{3}) \approx 3.439$, $b = (4/3)\sqrt{2} \approx 1.886$. Next we evaluate the Coulomb potential function

$$V(\xi) = \left(\frac{9\pi}{4} \right)^{1/3} \frac{m_\pi c^2}{\Delta e} \hat{\phi}(\xi), \quad (\text{A.8.10})$$

and by differentiation, the electric field

$$E(\xi) = - \left(\frac{3^5 \pi}{4} \right)^{1/6} \frac{\sqrt{\alpha} m_\pi^2 c^3}{\Delta^2 e \hbar} \hat{\phi}'(\xi). \quad (\text{A.8.11})$$

Details are given in Figs. A.30 and A.31.

A.8.4. Rotating Nuclear Matter Cores of Stellar Dimensions in Classical Electrodynamics

In section A.8.2 and A.8.3 we have seen that in the massive nuclear density cores the electric charge distribution is different from zero, although it is globally neutral. In this section we investigate the case when this charge distribution is allowed to rotate with the constant angular velocity Ω around the axis of symmetry. Thus the magnetic field of the resultant current density is calculated in terms of the charge distribution.

A. The Thomas-Fermi model: from nuclei to nuclear matter cores of stellar dimensions

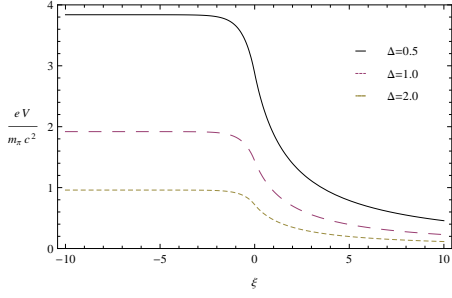


Figure A.30.: The electron Coulomb potential energy eV , in units of pion mass m_π is plotted as a function of the radial coordinate $\xi = \hat{x} - \hat{x}_c$, for selected values of the density parameter Δ .

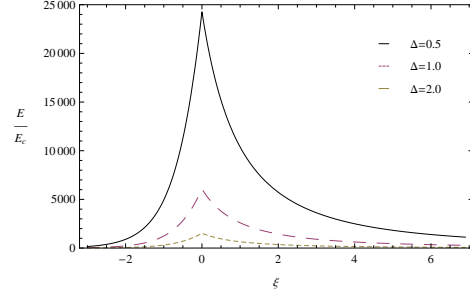


Figure A.31.: The electric field is plotted in units of the critical field E_c as a function of the radial coordinate ξ , showing a sharp peak at the core radius, for selected values of Δ .

Consider a charge distribution moving in a such way that at every point in space the charge density and the current density remain constant. In this case the magnetic field is defined by

$$\mathbf{B}(\mathbf{r}) = \nabla \times \mathbf{A}(\mathbf{r}), \quad \mathbf{A}(\mathbf{r}) = (\boldsymbol{\Omega}/c^2) \times \mathbf{F}(\mathbf{r}), \quad \mathbf{F}(\mathbf{r}) = \frac{1}{4\pi} \int \frac{\mathbf{r}'\rho(\mathbf{r}')d^3\mathbf{r}'}{|\mathbf{r}-\mathbf{r}'|}, \quad (\text{A.8.12})$$

where \mathbf{A} is the vector potential of the magnetic field, $\mathbf{F}(\mathbf{r})$ is the "superpotential" in general form. In the case of spherical symmetry, $\mathbf{F}(\mathbf{r})$ may be taken as radial (see Marsh Marsh (1982)). Writing $\mathbf{F}(\mathbf{r}) = \mathbf{e}_r F(r)$, where \mathbf{e}_r is the unit radial vector, one has

$$F(r) = \frac{1}{r^2} \int_0^r r'^2 \frac{d}{dr'} [r'V(r')] dr'. \quad (\text{A.8.13})$$

This expression allows to calculate the magnetic field due to rotation of any spherically symmetric distribution of charge in terms of its electrostatic Coulomb potential. Note that in fact due to rotation the shape of the neutron star must deviate from spherical symmetry. Since we are interested in the estimation of the order of the magnetic field the distortions to the shape of the star can be neglected for simplicity. Thus the magnetic field is defined by

$$\mathbf{B}(\mathbf{r}) = B_r \mathbf{e}_r + B_\theta \mathbf{e}_\theta, \quad B_r = \frac{2\Omega F}{c^2 r} \cos \theta, \quad B_\theta = -\frac{2\Omega}{c^2} \left[\frac{F}{r} + \frac{r}{2} \frac{d}{dr} \left(\frac{F}{r} \right) \right] \sin \theta, \quad (\text{A.8.14})$$

where B_r is the radial component and B_θ is the angular component of the magnetic field, θ is the angle between r and z axis, and \mathbf{e}_θ is the unit vector along θ . Consequently the expression for the magnitude (the absolute value)

of the magnetic field can be written as

$$B(r, \theta) = \frac{\Omega r}{c^2} \sqrt{\left(\frac{2F}{r^2}\right)^2 + \left\{ \frac{4F}{r^2} \frac{d}{dr} \left(\frac{F}{r}\right) + \left[\frac{d}{dr} \left(\frac{F}{r}\right) \right]^2 \right\} \sin^2 \theta}. \quad (\text{A.8.15})$$

Using the relation between r and ξ

$$r = R_c + \left(\frac{\pi}{12}\right)^{1/6} \frac{\Delta}{\sqrt{\alpha}} \frac{\hbar}{m_{\pi} c} \xi, \quad (\text{A.8.16})$$

one may estimate the value of the magnetic field. In Figs. A.32, A.33, A.34 and A.35 details are given.

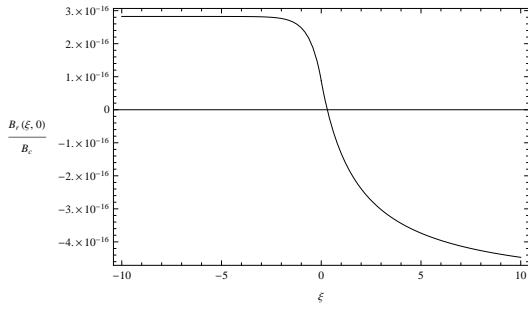


Figure A.32.: The radial component of the magnetic field is plotted as a function of the radial coordinate ξ in units of the critical field $B_c = m_c^2 c^3 / e \hbar \approx 4.5 \times 10^{13}$ G. Here the period is taken to be $P = 10$ ms, $\theta = 0$, $\Delta = 1$ and the radius of the core $R_c = 10$ km. Note that B_r is considered at the poles of star, where it has maximum value. Outside the star B_r has very small negative value and it tends to zero. Because of visualization difficulties it is not seen in the figure.

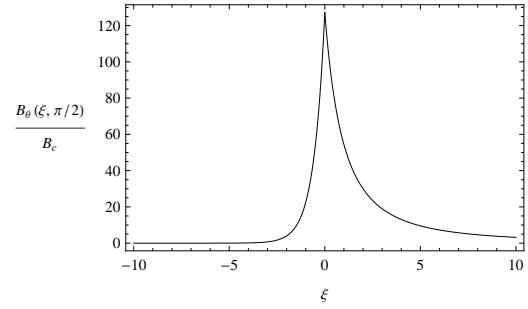


Figure A.33.: The angular component of the magnetic field is plotted in units of the B_c . Here $P = 10$ ms, $\theta = \pi/2$, $\Delta = 1$ and $R_c = 10$ km. Note that B_θ is considered at the equator, where it has maximum value. Inside the star it has very small constant negative value. Outside the star first it becomes negative (the value is very small) then it tends to zero. Because of scale problems this behavior is not seen from the figure.

Examining the Fig. A.32 one can see very small value of B_r which almost does not make a significant contribution to the magnitude of the field, except for the poles of the star. On the contrary, B_θ Fig. A.33 has values exceeding the critical magnetic field near the surface of the core although localized in a narrow region between positively and negatively charged shells as expected. Outside the core the magnetic field becomes negative. The magnitude of the

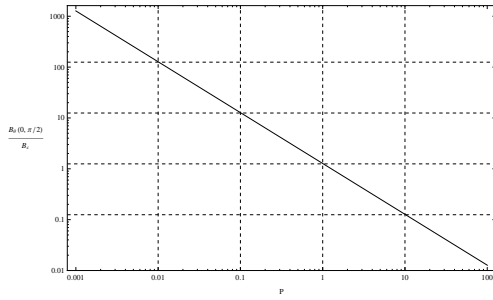


Figure A.34.: The magnitude of the magnetic field is plotted as a function of the period of the star P in the units of the critical field B_c at the surface of the core $R_c = 10 \text{ km}$ on the equator in the logarithmic scale.

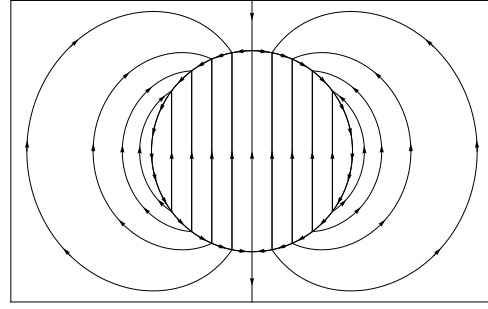


Figure A.35.: The magnetic lines of forces. Outside the star the magnetic field looks like a dipole field. Extra lines along the surface of the star indicate overcritical value of the field between positively and negatively charged shells.

field has very small and eventually vanishing values. This effect can not be seen from the figures, because of visualization difficulties.

In Fig. A.34 the magnitude of the magnetic field is presented as a function of the rotational period P on the surface of the core at the equator. Practically it demonstrates the upper limit of possible values of the magnetic field in the range between 1 ms and 100 s . Fig. A.35 represents magnetic lines of force inside, outside and on the surface of the star. It turned out that the lines of force of the overcritical magnetic field are oppressed between two shells along the surface of the core.

A.8.5. Conclusions

In this paper we have investigated the behavior of the magnetic field induced due to rotation on the basis of the research works considered in Ruffini et. al. Ruffini et al. (2007b) and Popov et. al. Popov et al. (2010) using the technique developed by Marsh Marsh (1982).

For this purpose considering a rotating neutron star with the period of 10 ms we have obtained the magnetic field of order of the critical field near the surface of the star and analyzed the magnetic lines of forces.

According to our results the magnetic fields of the neutron stars could be generated due to the rotation of the star as a whole rigid body. We believe that the generation of the magnetic field due to the rotation is the reason for the formation of the constant magnetic fields at the initial moments of neutron stars birth.

The problem of investigating the magnetic field in general relativity for a self-gravitating system of degenerate fermions in beta equilibrium is beyond

the scope of the present work. We expect to investigate this problem in the nearest future.

B. The Thomas-Fermi model in general relativistic systems

B.1. The general relativistic Thomas-Fermi theory of white-dwarfs

B.1.1. Introduction

The necessity of introducing the Fermi-Dirac statistics in order to overcome some conceptual difficulties in explaining the existence of white-dwarfs leading to the concept of degenerate stars was first advanced by R. H. Fowler in a classic paper (Fowler, 1926). Following that work, E. C. Stoner (Stoner, 1929) introduced the effect of special relativity into the Fowler considerations and, using what later became known as the exclusion principle, generally attributed in literature to Wolfgang Pauli, he discovered the concept of critical mass of white-dwarfs ¹

$$M_{\text{crit}}^{\text{Stoner}} = \frac{15}{16} \sqrt{5\pi} \frac{M_{\text{Pl}}^3}{\mu^2 m_n^2} \approx 3.72 \frac{M_{\text{Pl}}^3}{\mu^2 m_n^2}, \quad (\text{B.1.1})$$

where $M_{\text{Pl}} = \sqrt{\hbar c / G} \approx 10^{-5}$ g is the Planck mass, m_n is the neutron mass, and $\mu = A/Z \approx 2$ is the average molecular weight of matter which shows explicitly the dependence of the critical mass on the chemical composition of the star.

Following the Stoner's work, S. Chandrasekhar (Chandrasekhar, 1931b) at the time a 20 years old graduate student coming to Cambridge from India pointed out the relevance of describing white-dwarfs by using an approach, initiated by E. A. Milne (Milne, 1930), of using the powerful mathematical method of the solutions of the Lane-Emden polytropic equations (Emden, 1907). The same idea of using the Lane-Emden equations taking into account the special relativistic effects to the equilibrium of stellar matter for a degenerate system of fermions, came independently to L. D. Landau (Landau, 1932). Both the Chandrasekhar and Landau treatments were explicit in pointing out

¹For a lucid and scientifically correct historical reconstruction of the contributions to the critical mass concept see Nauenberg (2008).

the existence of the critical mass

$$M_{\text{crit}}^{\text{Ch-L}} = 2.015 \frac{\sqrt{3\pi}}{2} \frac{M_{\text{Pl}}^3}{\mu^2 m_n^2} \approx 3.09 \frac{M_{\text{Pl}}^3}{\mu^2 m_n^2}, \quad (\text{B.1.2})$$

where the first numerical factor on the right hand side of Eq. (B.1.2) comes from the boundary condition $-(r^2 du/dr)_{r=R} = 2.015$ (see last entry of Table 7 on Pag. 80 in Emden (1907)) of the $n = 3$ Lane-Emden polytropic equation. Namely for $M > M_{\text{crit}}^{\text{Ch-L}}$, no equilibrium configuration should exist.

This unexpected result created a wave of emotional reactions: Landau rejected the idea of the existence of such a critical mass as a “ridiculous tendency” (Landau, 1932). Chandrasekhar was confronted by a lively dispute with A. Eddington on the basic theoretical assumptions he adopted (see Wali (1982) for historical details). The dispute reached such a heated level that Chandrasekhar was confronted with the option either to change field of research or to leave Cambridge. As is well known he chose the second option transferring to Yerkes Observatory near Chicago where he published his results in his classic book (Chandrasekhar, 1939).

Some of the basic assumptions adopted by Chandrasekhar and Landau in their idealized approach were not justified e.g. the treatment of the electron as a free-gas without taking into due account the electromagnetic interactions, as well as the stability of the nuclear component against the gravitational interaction. It is not surprising that such an approach led to the criticisms of Eddington who considered that the physical foundation of the Chandrasekhar work did not inspire confidence. It goes to Eddington credit, at the time Plumian Professor at Cambridge, to have allowed the publication of the Chandrasekhar work although preceded by his own critical considerations (Eddington, 1935). It was unfortunate that the absence of interest of E. Fermi on the final evolution of stars did not allow Fermi himself to intervene in this contention and solve definitely these well-posed theoretical problems (Boccaletti and Ruffini, 2010). Indeed, we are showing in this article how the solution of the conceptual problems of the white-dwarf models, left open for years, can be duly addressed by considering the relativistic Thomas-Fermi model of the compressed atom (see Subsec. B.1.7 and Sec. B.1.11).

The original work on white-dwarfs was motivated by astrophysics and found in astrophysics strong observational support. From the theoretical physics point of view, which is the topic of this article, the study of white-dwarfs presented at the time and still presents today open issues of the greatest interest. The issue of the equilibrium of the electron gas and the associated nuclear component taking into account the electromagnetic, the gravitational and the weak interactions formulated in a correct special and general relativistic context has been and still is one of the most popular.

One of the earliest alternative approaches to the Chandrasekhar-Landau work was proposed by E. E. Salpeter in 1961 (Salpeter, 1961). He followed an

idea originally proposed by Y. I. Frenkel (Frenkel, 1928): to adopt in the study of white-dwarfs the concept of a Wigner-Seitz cell. Salpeter introduced to the lattice model of a point-like nucleus surrounded by a uniform cloud of electrons, corrections due to the non-uniformity of the electron fluid surrounding each nucleus. Thus, to the well-known lattice energy $E_C = -(9\alpha Z^2)/(10R_{ws})$ resulting from the Coulomb interaction between the point-like nucleus with the uniform surrounding electrons and from the electron-electron interaction, Salpeter introduced the non-uniform correction by assuming the electron distribution $n_e[1 + \epsilon(r)]$ being $\epsilon(r)$ infinitesimal and n_e the electron number density in the uniform approximation. The correction $\epsilon(r)$ is obtained through a first-order series expansion of the relativistic electron kinetic energy by considering the ratio eV/E_e^F between the Coulomb potential energy and the electron Fermi energy $E_e^F = \sqrt{[cP_e^F(r)]^2 + m_e^2c^4} - m_e c^2 - eV$ as infinitesimal (see Subsec. B.1.5 for details). In this way Salpeter obtained in (Salpeter, 1961) an analytic formula for the total energy in a Wigner-Seitz cell and derived the corresponding equation of state of matter composed by such cells, pointing out explicitly the relevance of taking into account the Coulomb interaction.

The consequences of taking into account these Coulomb interactions in the determination of the mass and radius of white-dwarfs, was pointed out in a subsequent paper by T. Hamada and E. E. Salpeter (Hamada and Salpeter, 1961) by using the equation of state constructed in Salpeter (1961). They found that the critical mass of white-dwarfs depends in a non-trivial way on the specific nuclear composition: the critical mass of Chandrasekhar-Landau which depends only on the mass to charge ratio of nuclei A/Z , now depends independently on the mass number A and on the proton number Z .

This fact can be seen from the approximate expression for the critical mass of white dwarfs obtained by Hamada and Salpeter (1961) in the ultrarelativistic limit for the electrons

$$M_{\text{crit}}^{\text{H\&S}} = 2.015 \frac{\sqrt{3\pi}}{2} \frac{1}{\mu_{\text{eff}}^2} \frac{M_{\text{Pl}}^3}{m_n^2}, \quad (\text{B.1.3})$$

where

$$\mu_{\text{eff}} = \mu \left(\frac{P_S}{P_{\text{Ch}}} \right)^{-3/4}, \quad (\text{B.1.4})$$

being P_S the pressure of the Wigner-Seitz cell obtained by Salpeter (1961) taking into account Coulomb interactions (see Subsec. B.1.5) and P_{Ch} is the pressure of a free-electron fluid used by Chandrasekhar (see Subsec. B.1.3). The ratio P_S/P_{Ch} is a function of the number of protons Z (see Eq. (20) in Salpeter (1961)) and it satisfies $P_S/P_{\text{Ch}} < 1$. Consequently, the effective molecular weight satisfies $\mu_{\text{eff}} > \mu$ and the critical mass of white-dwarfs turns to be smaller with respect to the original numerical value obtained by Chandrasekhar-Landau (see Eq. (B.1.2)).

In the mean time, the problem of the equilibrium gas in a white-dwarf taking into account possible global electromagnetic interactions between the nucleus and the electrons was addressed by E. Olson and M. Baily in (Olson and Baily, 1975, 1976). They well summarized the status of the problem: *“Traditional models for the white dwarf are non-relativistic and electrically neutral ... although a electric field is needed to support the pressureless nuclei against gravitational collapse, the star is treated essentially in terms of only one charge component, where charge neutrality is assumed”*. Their solution to the problem invokes the breakdown of the local charge neutrality and the presence of an overall electric field as a consequence of treating also the nuclei inside the white-dwarf as a fluid. They treated the white-dwarf matter through a two-fluid model not enforcing local charge neutrality. The closure equation for the Einstein-Maxwell system of equations was there obtained from a minimization procedure of the mass-energy of the configuration. This work was the first in pointing out the relevance of the Einstein-Maxwell equations in the description of an astrophysical system by requiring global and non local charge neutrality. As we will show here, this interesting approach does not apply to the case of white-dwarfs. It represents, however, a new development in the study of neutron stars (see e.g. Rueda et al. (2010c))

An alternative approach to the Salpeter treatment of a compressed atom was reconsidered by introducing the relativistic Thomas-Fermi treatment and the extended nucleus within a phenomenological description (Ferreirinho et al., 1980; Ruffini and Stella, 1981).

Recently, the study of a compressed atom has been revisited in (Rotondo et al., 2009) by extending to special relativity the powerful global approach of Feynman, Metropolis and Teller (Feynman et al., 1949), which takes into account all the Coulomb contributions duly expressed relativistically without the need of any piecewise description. In this model a unified approach is introduced bypassing the phenomenological mass-formula for nuclei. The relativistic Thomas-Fermi model has been solved by imposing in addition to the electromagnetic interaction also the weak interaction between neutrons, protons and electrons, self-consistently. This presents some conceptual differences with respect to previous approaches and can be used in order both to validate and to establish the limitations of previous approaches.

In this article we apply the considerations presented in (Rotondo et al., 2009) of a compressed atom in a Wigner-Seitz cell to the description of a non-rotating white-dwarf in general relativity. Paradoxically, after all this procedure which takes into account many additional theoretical features generalizing the Chandrasekhar-Landau work, a most simple equation is found to be fulfilled by the equilibrium configuration in a spherically symmetric metric. Assuming the metric

$$ds^2 = e^{\nu(r)} c^2 dt^2 - e^{\lambda(r)} dr^2 - r^2 d\theta^2 - r^2 \sin^2 \theta d\varphi^2, \quad (\text{B.1.5})$$

we demonstrate how the entire system of equations describing the equilibrium of white-dwarfs, taking into account the weak, the electromagnetic and the gravitational interactions as well as quantum statistics all expressed consistently in a general relativistic approach, is simply given by

$$\sqrt{g_{00}}\mu_{\text{ws}} = e^{\nu(r)/2}\mu_{\text{ws}}(r) = \text{constant}, \quad (\text{B.1.6})$$

which links the chemical potential of the Wigner-Seitz cell μ_{ws} , duly solved by considering the relativistic Feynman-Metropolis-Teller model following Rotondo et al. (2009), to the general relativistic gravitational potential at each point of the configuration. The overall system outside each Wigner-Seitz cell is strictly neutral and no global electric field exists, contrary to the results reported in (Olson and Bailyn, 1976). The same procedure will apply as well to the case of neutron star crusts.

The article is organized as follows. In Sec. B.1.2 we summarize the most common approaches used for the description of white-dwarfs and neutron star crusts: the uniform approximation for the electron fluid used by Chandrasekhar (1931b) in his theory of white-dwarfs; the lattice model of a point-like nucleus surrounded by a uniform electron cloud, used for instance by Baym et al. (1971b); the generalization of the lattice model due to Salpeter (1961) which introduces non-uniformity corrections on the electron fluid. Salpeter showed how the white-dwarf matter can be assumed as arranged in a Wigner-Seitz lattice composed of cells of radius R_{ws} filled by a relativistic gas of Z electrons in equilibrium with a nucleus of A nucleons. We turn then to the Feynman, Metropolis and Teller approach (Feynman et al., 1949) based on the the non-relativistic Thomas-Fermi model for a compressed atom and, to the relativistic generalization of the Feynman, Metropolis and Teller treatment recently introduced in (Rotondo et al., 2009).

In Sec. B.1.8 we formulate the general relativistic equations of equilibrium of the system and show how, from the self-consistent definition of chemical potential of the Wigner-Seitz cell and the Einstein equations, comes the equilibrium condition given by Eq. (B.1.6). In addition, we obtain the Newtonian and the first-order post-Newtonian equations of equilibrium through by expanding in the appropriate limits the general relativistic equations of equilibrium.

Finally, we show in Sec. B.1.11 the new results of the numerical integration of the general relativistic equations of equilibrium and discuss the corrections to the Stoner critical mass $M_{\text{crit}}^{\text{Stoner}}$, to the Chandrasekhar-Landau mass limit $M_{\text{crit}}^{\text{Ch-L}}$, as well as to the one of Hamada and Salpeter $M_{\text{crit}}^{\text{H\&S}}$, obtained when all effects are taken into account through the relativistic Feynman, Metropolis and Teller approach (Rotondo et al., 2009) in general relativity.

B.1.2. The Equation of State

There exists a large variety of approaches to model the equation of state of white-dwarf matter, each one characterized by a different way of treating or neglecting the Coulomb interaction inside each Wigner-Seitz cell, which we will briefly review here. Particular attention is given to the calculation of the self-consistent chemical potential of the Wigner-Seitz cell μ_{ws} , which plays a very important role in the conservation law (B.1.6) that we will derive below in Sec. B.1.8.

B.1.3. The uniform approximation

In the uniform approximation (see e.g. Chandrasekhar (1931b)), the electron distribution as well as the nucleons are assumed to be constant locally. In such a model no concept of Wigner-Seitz cell exists and then the condition of local charge neutrality

$$n_e = \frac{Z}{A}n_N, \quad (\text{B.1.7})$$

is applied. Then, the electromagnetic interaction is taken no into account either between electrons or between a well defined nucleus with surrounding electrons.

The electrons are considered as a fully degenerate free-gas and then described by Fermi-Dirac statistics. Thus, the electron density n_e is related to the electron Fermi-momentum by

$$n_e = \frac{(P_e^F)^3}{3\pi^2\hbar^3}, \quad (\text{B.1.8})$$

and the total electron energy-density and electron pressure are given by

$$\begin{aligned} \mathcal{E}_e &= \frac{2}{(2\pi\hbar)^3} \int_0^{P_e^F} \sqrt{c^2p^2 + m_e^2c^4} 4\pi p^2 dp \\ &= \frac{m_e^4c^5}{8\pi^2\hbar^3} [x_e \sqrt{1 + x_e^2(1 + 2x_e^2)} - \text{arcsinh}(x_e)], \end{aligned} \quad (\text{B.1.9})$$

$$\begin{aligned} P_e &= \frac{1}{3} \frac{2}{(2\pi\hbar)^3} \int_0^{P_e^F} \frac{c^2p^2}{\sqrt{c^2p^2 + m_e^2c^4}} 4\pi p^2 dp \\ &= \frac{m_e^4c^5}{8\pi^2\hbar^3} [x_e \sqrt{1 + x_e^2(2x_e^2/3 - 1)} \\ &\quad + \text{arcsinh}(x_e)]. \end{aligned} \quad (\text{B.1.10})$$

where we have introduced $x_e = P_e^F / (m_e c)$.

Then, for a given nucleus (A, Z) , the total energy-density of the configura-

tion can be written as

$$\mathcal{E} = \mathcal{E}_N + \mathcal{E}_e, \quad (\text{B.1.11})$$

being

$$\mathcal{E}_N = \frac{A}{Z} m_N c^2 n_e, \quad (\text{B.1.12})$$

where we have used Eq. (B.1.7) and m_N denotes the nucleon mass.

The total pressure is given by

$$P = P_N + P_e = P_e, \quad (\text{B.1.13})$$

where P_e is given by Eq. (B.1.10).

The total chemical potential is obtained from thermodynamical consistency as

$$\mu = \frac{\mathcal{E} + P}{n_e/Z}. \quad (\text{B.1.14})$$

Then, the chemical potential in the uniform approximation is given by

$$\mu = A m_N c^2 + Z \mu_e, \quad (\text{B.1.15})$$

where

$$\mu_e = \frac{\mathcal{E}_e + P_e}{n_e} = \sqrt{c^2 (P_e^F)^2 + m_e^2 c^4}, \quad (\text{B.1.16})$$

is the electron free-chemical potential. As a consequence of this effective approach which does not take into any account the Coulomb interaction, it is obtained the effective chemical potential (B.1.15). It can be interpreted as the chemical potential of an effective one-component electron-nucleon fluid where the kinetic pressure is given by electrons of mass m_e and their gravitational contribution is given by an effective mass $A m_N / Z$ attached to each electron.

B.1.4. Uniform approximation with point-like nucleus

The first correction to the above uniform model, corresponds to abandon the assumption of the electron-nucleon fluid. The concept of Wigner-Seitz cell is introduced where a point-like nucleus of charge $+Ze$ with A nucleons is surrounded by a uniformly distributed cloud of Z fully-degenerate electrons.

The global neutrality of the cell is given by

$$Z = V_{\text{ws}} n_e = \frac{n_e}{n_{\text{ws}}}, \quad (\text{B.1.17})$$

where $n_{\text{ws}} = 1/V_{\text{ws}}$ is the Wigner-Seitz cell density and $V_{\text{ws}} = 4\pi R_{\text{ws}}^3/3$ is the cell volume.

The total energy of the Wigner-Seitz cell is now written as the sum of the

nucleons energy, plus the electron kinetic energy, plus the Coulomb interaction energy

$$E_{\text{ws}} = E_N + E_k^{(e)} + E_C, \quad (\text{B.1.18})$$

being

$$E_N = Am_N c^2, \quad (\text{B.1.19})$$

$$E_k^{(e)} = \mathcal{E}_e V_{\text{ws}}, \quad (\text{B.1.20})$$

$$E_C = E_{e-N} + E_{e-e} = -\frac{9}{10} \frac{Z^2 e^2}{R_{\text{ws}}}, \quad (\text{B.1.21})$$

where \mathcal{E}_e is given by (B.1.9) and E_{e-N} and E_{e-e} are the electron-nucleus Coulomb energy and the electron-electron Coulomb energy, which are given by

$$\begin{aligned} E_{e-N} &= -\int_0^{R_{\text{ws}}} 4\pi r^2 \left(\frac{Ze}{r}\right) en_e dr \\ &= -\frac{3}{2} \frac{Z^2 e^2}{R_{\text{ws}}}, \end{aligned} \quad (\text{B.1.22})$$

$$E_{e-e} = \frac{3}{5} \frac{Z^2 e^2}{R_{\text{ws}}}. \quad (\text{B.1.23})$$

The energy given by Eq. (B.1.23) is the well-known Coulomb energy of a uniform distribution of charged particles. The total interaction energy (B.1.21) is the so-called lattice energy.

The self-consistent pressure of the Wigner-Seitz cell is then given by

$$P_{\text{ws}} = -\frac{\partial E_{\text{ws}}}{\partial V_{\text{ws}}} = P_N + P_k^{(e)} + P_C, \quad (\text{B.1.24})$$

being

$$P_N = -\frac{\partial E_N}{\partial V_{\text{ws}}} = 0, \quad (\text{B.1.25})$$

$$P_k^{(e)} = -\frac{\partial E_k^{(e)}}{\partial V_{\text{ws}}} = P_e(n_e), \quad (\text{B.1.26})$$

$$P_C = -\frac{\partial E_C}{\partial V_{\text{ws}}} = \frac{1}{3} \frac{E_C}{V_{\text{ws}}}, \quad (\text{B.1.27})$$

where P_e is given by Eq. (B.1.10). It is worth to recall that, the point-like assumption of the nucleus is incompatible with a relativistic treatment of the electron distribution (see Ferreira et al. (1980); Ruffini and Stella (1981) for details). It is a matter of fact that, such an inconsistency has been traditionally ignored by, applying within a point-like nucleus model, the relativistic formulas (B.1.9) and (B.1.10) and their corresponding ultrarelativistic limits

(see e.g. Salpeter (1961)).

The Wigner-Seitz cell chemical potential is, in this case, given by

$$\mu_{ws} = E_{ws} + P_{ws}V_{ws} = Am_Nc^2 + Z\mu_e + \frac{4}{3}E_C. \quad (\text{B.1.28})$$

It can be seen from Eq. (B.1.24) and (B.1.27) that the inclusion of the Coulomb interaction results in a decreasing of the pressure of the cell, due to the negative lattice energy E_C . The same conclusion is valid for the chemical potential μ_{ws} , as can be seen from Eq. (B.1.28).

B.1.5. Salpeter's approach

Keeping the point-like nucleus assumption, Salpeter (1961) studied the corrections to the above models due to the non-uniformity of the electron distribution inside the Wigner-Seitz cell.

The first contribution to the energy within the Salpeter treatment corresponds to the lattice energy (B.1.21), which results from the point-like nucleus-electron interaction and, from the electron-electron interaction inside the cell of radius R_{ws} .

The second contribution is given by a series-expansion of the Thomas-Fermi energy about the average electron density n_e given by the uniform approximation (B.1.17), i.e. $n_e = 3Z/(4\pi R_{ws}^3)$. The electron density is then assumed as $n_e[1 + \epsilon(r)]$, considering $\epsilon(r)$ as infinitesimal. The Coulomb potential energy is assumed to be the one of the point-like nucleus surrounded by a uniform distribution of electrons, so the correction given by $\epsilon(r)$ on the Coulomb potential is neglected. The electron distribution is then calculated at first-order by expanding the relativistic electron kinetic energy

$$\begin{aligned} \epsilon_k &= \sqrt{[cP_e^F(r)]^2 + m_e^2c^4} - m_e c^2 \\ &= \sqrt{\hbar^2c^2(3\pi^2n_e)^{2/3}[1 + \epsilon(r)]^{2/3} + m_e^2c^4} \\ &\quad - m_e c^2, \end{aligned} \quad (\text{B.1.29})$$

about its value in the uniform approximation

$$\epsilon_k^{\text{unif}} = \sqrt{\hbar^2c^2(3\pi^2n_e)^{2/3} + m_e^2c^4} - m_e c^2, \quad (\text{B.1.30})$$

considering as infinitesimal the ratio eV/E_e^F between the Coulomb potential energy eV and the electron Fermi energy

$$E_e^F = \sqrt{[cP_e^F(r)]^2 + m_e^2c^4} - m_e c^2 - eV. \quad (\text{B.1.31})$$

The influence of the Dirac electron-exchange correction (Dirac, 1930) on the equation of state was also considered by Salpeter (1961). However, adopting the general approach of Migdal et al. (1977), it has been shown that these effects are negligible in the relativistic regime (Rotondo et al., 2009). We will then consider here only the major correction of the Salpeter treatment.

The total energy of the Wigner-Seitz cell is then given by (see Salpeter (1961) for details)

$$E_{\text{ws}} = E_N + E_k^{(e)} + E_C + E_{TF}^S, \quad (\text{B.1.32})$$

being

$$E_N = Am_N c^2, \quad (\text{B.1.33})$$

$$E_k^{(e)} = \mathcal{E}_e V_{\text{ws}}, \quad (\text{B.1.34})$$

$$E_C = -\frac{9}{10} \frac{Z^2 e^2}{R_{\text{ws}}}, \quad (\text{B.1.35})$$

$$E_{TF}^S = -\frac{162}{175} \left(\frac{4}{9\pi} \right)^{2/3} \alpha^2 Z^{7/3} \mu_e, \quad (\text{B.1.36})$$

where \mathcal{E}_e is given by Eq. (B.1.9), μ_e is given by Eq. (B.1.16) and $\alpha = e^2/(\hbar c)$ is the fine structure constant.

The self-consistent pressure of the Wigner-Seitz cell is

$$P_{\text{ws}} = -\frac{\partial E_{\text{ws}}}{\partial V_{\text{ws}}} = P_N + P_k^{(e)} + P_C + P_{TF}^S, \quad (\text{B.1.37})$$

being

$$P_N = -\frac{\partial E_N}{\partial V_{\text{ws}}} = 0, \quad (\text{B.1.38})$$

$$P_k^{(e)} = -\frac{\partial E_k^{(e)}}{\partial V_{\text{ws}}} = P_e(n_e), \quad (\text{B.1.39})$$

$$P_C = -\frac{\partial E_C}{\partial V_{\text{ws}}} = \frac{1}{3} \frac{E_C}{V_{\text{ws}}}, \quad (\text{B.1.40})$$

$$P_{TF}^S = -\frac{\partial E_{TF}^S}{\partial V_{\text{ws}}} = \frac{1}{3} \left(\frac{P_e^F}{\mu_e} \right)^2 \frac{E_{TF}^S}{V_{\text{ws}}}, \quad (\text{B.1.41})$$

where P_e is given by Eq. (B.1.10) and the electron Fermi momentum P_e^F is related to the electron density by Eq. (B.1.8), and then to the number of electrons Z and the volume of the cell V_{ws} through Eq. (B.1.17).

The self-consistent Wigner-Seitz cell chemical potential can be then written

as

$$\begin{aligned} \mu_{\text{ws}} &= E_{\text{ws}} + P_{\text{ws}}V_{\text{ws}} = Am_Nc^2 + Z\mu_e + \frac{4}{3}E_C \\ &+ E_{TF}^S \left[1 + \frac{1}{3} \left(\frac{P_e^F}{\mu_e} \right)^2 \right]. \end{aligned} \quad (\text{B.1.42})$$

From Eqs. (B.1.37) and (B.1.42), we see that the inclusion of each additional Coulomb correction results in a decreasing of the pressure of the cell P_{ws} and of the chemical potential of the cell μ_{ws} . The Salpeter approach is very interesting in identifying piecewise Coulomb contribution to the total energy, to the total pressure and, to the Wigner-Seitz chemical potential. However, it does not have the full consistency of the global solutions obtained with the Feynman-Metropolis-Teller approach (Feynman et al., 1949) and its generalization to relativistic regimes (Rotondo et al., 2009) which we will discuss in detail below.

B.1.6. The Feynman-Metropolis-Teller treatment

Feynman, Metropolis and Teller (Feynman et al., 1949) showed how to derive the equation of state of matter at high pressures by considering a Thomas-Fermi model confined in a Wigner-Seitz cell of radius R_{ws} .

The condition of equilibrium of the electrons in the cell, in the non-relativistic case, is expressed by

$$E_e^F = \frac{(P_e^F)^2}{2m_e} - eV = \text{constant} > 0, \quad (\text{B.1.43})$$

where V denotes the Coulomb potential and E_e^F denotes the Fermi energy of electrons, which is positive for configurations subjected to external pressure, namely, for compressed cells.

Defining the function $\phi(r)$ by $eV(r) + E_e^F = e^2Z\phi(r)/r$, and introducing the dimensionless radial coordinate η by $r = b\eta$, where $b = \frac{(3\pi)^{2/3}\lambda_e}{2^{7/3}\alpha Z^{1/3}}$, being $\lambda_e = \hbar/(m_e c)$ the electron Compton wavelength; the Poisson equation from which the Coulomb potential V is calculated self-consistently becomes

$$\frac{d^2\phi(\eta)}{d\eta^2} = \frac{\phi(\eta)^{3/2}}{\eta^{1/2}}. \quad (\text{B.1.44})$$

The boundary conditions for Eq. (B.1.44) follow from the point-like structure of the nucleus $\phi(0) = 1$ and, from the global neutrality of the Wigner-Seitz cell $\phi(\eta_0) = \eta_0 d\phi/d\eta|_{\eta=\eta_0}$, where η_0 defines the dimensionless radius of the Wigner-Seitz cell by $\eta_0 = R_{\text{ws}}/b$.

For each value of the compression, for instance η_0 , it corresponds a value

of the electron Fermi energy E_e^F and a different solution of Eq. (B.1.44), which determines the self-consistent Coulomb potential energy eV as well as the self-consistent electron distribution inside the cell through

$$n_e(\eta) = \frac{Z}{4\pi b^3} \left[\frac{\phi(\eta)}{\eta} \right]^{3/2}. \quad (\text{B.1.45})$$

In the non-relativistic Thomas-Fermi model, the total energy of the Wigner-Seitz cell is given by (see Slater and Krutter (1935); Feynman et al. (1949) for details)

$$E_{\text{ws}} = E_N + E_k^{(e)} + E_C, \quad (\text{B.1.46})$$

being

$$E_N = Am_N c^2, \quad (\text{B.1.47})$$

$$\begin{aligned} E_k^{(e)} &= \int_0^{R_{\text{ws}}} 4\pi r^2 \mathcal{E}_e[n_e(r)] dr \\ &= \frac{3Z^2 e^2}{7b} \left[\frac{4}{5} \eta_0^{1/2} \phi^{5/2}(\eta_0) - \phi'(0) \right], \end{aligned} \quad (\text{B.1.48})$$

$$\begin{aligned} E_C &= E_{e-N} + E_{e-e} \\ &= -\frac{6Z^2 e^2}{7b} \left[\frac{1}{3} \eta_0^{1/2} \phi^{5/2}(\eta_0) - \phi'(0) \right], \end{aligned} \quad (\text{B.1.49})$$

where $\mathcal{E}_e[n_e(r)]$ is given by Eq. (B.1.9) and E_{e-N} and E_{e-e} are the electron-nucleus Coulomb energy and the electron-electron Coulomb energy, which are given by

$$E_{e-N} = - \int_0^{R_{\text{ws}}} 4\pi r^2 \left(\frac{Ze}{r} \right) e n_e(r) dr, \quad (\text{B.1.50})$$

$$\begin{aligned} E_{e-e} &= \frac{1}{2} \int_0^{R_{\text{ws}}} 4\pi r^2 e n_e(\vec{r}) dr \\ &\times \int_0^{R_{\text{ws}}} 4\pi r'^2 \frac{e n_e(\vec{r}')}{|\vec{r} - \vec{r}'|} dr'. \end{aligned} \quad (\text{B.1.51})$$

From Eqs. (B.1.48) and (B.1.49) we recover the well-known relation between the total kinetic energy and the total Coulomb energy in the Thomas-Fermi model (Slater and Krutter, 1935; Feynman et al., 1949)

$$E_k^{(e)} = E_k^{\text{unif}}[n_e(R_{\text{ws}})] - \frac{1}{2} E_C, \quad (\text{B.1.52})$$

where $E_k^{\text{unif}}[n_e(R_{\text{ws}})]$ denotes the non-relativistic kinetic energy of a uniform

electron distribution of density $n_e(R_{ws})$

$$E_k^{\text{unif}}[n_e(R_{ws})] = \frac{3}{5}Z^*\mu_e(R_{ws}), \quad (\text{B.1.53})$$

being Z^* the number of electrons given by a uniform electron distribution of density $n_e(R_{ws})$

$$Z^* = V_{ws}n_e(R_{ws}). \quad (\text{B.1.54})$$

The self-consistent pressure of the Wigner-Seitz cell given by the non-relativistic Thomas-Fermi model is

$$P_{ws} = -\frac{\partial E_{ws}}{\partial V_{ws}} = P_N + P_{TF}, \quad (\text{B.1.55})$$

being

$$P_N = -\frac{\partial E_N}{\partial V_{ws}} = 0, \quad (\text{B.1.56})$$

$$P_{TF} = -\frac{\partial (E_k^{(e)} + E_C)}{\partial V_{ws}} = \frac{2}{3} \frac{E_k^{\text{unif}}[n_e(R_{ws})]}{V_{ws}}, \quad (\text{B.1.57})$$

The electron chemical potential $\mu_e(R_{ws})$ is given by the non-relativistic limit of Eq. (B.1.16) calculated at the border of the cell R_{ws} , where $n_e(R_{ws})$ is the value of the electron density at the boundary of the Wigner-Seitz cell R_{ws} .

The pressure of the Thomas-Fermi model (B.1.57) is equal to the pressure of a free-electron distribution of density $n_e(R_{ws})$. Being the electron density inside the cell a decreasing function of the distance from the nucleus, the electron density at the radius of the cell $n_e(R_{ws})$ is smaller than the average electron distribution $3Z/(4\pi R_{ws}^3)$. Then, the pressure given by (B.1.57) is smaller than the one given by the non-relativistic expression (B.1.13) of the uniform model of Subsec. B.1.3. Such a smaller pressure, although faintfully given by the expression of a free-electron gas, contains in a self-consistent fashion all the Coulomb effects inside the Wigner-Seitz cell.

The chemical potential of the Wigner-Seitz cell of the non-relativistic Thomas-Fermi model can be then written as

$$\begin{aligned} \mu_{ws} &= E_{ws} + P_{ws}V_{ws} \\ &= Am_Nc^2 + E_k^{(e)} + E_C + \frac{2}{5}Z^*\mu_e(R_{ws}), \end{aligned} \quad (\text{B.1.58})$$

which, using Eqs. (B.1.52)–(B.1.54) becomes

$$\mu_{ws} = Am_Nc^2 + Z^*\mu_e(R_{ws}) + \frac{1}{2}E_C. \quad (\text{B.1.59})$$

Integrating by parts the total number of electrons as

$$Z = \int_0^{R_{\text{ws}}} 4\pi r^2 n_e(r) dr = Z^* + I(R_{\text{ws}}), \quad (\text{B.1.60})$$

where

$$I(R_{\text{ws}}) = \int_0^{R_{\text{ws}}} \frac{4\pi}{3} r^3 \frac{\partial n_e(r)}{\partial r} dr, \quad (\text{B.1.61})$$

we can rewrite finally the following semi-analytical expression of the chemical potential of the cell

$$\begin{aligned} \mu_{\text{ws}} = & Am_N c^2 + Z\mu_e^{\text{unif}} \left[1 + \frac{I(R_{\text{ws}})}{Z} \right]^{2/3} \\ & + \mu_e^{\text{unif}} I(R_{\text{ws}}) \left[1 + \frac{I(R_{\text{ws}})}{Z} \right]^{2/3} + \frac{1}{2} E_C, \end{aligned} \quad (\text{B.1.62})$$

where μ_e^{unif} is the electron free-chemical potential (B.1.16) calculated with the average electron density, namely, the electron chemical potential of the uniform approximation. The function $I(R_{\text{ws}})$ depends explicitly on the gradient of the electron density, i.e., on the non-uniformity of the electron distribution.

In the limit of no Coulomb interaction both the last term and the function $I(R_{\text{ws}})$ in Eq. (B.1.62) go to zero. Consequently, in such a limit the chemical potential of the Wigner-Seitz cell reduces to

$$\mu_{\text{ws}}^{\text{unif}} = Am_N c^2 + Z\mu_e^{\text{unif}}, \quad (\text{B.1.63})$$

which is, as expected, the chemical potential (B.1.15) within the uniform approximation.

B.1.7. The relativistic Feynman-Metropolis-Teller treatment

We recall now how the above classic Feynman, Metropolis, and Teller treatment of compressed atoms has been recently generalized to relativistic regimes (see Rotondo et al. (2009) for details). We recall first some of the main results of the Feynman, Metropolis, and Teller approach (Rotondo et al., 2009) and then proceed to apply them to the computation of the white-dwarf parameters.

One of the main differences in the relativistic generalization of the Thomas-Fermi equation is that, the point-like approximation of the nucleus, must be abandoned since the relativistic equilibrium condition of compressed atoms

$$E_e^F = \sqrt{c^2(P_e^F)^2 + m_e^2 c^4} - m_e c^2 - eV(r) = \text{constant} > 0, \quad (\text{B.1.64})$$

would lead to a non-integrable expression for the electron density near the

origin (see e.g. Ferreira et al. (1980); Ruffini and Stella (1981)).

It is then assumed a constant distribution of protons confined in a radius R_c defined by

$$R_c = \Delta \lambda_\pi Z^{1/3}, \quad (\text{B.1.65})$$

where $\lambda_\pi = \hbar/(m_\pi c)$ is the pion Compton wavelength. If the system is at nuclear density $\Delta \approx (r_0/\lambda_\pi)(A/Z)^{1/3}$ with $r_0 \approx 1.2$ fm. Thus, in the case of ordinary nuclei (i.e., for $A/Z \approx 2$) we have $\Delta \approx 1$. Consequently, the proton density can be written as

$$n_p(r) = \frac{Z}{\frac{4}{3}\pi R_c^3} \theta(r - R_c) = \frac{3}{4\pi} \left(\frac{1}{\Delta \lambda_\pi} \right)^3 \theta(r - R_c), \quad (\text{B.1.66})$$

where $\theta(r - R_c)$ denotes the Heaviside function centered at R_c . The electron density can be written as

$$n_e(r) = \frac{(P_e^F)^3}{3\pi^2 \hbar^3} = \frac{1}{3\pi^2 \hbar^3 c^3} \left[\hat{V}^2(r) + 2m_e c^2 \hat{V}(r) \right]^{3/2}, \quad (\text{B.1.67})$$

where $\hat{V} = eV + E_e^F$ and we have used Eq. (B.1.64).

The overall Coulomb potential satisfies the Poisson equation

$$\nabla^2 V(r) = -4\pi e [n_p(r) - n_e(r)], \quad (\text{B.1.68})$$

with the boundary conditions $dV/dr|_{r=R_{\text{ws}}} = 0$ and $V(R_{\text{ws}}) = 0$ due to the global charge neutrality of the cell.

By introducing the dimensionless quantities $x = r/\lambda_\pi$, $x_c = R_c/\lambda_\pi$, $\chi/r = \hat{V}(r)/(\hbar c)$ and replacing the particle densities (B.1.66) and (B.1.67) into the Poisson equation (B.1.68) we obtain the relativistic Thomas-Fermi equation

$$\begin{aligned} \frac{1}{3x} \frac{d^2 \chi(x)}{dx^2} &= -\frac{\alpha}{\Delta^3} \theta(x_c - x) \\ &+ \frac{4\alpha}{9\pi} \left[\frac{\chi^2(x)}{x^2} + 2 \frac{m_e}{m_\pi} \frac{\chi(x)}{x} \right]^{3/2}, \end{aligned} \quad (\text{B.1.69})$$

which must be integrated subjected to the boundary conditions $\chi(0) = 0$, $\chi(x_{\text{ws}}) \geq 0$ and $d\chi/dx|_{x=x_{\text{ws}}} = \chi(x_{\text{ws}})/x_{\text{ws}}$, where $x_{\text{ws}} = R_{\text{ws}}/\lambda_\pi$.

The neutron density $n_n(r)$, related to the neutron Fermi momentum $P_n^F = (3\pi^2 \hbar^3 n_n)^{1/3}$, is determined by imposing the condition of beta equilibrium

$$\begin{aligned} E_n^F &= \sqrt{c^2 (P_n^F)^2 + m_n^2 c^4} - m_n c^2 = \sqrt{c^2 (P_p^F)^2 + m_p^2 c^4} \\ &- m_p c^2 + eV(r) + E_e^F, \end{aligned} \quad (\text{B.1.70})$$

subjected to the baryon number conservation equation

$$A = \int_0^{R_c} 4\pi r^2 [n_n(r) + n_e(r)] dr. \quad (\text{B.1.71})$$

In Fig. B.1 we see how the relativistic generalization of the Feynman-Metropolis-Teller treatment leads to electron density distributions markedly different from the constant electron density approximation. The electron distribution is far from being uniform as a result of the solution of Eq. (B.1.69), which takes into account the electromagnetic interaction between electrons and between the electrons and the finite sized nucleus. Additional details are given in (Rotondo et al., 2009).

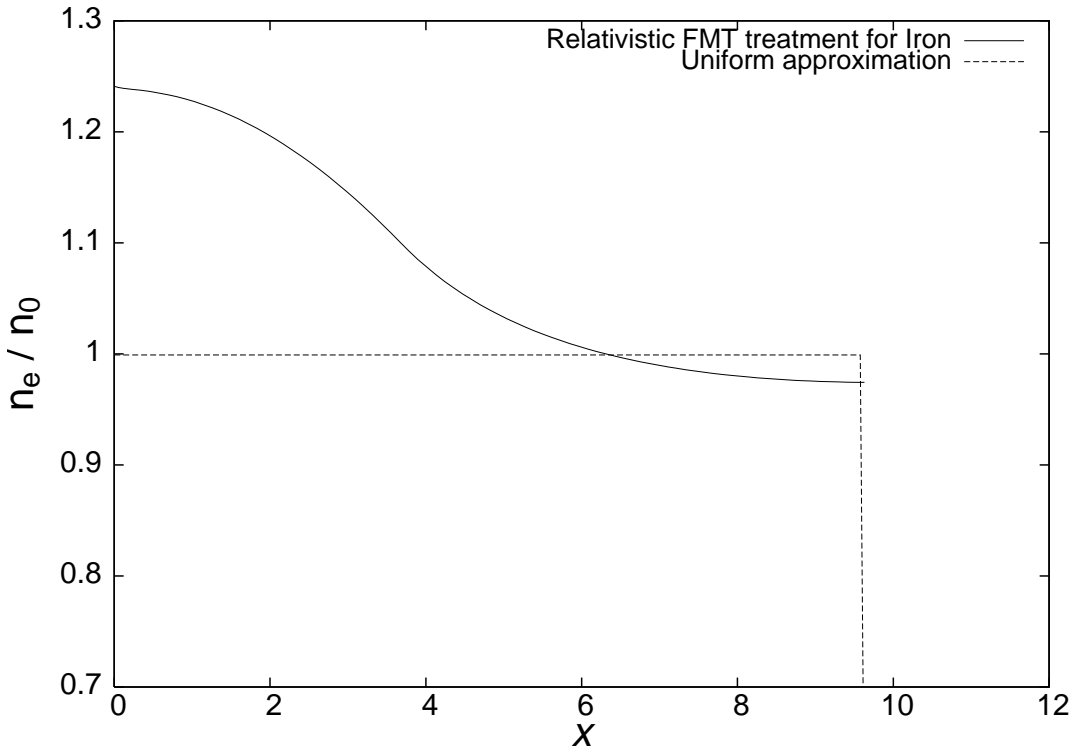


Figure B.1.: The electron number density n_e in units of the average electron number density $n_0 = 3Z/(4\pi R_{\text{ws}}^3)$ is plotted as a function of the dimensionless radial coordinate $x = r/\lambda_\pi$ for $x_{\text{ws}} = 9.7$ in both the relativistic Feynman-Metropolis-Teller approach and the uniform approximation respectively for Iron. The electron distribution for different levels of compression as well as for different nuclear compositions can be found in Rotondo et al. (2009).

V. Popov et al. (Popov et al., 2010) have shown how the solution of the relativistic Thomas-Fermi equation (B.1.69) together with the self-consistent implementation of the beta equilibrium condition (B.1.70) leads, in the case

of zero electron Fermi energy ($E_e^F = 0$), to a theoretical prediction of the beta equilibrium line, namely a theoretical Z - A relation (see the solid curve of Fig. B.2).

In the small mass number region $A \lesssim 10^2$, such a curve can be well approximated by the simple formula $Z \approx A/(2 + 0.030A^{2/3})$. Such a behavior resembles the semi-empirical relation $Z \approx A/(2 + 0.015A^{2/3})$ obtained from the mass formula of Weizsacker which fits the experimental masses of nuclei. The difference in the coefficient of the term $A^{2/3}$ between the theoretical and the semi-empirical relations is due to the simplicity of our nuclear model which takes no into account explicitly the strong interaction between nucleons. Then, within our model we overestimate the mass to charge ratio A/Z of nuclei; for instance, in the case of ${}^4\text{He}$ the overestimate is about 3.8%, for ${}^{12}\text{C}$ about 7.9%, for ${}^{16}\text{O}$ about 9.52%, and for ${}^{56}\text{Fe}$ about 13.2%. We focus here our attention on the effects due to the Coulomb interaction inside the Wigner-Seitz cells and specially we focus on their influence on the observable properties of white-dwarfs. Indeed, such small discrepancies due to the strong interactions disappear when a more refined model of the nucleus is adopted and will be reported elsewhere (Rueda et al., 2010b).

For light elements like ${}^4\text{He}$ and ${}^{12}\text{C}$ our estimates are quite good due to the fact that for lighter elements the beta equilibrium curve approaches the limit $Z \approx A/2$ (see dashed curve of Fig. B.2) which is a common limit of both our theoretical prediction and the semi-empirical formula.

For non-zero electron Fermi energies (i.e. in the case of compressed configurations) the Z - A relation depends on the density of matter. Then, at fixed mass number A the proton number Z becomes a function of the Fermi energy of the electrons and so a function of the density. At some critical density, the proton number changes from the initial value Z to the value $Z - 1$ which determines the onset of inverse beta decay of the initial nucleus. Thus, from the relativistic Feynman-Metropolis-Teller treatment (Rotondo et al., 2009) we are able to obtain in a self-consistent fashion theoretical predictions for the critical electron Fermi energy as well as for the critical matter density at which a given nucleus undergoes inverse beta decay. The influence of such a process on the stability of white-dwarfs will be discussed in Sec. B.1.11.

We turn now to the total energy of the Wigner-Seitz cell within the Feynman-Metropolis-Teller treatment which can be written as

$$E_{\text{ws}} = E_N + E_k + E_C, \quad (\text{B.1.72})$$

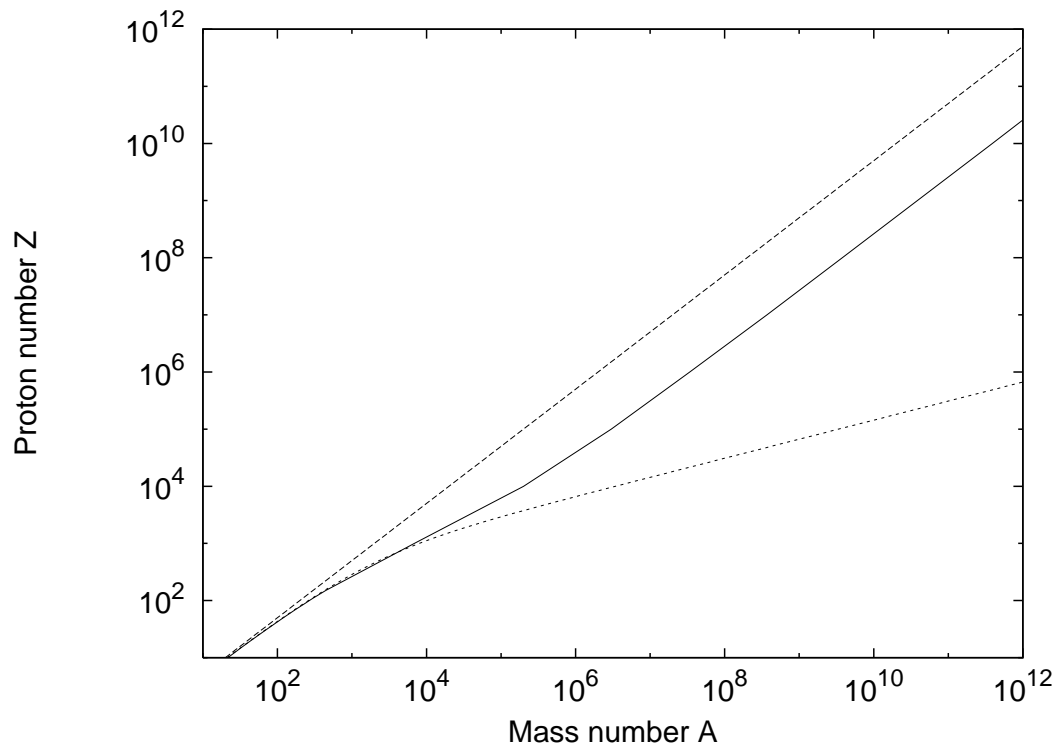


Figure B.2.: The beta-equilibrium curve obtained with: the relativistic Thomas-Fermi model (Popov et al., 2010) (solid line), the Weizsacker semi-empirical formula $Z \approx A/(2 + 0.015A^{2/3})$ (dotted line) and the curve $Z = A/2$ (dashed line).

being

$$E_N = (A - Z)m_n c^2 + Zm_p c^2, \quad (\text{B.1.73})$$

$$\begin{aligned} E_k &= \int_0^{R_{ws}} 4\pi r^2 \mathcal{E}_e[n_e(r)] dr \\ &+ \int_0^{R_c} 4\pi r^2 \{ \mathcal{E}_n[n_n(r)] - m_n c^2 n_n(r) \} dr \\ &+ \int_0^{R_c} 4\pi r^2 \{ \mathcal{E}_p[n_p(r)] - m_p c^2 n_p(r) \} dr, \end{aligned} \quad (\text{B.1.74})$$

$$E_C = \frac{1}{2} \int_0^{R_{ws}} 4\pi r^2 e[n_p(r) - n_e(r)] V(r) dr, \quad (\text{B.1.75})$$

where $\mathcal{E}_i[n_i(r)]$ is the energy-density containing the rest-mass density $m_i c^2 n_i$ given by Eq. (B.1.9), m_n is the neutron rest-mass, m_p is the proton rest-mass.

The total pressure of the Wigner-Seitz cell is given by

$$P_{ws} = -\frac{\partial E_{ws}}{\partial V_{ws}} = P_N + P_{\text{FMT}}^{\text{rel}}, \quad (\text{B.1.76})$$

where

$$\begin{aligned} P_N &= -\frac{\partial E_N}{\partial V_{ws}} = 0, \quad (\text{B.1.77}) \\ P_{\text{FMT}}^{\text{rel}} &= -\frac{\partial (E_k + E_C)}{\partial V_{ws}} = P_e[n_e(R_{ws})] \\ &= \frac{-E_k^{\text{unif}}[n_e(R_{ws})] + Z^* \mu_e(R_{ws})}{V_{ws}}, \end{aligned} \quad (\text{B.1.78})$$

being

$$E_k^{\text{unif}}[n_e(R_{ws})] = \mathcal{E}_e[n_e(R_{ws})] V_{ws}, \quad (\text{B.1.79})$$

the total kinetic energy of a uniform electron distribution of density $n_e(R_{ws})$. In addition, we have introduced the quantity Z^* which is given as before by Eq. (B.1.54) and $\mu_e(R_{ws})$ is the electron chemical potential (B.1.16) calculated at the border of the cell. As in the non-relativistic Thomas-Fermi model, in the relativistic case, the pressure at the boundary of the cell is given by the expression of a free-electron gas, whose density is the one of the electrons at the boundary of the cell $n_e(R_{ws})$.

The electron density at the boundary R_{ws} in the relativistic Feynman-Metropolis-Teller treatment is smaller with respect to the one given by the uniform density approximation (see Fig. B.1 for instance). Then, the relativistic pressure (B.1.76) gives systematically smaller values with respect to the uniform approximation pressure given by Eq. (B.1.13). A detailed comparison between the equations of state for Iron (^{56}Fe) obtained with the uniform

approximation, with the Salpeter analytic formulas and with the relativistic Feynman-Metropolis-Teller approach can be found in Table I of Rotondo et al. (2009).

The Wigner-Seitz cell chemical potential is then

$$\begin{aligned} \mu_{\text{ws}} &= E_{\text{ws}} + P_{\text{ws}} V_{\text{ws}} = (A - Z)m_n c^2 + Zm_p c^2 + E_k \\ &+ E_C - E_k^{\text{unif}}[n_e(R_{\text{ws}})] + Z^* \mu_e(R_{\text{ws}}), \end{aligned} \quad (\text{B.1.80})$$

which, contrary to the non-relativistic formula (B.1.58), can not be simplified in terms of its uniform counterparts. However, it is easy to check that, in the limit of no Coulomb interaction, we have $n_e(R_{\text{ws}}) \rightarrow 3Z/(4\pi R_{\text{ws}}^3)$, $Z^* \rightarrow Z$, $E_C \rightarrow 0$, and $E_k \rightarrow E_k^{\text{unif}}[n_e(R_{\text{ws}})]$. Then, approximating $m_p = m_n = m_N$ we finally obtain

$$\mu_{\text{ws}}^{\text{unif}} \rightarrow Am_N c^2 + Z\mu_e^{\text{unif}}, \quad (\text{B.1.81})$$

which corresponds to the Wigner-Seitz chemical potential (B.1.15) given by the uniform approximation.

B.1.8. General relativistic equations of equilibrium

Outside each Wigner-Seitz cell the system is electrically neutral, thus no overall electric field exists. Therefore, the above equation of state can be used to calculate the structure of the star through the Einstein equations. Introducing the spherically symmetric metric

$$ds^2 = e^{\nu(r)} c^2 dt^2 - e^{\lambda(r)} dr^2 - r^2 d\theta^2 - r^2 \sin^2 \theta d\phi^2, \quad (\text{B.1.82})$$

the Einstein equations can be written in the Oppenheimer and Volkoff (1939) form

$$\frac{dv(r)}{dr} = \frac{2G}{c^2} \frac{4\pi r^3 P(r) / c^2 + M(r)}{r^2 \left[1 - \frac{2GM(r)}{c^2 r} \right]}, \quad (\text{B.1.83})$$

$$\frac{dM(r)}{dr} = 4\pi r^2 \frac{\mathcal{E}(r)}{c^2}, \quad (\text{B.1.84})$$

$$\frac{dP(r)}{dr} = -\frac{1}{2} \frac{dv(r)}{dr} [\mathcal{E}(r) + P(r)], \quad (\text{B.1.85})$$

where we have introduced the mass enclosed at the distance r by $e^{\lambda(r)} = 1 - 2GM(r)/(c^2 r)$, $\mathcal{E}(r)$ is the energy-density and P is the total pressure.

We turn now to demonstrate how, from Eq. (B.1.85), it follows the general relativistic equation of equilibrium (B.1.6), for the self-consistent Wigner-Seitz chemical potential μ_{ws} . The first law of thermodynamics for a zero temperature fluid of N particles, total energy E , total volume V , total pressure

$P = -\partial E/\partial V$, and chemical potential $\mu = \partial E/\partial N$ reads

$$dE = -PdV + \mu dN, \quad (\text{B.1.86})$$

where the differentials denote arbitrary but simultaneous changes in the variables. Since for a system whose surface energy can be neglected with respect to volume energy, the total energy per particle E/N depends only on the particle density $n = N/V$, we can assume E/N as an homogeneous function of first-order in the variables N and V and hence, it follows the well-known thermodynamic relation

$$E = -PV + \mu N. \quad (\text{B.1.87})$$

In the case of the Wigner-Seitz cells, Eq. (B.1.87) reads

$$E_{\text{ws}} = -P_{\text{ws}}V_{\text{ws}} + \mu_{\text{ws}}, \quad (\text{B.1.88})$$

where we have introduced the fact that the Wigner-Seitz cell are the building blocks of the configuration and therefore we must put in Eq. (B.1.87) $N_{\text{ws}} = 1$. Through the entire article we have used Eq. (B.1.88) to obtain from the knowns energy and pressure, the Wigner-Seitz cell chemical potential (see e.g. Eqs. (B.1.15) and (B.1.28)). From Eqs. (B.1.86) and (B.1.87) we obtain the so-called Gibbs-Duhem relation

$$dP = nd\mu. \quad (\text{B.1.89})$$

In the case of the Wigner-Seitz cells in a white-dwarf, the pressure P and the chemical potential μ are decreasing functions of the distance from the origin. Then, the differentials in the above equations can be assumed as the gradients of the variables which, in the present spherically symmetric case, become just derivatives with respect to the radial coordinate r . Thus, it follows from the above relation the Gibbs-Duhem relation for the Wigner-Seitz cells in the white-dwarf

$$\frac{dP_{\text{ws}}}{dr} = n_{\text{ws}} \frac{d\mu_{\text{ws}}}{dr}, \quad (\text{B.1.90})$$

From Eqs. (B.1.85), (B.1.88) and (B.1.90) we obtain

$$n_{\text{ws}}(r) \frac{d\mu_{\text{ws}}(r)}{dr} = -\frac{1}{2} \frac{dv(r)}{dr} n_{\text{ws}}(r) \mu_{\text{ws}}(r), \quad (\text{B.1.91})$$

which can be straightforwardly integrated to obtain

$$e^{v(r)/2} \mu_{\text{ws}}(r) = \text{constant}. \quad (\text{B.1.92})$$

The above equilibrium condition is completely general and applies also for non-zero temperature configurations (Klein, 1949). In such a case, it can be shown that in addition to the equilibrium condition (B.1.92) the temperature

of the system satisfies $e^{\nu(r)/2}T(r) = \text{constant}$.

B.1.9. The weak-field non-relativistic limit

In the weak-field limit we have $e^{\nu/2} \approx 1 + \Phi/c^2$, where the Newtonian gravitational potential has been defined by $\Phi(r) = c^2\nu(r)/2$. In the non-relativistic mechanics limit $c \rightarrow \infty$, the chemical potential $\mu_{\text{ws}} \rightarrow \tilde{\mu}_{\text{ws}} + M_{\text{ws}}c^2$, where $\tilde{\mu}_{\text{ws}}$ denotes the non-relativistic free-chemical potential of the Wigner-Seitz cell and M_{ws} is the rest-mass of the Wigner-Seitz cell, namely, the rest-mass of the nucleus plus the rest-mass of the electrons. Applying these considerations to Eq. (B.1.92) we obtain

$$e^{\nu/2}\mu_{\text{ws}} \approx M_{\text{ws}}c^2 + \tilde{\mu}_{\text{ws}} + M_{\text{ws}}\Phi = \text{constant}. \quad (\text{B.1.93})$$

Absorbing the Wigner-Seitz rest-mass energy $M_{\text{ws}}c^2$ in the constant on the right-hand-side we obtain

$$\tilde{\mu}_{\text{ws}} + M_{\text{ws}}\Phi = \text{constant}. \quad (\text{B.1.94})$$

In the weak-field non-relativistic limit the Einstein equations (B.1.83)–(B.1.85) reduce to

$$\frac{d\Phi(r)}{dr} = \frac{GM(r)}{r^2}, \quad (\text{B.1.95})$$

$$\frac{dM(r)}{dr} = 4\pi r^2 \rho(r), \quad (\text{B.1.96})$$

$$\frac{dP(r)}{dr} = -\frac{GM(r)}{r^2}\rho(r), \quad (\text{B.1.97})$$

where $\rho(r)$ denotes the rest-mass density. The Eqs. (B.1.95)–(B.1.96) can be combined to obtain the gravitational Poisson equation

$$\frac{d^2\Phi(r)}{dr^2} + \frac{2}{r}\frac{d\Phi(r)}{dr} = 4\pi G\rho(r). \quad (\text{B.1.98})$$

In the uniform approximation (see Subsec. B.1.3), the equilibrium condition given by Eq. (B.1.94) reads

$$\tilde{\mu}_e + \frac{A}{Z}m_N\Phi = \text{constant}, \quad (\text{B.1.99})$$

where we have neglected the electron rest-mass with respect to the nucleus rest-mass and we have divided the equation by the total number of electrons Z . This equilibrium equation is the classical condition of thermodynamic equilibrium assumed for non-relativistic white-dwarf models (see e.g. Landau and Lifshitz (1980) for details).

Introducing the above equilibrium condition (B.1.99) into Eq. (B.1.98), and using the relation between the non-relativistic electron chemical potential and the particle density $n_e = (2m_e)^{3/2} \tilde{\mu}_e^{3/2} / (3\pi^2 \hbar^3)$, we obtain

$$\frac{d^2 \tilde{\mu}_e(r)}{dr^2} + \frac{2}{r} \frac{d\tilde{\mu}_e(r)}{dr} = - \frac{2^{7/3} m_e^{3/2} (A/Z)^2 m_N^2 G}{3\pi \hbar^3} \tilde{\mu}_e^{3/2}(r), \quad (\text{B.1.100})$$

which is the correct equation of equilibrium of white-dwarfs within Newtonian gravitational theory (Landau and Lifshitz, 1980). It is remarkable that the equation of equilibrium (B.1.100), obtained from the correct application of the Newtonian limit, does not coincide with the equation given by Chandrasekhar (1931b,a, 1935, 1939), which, as correctly pointed out by Eddington (1935), is a mixture of both relativistic and non-relativistic approaches. Indeed, the consistent relativistic equations should be Eq. (B.1.92). Therefore a dual relativistic and non-relativistic equation of state was used by Chandrasekhar. The pressure on the left-hand-side of Eq. (B.1.97) is taken to be given by relativistic electrons while, the term on the right-hand-side of Eq. (B.1.96) and (B.1.97) (or the source of Eq. (B.1.98)), is taken to be the rest-mass density of the system instead of the total relativistic energy-density. Such a procedure is equivalent to take the chemical potential in Eq. (B.1.94) as a relativistic quantity. As we have seen, this is inconsistent with the weak-field non-relativistic limit of the general relativistic equations.

B.1.10. The Post-Newtonian limit

Although quantitatively justifiable (see next section), the Chandrasekhar approach was strongly criticized by Eddington because it was conceptually unjustified. Indeed, if one were to treat the problem of white-dwarfs approximately without going to the sophistications of general relativity, but including the effects of relativistic mechanics, one should use at least the equations in the post-Newtonian limit. The first-order post-Newtonian expansion of the Einstein equations (B.1.83)–(B.1.85) in powers of P/\mathcal{E} and $GM/(c^2 r)$ leads to the equilibrium equations (Ciufolini and Ruffini, 1983)

$$\frac{d\Phi(r)}{dr} = - \frac{1}{\mathcal{E}(r)} \left[1 - \frac{P(r)}{\mathcal{E}(r)} \right] \frac{dP(r)}{dr}, \quad (\text{B.1.101})$$

$$\frac{dM(r)}{dr} = 4\pi r^2 \frac{\mathcal{E}(r)}{c^2}, \quad (\text{B.1.102})$$

$$\begin{aligned} \frac{dP(r)}{dr} = & - \frac{GM(r)}{r^2} \frac{\mathcal{E}(r)}{c^2} \left[1 + \frac{P(r)}{\mathcal{E}(r)} + \frac{4\pi r^3 P(r)}{M(r)c^2} \right. \\ & \left. + \frac{2GM(r)}{c^2 r} \right], \end{aligned} \quad (\text{B.1.103})$$

where Eq. (B.1.103) is the post-Newtonian version of the Tolman-Oppenheimer-Volkoff equation (B.1.85).

Replacing Eq. (B.1.90) into Eq. (B.1.101) we obtain

$$\left[1 - \frac{P(r)}{\mathcal{E}(r)}\right] \frac{d\mu_{\text{ws}}(r)}{dr} + \frac{\mathcal{E}(r)/c^2}{n_{\text{ws}}(r)} \frac{d\Phi(r)}{dr} = 0. \quad (\text{B.1.104})$$

It is convenient to split the energy-density as $\mathcal{E} = c^2\rho + U$, where $c^2\rho = M_{\text{ws}}c^2n_{\text{ws}}$ is the rest-energy density and U the internal energy. Eq. (B.1.104) becomes

$$\begin{aligned} \frac{d\mu_{\text{ws}}(r)}{dr} + M_{\text{ws}} \frac{d\Phi(r)}{dr} - \frac{P(r)}{\mathcal{E}(r)} \frac{d\mu_{\text{ws}}(r)}{dr} \\ + \frac{U/c^2}{n_{\text{ws}}(r)} \frac{d\Phi(r)}{dr} = 0, \end{aligned} \quad (\text{B.1.105})$$

which is the differential post-Newtonian version of the equilibrium equation (B.1.92) and where the post-Newtonian corrections of equilibrium can be clearly seen. Applying the non-relativistic limit $c \rightarrow \infty$ to Eq. (B.1.105): $1 - P/\mathcal{E} \rightarrow 1$, $\mathcal{E}/(c^2n_{\text{ws}}) \rightarrow M_{\text{ws}}$, and $\mu_{\text{ws}} \rightarrow M_{\text{ws}}c^2 + \tilde{\mu}_{\text{ws}}$, we recover the Newtonian equation of equilibrium given by Eq. (B.1.94).

B.1.11. Mass and radius of general relativistic stable white-dwarfs

Inverse beta-decay instability

In 1938, following the earlier suggestions by F. Hund (Hund, 1936), Landau (1938) pointed out *“it is well-known that matter consists of nuclei and electrons. Nevertheless it can be shown that in bodies of very large mass, this usual electronic state of matter can become unstable. The reason for this lies in the fact that the electronic state of matter does not lead to extremely great densities, because at such densities electrons form a Fermi gas having an immense pressure. On the other hand, it is easy to see that matter can go into another state which is much more compressible—the state where all nuclei and electrons have combined to form neutrons”*. Later I. B. Zel’dovich (Zel’Dovich, 1958) pointed out, quantitatively, that this neutron condensation for inverse beta decay starts to occur for hydrogen already at 10^7 g cm^{-3} . Then B. K. Harrison et al. (Harrison et al., 1958), based on a pulsational analysis pointed out that all configurations of white-dwarfs after the onset of the inverse beta decay are indeed unstable and the critical mass is reached not at an infinite density but at precisely the finite density marked by the onset of inverse beta decay. The onset for inverse beta decay of a nucleus (Z, A) is reached when the kinetic energy of electrons is higher than the mass-energy difference between such a nucleus and the nucleus $(Z - 1, A)$.

For instance, the experimental value of the inverse beta-decay energy $\epsilon_{\text{crit}}^{\text{exp}}$ for ${}^4\text{He}$ and for ${}^{56}\text{Fe}$ is 20.596 MeV and 3.695 MeV respectively (see Table B.1).

In previous works (see e.g. Salpeter (1961); Hamada and Salpeter (1961); Bertone and Ruffini (2000); H. Gursky, R. Ruffini, & L. Stella (2000)) where, the condition of beta equilibrium has not been taken self-consistently into account in the construction of the equation of state, the critical density at which a given chemical element becomes unstable against inverse beta decay has been obtained using experimental nuclear data. For instance, when the uniform approximation for the electron fluid is assumed (see e.g. Salpeter (1961); Hamada and Salpeter (1961)), the critical density for the onset of inverse beta decay is given by

$$\rho_{\text{crit}}^{\text{unif}} = \frac{Z}{A} \frac{m_N}{3\pi^2 \hbar^3 c^3} [(\epsilon_{\text{crit}}^{\text{exp}})^2 + 2m_e c^2 \epsilon_{\text{crit}}^{\text{exp}}]^{3/2}. \quad (\text{B.1.106})$$

where the density of the system has been approximated by $\rho \approx (A/Z)m_N n_e$ and consequently the electron Fermi momentum $P_e^F \approx \hbar [3\pi^2 (Z/A)\rho/m_N]^{1/3}$ has been used.

Then, replacing the experimental inverse beta-decay energy for ${}^4\text{He}$ and for ${}^{56}\text{Fe}$ it is obtained for the critical density $1.37 \times 10^{11} \text{ g cm}^{-3}$ and $1.14 \times 10^9 \text{ g cm}^{-3}$ respectively (see Table B.1 and e.g. Salpeter (1961)). These numerical values for the critical densities for the onset of inverse beta decay can be considered as good estimates. However, such estimates are based on the hybrid employment of empirical onset energies together with model approximations and therefore they do not ensure full self-consistency.

As we mentioned in Subsec. B.1.7, from a self-consistent treatment we should obtain a Z - A relation that depends on the density of matter (or equivalently, on the electron Fermi energy). Such a relation has been obtained recently in Rotondo et al. (2009) within the relativistic generalization of the Feynman-Metropolis-Teller treatment by implementing the beta equilibrium condition between neutrons, protons and electrons at each matter density, namely at each level of compression of the Wigner-Seitz cells (see Subsec. B.1.7 and Rotondo et al. (2009) for details). This implies the numerical solution of Eq. (B.1.69) subjected to the beta equilibrium condition (B.1.70). At constant mass number A , we then obtain a non trivial (numerical) relation $Z = Z(\rho)$ or $Z = Z(E_e^F)$ between the number of protons Z inside each nucleus and the matter density ρ or the electron Fermi energy E_e^F . We are then able to obtain, starting for a given nucleus (Z, A) , the critical matter density (or critical electron Fermi energy) at which the initial nucleus becomes $(Z - 1, A)$ undergoing inverse beta decay. In Table B.1 we report the critical density and the critical electron Fermi energy for the onset of inverse beta-decay as obtained from the numerical integrations of the relativistic Thomas-Fermi equations of equilibrium (Rotondo et al., 2009) in the case of ${}^4\text{He}$ and ${}^{56}\text{Fe}$.

The differences between the numerical values we have obtained and the

	$\rho_{\text{crit}}^{\text{relTF}}$	$(E_e^F)_{\text{crit}}$	$\rho_{\text{crit}}^{\text{unif}}$	$\epsilon_{\text{crit}}^{\text{exp}}$
${}^4\text{He}$	1.2×10^{12}	23.37	1.37×10^{11}	20.596
${}^4\text{Fe}$	8.6×10^8	2.03	1.14×10^9	3.695

Table B.1.: Onset of inverse beta decay instability for ${}^4\text{He}$ and ${}^{56}\text{Fe}$. The experimental inverse beta-decay energy $\epsilon_{\text{crit}}^{\text{exp}}$ is given in MeV, the corresponding critical density for the uniform electron density model $\rho_{\text{crit}}^{\text{unif}}$ given by Eq. (B.1.106) is given in g cm^{-3} . The self-consistent values for both the inverse beta decay energy as well as the corresponding critical density obtained with the relativistic Feynman-Metropolis-Teller treatment are denoted by $(E_e^F)_{\text{crit}}$ and $\rho_{\text{crit}}^{\text{relTF}}$ and are given in MeV and in g cm^{-3} respectively.

experimental ones are due to the fact that, we have implemented a refined model for the electron component and the Coulomb interaction, and we have adopted a simplified model for the nucleus with constant proton density (see Rotondo et al. (2009) and Subsec. B.1.7 for details). However, it is remarkable that from such a simple model which implements the beta equilibrium condition between the neutrons and protons of the nucleus with the electrons it is possible to overcome some of the current difficulties models such as, the adoption of ad-hoc nuclear models through phenomenological or semi-empirical equations (see e.g. Bertone and Ruffini (2000); H. Gursky, R. Ruffini, & L. Stella (2000)) which are not self-consistent for non-zero electron Fermi energies and, the employment of experimental data to obtain the critical density for inverse beta decay without taking into account the value of the Fermi energy (see e.g. Salpeter (1961) and Eq. (B.1.106)).

The relativistic Feynman-Metropolis-Teller treatment (Rotondo et al., 2009) which we apply below to construct general relativistic white-dwarf equilibrium configurations is a first step towards a fully self-consistent theory of the description of equilibrium configurations composed by white-dwarf like matter which shows the essential physics governing these systems. Although the relativistic Feynman-Metropolis-Teller treatment is here applied in order to point out the influence of Coulomb effects as well as of special relativistic effects on the properties of white-dwarfs, the treatment can be refined with respect to the nucleus model by including strong interaction effects (Rueda et al., 2010b). However, such a refinement of the model does not change the essential physics introduced by the relativistic Feynman-Metropolis-Teller approach (Rotondo et al., 2009). Instead, this refinement only smears out the small differences between the experimental values and the theoretical prediction obtained for instance for the Z - A relation at zero matter density as well as in the important case of compressed matter (Rueda et al., 2010b).

General relativity instability

The concept of the critical maximum mass introduced by Chandrasekhar has played a major role in the theory of stellar evolution. For Newtonian white-dwarf stars, however, such a critical mass is reached only asymptotically at infinite central densities of the object. One of the most important general relativistic effects is that such a critical mass is reached at finite densities when general relativity is introduced.

This general relativistic effect is an additional source of instability with respect to the readily discussed instability due to the onset of inverse beta-decay which, contrary to the present general relativistic one, applies also in the Newtonian case by shifting the maximum mass of Newtonian white-dwarfs to finite densities (Harrison et al., 1958).

In Figs. B.3–B.6 we have plotted respectively the mass-central density relation and the mass-radius relation of general relativistic for ${}^4\text{He}$ and ${}^{56}\text{Fe}$ white-dwarfs. In particular, we show the results for general relativistic white-dwarfs obtained with the Salpeter equation of state (see Subsec. B.1.5 and Hamada and Salpeter (1961) for details), for general relativistic white-dwarfs obtained with the relativistic Feynman-Metropolis-Teller equation of state (see Subsec. B.1.7), and for the Newtonian white-dwarfs of Chandrasekhar (see Subsec. B.1.3). A comparison of the numerical value of the critical mass as given by Stoner (1929), by Chandrasekhar (1931b) and Landau (1932), by Hamada and Salpeter (1961) and, by the treatment presented here can be found in Table B.2.

Since our approach takes into account self-consistently both beta decay equilibrium and general relativity, we can determine if the critical mass is reached due either to the inverse beta-decay instability or to the general relativity instability. In fact, we find that ${}^4\text{He}$ white-dwarfs becomes unstable at a density smaller than the critical density for the onset of inverse beta-decay (see Fig. B.3 and Table B.1) and therefore we see that the instability of white-dwarfs composed by light material (like ${}^4\text{He}$) is due to general relativity effects. On the other hand, in the case of white-dwarfs composed by heavy material (like ${}^{56}\text{Fe}$) the instability is due to inverse beta-decay (see Fig. B.5 and Table B.1).

B.1.12. Conclusions

We have addressed the theoretical physics aspects of the white-dwarf configurations of equilibrium, quite apart from the astrophysical application.

In the introduction we have recalled how the study of white-dwarfs has often stimulated and taken advantage of crucial progress in theoretical physics and applied mathematics. It is clear that the early considerations of the critical mass of a white-dwarf were routed in the concept of quantum statistics

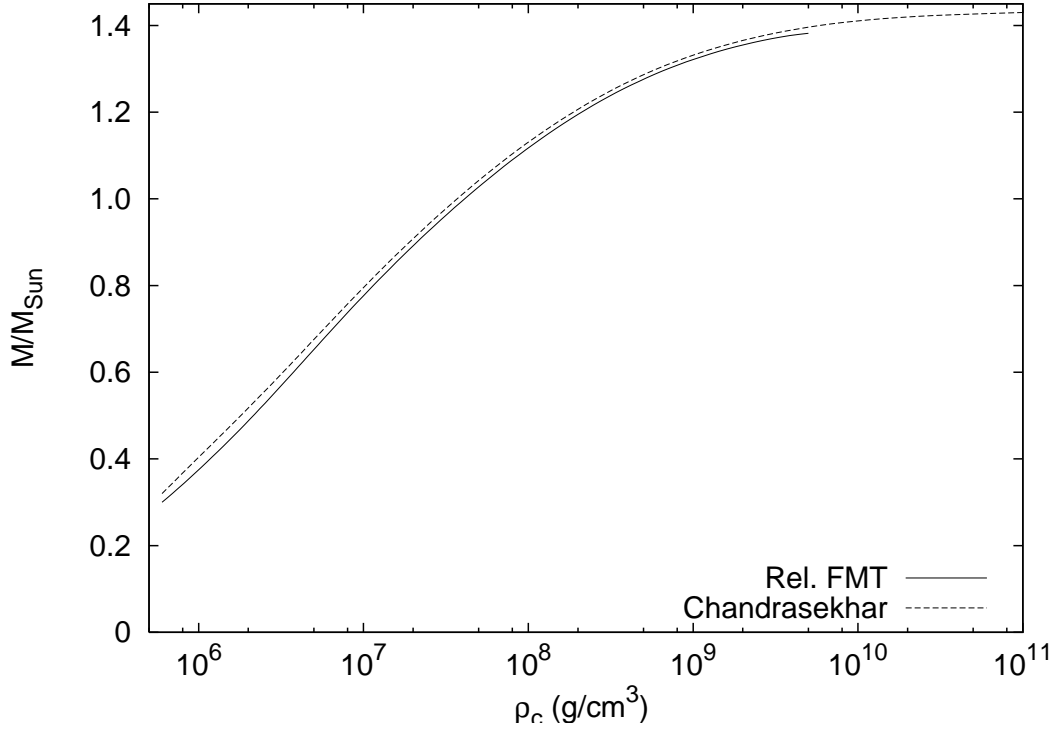


Figure B.3.: Mass in solar masses as a function of the central density in g cm^{-3} for ${}^4\text{He}$ white-dwarfs. The solid curve corresponds to the general relativistic ${}^4\text{He}$ white-dwarfs using the equation of state given by the relativistic Feynman-Metropolis-Teller approach while, the dotted curve, are the corresponding Newtonian ${}^4\text{He}$ white-dwarfs of Chandrasekhar.

	$M_{\text{crit}}^{\text{Stoner}}/M_{\odot}$	$M_{\text{crit}}^{\text{Ch-L}}/M_{\odot}$	$M_{\text{crit}}^{\text{H\&S}}/M_{\odot}$	$M_{\text{crit}}^{\text{FMTrel}}/M_{\odot}$
${}^4\text{He}$	1.73	1.44	1.42	1.38
${}^56\text{Fe}$	1.49	1.24	1.11	1.08

Table B.2.: Critical mass of ${}^4\text{He}$ and ${}^{56}\text{Fe}$ white-dwarfs in solar masses. The critical mass of Stoner $M_{\text{crit}}^{\text{Stoner}}$ is given by Eq. (B.1.1), the Chandrasekhar-Landau limiting mass $M_{\text{crit}}^{\text{Ch-L}}$ is given by Eq. (B.1.2). The critical mass of Hamada and Salpeter $M_{\text{crit}}^{\text{H\&S}}$ is obtained, for ${}^4\text{He}$ white-dwarfs from the approximated expression (B.1.3) with $\mu_{\text{eff}} = 2.011$ while, for ${}^{56}\text{Fe}$ white-dwarfs from Table 2 of Hamada and Salpeter (1961). The critical mass obtained in the present work is denoted by $M_{\text{crit}}^{\text{FMTrel}}$.

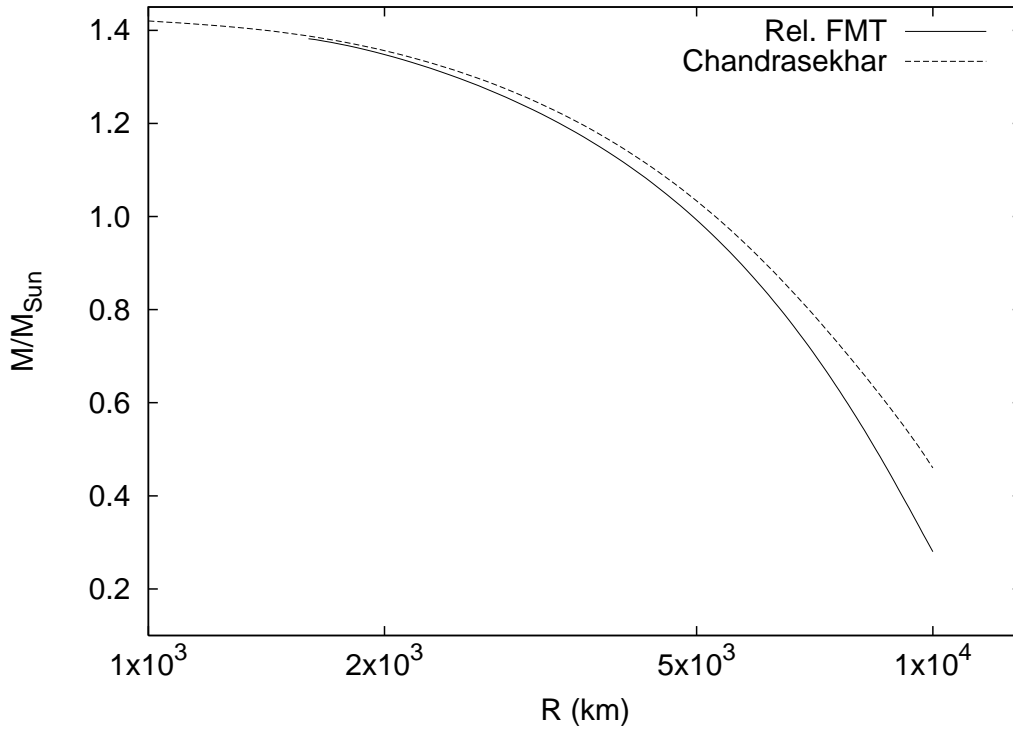


Figure B.4.: Mass in solar masses as a function of the radius in km for ${}^4\text{He}$ white-dwarfs. The solid curve corresponds to the general relativistic ${}^4\text{He}$ white-dwarfs using the equation of state given by the relativistic Feynman-Metropolis-Teller approach while, the dotted curve, are the corresponding Newtonian ${}^4\text{He}$ white-dwarfs of Chandrasekhar.

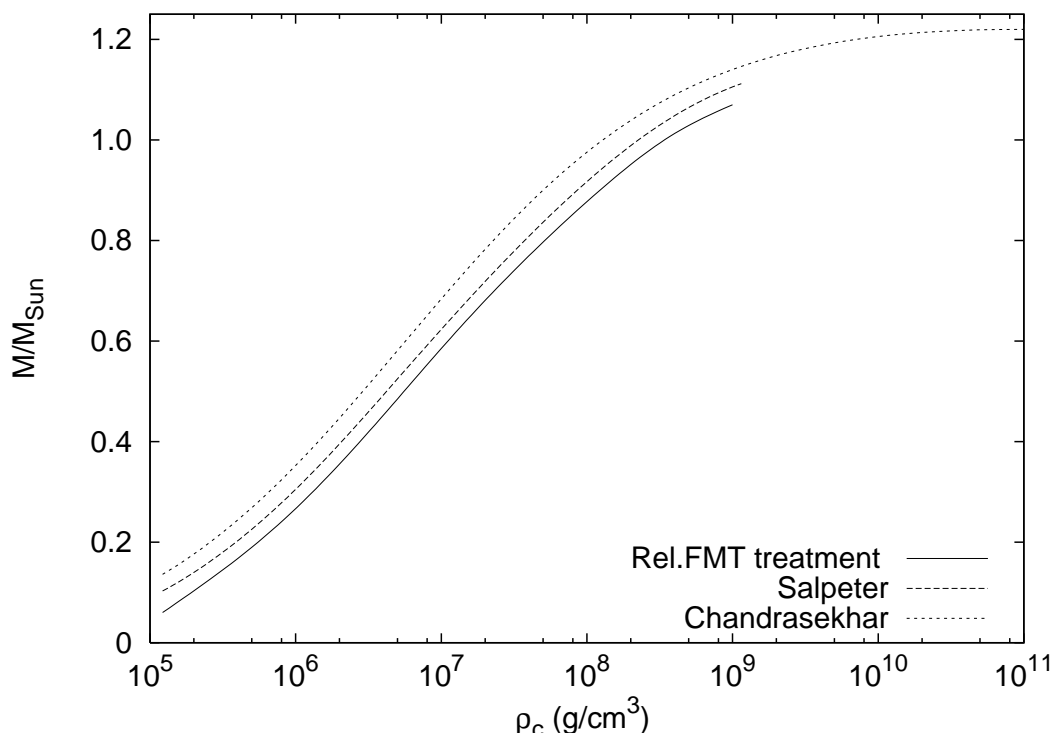


Figure B.5.: Mass in solar masses as a function of the central density in g cm^{-3} for ^{56}Fe white-dwarfs. The solid curve corresponds to the general relativistic ^{56}Fe white-dwarfs using the equation of state given by the relativistic Feynman-Metropolis-Teller approach. The dashed curve corresponds to the general relativistic ^{56}Fe white-dwarfs of Hamada and Salpeter (1961) while, the dotted curve, are the corresponding Newtonian ^{56}Fe white-dwarfs of Chandrasekhar (1931b).

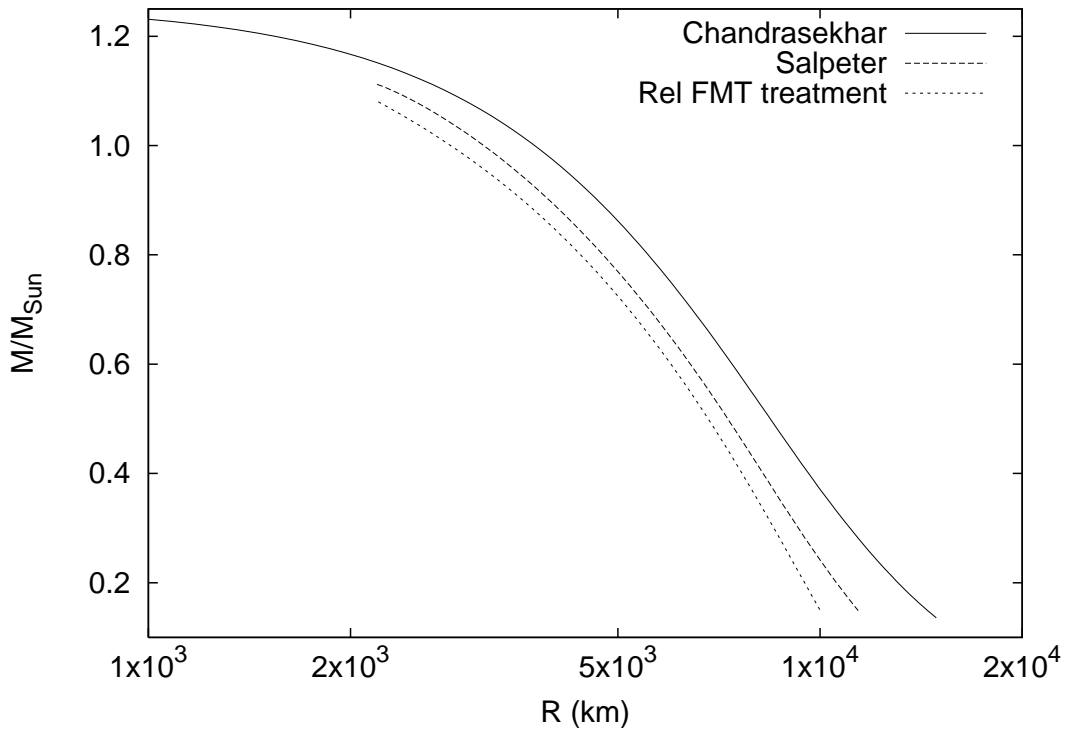


Figure B.6.: Mass in solar masses as a function of the radius in km for ^{56}Fe white-dwarfs. The solid curve corresponds to the general relativistic ^{56}Fe white-dwarfs using the equation of state given by the relativistic Feynman-Metropolis-Teller approach. The dashed curve corresponds to the general relativistic ^{56}Fe white-dwarfs of Hamada and Salpeter (1961) while, the dotted curve, are the corresponding Newtonian ^{56}Fe white-dwarfs of Chandrasekhar (1931b).

and the fermion exclusion principle² considered by Fowler (1926) and Stoner (1924) leading to the value (Stoner, 1929)

$$M_{\text{crit}}^{\text{Stoner}} = \frac{15}{16} \sqrt{5\pi} \frac{M_{\text{Pl}}^3}{\mu^2 m_n^2}. \quad (\text{B.1.107})$$

The following progress was made by Chandrasekhar (1931b) and Landau (1932) adopting the monumental work of applied mathematics by Emden (1907) on the solution of the nonlinear Lane-Emden polytropic differential equations. They obtained the critical mass

$$M_{\text{crit}}^{\text{Ch-L}} = 2.015 \frac{\sqrt{3\pi}}{2} \frac{M_{\text{Pl}}^3}{\mu^2 m_n^2}. \quad (\text{B.1.108})$$

It was Salpeter (1961) and later Hamada and Salpeter (1961) who brought to full fruition the additional conceptual theoretical physics progress of Wigner and Seitz (1933, 1934). Salpeter indeed adopted the Wigner-Seitz cell for the description of white-dwarfs by studying the perturbation to the uniform electron distribution, given by the Coulomb interactions and their special relativity corrections. The value of the critical mass, although obtained only through numerical integration, can be expressed approximately as (see Eq. (3) of Hamada and Salpeter (1961))

$$M_{\text{crit}}^{\text{H\&S}} = 2.015 \frac{\sqrt{3\pi}}{2} \frac{1}{\mu_{\text{eff}}^2} \frac{M_{\text{Pl}}^3}{m_n^2}, \quad (\text{B.1.109})$$

where $\mu_{\text{eff}} > \mu$ is the effective molecular weight of the white-dwarf given by Eq. (B.1.4), which becomes here a function of the nuclear composition.

Still many inconsistencies existed in the theoretical model. It has been recently accomplished (Rotondo et al., 2009) the description of a compressed atom within the global and powerful approach of the relativistic Feynman, Metropolis and Teller treatment, by using in the relativistic regime the Thomas-Fermi equation. This new theoretical result is here applied within the Wigner-Seitz cell and solved in the framework of general relativity. From a theoretical physics point of view, this is the first unified approach of white-dwarfs taking into account consistently the gravitational, the weak, the strong and the electromagnetic interactions, and it answers open theoretical physics issues in this matter. No analytic formula for the critical mass of white-dwarfs can be derived and, on the contrary, the critical mass can be obtained only through the numerical integration of the general relativistic equations of equilibrium together with the relativistic Feynman-Metropolis-Teller equation of state (see Figs. B.3–B.6).

Turning now to astrophysics, the critical mass of white-dwarfs is today ac-

²For historical details about the exclusion principle see Heilbron (1983); Nauenberg (2008).

quiring a renewed interest in view of its central role in the explanation of the supernova phenomena (Phillips, 1993; Riess et al., 1998; Perlmutter et al., 1999; Riess et al., 2004). The central role of the critical mass of white-dwarfs as related to supernova was forcefully presented by F. Hoyle and W. A. Fowler (Hoyle and Fowler, 1960) explaining the difference between type I and type II Supernova. This field has developed in the intervening years to a topic of high precision research in astrophysics and, very likely, the relativistic effect outlined in this article will become topic of active confrontation between theory and observation.

Paradoxically, the concept of critical mass was not pursued by Chandrasekhar in order to explain the supernova phenomena, on the contrary, Chandrasekhar purported on the role of the critical mass in discriminating star masses leading to the formation of a white-dwarf versus stars never reaching a configuration of equilibrium due to radiation pressure (Arnett, 2010; Giacconi and Ruffini, 1978)³.

The value of the critical mass and the radius of white-dwarfs in our treatment and in the Hamada and Salpeter (1961) treatment become a function of the composition of the star. Specific examples have been given in the limiting cases of ^4He and ^{56}Fe and the results of Chandrasekhar, of Salpeter and ours have been compared and contrasted (see Table B.2). The formalism we have introduced by presenting the study of inverse beta decay equilibrium allows in principle to evaluate subtle effects of a nuclear density distribution as a function of the radius and of the Fermi energy of the electrons and of the varying depth of the general relativistic gravitational potential.

We have finally obtained a general formula in Eq. (B.1.92) as a “first integral” of the general relativistic equations of equilibrium. This formula relates the chemical potential of the Wigner-Seitz cells, duly obtained from the relativistic Feynman-Metropolis-Teller model (Rotondo et al., 2009) taking into account weak, nuclear and electromagnetic interactions, to the general relativistic gravitational potential at each point of the configuration. Besides its esthetic value, this result relates the general relativistic gravitational potential at each point to the chemical potential of the relativistic Wigner-Seitz cell. This is an important tool to examine the radial dependence of the white-dwarf properties and, even more important, it can be applied to the crust of a neutron star as it approaches to the physical important regime of neutron star cores.

We have discussed many theoretical issues open for years on white-dwarfs, including the legitimately posed by A. Eddington (Eddington, 1935).

³Chandrasekhar, in an interview with S. Weart Weart (1977), recognized “... at first I didnt understand what this limit meant and I didnt know how it would end, and how it related to the 3/2 low mass polytropes ...”

B.2. On the self-consistent general relativistic equilibrium equations of neutron stars

One of the fundamental issues in physics and astrophysics is the creation of an electron-positron plasma in overcritical electric fields larger than $E_c = m_e^2 c^3 / (e\hbar)$ (see Ruffini et al. (2010) and references therein). Basic progress toward the understanding of the thermalization process of such a plasma have been achieved Aksenov et al. (2007). The existence of such an electron-positron plasma has a central role in a variety of problems ranging from the acceleration process in gamma ray bursts (GRBs) Ruffini et al. (2010) to the sharp trigger process in supernova phenomena Pagliaroli et al. (2009b,a). This has motivated us to reconsider the standard treatment of neutron stars in order to find a theoretical explanation for the emergence of a wide variety of astrophysical situations involving such overcritical electric fields. In a classic article Baym, Bethe and Pethick Baym et al. (1971a) presented the problem of matching to the crust in a neutron star a liquid core composed of N_n neutrons, N_p protons and N_e electrons. After discussing various aspects of the problem they conclude: ‘the details of this picture requires further elaboration; this is a situation for which the Thomas-Fermi method is useful.’ In this letter we focus on relaxing the traditional condition of local charge neutrality $n_e = n_p$, which appears to have been assumed only for mathematical convenience without any physical justification. Instead, we adopt the more general condition of global charge neutrality $N_e = N_p$. The corresponding equilibrium equations then follow from self-consistent solution of the relativistic Thomas-Fermi equation, the Einstein-Maxwell equations and the β -equilibrium condition, properly expressed in general relativity.

The pressure and the density of the core are mainly due to the baryons while the pressure of the crust is mainly due to the electrons with the density due to the nuclei and possibly some free neutrons due to neutron drip (see e.g. Baym et al. (1971a)). The boundary conditions determined by the matching of the electron distribution in the core with that of the electrons of the crust are fundamental for the self-consistent construction of the equilibrium configurations.

We consider the case of a non-rotating neutron star with metric

$$ds^2 = e^\nu dt^2 - e^\lambda dr^2 - r^2 d\theta^2 - r^2 \sin^2 \theta d\phi^2, \quad (\text{B.2.1})$$

where ν and λ are functions only of r . We assume units where $G = \hbar = c = 1$ and let α denote the fine structure constant. As usual we define the mass of the star $M(r)$ by $e^{-\lambda} = 1 - 2M/r + r^2 E^2$, and denote the Coulomb potential by $V(r)$, which determines the electric field $E = e^{-(\nu+\lambda)/2} V'$, where a prime indicates the radial derivative. The combined energy-momentum tensor of

the matter and fields $T_{\mu\nu}$ is given by

$$T_{\beta}^{\alpha} = \text{diag}(\mathcal{E} + \mathcal{E}^{em}, -P - P^{em}, -P + P^{em}, -P + P^{em}), \quad (\text{B.2.2})$$

where $\mathcal{E}^{em} = -P^{em} = E^2/(8\pi)$, and \mathcal{E} and P are the energy density and pressure of matter. With all the above definitions, the time-independent Einstein-Maxwell field equations read

$$M' = 4\pi r^2 \mathcal{E} + 4\pi e^{\lambda/2} r^3 e E (n_p - n_e), \quad (\text{B.2.3})$$

$$e^{-\lambda} \left(\frac{v'}{r} + \frac{1}{r^2} \right) - \frac{1}{r^2} = -8\pi T_1^1, \quad (\text{B.2.4})$$

$$e^{-\lambda} \left[v'' + (v' - \lambda') \left(\frac{v'}{2} + \frac{1}{r} \right) \right] = -16\pi T_2^2, \quad (\text{B.2.5})$$

$$(eV)'' + (eV)' \left[\frac{2}{r} - \frac{(v' + \lambda')}{2} \right] = -4\pi \alpha e^{v/2} e^{\lambda} (n_p - n_e). \quad (\text{B.2.6})$$

In order to close the system of equilibrium equations, the condition of local charge neutrality $n_e = n_p$ has been traditionally imposed for mathematical simplicity. In this case the problem is reduced to solving only the Einstein equations for a Schwarzschild metric. When this condition is relaxed, imposing only global charge neutrality $N_e = N_p$, we need to satisfy the Einstein-Maxwell equations (B.2.3)–(B.2.6). In order to impose global charge neutrality as well as quantum statistics on the leptonic component, the general relativistic Thomas-Fermi equation must also be satisfied.

The general relativistic electron Fermi energy is given by

$$E_e^F = e^{v/2} \mu_e - eV = \text{constant}, \quad (\text{B.2.7})$$

where $\mu_e = \sqrt{(P_e^F)^2 + m_e^2}$ and $P_e^F = (3\pi^2 n_e)^{1/3}$ are respectively the chemical potential and Fermi momentum of degenerate electrons. From Eqs. (B.2.6) and (B.2.7) we obtain the general relativistic Thomas-Fermi equation

$$(eV)'' + (eV)' \left[\frac{2}{r} - \frac{(v' + \lambda')}{2} \right] = -4\pi \alpha e^{v/2} e^{\lambda} \left\{ n_p - \frac{e^{-3v/2}}{3\pi^2} [(E_e^F + eV)^2 - m_e^2 e^v]^{3/2} \right\}. \quad (\text{B.2.8})$$

The β -equilibrium condition is expressed by

$$\mu_n = \mu_e + \mu_p. \quad (\text{B.2.9})$$

In order to take into account the effect of the compression of the crust on the leptonic component of the core we solve the equilibrium conditions for the core within a Wigner-Seitz cell Rotondo et al. (2009). The radius R_{WS} of

this cell determines the Fermi energy of the electrons of the core which has to be matched with the Fermi energy of the leptonic component of the crust. Global charge neutrality is specified by

$$\int_0^{R_{WS}} e^{\lambda/2} n_p d^3r = \int_0^{R_{WS}} e^{\lambda/2} n_e d^3r. \quad (\text{B.2.10})$$

From Eqs. (B.2.9) and (B.2.10) we can determine self-consistently the proton, neutron, electron fractions inside the core as well as the radius R_{WS} of the Wigner-Seitz cell of the core Rotondo et al. (2009).

The coupled system of equations consisting of the Einstein-Maxwell equations (B.2.3)–(B.2.5), the general relativistic Thomas-Fermi equation (B.2.8), the β -equilibrium condition (B.2.9) along with the constraint (B.2.10) needs, in order to be closed, an equation of state (EOS) for the baryonic component in the core and for the leptonic component of the crust.

In order to illustrate the application of this approach we adopt, as an example, the Baym, Bethe, and Pethick (BBP) Baym et al. (1971a) strong interaction model for the baryonic matter in the core as well as for the white-dwarf-like material of the crust. The general conclusions we reach will in fact be independent of the details of this model.

At the neutron star radius $r = R$, all the electro-dynamical quantities must be zero as a consequence of the global charge neutrality condition. Consequently, we have a matching condition with the Schwarzschild spacetime which imposes the boundary condition

$$e^{v(R)/2} = \sqrt{1 - \frac{2M(R)}{R}}. \quad (\text{B.2.11})$$

The boundary conditions at the center correspond to $M(0) = 0$ and the regularity condition to $n_e(0) = n_p(0)$. From the β -equilibrium condition (B.2.9), we can evaluate the central chemical potentials $\mu_e(0)$, $\mu_p(0)$, and $\mu_n(0)$, or equivalently, the central number densities $n_e(0)$, $n_p(0)$, and $n_n(0)$ Rueda et al. (2010a). From Eq. (B.2.7) we also have the relation

$$e^{v(0)/2} = \frac{E_e^F + eV(0)}{\mu_e(0)}. \quad (\text{B.2.12})$$

Having determined the boundary conditions at infinity and at the center, we turn now to the matching conditions at the surface of the core. Following BBP Baym et al. (1971a), the neutron profile at the core-crust interface is given by

$$n_n(z) = n_n^{crust} + (n_n^{core} - n_n^{crust})f(z/b). \quad (\text{B.2.13})$$

We have defined $n_n^{core} = n_n(R_c)$ and $n_n^{crust} = n_n(R_{WS})$. Here R_c is the radius of the core defined as the point where the rest-mass density reaches

the nuclear saturation density, i.e., $\rho(R_c) = \rho_0 \simeq 2.7 \times 10^{14} \text{ g cm}^{-3}$ Baym et al. (1971a). The function $f(z/b)$ satisfies $f(-\infty) = 1$, $f(\infty) = 0$, where $b \simeq (n_n^{core} - n_n^{crust})^{-1/3} \simeq 1/m_\pi$ Baym et al. (1971a). As proposed by BBP, an appropriate choice for the function $f(z/b)$ is the Woods-Saxon profile $f(z/b) = (1 + e^{z/b})^{-1}$. The z -coordinate lines are perpendicular to the sharp surface separating two semi-infinite regions (core and crust) in the planar approximation Baym et al. (1971a); the neutron density approaches n_n^{core} as $z \rightarrow -\infty$ and n_n^{crust} as $z \rightarrow \infty$.

The matching between the core and the crust occurs at the radius R_{WS} , where we have $V'(R_{WS}) = 0$ by virtue of the global neutrality condition given by Eq. (B.2.10), and we also choose the value of the Coulomb potential $V(R_{WS}) = 0$. From the electron chemical potential $\mu_e(R_{WS})$ at the edge of the crust, we calculate the corresponding neutron chemical potential $\mu_n(R_{WS})$ according to the BBP treatment. If $\mu_n(R_{WS}) - m_n > 0$, neutron drip occurs. In this case, the pressure is due to the neutrons as well as to the leptonic component, so we have the inner crust (see Table B.3 and Baym et al. (1971a) for details). For larger values of the radii, i.e., for $r > R_{WS}$ the condition $\mu_n(r) - m_n < 0$ is reached at $\rho_{drip} \simeq 4.3 \times 10^{11} \text{ g cm}^{-3}$ and there the outer crust starts, with the pressure only determined by the leptonic component. If $\mu_n(R_{WS}) - m_n < 0$, only the outer crust exists.

For a fixed central rest-mass density $\rho(0) \simeq 9.8 \times 10^{14} \text{ g cm}^{-3}$ and selected values of E_e^F we have integrated the system of equations composed by the general relativistic Thomas-Fermi equation (B.2.8), the β -equilibrium condition (B.2.9), the Einstein-Maxwell equations (B.2.3)-(B.2.5), with the constraint of overall neutrality (B.2.10).

We found that although the electro-dynamical properties of the core are very sensitive to the Fermi energy of the electrons (see Table B.3 for details), the bulk properties of the core like its mass and radius are not sensitive to the value of E_e^F . This is perfectly in line with the results of Ruffini et al. in Rotondo et al. (2009).

Particularly interesting are the electro-dynamical structure and the distribution of neutrons, protons, and electrons as the surface of the core is approached (see Fig. B.7). It is interesting to compare and contrast these results with the preliminary ones obtained in the simplified model of massive nuclear density cores Rotondo et al. (2009). The values of the electric field are quite close and are not affected by the constant proton density distribution assumed there. In the present case, the proton distribution is far from constant and increases outward as the core surface is approached.

In conclusion, for any given value of the central density an entire new family of equilibrium configurations exists. Each configuration is characterized by a strong electric field at the core-crust interface. Such an electric field extends over a thin shell of thickness $\sim 1/m_e$ and becomes largely overcritical in the limit of decreasing values of the crust mass and size (see Table B.3 and Fig. B.7).

$\frac{E_e^F}{m_\pi}$	$\frac{M(R_c)}{M_\odot}$	R_c (km)	$\frac{eV(0)}{m_\pi}$	$\frac{eV(R_c)}{m_\pi}$	$\frac{E_{max}}{E_c}$	$\frac{\rho_{crust}}{\rho_{drip}}$	$\frac{M_{crust}}{10^{-5}M_\odot}$	Δ_r^{ic} (m)	Δ_r^{oc} (km)
0.10	0.24	5.98	1.085	0.60	388.72	0.125	0.245	0.00	0.797
0.15	0.24	5.98	0.985	0.55	381.04	0.384	1.150	0.00	1.251
0.20	0.24	5.98	0.935	0.50	370.89	1.000	4.450	0.00	1.899
0.30	0.24	5.98	0.835	0.40	346.67	46.19	4.830	1.89	1.899
0.35	0.24	5.98	0.785	0.35	332.43	80.83	5.420	2.85	1.899

Table B.3.: Results of the numerical integration of the BBP model for selected values of E_e^F for $\rho(0) \simeq 9.8 \times 10^{14} \text{ g cm}^{-3}$. We show the mass and radius of the core $M(R_c)$ and R_c , the Coulomb potential at the center and at the core surface $eV(0)$ and $eV(R_c)$, the peak of the electric field in the core-crust interface E_{max} , the rest-mass density at the edge of the crust $\rho_{crust} \equiv \rho(R_{WS})$, the mass of the crust M_{crust} , and the inner and outer crust thickness Δ_r^{ic} and Δ_r^{oc} .

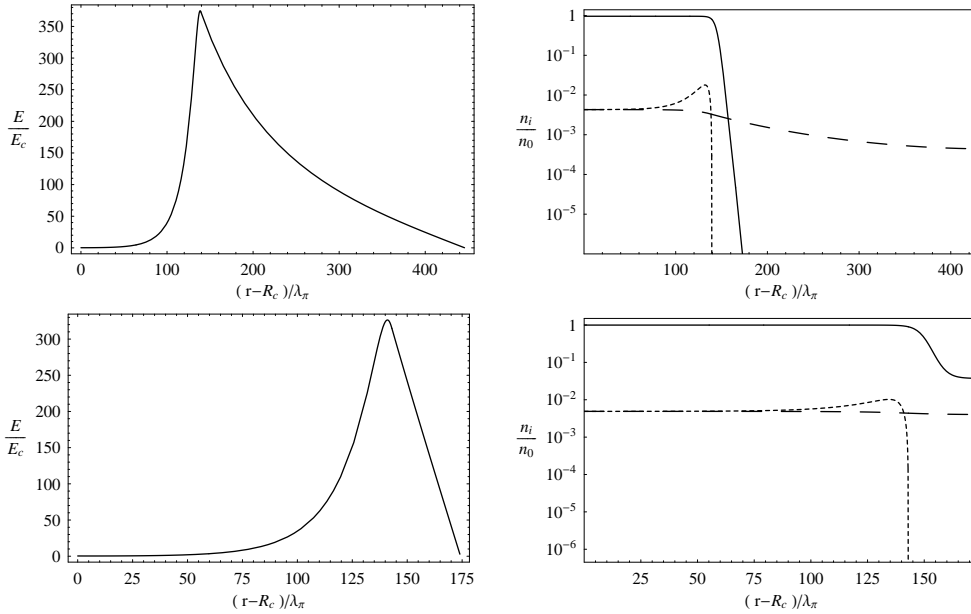


Figure B.7.: Left column: the surface electric field in units of the critical field. Right column: the surface particle number density of neutrons (solid), protons (short-dashed), and electrons (long-dashed) normalized to the nuclear density for selected values of E_e^F . First row: $E_e^F = 0.20m_\pi$, second row $E_e^F = 0.35m_\pi$.

These configurations endowed with overcritical electric fields are indeed stable against the quantum instability of pair creation because of the Pauli blocking of the degenerate electrons Ruffini et al. (2010). It is expected that during the gravitational collapse phases leading to the formation of a neutron star, a large emission of electron-positron pairs will occur prior to reaching a stable ground state configuration. Similarly during the merging of two neutron stars or a neutron star and a white-dwarf leading to the formation of a black hole, an effective dyadotorus Cherubini et al. (2009) will be formed leading to very strong creation of an electron-positron plasma. In both cases the basic mechanism which makes gravitational collapse depart from a pure gravitational phenomena is due to the electro-dynamical process introduced in this letter.

Finally, it is appropriate to recall that the existence of overcritical fields on macroscopic objects of $M \sim M_{\odot}$ and $R \sim 10$ km was first noted in the treatment of quark stars Witten (1984); Itoh (1970); Alcock et al. (1986); Kettner et al. (1995). In that case the relativistic Thomas-Fermi equations were also considered. However, in all of these investigations, a hybrid combination of general and special relativistic treatments was adopted, resulting in an inconsistency in the boundary conditions. The treatment given here in this letter is the first self-consistent treatment of the general relativistic Thomas-Fermi equations, the beta equilibrium condition and the Einstein-Maxwell equations. Critical fields are indeed obtained on the surface of the neutron star core involving only neutrons, protons, and electrons, their fundamental interactions, and with no quarks present.

While we were preparing our work an extremely interesting observational problematic has emerged from the Chandra observations of Cas A CCO Pavlov and Luna (2009); Ho and Heinke (2009). It is with a similar steadily emitting and non-pulsating neutron star that our theoretical predictions can be tested. In particular, the existence for each central density of a new family of neutron stars with a smaller crust than the one obtained when the local neutrality condition is adopted.

Indeed, the existence of neutron stars with huge crusts, i.e., with both inner and outer crusts, is mainly a consequence of assuming no electro-dynamical structure (i.e., assuming local neutrality) and of allowing electrons to have larger values of their Fermi energy E_e^F Rotondo et al. (2009). It can also be demonstrated that no consistent solution of the Einstein-Maxwell equations satisfying the local $n_e = n_p$ condition exists, even as a limiting case Rotondo et al. (2009).

B.3. The Outer Crust of Neutron Stars

B.3.1. The General Relativistic Model

The Outer Crust of Neutron Stars is the region of Neutron Stars characterized by a mass density less than the “neutron drip” density $\rho_{drip} = 4.3 \cdot 10^{11} \text{ g cm}^{-3}$ Baym et al. (1971b) and composed by White Dwarf - like material (fully ionized nuclei and free electrons). Its internal structure can be described by the Tolman-Oppenheimer-Volkoff (TOV) equation

$$\frac{dP}{dr} = -\frac{G \left(\rho + \frac{P}{c^2} \right) \left(m + \frac{4\pi r^3 P}{c^2} \right)}{r^2 \left(1 - \frac{2Gm}{rc^2} \right)}, \quad (\text{B.3.1})$$

together with the equation

$$\frac{dm}{dr} = 4\pi r^2 \rho, \quad (\text{B.3.2})$$

where m , ρ and P are the mass, the density and the pressure of the system. We have determined M_{crust} and ΔR_{crust} by integrating eq. (B.3.1) and (B.3.2) from $r_{in} = R_{is}$, where R_{is} is the radius of the inner part of the star (the base of the Outer Crust).

The pressure and the mass density of the system are

$$P \approx P_e, \quad (\text{B.3.3})$$

$$\rho \approx \mu_e m_n n_e. \quad (\text{B.3.4})$$

P_e is the pressure of electrons, given by Shapiro and Teukolsky (1983)

$$P_e = k_e \phi_e, \quad (\text{B.3.5})$$

where

$$k_e = \frac{m_e c^2}{8\pi^2 \lambda_e^3}, \quad (\text{B.3.6})$$

$$\phi_e = \quad (\text{B.3.7})$$

$$\xi_e \left(\frac{2}{3} \xi_e^2 - 1 \right) \sqrt{\xi_e^2 - 1} + \log \left(\xi_e + \sqrt{\xi_e^2 - 1} \right), \quad (\text{B.3.8})$$

with λ_e the Compton wavelength of electrons, $\xi_e = \sqrt{1 + x_e^2}$ and x_e the Fermi momentum of electrons normalized to $(m_e c)$. μ_e is the mean molecular weight per electron that, for a completely ionized element of atomic weight A and number Z , is equal to A/Z (for simplicity, we assume $\mu_e = 2$), m_n is

the mass of neutrons and n_e is the number density of electrons

$$n_e = \frac{x_e^3}{3\pi^2\lambda_e^3}. \quad (\text{B.3.9})$$

In eq. (B.3.4) we have assumed the local charge neutrality of the system.

B.3.2. The mass and the thickness of the crust

We have integrated eq. (B.3.1) and (B.3.2) for different sets of initial conditions; in fig. B.8 are shown the results obtained assuming

$$\begin{aligned} 10 \text{ km} &\leq R_{is} \leq 20 \text{ km}, \\ 1M_\odot &\leq M_{is} \leq 3M_\odot \end{aligned}$$

and an initial pressure equal to $1.6 \cdot 10^{30} \text{ dyne cm}^{-2}$, that corresponds to a mass density equal to ρ_{drip} .

It can be seen that M_{crust} has values ranging from $10^{-6}M_\odot$ to $10^{-3}M_\odot$; both M_{crust} and ΔR_{crust} increase by increasing R_{is} and decreasing M_{is} (see fig. B.8, B.9).

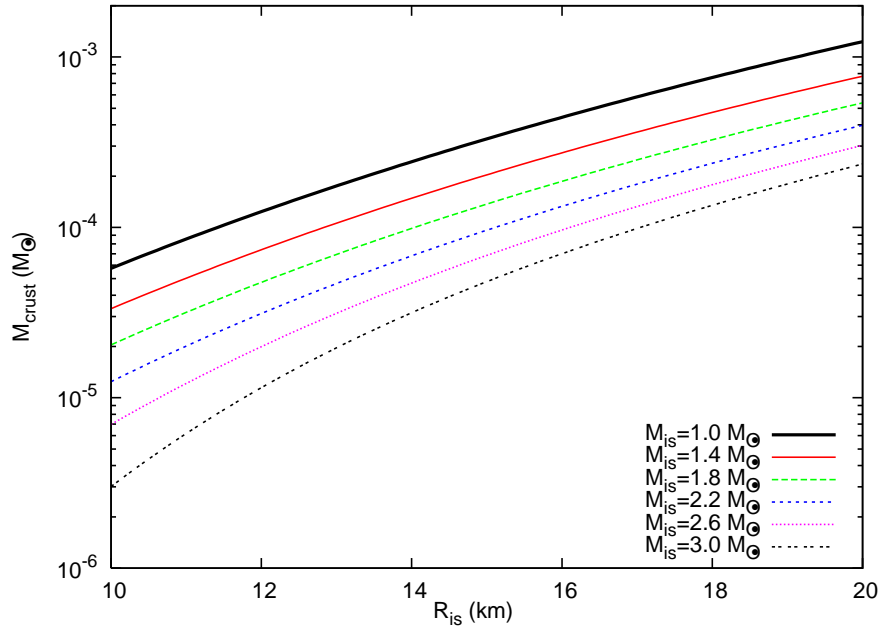


Figure B.8: Values of M_{crust} in units of solar masses, as function of R_{is} , for different values of M_{is} (see legend).

It's important to note that the values estimated for M_{crust} strongly depend on the values of M_{is} and R_{is} used; in particular, the values of M_{is} considered are greater than the maximum mass calculated for neutron stars with a core

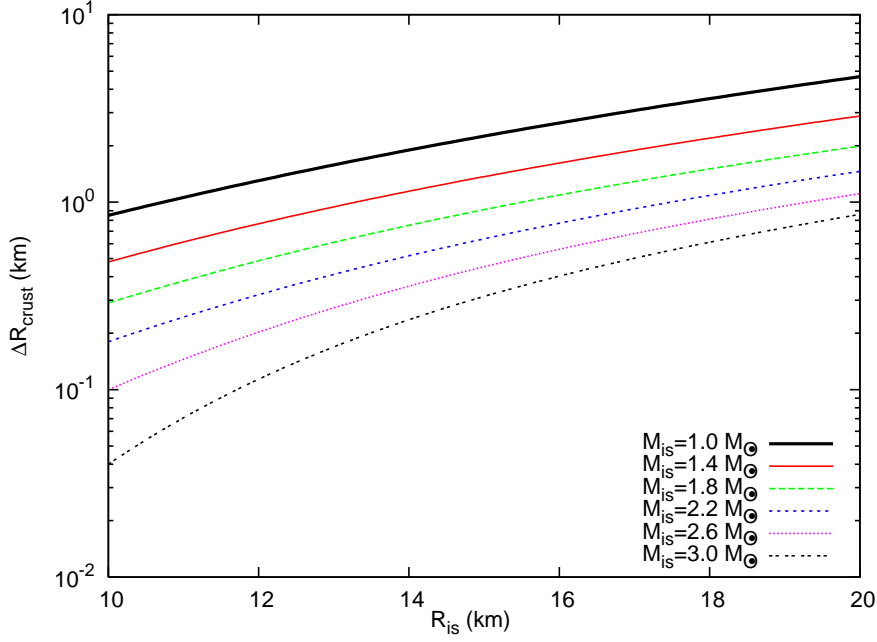


Figure B.9.: Values of thickness of the Outer Crust ΔR_{crust} in km, as function of R_{is} , for different values of M_{is} (see legend).

of degenerate relativistic electrons, protons and neutrons in local charge neutrality ($M_{max} = 0.7M_{\odot}$ Oppenheimer and Volkoff (1939)). The outstanding theoretical problem to address is to identify the physical forces influencing such a strong departure; the two obvious candidate are the electromagnetic structure in the core and/or the strong interactions.

B.3.3. The Fireshell Model of GRBs

In the Fireshell Model H. Kleinert, R. T. Jantzen, R. Ruffini (2008) GRBs are generated by the gravitational collapse of the star progenitor to a charged black hole. The electron-positron plasma created in the process of black hole (BH) formation expands as a spherically symmetric “fireshell”. It evolves and encounters the *baryonic remnant* of the star progenitor of the newly formed BH, then is loaded with baryons and expands until the transparency condition is reached and the Proper - GRB is emitted. The afterglow emission starts due to the collision between the remaining optically thin fireshell and the CircumBurst Medium. A schematization of the model is shown in fig. B.10.

The baryon loading is measured by the dimensionless quantity

$$B = \frac{M_B c^2}{E_{dya}}, \quad (\text{B.3.10})$$

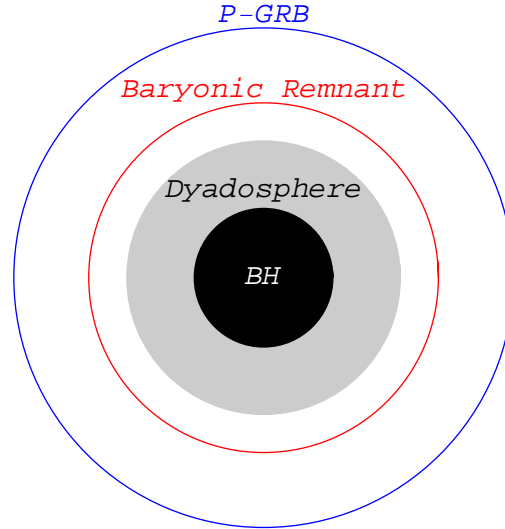


Figure B.10.: Schematization of the Fireshell Model of GRBs.

where M_B is the mass of the baryonic remnant and E_{dya} is the energy of the dyadosphere, the region outside the horizon of a BH where the electric field is of the order of the critical value for electron positron pair creation Heisenberg and Euler (1936), Sauter (1931) and Schwinger (1951, 1954a,b)

$$E_c = \frac{m_e^2 c^3}{e \hbar} \approx 10^{16} \text{ V cm}^{-1}. \quad (\text{B.3.11})$$

B and E_{dya} are the two free parameters of the model.

B.3.4. The mass of the crust and M_B

Using the values of B and E_{dya} constrained by the observational data of several GRBs and eq. (B.3.10), we have obtained the correspondent values of M_B (see table B.4).

It can be seen that these values are compatible with the ones of M_{crust} .

GRB	M_B/M_\odot
970228	5.0×10^{-3}
050315	4.3×10^{-3}
061007	1.3×10^{-3}
991216	7.3×10^{-4}
011121	9.4×10^{-5}
030329	5.7×10^{-5}
060614	4.6×10^{-6}
060218	1.3×10^{-6}

Table B.4.: GRBs and correspondent values of M_B used to reproduce the observed data within the Fireshell Model, in units of solar masses.

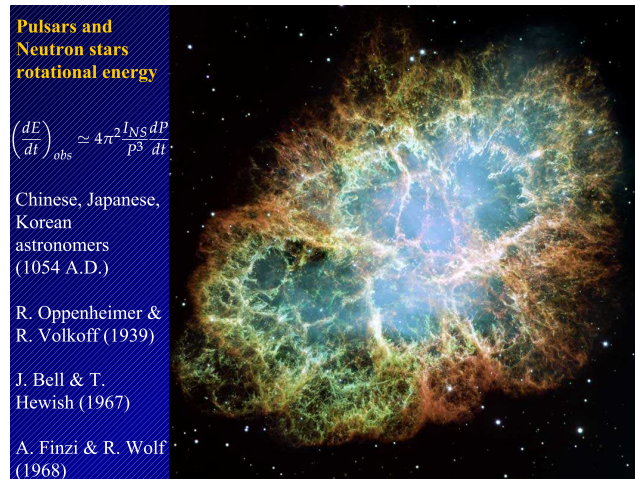
B.4. The Role of Thomas-Fermi approach in Neutron Star Matter

B.4.1. Introduction

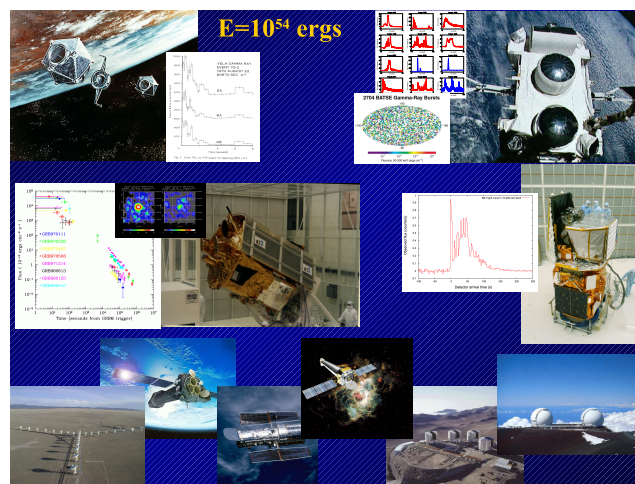
We first recall how certainly one of the greatest success in human understanding of the Universe has been the research activity started in 1054 by Chinese, Korean and Japanese astronomers by the observations of a “Guest Star”(see e.g. Shklovsky Shklovskii (1968)), followed by the discovery of the Pulsar *NPO532* in the Crab Nebula in 1967, (see e.g. Manchester and Taylor Manchester and Taylor (1977)), still presenting challenges in the yet not identified physical process originating the expulsion of the remnant in the Supernova explosion (see e.g. Mezzacappa and Fuller Mezzacappa (2005) and Fig. B.11(a)). We are currently exploring the neutron star equilibrium configuration for a missing process which may lead to the solution of the above mentioned astrophysical puzzle.

We also recall an additional astrophysical observation which is currently capturing the attention of Astrophysicists worldwide: the Gamma ray Bursts or for short GRBs. Their discovery was accidental and triggered by a very unconventional idea proposed by Yacov Borisovich Zel’dovich. It is likely that this idea served as an additional motivation for the United States of America to put a set of four Vela Satellites into orbit, 150,000 miles above the Earth. They were top-secret omnidirectional detectors using atomic clocks to precisely record the arrival times of both X-rays and γ -rays (see Fig. B.11(b)). When they were made operational they immediately produced results (see Fig. B.11(b)). It was thought at first that the signals originated from nuclear bomb explosions on the earth but they were much too frequent, one per day! A systematic analysis showed that they had not originated on the earth, nor even in the solar system. These Vela satellites had discovered GRBs! The first public announcement of this came at the AAAS meeting in San Francisco in a special session on neutron stars, black holes and binary X-ray sources, organized by Herb Gursky and myself Gursky and Ruffini (1975).

A few months later, Thibault Damour and myself published a theoretical framework for GRBs based on the vacuum polarization process in the field of a Kerr–Newman black hole Damour and Ruffini (1975). We showed how the pair creation predicted by the Heisenberg-Euler-Schwinger theory Heisenberg and Euler (1936); Schwinger (1951, 1954a,b) would lead to a transformation of the black hole, asymptotically close to reversibility. The electron-positron pairs created by this process were generated by what we now call the blackholic energy. In that paper we concluded that this “naturally leads to a very simple model for the explanation of the recently discovered GRBs”. Our theory had two very clear signatures. It could only operate for black holes with mass M_{BH} in the range $3.2-10^6 M_{\odot}$ and the energy released had a



(a)



(b)

Figure B.11.: (a) The expanding shell of the remnant of the Crab Nebulae as observed by the Hubble Space Telescope. Reproduced from Hubble Telescope web site with their kind permission (News Release Number: STScI-2005-37). (b) On the upper left the Vela 5A and 5B satellites and a typical event as recorded by three of the Vela satellites; on the upper right the Compton satellite and the first evidence of the isotropy of distribution of GRB in the sky; on the center left the Beppo Sax satellite and the discovery of the after glow; on the center right a GRB from Integral satellite; in the lower part the Socorro very large array radiotelescope ,the Hubble, the Chandra and the XMM telescopes, as well as the VLT of Chile and KECK observatory in Hawaii. All these instruments are operating for the observations of GRBs Ruffini et al. (2007a).

characteristic value of

$$E = 1.8 \times 10^{54} M_{BH} / M_{\odot} \text{ ergs} . \quad (\text{B.4.1})$$

Since nothing was then known about the location and the energetics of these sources we stopped working in the field, waiting for a clarification of the astrophysical scenario.

The situation changed drastically with the discovery of the “afterglow” of GRBs Costa et al. (1997) by the joint Italian-Dutch satellite BeppoSAX (see Fig. B.11(b)). This X-ray emission lasted for months after the “prompt” emission of a few seconds duration and allowed the GRB sources to be identified much more accurately. This then led to the optical identification of the GRBs by the largest telescopes in the world, including the Hubble Space Telescope, the KECK telescope in Hawaii and the VLT in Chile (see Fig. B.11(b)). Also, the very large array in Socorro made the radio identification of GRBs possible. The optical identification of GRBs made the determination of their distances possible. The first distance measurement for a GRB was made in 1997 for GRB970228 and the truly enormous of isotropical energy of this was determined to be 10^{54} ergs per burst. This proved the existence of a single astrophysical system emitting as much energy during its short lifetime as that emitted in the same time by all other stars of all galaxies in the Universe!^a It is interesting that this “quantum” of astrophysical energy coincided with the one Thibault Damour and I had already predicted, see Eq. (B.4.1). Much more has been learned on GRBs in recent years confirming this basic result (see e.g. H. Kleinert, R. T. Jantzen, R. Ruffini (2008)). The critical new important step now is to understand the physical process leading to the critical fields needed for the pair creation process during the gravitational collapse process from a Neutron Stars to a Black Hole.

As third example, we recall the galactic ‘X-ray bursters’ as well as some observed X-ray emission precursor of supernovae events. It is our opinion that the solution of: **a)** the problem of explaining the energetics of the emission of the remnant during the collapse to a Neutron Star, **b)** the problem of formation of the supercritical fields during the collapse to a Black Hole, **c)** the less energetics of galactic ‘X-ray bursters’ and of the precursor of the supernovae explosion event, will find their natural explanation from a yet unexplored field: the electro-dynamical structure of a neutron star. We will outline a few crucial ideas of how a Thomas-Fermi approach to a neutron star can indeed represent an important step in identify this crucial new feature.

¹Luminosity of average star = 10^{33} erg/s, Stars per galaxy = 10^{12} , Number of galaxies = 10^9 . Finally, $33 + 12 + 9 = 54!$

B.4.2. Thomas-Fermi model

We first recall the basic Thomas-Fermi non relativistic Equations (see e.g. Landau and Lifshitz Landau and Lifshitz (1980)). They describe a degenerate Fermi gas of N_{el} electrons in the field of a point-like nucleus of charge Ze . The Coulomb potential $V(r)$ satisfies the Poisson equation

$$\nabla^2 V(r) = 4\pi en, \quad (\text{B.4.2})$$

where the electron number density $n(r)$ is related to the Fermi momentum p_F by $n = p_F^3 / (3\pi^2 \hbar^3)$. The equilibrium condition for an electron, of mass m , inside the atom is expressed by $\frac{p_F^2}{2m} - eV = E_F$. To put Eq. (B.4.2) in dimensionless form, we introduce a function ϕ , related to Coulomb potential by $\phi(r) = V(r) + \frac{E_F}{e} = Ze \frac{\chi(r)}{r}$. Assuming $r = bx$, with $b = \frac{(3\pi)^{3/2}}{2^{7/3}} \frac{1}{Z^{1/3}} \frac{\hbar^2}{me^2}$, we then have the universal equation Thomas (1927); Fermi (1927)

$$\frac{d^2 \chi(x)}{dx^2} = \frac{\chi(x)^{3/2}}{x^{1/2}}. \quad (\text{B.4.3})$$

The first boundary condition for this equation follows from the request that approaching the nucleus one gets the ordinary Coulomb potential therefore $\chi(0) = 1$. The second boundary condition comes from the fact that the number of electrons N_{el} is $1 - \frac{N_{el}}{Z} = \chi(x_0) - x_0 \chi'(x_0)$.

B.4.3. White dwarfs and Neutron Stars as Thomas-Fermi systems

It was at the 1972 Les Houches organized by Bryce and Cecille de Witt summer School (see Fig. B.12(a) and C. De Witt, B. S. De Witt (1972)) that, generalizing a splendid paper by Landau Landau (1932), I introduced a Thomas-Fermi description of both White Dwarfs and Neutron Stars within a Newtonian gravitational theory and describing the microphysical quantities by a relativistic treatment. The equilibrium condition for a self-gravitating system of fermions, in relativistic regime is $c \sqrt{p_F^2 + m_n^2 c^2} - m_n c^2 - m_n V = -m_n V_0$, where p_F is the Fermi momentum of a particle of mass m_n , related to the particle density n by $n = \frac{1}{3\pi^2 \hbar^3} p_F^3$. $V(r)$ is the gravitational potential at a point at distance r from the center of the configuration and V_0 is the value of the potential at the boundary R_c of the configuration $V_0 = \frac{GNm_n}{R_c}$. N is the total number of particles. The Poisson equation is $\nabla^2 V = -4\pi G m_n n$. Assuming $V - V_0 = GNm_n \frac{\chi(r)}{r}$ and $r = bx$, with $b = \frac{(3\pi)^{2/3}}{2^{7/3}} \frac{1}{N^{1/3}} \left(\frac{\hbar}{m_n c} \right) \left(\frac{m_{\text{Planck}}}{m_n} \right)^2$ we obtain the gravitational Thomas-Fermi equation

$$\frac{d^2\chi}{dx^2} = -\frac{\chi^{3/2}}{\sqrt{x}} \left[1 + \left(\frac{N}{N^*} \right)^{4/3} \frac{\chi}{x} \right]^{3/2}, \quad (\text{B.4.4})$$

where $N^* = \left(\frac{3\pi}{4} \right)^{1/2} \left(\frac{m_{\text{Planck}}}{m_n} \right)^3$. Eq.(B.4.4) has to be integrated with the boundary conditions $\chi(0) = 0$, $-x_b \left(\frac{d\chi}{dx} \right)_{x=x_b} = 1$. Eq. (B.4.4) can be applied as well to the case of white dwarfs.

It is sufficient to assume

$$b = \frac{(3\pi)^{2/3}}{2^{7/3}} \frac{1}{N^{1/3}} \left(\frac{\hbar}{m_e c} \right) \left(\frac{m_{\text{Planck}}}{\mu m_n} \right)^2,$$

$$N^* = \left(\frac{3\pi}{4} \right)^{1/2} \left(\frac{m_{\text{Planck}}}{\mu m_n} \right)^3,$$

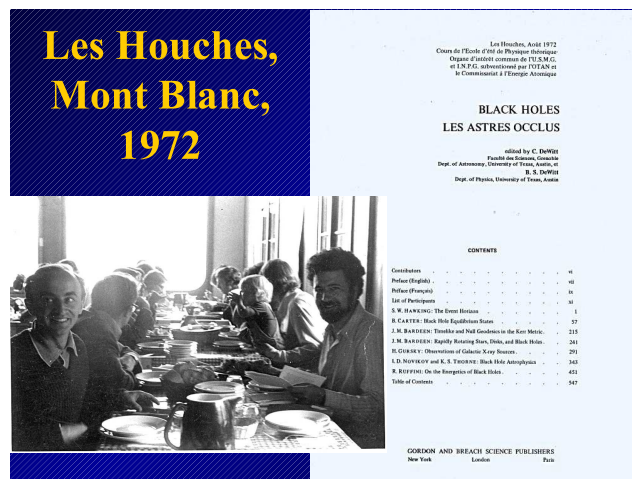
$$M = \int_0^{R_c} 4\pi r^2 n_e(r) \mu m_n dr.$$

For the equilibrium condition $c\sqrt{p_F^2 + m^2c^2} - mc^2 - \mu m_n V = -\mu m_n V_0$, in order to obtain for the critical mass the value $M_{\text{crit}} \approx 5.7 M_{\text{sun}} \mu_e^{-2} \approx 1.5 M_{\text{sun}}$.

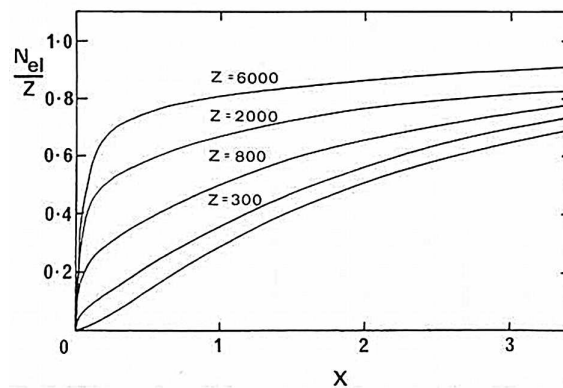
B.4.4. The relativistic Thomas-Fermi equation

In the intervening years my attention was dedicated to an apparently academic problem: the solution of a relativistic Thomas-Fermi Equation and extrapolating the Thomas-Fermi solution to large atomic numbers of $Z \approx 10^4 - 10^6$. Three new features were outlined: **a)** the necessity of introducing a physical size for the nucleus, **b)** the penetration of the electrons in the nucleus, **c)** the definition of an effective nuclear charge Ferreira et al. (1980); Ruffini and Stella (1981). The electrostatic potential is given by $\nabla^2 V(r) = 4\pi e n$, where the number density of electrons is related to the Fermi momentum p_F by $n = \frac{p_F^3}{3\pi^2 \hbar^3}$. In order to have equilibrium we have $c\sqrt{p_F^2 + m^2c^2} - mc^2 - eV(r) = E_F$. Assuming $\phi(r) = V(r) + \frac{E_F}{e} = Ze \frac{\chi(r)}{r}$, $Z_c = \left(\frac{3\pi}{4} \right)^{1/2} \left(\frac{\hbar c}{e^2} \right)^{3/2}$, and $r = bx$, with $b = \frac{(3\pi)^{3/2}}{2^{7/3}} \frac{1}{Z^{1/3}} \frac{\hbar^2}{me^2}$, the Eq. (B.4.3) becomes

$$\frac{d^2\chi(x)}{dx^2} = \frac{\chi(x)^{3/2}}{x^{1/2}} \left[1 + \left(\frac{Z}{Z_c} \right)^{4/3} \frac{\chi(x)}{x} \right]^{3/2}. \quad (\text{B.4.5})$$



(a)



(b)

Figure B.12.: (a) Lunch at Les Louces summer school on 'Black Holes'. In front, face to face, Igor Novikov and the author; in the right the title of the book in English and in French. It is interesting that in that occasion Cecile de Witt founded the French translation of the word 'Back Hole' in 'Trou Noir' objectionable and she introduced instead the even more objectionable term 'Astres Occlus'. The French nevertheless happily adopted in the following years the literally translated word 'Trou Noir' for the astrophysical concept I introduced in 1971 with J.A. Wheeler (Ruffini and Wheeler (1971)). (b) The number of electrons contained within a distance x of the origin, as a function of the total number Z for a neutral atom. The lowest curve is that given by the solution of the non-relativistic Thomas-Fermi equation.

B.4.5. The essential role of the non point-like nucleus

The point-like assumption for the nucleus leads, in the relativistic case, to a non-integrable expression for the electron density near the origin. We assumed a uniformly charged nucleus with a radius r_{nuc} and a mass number A given by the following semi-empirical formulae

$$r_{nuc} = r_0 A^{1/3}, \quad r_0 \approx 1.5 \times 10^{-13} \text{ cm}, \quad (\text{B.4.6})$$

$$Z \simeq \left[\frac{2}{A} + \frac{3}{200} \frac{1}{A^{1/3}} \right]^{-1}, \quad (\text{B.4.7})$$

Eq.(B.4.5) then becomes

$$\frac{d^2 \chi(x)}{dx^2} = \frac{\chi(x)^{3/2}}{x^{1/2}} \left[1 + \left(\frac{Z}{Z_c} \right)^{4/3} \frac{\chi(x)}{x} \right]^{3/2} - \frac{3x}{x_{nuc}^3} \theta(x_{nuc} - x), \quad (\text{B.4.8})$$

where $\theta = 1$ for $r < r_{nuc}$, $\theta = 0$ for $r > r_{nuc}$, $\chi(0) = 0$, $\chi(\infty) = 0$.

Eq.(B.4.8) has been integrated numerically for selected values of Z (see Fig. B.12(b) and Ferreira et al. (1980); Ruffini and Stella (1981)). Similar results had been obtained by Greiner and his school and by Popov and his school with special emphasis on the existence of critical electric field at the surface of heavy nuclei. Their work was mainly interested in the study of the possibility of having process of vacuum polarization at the surface of heavy nuclei to be possibly achieved by heavy nuclei collisions. Paradoxically at the time we were not interested in this very important aspect and we did not compute the strength of the field in our relativistic Thomas-Fermi model which is indeed of the order of the Critical Field $E_c = m^2 c^3 / e \hbar$.

B.4.6. Nuclear matter in bulk: $A \approx 300$ or $A \approx (m_{Planck}/m_n)^3$

The situation clearly changed with the discovery of GRBs and the understanding that the process of vacuum polarization unsuccessfully sought in earthbound experiments could indeed be observed in the process of formation of a Black Hole from the gravitational collapse of a neutron star. The concept of a Dyadosphere, Ruffini (1998); Preparata et al. (1998), was introduced around an already formed Black Hole and it became clear that this concept was of paramount importance in the understanding the energy source for GRBs. It soon became clear that the initial conditions for such a process had to be found in the electro-dynamical properties of neutron stars. Similarly manifest came the crucial factor which had hampered the analysis of the true electro dynamical properties of a neutron star; the unjustified imposition of local charge neutrality as opposed to the global charge neutrality of

the system. We have therefore proceeded to make a model of a nuclear matter core of $A \approx (m_{\text{Planck}}/m_n)^3$ nucleons Ruffini et al. (2007b). We generalized to this more general case the concept introduced in their important work by W. Greiner and V. Popov (see Fig. B.13) as follows.

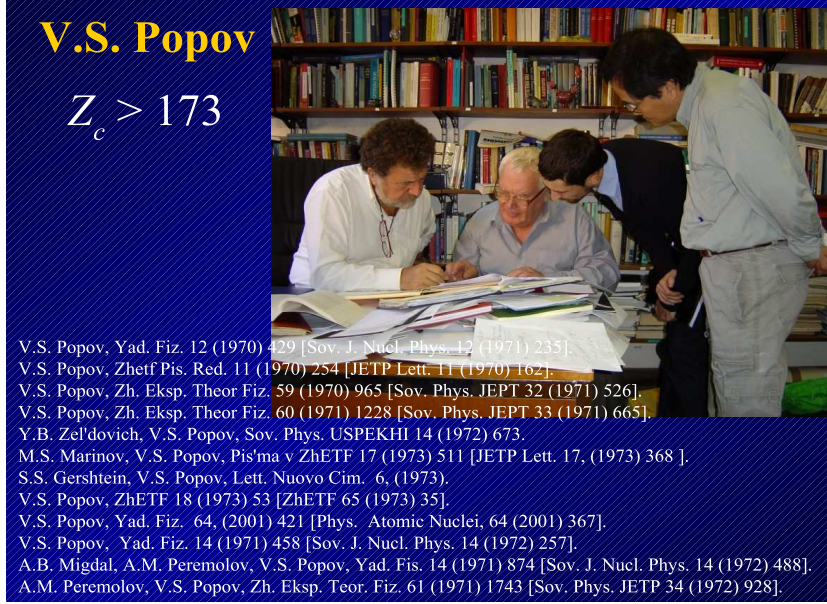


Figure B.13.: Vladimir Popov discussing with the author and Professors She Sheng Xue and Gregory Vereshchagin (Roma 2007). Also quoted the classical contributions of Popov and his school.

I have assumed that the proton number density is constant inside the core $r \leq R_c$ and vanishes outside the core $r > R_c$:

$$n_p = \frac{1}{3\pi^2\hbar^3}(P_p^F)^3 = \frac{3N_p}{4\pi R_c^3}\theta(R_c - r), \quad R_c = \Delta \frac{\hbar}{m_{\pi}c}N_p^{1/3},$$

where P_p^F is the Fermi momentum of protons, $\theta(R_c - r)$ is the step-function and Δ is a parameter. The proton Fermi energy is

$$\varepsilon_p(P_p^F) = [(P_p^F c)^2 + m_p^2 c^4]^{1/2} - m_p c^2 + eV, \quad (\text{B.4.9})$$

where e is the proton charge and V is the Coulomb potential. Based on the Gauss law, $V(r)$ obeys the Poisson equation $\nabla^2 V(r) = -4\pi e [n_p(r) - n_e(r)]$ and boundary conditions $V(\infty) = 0$, $V(0) = \text{finite}$, where the electron number density $n_e(r)$ is given by

$$n_e(r) = \frac{1}{3\pi^2\hbar^3}(P_e^F)^3, \quad (\text{B.4.10})$$

being P_e^F the electron Fermi momentum. The electron Fermi energy is

$$\mathcal{E}_e(P_e^F) = [(P_e^F c)^2 + m^2 c^4]^{1/2} - mc^2 - eV. \quad (\text{B.4.11})$$

The energetic equation for an electrodynamic equilibrium of electrons in the Coulomb potential $V(r)$ is $\mathcal{E}_e(P_e^F) = 0$, hence the Fermi momentum and the electron number density can be written as

$$n_e(r) = \frac{1}{3\pi^2 \hbar^3 c^3} \left[e^2 V^2(r) + 2mc^2 eV(r) \right]^{3/2}.$$

Introducing the new variable $x = r/(\hbar/m_\pi c)$ (the radial coordinate in unit of pion Compton length $(\hbar/m_\pi c)$, $x_c = x(r = R_c)$), I have obtained the following relativistic Thomas-Fermi Equation (Patricelli et al. (2008)):

$$\frac{1}{3x} \frac{d^2 \chi(x)}{dx^2} = -\alpha \left\{ \frac{1}{\Delta^3} \theta(x_c - x) - \frac{4}{9\pi} \left[\frac{\chi^2(x)}{x^2} + 2 \frac{m}{m_\pi} \frac{\chi}{x} \right]^{3/2} \right\}, \quad (\text{B.4.12})$$

where χ is a dimensionless function defined by $\frac{\chi}{r} = \frac{eV}{\hbar c}$ and α is the fine structure constant $\alpha = e^2/(\hbar c)$. The boundary conditions of the function $\chi(x)$ are $\chi(0) = 0$, $\chi(\infty) = 0$ and $N_e = \int_0^\infty 4\pi r^2 dr n_e(r)$. Instead of using the phenomenological relation between Z and A , given by Eqs. (B.4.6) and (B.4.7), we determine directly the relation between A and Z by requiring the β -equilibrium

$$\mathcal{E}_n = \mathcal{E}_p + \mathcal{E}_e. \quad (\text{B.4.13})$$

The number-density of degenerate neutrons is given by $n_n(r) = \frac{1}{3\pi^2 \hbar^3} (P_n^F)^3$, where P_n^F is the Fermi momentum of neutrons. The Fermi energy of degenerate neutrons is

$$\mathcal{E}_n(P_n^F) = [(P_n^F c)^2 + m_n^2 c^4]^{1/2} - m_n c^2, \quad (\text{B.4.14})$$

where m_n is the neutron mass. Substituting Eqs. (B.4.9, B.4.11, B.4.14) into Eq. (B.4.13), we obtain $[(P_n^F c)^2 + m_n^2 c^4]^{1/2} - m_n c^2 = [(P_p^F c)^2 + m_p^2 c^4]^{1/2} - m_p c^2 + eV$. These equations and boundary conditions form a close set of non-linear boundary value problem for a unique solution for Coulomb potential $V(r)$ and electron distribution (B.4.10), as functions of the parameter Δ , i.e., the proton number-density n_p . The solution is given in Fig. B.14(a). A relevant quantity for exploring the physical significance of the solution is given by the number of electrons within a given radius r , $N_e(r) = \int_0^r 4\pi (r')^2 n_e(r') dr'$. This allows to determine, for selected values of the $A = N_p + N_n$ parameter, the distribution of the electrons within and outside the core and follow the progressive penetration of the electrons in the core at increasing values of A (see Fig. B.14(b)). We can then evaluate, generalizing the results in Ferreir-

inho et al. (1980); Ruffini and Stella (1981) , the net charge inside the core $N_{\text{net}} = N_p - N_e(R_c) < N_p$, and consequently determine of the electric field at the core surface, as well as within and outside the core (see Fig. A.18).

B.4.7. The energetically favorable configurations

Introducing the new function ϕ defined by $\phi = \Delta \left[\frac{4}{9\pi} \right]^{1/3} \frac{\chi}{x}$, and putting $\hat{x} = \Delta^{-1} \sqrt{\alpha} (12/\pi)^{1/6} x$, $\xi = \hat{x} - \hat{x}_c$ the ultra-relativistic Thomas-Fermi equation can be written as

$$\frac{d^2 \hat{\phi}(\xi)}{d\xi^2} = -\theta(-\xi) + \hat{\phi}(\xi)^3, \quad (\text{B.4.15})$$

where $\hat{\phi}(\xi) = \phi(\xi + \hat{x}_c)$. The boundary conditions on $\hat{\phi}$ are: $\hat{\phi}(\xi) \rightarrow 1$ as $\xi \rightarrow -\hat{x}_c \ll 0$ (at massive core center) and $\hat{\phi}(\xi) \rightarrow 0$ as $\xi \rightarrow \infty$. We must also have the continuity of the function $\hat{\phi}$ and the continuity of its first derivative $\hat{\phi}'$ at the surface of massive core $\xi = 0$.

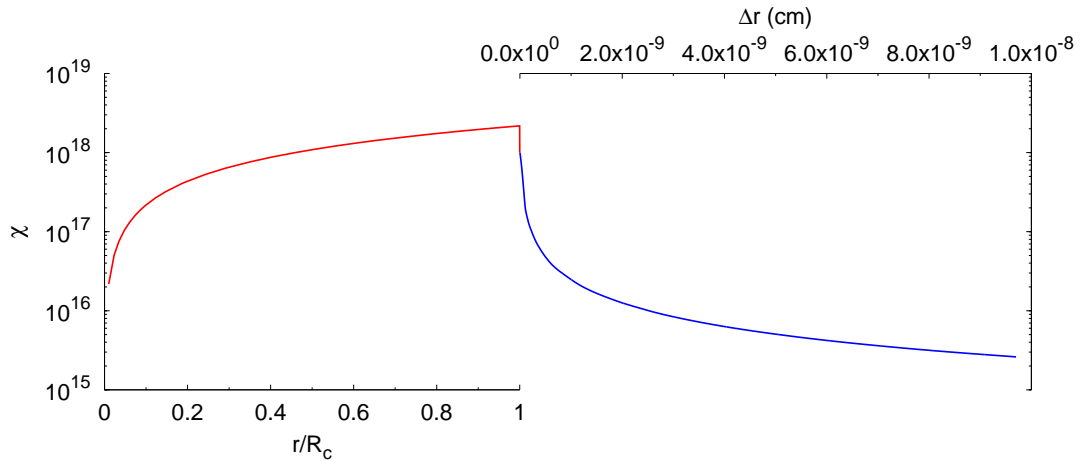
Eq. (B.4.15) admits an exact solution

$$\hat{\phi}(\xi) = \begin{cases} 1 - 3 \left[1 + 2^{-1/2} \sinh(a - \sqrt{3}\xi) \right]^{-1}, & \xi < 0, \\ \frac{\sqrt{2}}{(\xi+b)',} & \xi > 0, \end{cases} \quad (\text{B.4.16})$$

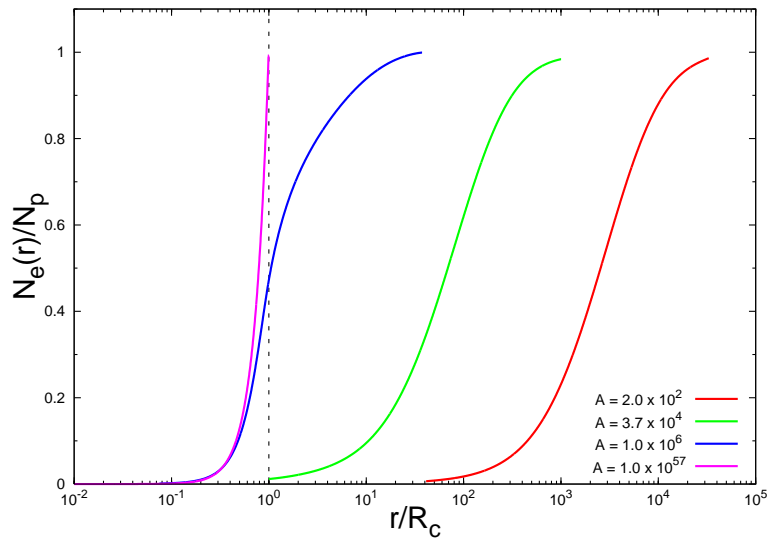
where integration constants a and b are: $\sinh a = 11\sqrt{2}$, $a = 3.439$; $b = (4/3)\sqrt{2}$.

We than have for the Coulomb potential energy, in terms of the variable ξ , $eV(\xi) = \left(\frac{1}{\Delta^3} \frac{9\pi}{4} \right)^{1/3} m_\pi c^2 \hat{\phi}(\xi)$, and at the center of massive core $eV(0) = \hbar c (3\pi^2 n_p)^{1/3} = \left(\frac{1}{\Delta^3} \frac{9\pi}{4} \right)^{1/3} m_\pi c^2$, which plays a fundamental role in order to determine the stability of the configuration.

It is possible to compare energetic properties of different configurations satisfying the different neutrality conditions $n_e = n_p$ and $N_e = N_p$, with the same core radius R_c and total nucleon number A . The total energy in the case $n_e = n_p$ is



(a)



(b)

Figure B.14.: (a) The solution χ of the relativistic Thomas-Fermi Equation for $A = 10^{57}$ and core radius $R_c = 10\text{km}$, is plotted as a function of radial coordinate. The left solid line corresponds to the internal solution and it is plotted as a function of radial coordinate in unit of R_c in logarithmic scale. The right dotted line corresponds to the solution external to the core and it is plotted as function of the distance Δr from the surface in the logarithmic scale in centimeter. (b) The electron number in the unit of the total proton number N_p , for selected values of A , is given as function of radial distance in the unit of the core radius R_c , again in logarithmic scale. It is clear how by increasing the value of A the penetration of electrons inside the core increases.

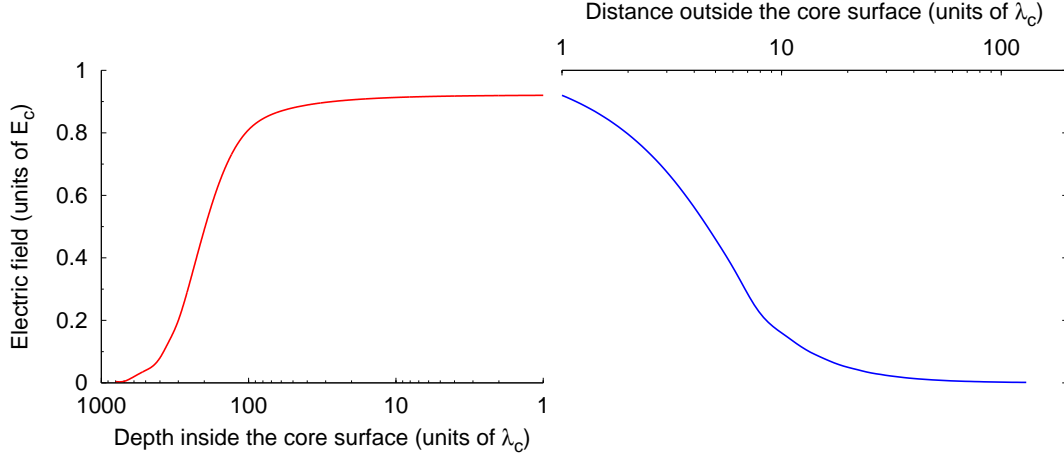


Figure B.15.: The electric field in the unit of the critical field E_c is plotted around the core radius R_c . The left (right) solid (dotted) diagram refers to the region just inside (outside) the core radius plotted logarithmically. By increasing the density of the star the field approaches the critical field.

$$\begin{aligned}\mathcal{E}_{\text{tot}}^{\text{loc}} &= \sum_{i=e,p,n} \mathcal{E}_{\text{loc}}^i \\ \mathcal{E}_{\text{loc}}^i &= 2 \int \frac{d^3 r d^3 p}{(2\pi\hbar)^3} \epsilon_{\text{loc}}^i(p) = \\ &= \frac{cV_c}{8\pi^2\hbar^3} \left\{ \bar{P}_i^F [2(\bar{P}_i^F)^2 + (m_i c)^2] [(\bar{P}_i^F)^2 + (m_i c)^2]^{1/2} - (m_i c)^4 \text{Arsh} \left(\frac{\bar{P}_i^F}{m_i c} \right) \right\}\end{aligned}$$

The total energy in the case $N_e = N_p$ is

$$\begin{aligned}\mathcal{E}_{\text{tot}}^{\text{glob}} &= \mathcal{E}_{\text{elec}} + \mathcal{E}_{\text{binding}} + \sum_{i=e,p,n} \mathcal{E}_{\text{glob}}^i \\ \mathcal{E}_{\text{elec}} &= \int \frac{E^2}{8\pi} d^3 r \approx \frac{3^{3/2} \pi^{1/2} N_p^{2/3}}{4 \sqrt{\alpha} \Delta c} m_\pi \int_{-\kappa R_c}^{+\infty} dx [\phi'(x)]^2 \\ \mathcal{E}_{\text{binding}} &= -2 \int \frac{d^3 r d^3 p}{(2\pi\hbar)^3} eV(r) \approx -\frac{V_c}{3\pi^2\hbar^3} (P_e^F)^3 eV(0) \\ \mathcal{E}_{\text{glob}}^i &= 2 \int \frac{d^3 r d^3 p}{(2\pi\hbar)^3} \epsilon_{\text{glob}}^i(p) = \\ &= \frac{cV_c}{8\pi^2\hbar^3} \left\{ P_i^F [2(P_i^F)^2 + (m_i c)^2] [(P_i^F)^2 + (m_i c)^2]^{1/2} - (m_i c)^4 \text{Arsh} \left(\frac{P_i^F}{m_i c} \right) \right\}.\end{aligned}$$

We have indicated with \bar{P}_i^F ($i = n, e, p$) the Fermi momentum in the case of local charge neutrality ($V = 0$) and with P_i^F ($i = n, e, p$) the Fermi momentum in the case of global charge neutrality ($V \neq 0$). The energetic difference between local neutrality and global neutrality configurations is positive, $\Delta\mathcal{E} = \mathcal{E}_{tot}^{loc} - \mathcal{E}_{tot}^{glob} > 0$, so configurations which obey to the condition of global charge neutrality are energetically favorable with respect to one which obey to the condition of local charge neutrality. For a core of 10 Km the difference in binding energy reaches 10^{49} ergs which gives an upper limit to the energy emittable by a neutron star, reaching its electrodynamical ground state. The current work is three fold: **a)** generalize our results considering the heavy nuclei as special limiting cases of macroscopic nuclear matter cores Patricelli et al. (2008), **b)** describe a macroscopic nuclear matter core within the realm of General Relativity fulfilling the generalized Tolman, Oppenheimer, Volkoff equation, **c)** Generalize the concept of a Dyadosphere to a Kerr-Newman Geometry.

B.4.8. Conclusions

It is clear that any neutron star has two very different components: the core with pressure dominated by a baryonic component and the outer crust with pressure dominated by a leptonic component and density dominated by the nuclear species. The considerations that we have presented above apply to the first component where the baryonic pressure dominates. It is clear that when the density increases and baryons become ultra-relativistic is this baryonic component which undergoes the process of gravitational collapse and its dynamics is completely dominated by the electrodynamical process which we have presented in this talk.

B.5. A Self-consistent Approach to Neutron Stars

B.5.1. Introduction

Since the seminal work of Oppenheimer and Volkoff (1939) on the general relativistic equilibrium state of a degenerate gas of neutrons, a colossal amount of research has been devoted to neutron star physics. In scientific literature on neutron stars, a “local approach”, where the equation of state of neutron star matter is constructed ignoring global gravitational and Coulombian effects by assuming not only flat space but also local charge neutrality, has been traditionally used. A barotropic relation $P = P(\mathcal{E})$ between the energy-density \mathcal{E} and the pressure P is then obtained (see e.g. Haensel et al. (2007) for a recent compilation of modern neutron star matter equations of state). The gravitational effects are then taken into account by embedding such an equation of state into the so-called Tolman-Oppenheimer-Volkoff equation of hydrostatic equilibrium in spherical symmetry (we use units with $\hbar = c = 1$ hereafter):

$$P' = -\frac{(\mathcal{E} + P)(4\pi Gr^3 P + GM)}{r(r - 2GM)}, \quad (\text{B.5.1})$$

where the mass $M(r)$ is given by

$$M' = 4\pi r^2 \mathcal{E}, \quad (\text{B.5.2})$$

we denote radial derivatives with primes, and $G = 1/m_{\text{Pl}}^2$ with m_{Pl} being the Planck mass. Thus, in the local approach, the problem of the equilibrium state of a self-gravitating system composed of different degenerate fermion-species is reduced to an effective one-component fluid problem by solving the system of equations, given by Eqs. (B.5.1) and (B.5.2), for a barotropic equation of state $P(\mathcal{E})$.

We should consider such an approach as an effective solution of the problem that gives good estimates for the mass and the radius of a neutron star through an oversimplification of the real physical situation. However, recent developments in high-energy astrophysics point to the relevance of overcritical electric fields in neutron stars and black holes Ruffini et al. (2010). It has then become apparent that a new approach to neutron stars is necessary and that fundamental gravito-electrodynamical effects are missing in the traditional approach.

We present here the self-consistent equilibrium equations governing a degenerate neutron, proton and electron fluid in beta equilibrium within the framework of relativistic quantum statistics and of the Einstein-Maxwell equations. From this formulation descend the general relativistic Thomas-Fermi equation, which, as in the case of atoms, plays a crucial role by joining Coulombian, gravitational and quantum-statistical effects associated with the equilib-

rium state of a self-gravitating system of degenerate fermions.

B.5.2. The Equilibrium Equations

We consider the equilibrium configurations of a degenerate gas of neutrons, protons and electrons with total matter energy density and pressure

$$\mathcal{E} = \sum_{i=n,p,e} \mathcal{E}_i, \quad (\text{B.5.3})$$

$$P = \sum_{i=n,p,e} P_i, \quad (\text{B.5.4})$$

that satisfy the condition of beta equilibrium

$$\mu_n = \mu_p + \mu_e, \quad (\text{B.5.5})$$

where $\mu_i = \partial\mathcal{E}/\partial n_i$ denotes the free chemical potential of the particle species with number density n_i . In addition, we introduce the extension to general relativity of the Thomas-Fermi equilibrium condition on the generalized Fermi energy E_e^F of the electron component:

$$E_e^F = e^{v/2} \mu_e - m_e - eV = \text{constant}, \quad (\text{B.5.6})$$

where e is the fundamental charge, V is the Coulomb potential of the configuration and we have introduced the metric

$$ds^2 = e^{v(r)} dt^2 - e^{\lambda(r)} dr^2 - r^2 d\theta^2 - r^2 \sin^2 \theta d\varphi^2, \quad (\text{B.5.7})$$

for a spherically-symmetric non-rotating neutron star. The metric function λ is related to the mass $M(r)$ and the electric field $E(r) = -e^{-(v+\lambda)/2} V'$ through

$$e^{-\lambda} = 1 - \frac{2GM(r)}{r} + Gr^2 E^2(r). \quad (\text{B.5.8})$$

Thus, the equations for the neutron star equilibrium configuration consist of the following Einstein-Maxwell equations and general relativistic Thomas-

Fermi equation:

$$\begin{aligned}
 M' &= 4\pi r^2 \mathcal{E} - 4\pi r^3 e^{-\nu/2} \hat{V}' (n_p + n_e) \quad (\text{B.5.9}) \\
 \frac{\nu'}{r} + \frac{1 - e^\lambda}{r^2} &= 8\pi G e^\lambda \left[P - \frac{e^{-(\nu+\lambda)}}{8\pi\alpha} (\hat{V}')^3 \right] \quad (\text{B.5.10}) \\
 P' + \frac{\nu'}{2} (\mathcal{E} + P) &= -(P^{\text{em}})' - \frac{4P^{\text{em}}}{r}, \quad (\text{B.5.11}) \\
 \hat{V}'' + \hat{V}' \left[\frac{2}{r} - \frac{(\nu' + \lambda')}{2} \right] &= -4\pi\alpha e^{\nu/2} e^\lambda \left\{ n_p \right. \\
 &\quad \left. - \frac{e^{-3\nu/2}}{3\pi^2} [(\hat{V} + m_e)^2 - m_e^2 e^{\nu}]^{3/2} \right\}, \quad (\text{B.5.12})
 \end{aligned}$$

where α denotes the fine structure constant, $\hat{V} = E_e^F + eV$ and $P^{\text{em}} = -E^2/(8\pi)$.

The assumption of the equilibrium condition in Eq. (B.5.6), together with the beta equilibrium condition in Eq. (B.5.5) and the hydrostatic equilibrium in Eq. (B.5.11), along with the thermodynamic relation $\mathcal{E}_i + P_i = n_i \mu_i$, can be demonstrated to be enough to guarantee the constancy of the generalized Fermi energy

$$E_i^F = e^{\nu/2} \mu_i - m_i + q_i V, \quad i = n, p, e, \quad (\text{B.5.13})$$

for all particle species separately. Here, q_i denotes the particle unit charge of the i -species. Indeed, as shown by Olson and Bailyn Olson and Bailyn (1975), when the fermion nature of the constituents and their degeneracy are taken into account, in the configuration of minimum energy, the generalized Fermi energies E_i^F defined by Eq. (B.5.13) must be constant over the entire configuration, i.e. r -independent. These minimum energy conditions generalize the equilibrium conditions of Klein Klein (1949) and of Kodama and Yamada Kodama and Yamada (1972) to the case of degenerate multicomponent fluids with particle species with non-zero unit charge. Therefore, the solution to the system of equations composed by Eq. (B.5.5), by Eq. (B.5.6), and by Eqs. (B.5.9)–(B.5.12) represents the ground-state equilibrium configuration.

B.5.3. Some Specific Solutions

The inconsistency of the local charge neutrality condition $n_e(r) = n_p(r)$ with this system of equations was proven in Rueda et al. (2010a), where, in addition, a globally neutral solution was obtained by solving the above self-consistent equations in the case of non-strongly interacting degenerate neutrons, protons and electrons extending from the center of the star all the way to the border. Although the configuration described in Rueda et al. (2010a) cannot represent a realistic neutron star, the gravito-electrodynamical effects discovered there deserve further attention. In addition, the results found in Rueda et al. (2010a) agree with those predicted in Rotondo et al. (2009) in the

simpler case of a beta-equilibrated degenerate neutron, proton and electron fluid at nuclear density fulfilling the relativistic Thomas-Fermi equation with constant proton density.

In a realistic neutron star, the degenerate neutron, proton and electron fluid is confined to the core and is subjected to the external pressure of the crust formed around by white-dwarf-like material. In this more general case, the constancy of the generalized Fermi energy of the electrons still plays a fundamental role in order to fulfill the matching conditions and in the boundary-value problem Rueda et al. (2010c). It can be shown that as a consequence of the fulfillment of the core-crust matching conditions and the self-consistent minimum energy equilibrium equations described here, the surface of the core develops a sharp exponential transition surrounded by the neutron star's crust Rueda et al. (2010c). Furthermore, together with such an exponential density transition, an electric field with an intensity larger than that of the critical field for vacuum polarization,

$$E_c = \frac{m_e^2}{\sqrt{\alpha}}, \quad (\text{B.5.14})$$

extending over all the entire surface of the transition surface, whose thickness is of the order of several electron Compton wavelength $\lambda_e = 1/m_e$, appears.

B.5.4. Conclusions

We have presented the coupled system of equations that must be solved in order to calculate the ground-state equilibrium configuration of a neutron star. In addition, we have shown that the minimum energy configuration exhibits an r -independent generalized particle Fermi energy for all particle species composing the internal fluid. We have also demonstrated that the minimum energy problem of neutron stars can be reformulated as an extension to general relativity of the Thomas-Fermi atom.

The contribution of the hadronic fields to the energy-momentum tensor, to the four-vector current and, consequently, to the Einstein-Maxwell equations are currently under consideration in order to establish a more general formulation of the problem Pugliese et al. (2010). The introduction of strong interactions preserves the r -independence of the generalized Fermi energy of the electrons, requires the fulfillment of the general relativistic Thomas-Fermi equation, and confirms all the gravito-electrodynamical effects here described in the simplest possible example Pugliese et al. (2010).

B.6. On the electrostatic structure of neutron stars

B.6.1. Introduction

From the point of view of Newtonian gravity, an spherically symmetric object composed by a free degenerate gas of neutrons has a maximum mass about $M_{\max} \simeq 5.8M_{\odot}$ Landau and Lifshitz (1980). Nevertheless, the strong gravity expected in neutron star interiors imposes the use of general relativity equations as structure equations. For the same free gas of neutrons, Einstein theory strongly reduces the maximum mass limit to $M_{\max} \simeq 0.7M_{\odot}$ as calculated by Oppenheimer & Volkoff (OV) in their seminal paper Oppenheimer and Volkoff (1939).

Observations of X-Ray Binary systems ruled out rapidly the OV work finding that usually neutron stars have masses $M_{NS} \gtrsim 1.4M_{\odot}$. Even very recently an extraordinary high value of $M = 2.74 \pm 0.21M_{\odot}$ has been reported for the millisecond pulsar PSR J1748-2021B Freire et al. (2008). Therefore, researchers directed their attention to the theoretical study of the properties of neutron stars. In particular, the improvement of the Equation of State (EoS) for nuclear matter at densities above the so-called saturation density of ordinary nuclei $\rho_0 \simeq 2.7 \times 10^{14} \text{ g cm}^{-3}$, has been one of the challenges of theoretical physics in the last 40 years.

Despite the effort to understand the nuclear EoS above saturation density ρ_0 , the problem is by far unsolved, due mainly to the lack of a theory for the strong interaction, and to the lack of ground-based experiments able to simulate the extreme conditions expected in neutron star interiors. Consequently, a proliferation of nuclear EoS approaching in different ways the strong interaction is growing day after day. Thus, to avoid any discussion of validity of the EoS we use, we will construct here a simple phenomenological EoS based on the Weizsacker mass formula in nuclear physics, which let us to concentrate the attention to the real scope of the paper, which is devoted to the self-consistent introduction of the electromagnetic interaction inside the equilibrium equations governing neutron stars.

The standard picture of a neutron star assumes at least the existence of three regions: core, inner crust and outer crust. Starting for the more external one, the outer crust is composed by a nuclei lattice (or Coulomb lattice) immersed in sea of free electrons, and extents until a density $\rho_d \simeq 4 \times 10^{11} \text{ g cm}^{-3}$ or neutron drip density. At this density, the dripped neutrons start to form a background of neutrons. This region composed by a nuclei lattice in a background of electrons and neutrons is known as inner crust and exists approximately until the nuclear saturation density $\rho_0 \simeq 2.7 \times 10^{14} \text{ g cm}^{-3}$. At even higher densities, the core of the star is assumed to be a uniform gas composed mainly by neutrons, and a smaller presence of protons and electrons under the constraints of β -equilibrium and local charge neutrality $n_e = n_p$. Here n_e and n_p stand for the electron and proton number densities. There-

fore, in the interior of a neutron star conjugate all the interactions we know in nature, namely, weak, strong, electromagnetic and gravitational. Nevertheless, as we have mentioned, the electromagnetic interaction is not taken into account because the very stringent assumption of local charge neutrality condition $n_e = n_p$ is assumed. In this paper we will relax this condition and impose the more general one $N_e = N_p$ where N_e, N_p are the total number of electrons and protons respectively.

As a natural consequence of global neutrality it appears a transition surface-shell between the core and the crust. The thickness δR of this surface-shell is of order of the electron Compton wavelength $\lambda_e = 1/m_e$ (we use hereafter $\hbar = c = 1$), i.e., of the order of some fermi. Inside the surface-shell a strong electric field develops. It grows until some maximum value and after drops down up to some distance δR from the core radius R_c where it becomes null and the configuration becomes neutral. Therefore, the thickness of the surface-shell δR is given by the global neutrality condition

$$\varphi(R_c + \delta R) = 0, \quad \varphi'(R_c + \delta R) = 0, \quad (\text{B.6.1})$$

where φ is the electrostatic potential.

B.6.2. Structure Equations

The metric for a spherically symmetric spacetime can be written as

$$ds^2 = e^\nu dt^2 - e^\lambda dr^2 - r^2 d\theta^2 - r^2 \sin^2 \theta d\phi^2, \quad (\text{B.6.2})$$

where ν and λ are functions of r only. For this metric the Einstein-Maxwell field equations are

$$M' = 4\pi r^2 (T_0^0 - \mathcal{E}_{\text{em}}) + 4\pi e^{\lambda/2} r^3 e E (n_p - n_e) \quad (\text{B.6.3})$$

$$e^{-\lambda} \left(\frac{\nu'}{r} + \frac{1}{r^2} \right) - \frac{1}{r^2} = -8\pi G T_1^1 \quad (\text{B.6.4})$$

$$e^{-\lambda} \left[\nu'' + (\nu' - \lambda') \left(\frac{\nu'}{2} + \frac{1}{r} \right) \right] = -16\pi G T_2^2 \quad (\text{B.6.5})$$

$$\begin{aligned} (e\varphi)'' + (e\varphi)' \left[\frac{2}{r} - \frac{(\nu' + \lambda')}{2} \right] \\ = -4\pi \alpha e^{\nu/2} e^\lambda (n_p - n_e), \end{aligned} \quad (\text{B.6.6})$$

where T_ν^μ is the energy-momentum tensor of matter and fields, E is the electrostatic field and $\mathcal{E}_{\text{em}} = E^2/2$ is the electromagnetic energy density.

B.6.3. The Equation of State

Core EoS

In phenomenological nuclear physics, the Weizsacker binding energy per nucleon is given by

$$\frac{E_W}{A} = -a_v + a_s \frac{(N-Z)^2}{A^2} + a_C \frac{Z^2}{A^{4/3}} + a_{\text{surf}} A^{-1/3} + \frac{\delta_{\text{even-odd}}}{A}, \quad (\text{B.6.7})$$

where

$$a_v = 15.8 \text{ MeV} \quad a_{\text{surf}} = 18.3 \text{ MeV} \quad a_s = 23.3 \text{ MeV} \\ a_C = 0.714 \text{ MeV} \quad \delta_{\text{even-odd}} \simeq 12 \text{ MeV},$$

are the volume, surface, symmetry, Coulomb, and pairing contributions.

If we assume the above formula valid also in the case of neutron rich matter $N \gg Z$ we have

$$\frac{E_W}{A} \simeq -a_v + a_s > 0, \quad (\text{B.6.8})$$

which implies that neutron rich matter is unbounded. However, for a large number of baryons A , the gravitational potential plays an important role. In order to see that, let us to modify the Weizsacker formula by including the gravitational interaction (in the constant density case)

$$\frac{E_W}{A} \simeq -a_v + a_s - \frac{3}{5r_0} \left(\frac{m_n}{m_{\text{Planck}}} \right)^2 A^{2/3}, \quad (\text{B.6.9})$$

where we have assumed

$$M \simeq m_n A, \quad R \simeq r_0 A^{1/3}, \quad m_n \simeq 939 \text{ MeV}. \quad (\text{B.6.10})$$

Then neutron matter is bounded for

$$A > A^* = \left[\frac{5r_0}{3} (-a_v + a_s) \right]^{3/2} \left(\frac{m_{\text{Planck}}}{m_n} \right)^3 \simeq 0.8 \times 10^{56}. \quad (\text{B.6.11})$$

Using this minimum mass number A^* for bounding we calculate the minimum mass as given by the modified Weizsacker formula (B.6.9)

$$M_W \gtrsim m_n A^* \simeq 0.07 M_\odot, \quad (\text{B.6.12})$$

which is very close to the value given by most accepted nuclear EoS.

Therefore the nuclear potential energy should properly be included into the

mass–energy of neutron star cores. Applying the Weizsacker formula (B.6.7) to a local thin–shell of neutron star cores, we write the energy density for the core in the form

$$\mathcal{E} = \mathcal{E}_k + \mathcal{E}_W + \mathcal{E}_{em} \quad (\text{B.6.13})$$

where

$$\mathcal{E}_k = \frac{2}{(2\pi)^3} \sum_{i=e,p,n} \int_0^{k_i^F} 4\pi k^2 \sqrt{k^2 + m_i^2} dk, \quad (\text{B.6.14})$$

$$\mathcal{E}_W = -a_v^* n + a_s^* n T^2 + a_{\text{surf}} n^{2/3} \delta(r - R_c), \quad (\text{B.6.15})$$

where

$$T \equiv \frac{n_n - n_p}{n}, \quad n \equiv n_p + n_n, \quad (\text{B.6.16})$$

are the asymmetry parameter and the baryon number density. The parameters a_v^* and a_s^* must be calculated avoiding double counting of the kinetic contribution to the volume and symmetry energy. For the surface contribution we have introduced a δ -distribution about the core radius R_c to recall that it acts just on the surface of the core. The radius of the core is defined as the radius at which the rest-mass density of the core reach nuclear density, namely, $\rho(R_c) = \rho_0 \simeq 2.7 \times 10^{14} \text{ g cm}^{-3}$. The delta distribution has dimension L^{-1} , and it is given by the characteristic range of the strong interaction, so it should be of the order of some fermi.

To obtain the parameters a_v^* and a_s^* , we expand the kinetic energy (B.6.13) about $n_n = n_p$ ($T = 0$), i.e. for symmetric nuclear matter

$$\frac{\mathcal{E}_k}{n} - m = \tilde{a}_v + \tilde{a}_s T^2 + \dots, \quad (\text{B.6.17})$$

$$\tilde{a}_v \simeq 21.84 \text{ MeV}, \quad \tilde{a}_s = \frac{k_0^F}{6\sqrt{(k_0^F)^2 + m^2}} \simeq 11.84 \text{ MeV}, \quad (\text{B.6.18})$$

where we have assumed $m_p \simeq m_n \simeq m = 939 \text{ MeV}$, and

$$k_p^F = k_n^F = k_0^F = \left(\frac{3\pi^2 n_0}{2} \right)^{1/3} \simeq 263.26 \text{ MeV}, \quad (\text{B.6.19})$$

where $n_0 \simeq 0.16 \text{ fm}^{-3}$. Then we obtain

$$a_v^* = a_v - \tilde{a}_v \simeq 37.64 \text{ MeV}, \quad (\text{B.6.20})$$

$$a_{as}^* = a_s - \tilde{a}_s \simeq 11.45 \text{ MeV}. \quad (\text{B.6.21})$$

Therefore, the relevant components of the energy-momentum tensor in the

core are

$$T_0^0 = \mathcal{E}_k + \mathcal{E}_{\text{em}} + \mathcal{E}_W, \quad (\text{B.6.22})$$

$$T_1^1 = -P_k + \mathcal{E}_{\text{em}} - P_W, \quad (\text{B.6.23})$$

$$T_2^2 = -P_k - \mathcal{E}_{\text{em}} - P_W. \quad (\text{B.6.24})$$

The pressure terms are calculated by thermodynamical self-consistency as

$$P_i = n^2 \frac{\partial \mathcal{E}_i / n}{\partial n}. \quad (\text{B.6.25})$$

where $i = k, \text{em}, W$ respectively indicates kinetic, electromagnetic and nuclear components. In addition, we calculate chemical potentials of neutrons, protons and electrons by using usual definition

$$\mu_{n,p,e} = \frac{\partial \mathcal{E}}{\partial n_{n,p,e}}. \quad (\text{B.6.26})$$

The system must satisfy some additional constraints. The first one is related with the equilibrium of the electron gas which can be written as

$$E_e^F = e^{\nu/2} \mu_e - e\varphi = \text{constant} > 0, \quad (\text{B.6.27})$$

while the second one is the β -equilibrium of the system given by

$$E_n^F = E_e^F + E_p^F, \quad (\text{B.6.28})$$

where

$$E_p^F = e^{\nu/2} \mu_p + e\varphi. \quad (\text{B.6.29})$$

Using the above constraints, we can write the electron and neutron number densities as

$$n_e = \frac{[e^{-\nu/2} (E_e^F + e\varphi)]^3}{3\pi^2} \quad (\text{B.6.30})$$

$$n_n = \frac{(e^{-\nu/2})^3}{3\pi^2} \{ (E_e^F + E_p^F + m_n)^2 - m_n^2 e^\nu \}^{3/2}, \quad (\text{B.6.31})$$

where we have used the ultra-relativistic approximation for the electrons $\mu_e \simeq P_e^F$, with P_e^F the electron Fermi momentum.

Crust EoS

For the inner crust we adopt the well-known EoS by Baym, Bethe and Pethick (BBP) Baym et al. (1971a), which is well fitted by the following polytropic-like

form

$$P = K \mathcal{E}^\Gamma, \quad K = 0.000287961, \quad \Gamma = 1.68051, \quad (\text{B.6.32})$$

where P and \mathcal{E} are the total pressure and energy density. Of course for each value of pressure (and density) we need the self-consistent values of the chemical potential of neutrons and electrons, which can be obtained from the entries on the tables in Baym et al. (1971a).

In the outer crust we have white-dwarf-like material, so we can obtain most of its properties from the equilibrium condition Landau and Lifshitz (1980)

$$e^{\nu/2}(\mu_e + 2m_n) = \text{constant} = e^{\nu(R)/2}(m_e + 2m_n), \quad (\text{B.6.33})$$

where R is the radius of the configuration, which is calculated as the point where $P(R) = 0$. From the matching conditions with the exterior spacetime, which must be the Schwarzschild solution we obtain

$$e^{\nu(R)/2} = \sqrt{1 - \frac{2M(R)}{R}}. \quad (\text{B.6.34})$$

B.6.4. Numerical Integration

We describe now the main steps to construct the solutions:

1. Select a value for the central rest-mass density

$$\rho(0) = \sum_{i=e,p,n} m_i n_i(0). \quad (\text{B.6.35})$$

2. Select a positive value for E_e^F . It determines the electron chemical potential at the edge of the crust

$$\mu_e^{crust} = \mu_e(R_c + \delta R) = e^{-\nu(R_c)/2} E_e^F, \quad (\text{B.6.36})$$

where we have used the global neutrality condition and the fact that at very small scales the gravitational potential is constant, which is exactly the case for the region $R_c \leq r \leq R_c + \delta R$, for $\delta R \ll R_c$.

3. From the regular behavior at the center $r = 0$ we have $n_e(0) = n_p(0)$.
4. From 1–3 and the β -equilibrium condition (B.6.28) we obtain the central particle chemical potential $\mu_e(0)$, $\mu_p(0)$, and $\mu_n(0)$.
5. Select a value for the central electrostatic potential $\varphi(0)$.
6. Now we can calculate the central gravitational potential using (B.6.27) by

$$e^{\nu(0)/2} = \frac{E_e^F + e\varphi(0)}{\mu_e(0)}. \quad (\text{B.6.37})$$

7. Having all the initial conditions determined, it is possible to integrate the equations in the core up to the a radius R_c defined by $\rho(R_c) = \rho_0$, i.e., until the surface of the core.
8. The next step is to calculate the properties of the transition surface-shell between the core and the crust. Due to the surface tension neutron and proton profiles will drop down. In this work the value of the surface tension is taken to be the one given by the Weizsacker formula (B.6.15). We calculate properly the electric field coming out from the surface charge separation between electrons and protons. The transition surface finishes when we reach global charge neutrality.
9. Finally we integrate the crust equations until reach at the radius of the configuration $P(R) = 0$. At the end of the integration we verify the matching condition with the Schwarzschild solution given by (B.6.34). If it is not satisfied we change the central gravitational potential value by changing the central potential as dictated by (B.6.37). In other words, the correct value of the central electrostatic potential is the one for which we satisfy correctly all the boundary conditions of the system.

Below we show an example of the integration for the initial conditions $\rho(0) \simeq 5.7\rho_0$ and $P(0) \simeq 40.63 \text{ MeV}/\text{fm}^3$. In Fig. B.16 we have plotted the mass function in the core of the star in solar masses, while in Fig. B.17 we show the electrostatic field in the core in unit of the critical electric field for vacuum polarization $E_c = m_e^2 c^3 / e\hbar \sim 10^{16} \text{ V}/\text{cm}$. Fig. B.18 shows the electrostatic potential energy of protons in the core in units of the pion mass and in Fig. B.19 we show the number density of neutrons, protons, and electrons normalized to the nuclear number density n_0 in the core. In Fig. B.20 it is shown the internal pressure in the core. In Figs. B.21 and B.22 we show the electrostatic field and proton Coulomb energy in the transition surface-shell between the core and the crust, while in Figs. B.23 and B.24 we have plotted the number density of particles and internal pressure in the surface-shell.

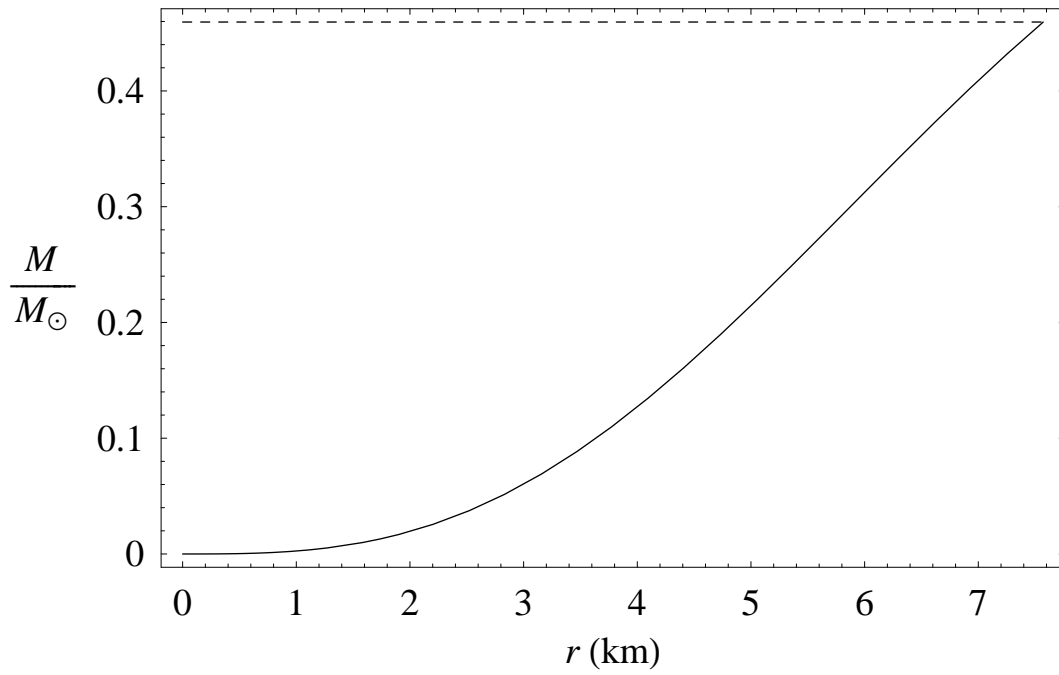


Figure B.16.: Mass of the core in solar masses.

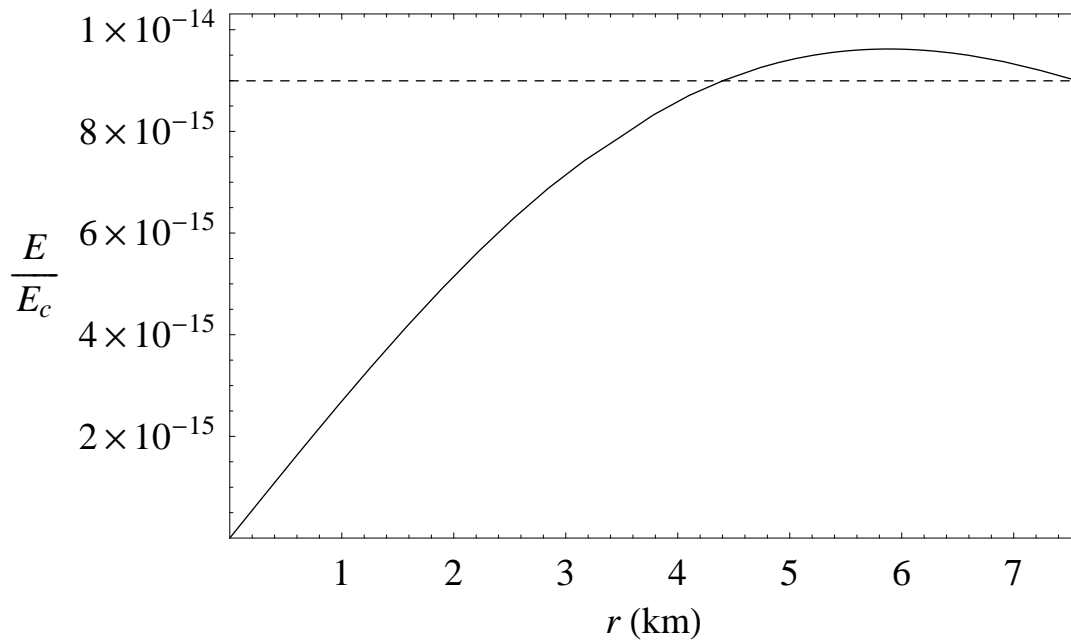


Figure B.17.: Electric field of the core in units of the critical field

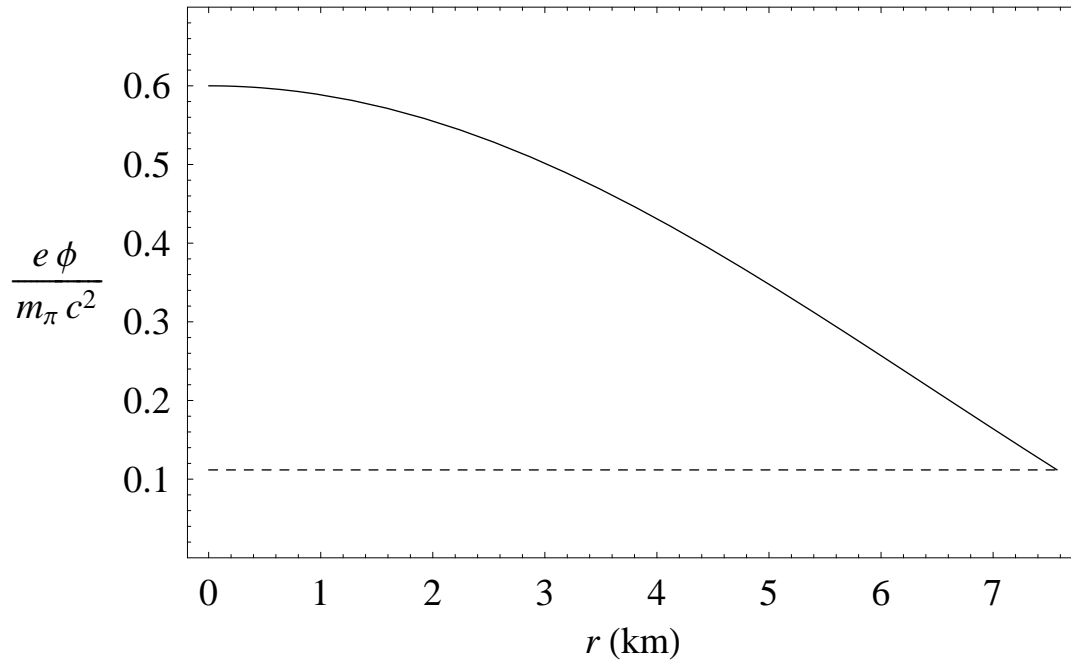


Figure B.18.: Electrostatic potential of the core in units of the pion mass.

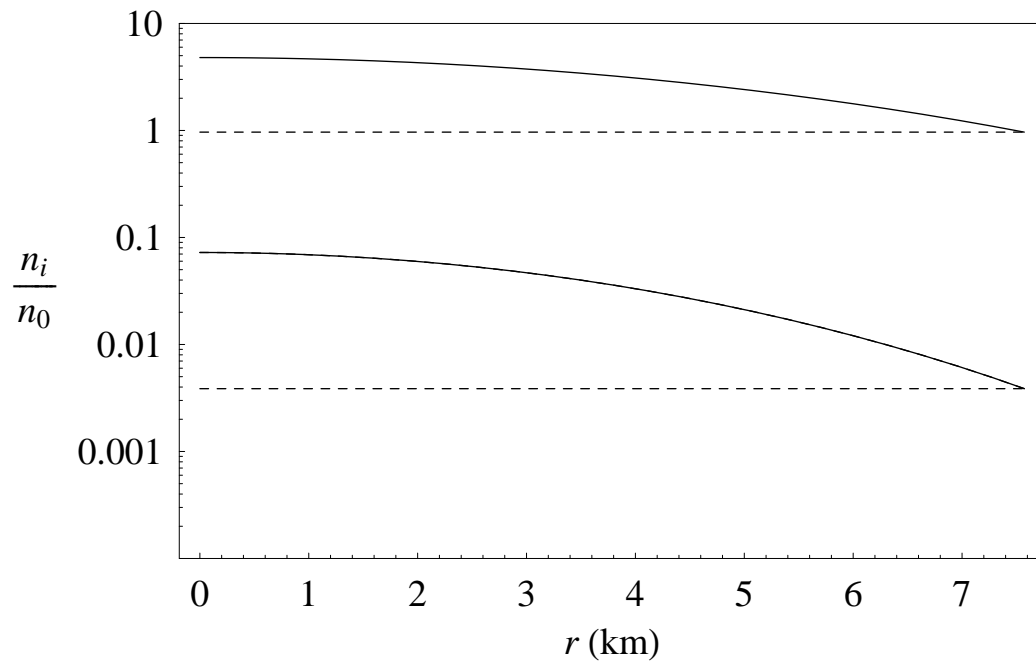


Figure B.19.: Number densities inside the core in units of the nuclear density n_0 .

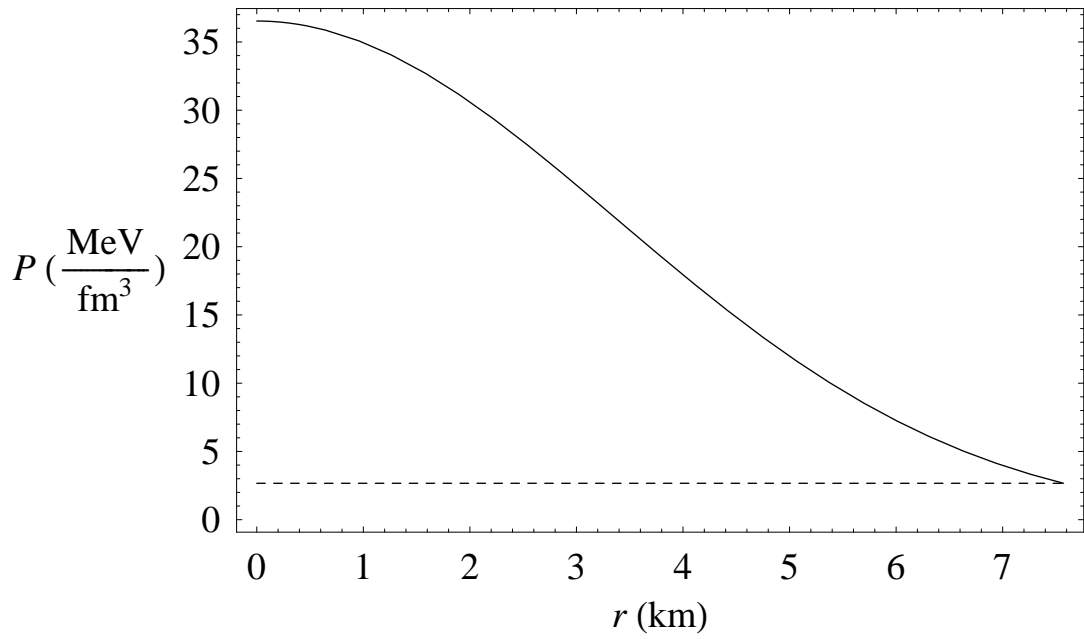


Figure B.20.: Pressure inside the core.

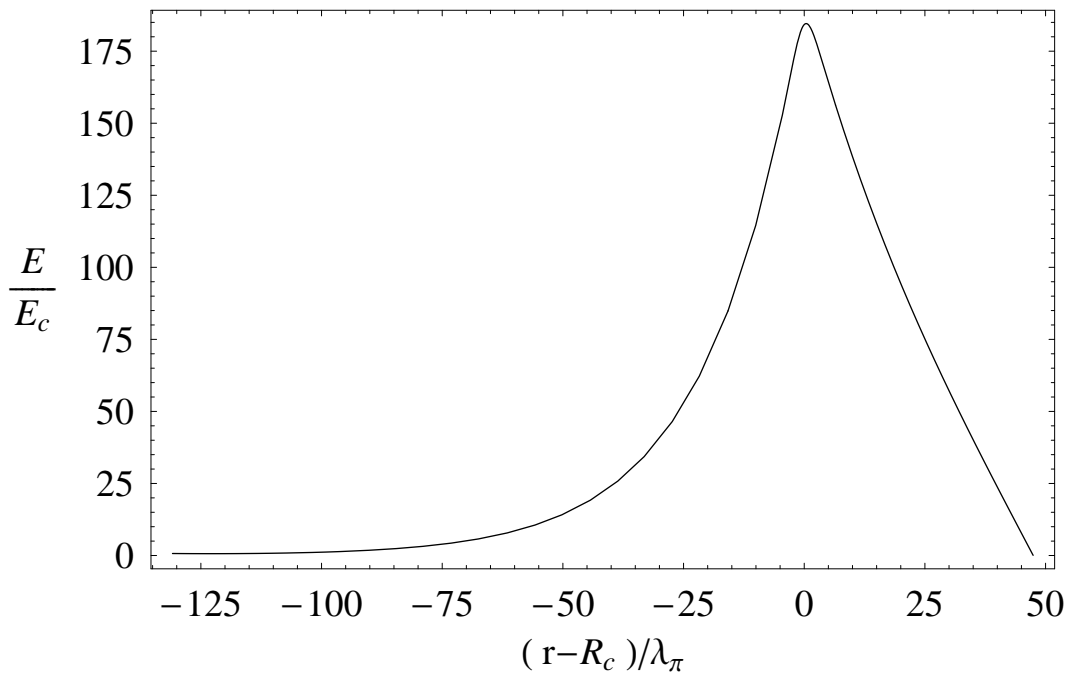


Figure B.21.: Surface electric field in units of the critical field.

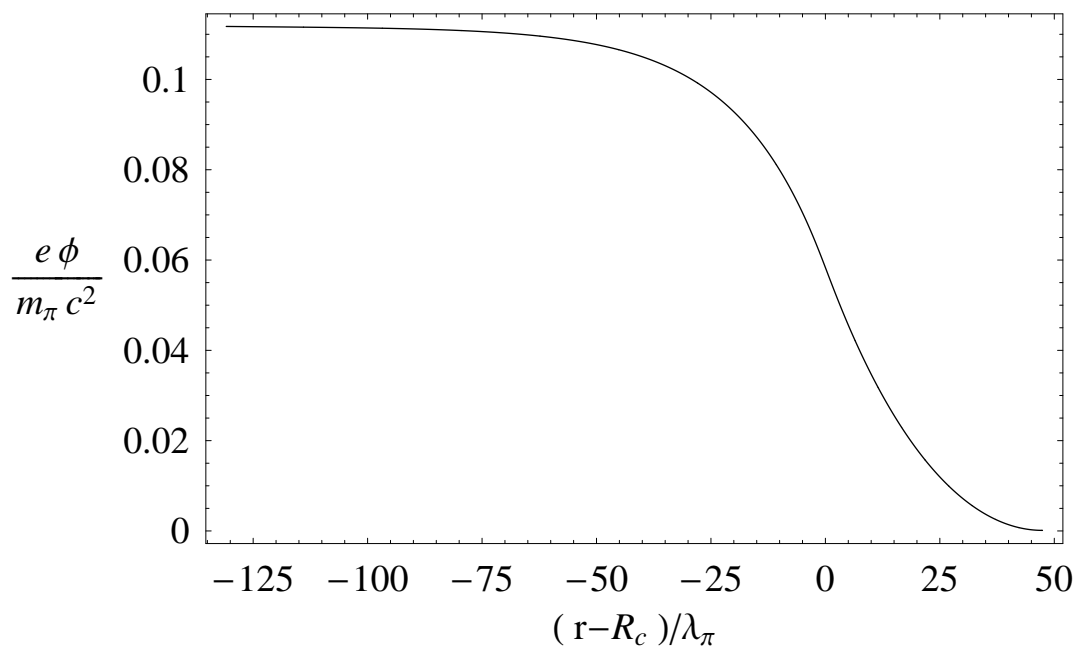


Figure B.22.: Surface electrostatic potential of the core in units of the pion mass.

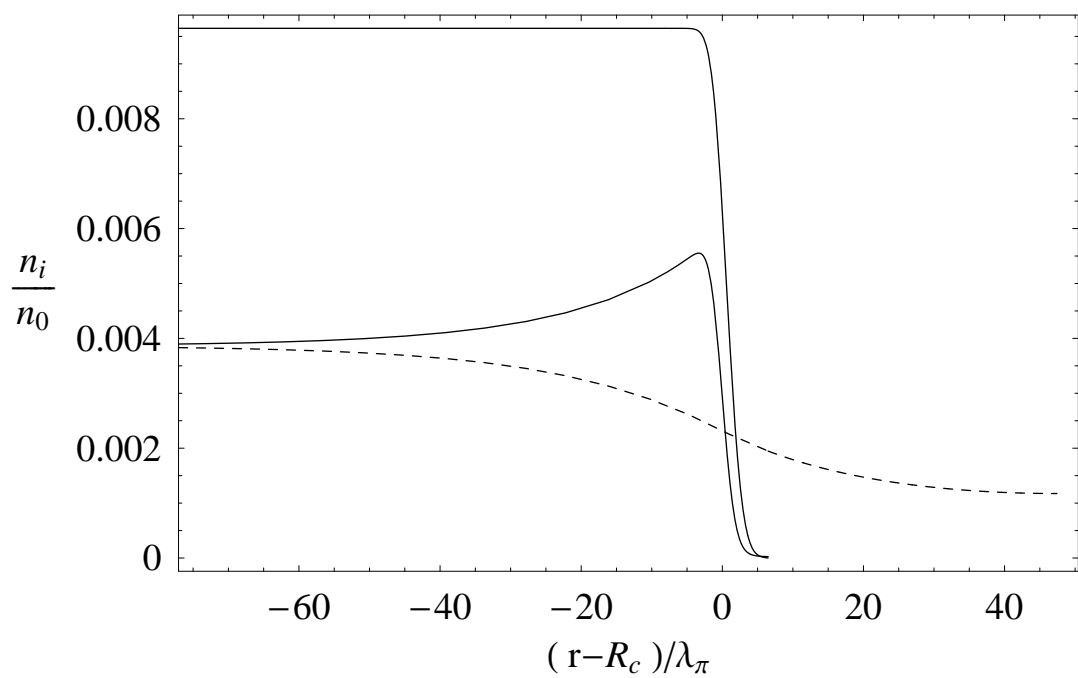


Figure B.23.: Surface number densities in units of the nuclear density n_0 .

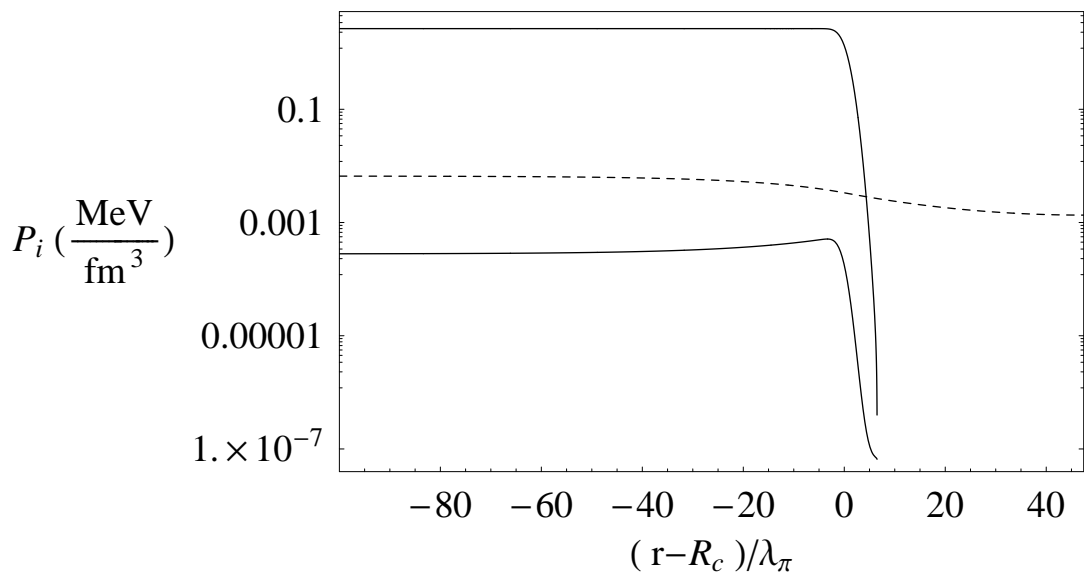


Figure B.24.: Surface pressure

B.7. A New Family of Neutron Star Models: Global Neutrality vs. Local Neutrality

B.7.1. Introduction

Traditionally, neutron star equilibrium configurations have been constructed following a “local approach”. In such an approach, the equation of state of neutron star matter is constructed ignoring global gravitational and Coulomb effects by assuming flat spacetime as well as local charge neutrality. Then, it is obtained a relation $P = P(\mathcal{E})$ between the energy-density \mathcal{E} and the pressure P (see Haensel et al. (2007) for a recent compilation of modern neutron star matter equations of state). The gravitational effects are then taken into account by embedding such an equation of state into the so-called Tolman-Oppenheimer-Volkoff equation of hydrostatic equilibrium in spherical symmetry

$$\frac{dP(r)}{dr} = -\frac{G[\mathcal{E}(r) + P(r)][4\pi r^3 P(r)/c^2 + M(r)]}{c^2 r(r - 2GM(r)/c^2)}, \quad (\text{B.7.1})$$

where the mass $M(r)$ is obtained from $dM(r)/dr = 4\pi r^2 \mathcal{E}(r)/c^2$. Thus, in the local approach, the problem of the equilibrium state of a self-gravitating system composed of different particle-species is reduced to an effective one-component fluid problem by solving the above equations for a certain equation of state $P(\mathcal{E})$.

This approach, although gives good estimates for the mass and the radius of a neutron star, should be consider as an effective solution of the problem that oversimplifies the real physical situation, where fundamental gravito-electrodynamical effects exist. We present here the self-consistent equilibrium equations governing a degenerate neutron, proton and electron fluid in beta equilibrium within the framework of relativistic quantum statistics and of the Einstein-Maxwell equations. From this formulation descend the general relativistic Thomas-Fermi equation, which, as in the case of atoms, plays a crucial role by joining Coulombian, gravitational and quantum-statistical effects associated with the equilibrium state of a self-gravitating system of degenerate fermions.

B.7.2. The equilibrium equations

We consider equilibrium configurations of a degenerate gas of neutrons, protons and electrons with total matter energy density $\mathcal{E} = \sum_{i=n,p,e} \mathcal{E}_i$ and pressure $P = \sum_{i=n,p,e} P_i$ where \mathcal{E}_i and P_i are the energy density and pressure of a degenerate fluid of 1/2-spin fermions of mass m_i , Fermi momentum P_i^F and number density $n_i = (P_i^F)^3 / (3\pi^2 \hbar^3)$.

We define at first, the generalized Fermi energy $E_i^F = e^{\nu/2} \mu_i - m_i c^2 + q_i V$

for the i -particle specie, where q_i is the particle unit charge, $\mu_i = \partial\mathcal{E}/\partial n_i$ is the free-chemical potential, and V denotes the Coulomb potential of the configuration. Thus, the equations for the neutron star equilibrium configuration are given by the beta equilibrium condition, the general relativistic Thomas-Fermi equilibrium condition for electrons and the Einstein-Maxwell equations Rueda et al. (2010c,a)

$$E_n^F + m_n c^2 = E_p^F + m_p c^2 + E_e^F + m_e c^2, \quad (\text{B.7.2})$$

$$E_e^F = e^{v/2} \mu_e - m_e c^2 - eV = \text{constant}, \quad (\text{B.7.3})$$

$$\frac{dM}{dr} = 4\pi r^2 \frac{\mathcal{E}}{c^2} - 4\pi r^3 e^{-v/2} \frac{d\hat{V}/c^2}{dr} (n_p - n_e), \quad (\text{B.7.4})$$

$$\frac{1}{r} \frac{dv}{dr} + \frac{1 - e^\lambda}{r^2} = \frac{8\pi G}{c^4} e^\lambda \left[P - \frac{e^{-(v+\lambda)}}{8\pi\alpha \hbar c} \left(\frac{d\hat{V}}{dr} \right)^2 \right], \quad (\text{B.7.5})$$

$$\frac{dP}{dr} + \frac{1}{2} \frac{dv}{dr} (\mathcal{E} + P) = -\frac{dP^{\text{em}}}{dr} - \frac{4P^{\text{em}}}{r}, \quad (\text{B.7.6})$$

$$\begin{aligned} & \frac{d^2\hat{V}}{dr^2} + \frac{d\hat{V}}{dr} \left[\frac{2}{r} - \frac{1}{2} \left(\frac{dv}{dr} + \frac{d\lambda}{dr} \right) \right] = -4\pi\alpha \hbar c e^{v/2} e^\lambda \left\{ n_p \right. \\ & \left. - \frac{e^{-3v/2}}{3\pi^2 \hbar^3 c^3} [(\hat{V} + m_e c^2)^2 - m_e^2 c^4 e^v]^{3/2} \right\}, \end{aligned} \quad (\text{B.7.7})$$

where α denotes the fine structure constant, $\hat{V} = E_e^F + eV$ and $P^{\text{em}} = -E^2/(8\pi)$ and we have introduced the metric $g_{\alpha\beta} = \text{diag}(e^{v(r)}, -e^{\lambda(r)}, -r^2, -r^2 \sin^2 \theta)$ for a spherically-symmetric non-rotating neutron star. The metric function λ is related to the mass $M(r)$ and the electric field $E(r) = -e^{-(v+\lambda)/2} dV/dr$ through

$$e^{-\lambda} = 1 - \frac{2GM(r)}{c^2 r} + \frac{Gr^2 E^2(r)}{c^4}. \quad (\text{B.7.8})$$

It has been demonstrated in Rueda et al. (2010a) that, from the above system of equations follows that indeed all the generalized particle Fermi energies E_i^F are constant through the entire configuration, for all particle-species separately. This is in line with the results of Klein Klein (1949), of Kodama and Yamada Kodama and Yamada (1972), and of Olson and Bailyn Olson and Bailyn (1975).

B.7.3. Discussion

The inconsistency of locally neutral neutron stars was proven in Rueda et al. (2010a), where violation of the thermodynamic equilibrium condition of constancy of the generalized particle Fermi energies was explicitly shown for such configurations. Instead, globally neutral systems can be obtained from the above self-consistent equations. The specific solution for non-strongly

interacting degenerate neutrons, protons and electrons extending from the center of the star all the way to the border was obtained in Ref. Rueda et al. (2010a). Although such a system cannot represent a realistic neutron star, essential gravito-electrodynamical effects were shown and the typical depth of the Coulomb potential was obtained.

In realistic neutron stars, the degenerate neutrons, protons and electrons are confined to the core and are subjected to the external pressure of the crust. In this more general case, the constancy of the generalized Fermi energy of the electrons still plays a fundamental role in the matching and boundary conditions Rueda et al. (2010c). It was shown in Ref. Rueda et al. (2010c) that, as a consequence of the fulfillment of the core-crust matching conditions and the self-consistent equilibrium equations described here, the surface of the core develops a sharp exponential transition surrounded by the neutron star crust. Furthermore, together with the exponential density transition, an electric field with an intensity larger than that of the critical field $E_c = m_e^2 c^3 / (e \hbar)$ extending over all the entire surface of the transition surface, whose thickness is of the order of several electron Compton wavelength $\lambda_e = \hbar / (m_e c)$, appears.

All the new gravito-electrodynamical effects discussed here deserve further analysis in view of the recent developments in high-energy astrophysics pointing to the relevance of overcritical electric fields in neutron stars and black holes Ruffini et al. (2010). The introduction of strong interactions to the energy-momentum tensor, to the four-vector current and, consequently, to the Einstein-Maxwell equations are currently under consideration in order to establish a more general formulation of the problem Pugliese et al. (2010).

B.8. A general relativistic Thomas Fermi treatment of neutron star cores II. Generalized Fermi energies and beta equilibrium.

B.8.1. Introduction

It is well known that, in addition to the constancy of the temperature, thermodynamic equilibrium demands, in absence of any external field, the constancy of the particle chemical potential throughout the configuration. In presence of an external field, such a condition becomes Landau and Lifshitz (1980) $\mu_0 + U = \text{constant}$, where U denotes the external potential and μ_0 is the free-particle chemical potential. The extension of these equilibrium conditions to the case of general relativity were obtained by O. Klein (1949), who investigated the thermodynamic equilibrium conditions of a self-gravitating one-component fluid of non-interacting neutral particles in spherical symmetry. The generalization of the Klein's equilibrium conditions to the case of a multi-component fluid of non-interacting neutral particles was given by T. Kodama and M. Yamada (1972). E. Olson and M. Bailyn (1975) went one step further obtaining the equilibrium conditions for a self-gravitating multi-component fluid of charged particles taking into account the Coulomb interaction. Having in mind the case of neutron star interiors, in this article we make a brief description of the generalization of the above works to include the strong interaction for the hadronic species and the Coulomb interaction for the charged species within a self-consistent general relativistic treatment. In particular, we assume neutron star cores composed of interacting degenerate neutrons, protons and electrons in beta equilibrium. Thus, we shall develop a general relativistic Thomas-Fermi treatment of neutron star cores within the framework of quantum statistics and of the general relativistic field theory for the gravitational, the electromagnetic and the hadronic fields. We consider the electromagnetic interaction between electrons and protons and, for the hadronic interaction, we follow the so-called Walecka model or quantum hadrodynamical model Duerr (1956); Walecka (1974), in which the strong interaction is modeled by meson-exchange through the sigma, omega and rho meson-fields. Throughout the paper we adopt units with $\hbar = c = 1$. The Latin indexes vary from 1 to 3, Greek indexes from 0 to 4.

B.8.2. General formulation

The total Lagrangian density of the system is given by

$$\mathcal{L} = \mathcal{L}_g + \mathcal{L}_f + \mathcal{L}_\sigma + \mathcal{L}_\omega + \mathcal{L}_\rho + \mathcal{L}_\gamma + \mathcal{L}_{int}, \quad (\text{B.8.1})$$

where σ is an isoscalar meson field, providing the attractive long-range nuclear force, ω is the massive vector field, modeling the repulsive short range nuclear force and ρ is the massive isovector field that takes account of the surface effects of nuclei modeling a repulsive nuclear force Duerr (1956); Walecka (1974); Boguta and Bodmer (1977); Ring (1996). Therefore the Lagrangian densities for the free fields are

$$\begin{aligned} \mathcal{L}_f &= \sum_{i=e,N} \bar{\psi}_i (i\gamma^\mu \partial_\mu - m_i) \psi_i, & \mathcal{L}_\sigma &= \frac{1}{2} \nabla_\mu \sigma \nabla^\mu \sigma - U(\sigma), \\ \mathcal{L}_\omega &= -\frac{1}{4} \Omega_{\mu\nu} \Omega^{\mu\nu} + \frac{1}{2} m_\omega^2 \omega_\mu \omega^\mu, & \mathcal{L}_\gamma &= -\frac{1}{4} F_{\mu\nu} F^{\mu\nu} \\ \mathcal{L}_\rho &= -\frac{1}{4} \mathcal{R}_{\mu\nu} \mathcal{R}^{\mu\nu} + \frac{1}{2} m_\rho^2 \rho_\mu \rho^\mu, & \mathcal{L}_g &= -\frac{R}{16\pi G}, \end{aligned} \quad (\text{B.8.2})$$

where ψ_N is the nucleon isospin doublet, ψ_e is the electronic singlet, m_i states for the mass of each particle-specie and $\Omega_{\mu\nu} \equiv \partial_\mu \omega_\nu - \partial_\nu \omega_\mu$, $\mathcal{R}_{\mu\nu} \equiv \partial_\mu \rho_\nu - \partial_\nu \rho_\mu$, $F_{\mu\nu} \equiv \partial_\mu A_\nu - \partial_\nu A_\mu$ the field strengths for the ω^μ , ρ and A^μ fields respectively. $U(\sigma)$ denotes the self interaction scalar field potential, which is a quartic-order polynom for a renormalizable theory Lee and Wick (1974); Lee (1975); Lee and Margulies (1975); Lee and Pang (1987), and R is the Ricci scalar. The interacting part of the Lagrangian density is

$$\mathcal{L}_{int} = -g_\sigma \sigma \bar{\psi}_N \psi_N - g_\omega \omega_\mu J_\omega^\mu - g_\rho \rho_\mu J_\rho^\mu + e A_\mu J_{\gamma,e}^\mu - e A_\mu J_{\gamma,N}^\mu \quad (\text{B.8.3})$$

where the currents are $J_\omega^\mu \equiv \bar{\psi}_N \gamma^\mu \psi_N$, $J_\rho^\mu \equiv \bar{\psi}_N \tau_3 \gamma^\mu \psi_N$, $J_{\gamma,e}^\mu \equiv \bar{\psi}_e \gamma^\mu \psi_e$ and $J_{\gamma,N}^\mu \equiv \bar{\psi}_N \left(\frac{1+\tau_3}{2} \right) \gamma^\mu \psi_N$ with a bar denoting usual Hermitian conjugation. The coupling constants of the σ , ω and ρ -fields are g_σ , g_ω and g_ρ , and e is the fundamental electric charge. The Dirac matrices γ^μ and the isospin Pauli matrices satisfy the Dirac algebra in curved spacetime Lee and Pang (1987) $\{\gamma^\mu, \gamma^\nu\} = 2g^{\mu\nu}$, $\{\gamma_\mu, \gamma_\nu\} = 2g_{\mu\nu}$, $\{\gamma^\mu, \gamma_\nu\} = 2\delta_\nu^\mu$, $[\tau_i, \tau_j] = 2i\epsilon_{ijk} \tau^k$.

The Einstein-Maxwell-Dirac system of equations is then given by

$$G_{\mu\nu} + 8\pi G T_{\mu\nu} = 0, \quad \nabla_\mu \nabla^\mu \sigma + \partial_\sigma U(\sigma) + g_s \bar{\psi}_N \psi_N = 0, \quad (\text{B.8.4})$$

$$\nabla_\mu \Omega^{\mu\nu} + m_\omega^2 \omega^\nu - g_\omega J_\omega^\nu = 0, \quad \nabla_\mu \mathcal{R}^{\mu\nu} + m_\rho^2 \rho^\nu - g_\rho J_\rho^\nu = 0, \quad (\text{B.8.5})$$

$$[\gamma_\mu (i\partial^\mu + eA^\mu) - m_e] \psi_e = 0, \quad [\gamma_\mu (i\partial^\mu - V_N) - \tilde{m}_N] \psi_N = 0, \quad (\text{B.8.6})$$

$$\nabla_\mu F^{\mu\nu} - e J_{ch}^\nu = 0, \quad (\text{B.8.7})$$

where $V_N \equiv g_\omega \omega^\mu + g_\rho \tau \rho^\mu + e \left(\frac{1+\tau_3}{2} \right) A^\mu$ is the effective four potential of nucleons, and the nucleon effective mass is $\tilde{m}_N \equiv m_N + g_\sigma \sigma$. The energy momentum tensor $T^{\mu\nu}$ can be written as the sum of the contributions of all the fields:

$$\begin{aligned} T_\sigma^{\mu\nu} &= \nabla^\mu \nabla^\nu \sigma - g^{\mu\nu} \left[\frac{1}{2} \nabla_\sigma \sigma \nabla^\sigma \sigma - U(\sigma) \right], & T_\gamma^{\mu\nu} &= -F_\alpha^\mu F^{\alpha\nu} - \frac{1}{4} g^{\mu\nu} F_{\alpha\beta} F^{\alpha\beta}, \\ T_\omega^{\mu\nu} &= -\Omega_\alpha^\mu \Omega^{\alpha\nu} - \frac{1}{4} g^{\mu\nu} \Omega_{\alpha\beta} \Omega^{\alpha\beta} + m_\omega^2 \left(\omega^\mu \omega^\nu - \frac{1}{2} g^{\mu\nu} \omega_\alpha \omega^\alpha \right), \\ T_\rho^{\mu\nu} &= -\mathcal{R}_\alpha^\mu \mathcal{R}^{\alpha\nu} - \frac{1}{4} g^{\mu\nu} \mathcal{R}_{\alpha\beta} \mathcal{R}^{\alpha\beta} + m_\rho^2 \left(\mathcal{R}^\mu \mathcal{R}^\nu - \frac{1}{2} g^{\mu\nu} \mathcal{R}_\alpha \omega^\alpha \right), \\ T_f^{\mu\nu} &= (\mathcal{E} + \mathcal{P}) u^\mu u^\nu - \mathcal{P} g^{\mu\nu}, \end{aligned} \quad (\text{B.8.8})$$

where u^μ denotes the four-velocity. The energy-density \mathcal{E} and the pressure \mathcal{P} of the fermion fluid are

$$\mathcal{E} = \frac{2}{(2\pi)^3} \sum_{i=n,p,e} \int_0^{K_i^F} \epsilon_i d^3k, \quad \mathcal{P} = \frac{2}{3(2\pi)^3} \sum_{i=n,p,e} \int_0^{K_i^F} \frac{k^2}{\epsilon_i} d^3k, \quad (\text{B.8.9})$$

where $\epsilon_i = \sqrt{k^2 + (\tilde{m}_i)^2}$ denotes the single-particle energy spectrum (we recall that for electrons $\tilde{m}_e = m_e$) and K_i^F denotes the Fermi momentum of each particle specie. From Eq. (B.8.9) it follows the thermodynamic relation

$$\mathcal{E} + \mathcal{P} = \sum_{i=n,p,e} n_i \mu_i, \quad (\text{B.8.10})$$

where $\mu_i = \sqrt{(K_i^F)^2 + (\tilde{m}_i)^2}$ and $n_i = (K_i^F)^3 / (3\pi^2)$ are the free-chemical potential and number density of the i -specie. In addition, from Eq. (B.8.10) and the scalar density $n_s = \partial \mathcal{E} / \partial \tilde{m}_N$, we obtain the generalized Gibbs-Duhem relation

$$d\mathcal{P} = \sum_{i=n,p,e} n_i d\mu_i - g_\sigma n_s d\sigma. \quad (\text{B.8.11})$$

We consider non-rotating spherically symmetric neutron stars, so we introduce the spacetime metric

$$ds^2 = e^{\nu(r)} dt^2 - e^{\lambda(r)} dr^2 - r^2 d\theta^2 - r^2 \sin^2 \theta d\varphi^2, \quad (\text{B.8.12})$$

for which the Einstein-Maxwell-Dirac equations (B.8.4)-(B.8.7) read

$$e^{-\lambda(r)} \left(\frac{1}{r^2} - \frac{\lambda'}{r} \right) - \frac{1}{r^2} = -8\pi GT_0^0, \quad (\text{B.8.13})$$

$$e^{-\lambda(r)} \left(\frac{1}{r^2} + \frac{\nu'}{r} \right) - \frac{1}{r^2} = -8\pi GT_1^1, \quad (\text{B.8.14})$$

$$\mathcal{P}' + \frac{\nu'}{2}(\mathcal{E} + \mathcal{P}) = -g_\sigma n_s \sigma' - \omega' g_\omega J_\omega^0 - \rho' g_\rho J_\rho^0 - V' e J_{ch}^0, \quad (\text{B.8.15})$$

$$V'' + V' \left[\frac{2}{r} - \frac{(\nu' + \lambda')}{2} \right] = -e^\lambda e J_{ch}^0, \quad (\text{B.8.16})$$

$$\sigma'' + \sigma' \left[\frac{2}{r} + \frac{(\nu' - \lambda')}{2} \right] = e^\lambda [\partial_\sigma U(\sigma) + g_s n_s], \quad (\text{B.8.17})$$

$$\omega'' + \omega' \left[\frac{2}{r} - \frac{(\nu' + \lambda')}{2} \right] = -e^\lambda [g_\omega J_\omega^0 - m_\omega^2 \omega], \quad (\text{B.8.18})$$

$$\rho'' + \rho' \left[\frac{2}{r} - \frac{(\nu' + \lambda')}{2} \right] = -e^\lambda [g_\rho J_\rho^0 - m_\rho^2 \rho], \quad (\text{B.8.19})$$

where we use the notation $\omega_0 = \omega$, $\rho_0 = \rho$ and $A_0 = V$, a prime stands for radial derivative, the zero-covariant component of the currents are $J_0^\omega = n_b u_0 = (n_n + n_p) e^{\nu/2}$, $J_0^\rho = n_3 u_0 = (n_p - n_n) e^{\nu/2}$ and $J_0^{ch} = n_{ch} u_0 = (n_p - n_e) e^{\nu/2}$, and n_b , n_p , n_n and n_e are the baryon, proton, neutron and electron number density. The scalar density n_s is given by $n_s = \bar{\psi}_N \psi_N = \partial \mathcal{E} / \partial \bar{m}_N = \frac{2}{(2\pi)^3} \sum_{i=n,p} \int_0^{K_i^F} \frac{\bar{m}_N}{\epsilon_i} d^3 k$.

B.8.3. Generalized Fermi energies and beta equilibrium

The nucleon doublet and the electronic spinor written in the phase-space are $\psi_i = \psi_i(k) e^{-ik_\mu x^\mu}$. From the Dirac equations (B.8.6) we obtain the following equations $(\gamma_\mu \mathcal{K}^\mu - \tilde{m}_i) \psi_i(k) = 0$ with $\mathcal{K}^\mu \equiv k^\mu - V_i^\mu$, $V_e = -eV$. Making a quadrature of the Dirac operators in the phase-space we obtain the Fermi energy for electrons E_e^F , neutrons E_n^F and protons E_p^F

$$E_e^F = \sqrt{g_{00}} \mu_e - eV = e^{\nu/2} \mu_e - eV, \quad (\text{B.8.20})$$

$$E_n^F = \sqrt{g_{00}} \mu_n + g_\omega \omega - g_\rho \rho = e^{\nu/2} \mu_n + g_\omega \omega - g_\rho \rho, \quad (\text{B.8.21})$$

$$E_p^F = \sqrt{g_{00}} \mu_p + g_\omega \omega + g_\rho \rho + eV = e^{\nu/2} \mu_p + g_\omega \omega + g_\rho \rho + eV. \quad (\text{B.8.22})$$

Consequently, the beta equilibrium condition $E_n^F = E_p^F + E_e^F$, becomes

$$\mu_n = \mu_p + \mu_e + 2g_\rho \rho e^{-\nu/2}. \quad (\text{B.8.23})$$

B.8.4. Constancy of the generalized Fermi energies

The energy-momentum conservation is given by the last equation in (B.8.19), and can be called generalized Tolman-Oppenheimer-Volkoff equation. Using the equations of motion for the fields ρ , ω and σ , and using the generalized Gibbs-Duhem relation (B.8.11), such an energy-momentum conservation equation can be rewritten as

$$\sum_{i=n,p,e} n_i d(e^{v/2} \mu_i) + g_\omega n_b d\omega + g_\rho n_3 d\rho + e n_{ch} dV = 0. \quad (\text{B.8.24})$$

Using the expressions (B.8.20)-(B.8.22) and the beta equilibrium condition (B.8.23), the Eq. (B.8.24) becomes

$$\sum_{i=p,e} (n_i + n_e) dE_i^F = 0. \quad (\text{B.8.25})$$

It was demonstrated in the non interacting case Olson and Baily (1975) that from the minimization energy procedure it follows the thermodynamic energy condition of constancy of the generalized particle Fermi energy of all particle species. It can be seen from Eq. (B.8.25) that it is enough to request the constancy of the generalized electron Fermi energy

$$E_e^F = e^{v/2} \mu_e - eV = \text{constant}, \quad (\text{B.8.26})$$

to obtain the constancy of E_p^F and consequently, from beta equilibrium, the constancy of E_n^F Rueda et al. (2010c,a). Then, in addition to the electron equilibrium condition (B.8.26) we obtain for the nucleon components

$$E_{n,p}^F = e^{v/2} \mu_{n,p} + \mathcal{V}_{n,p} = \text{constant}, \quad \mathcal{V}_{n,p} \equiv g_\omega \omega + g_\rho \tau \rho + e \left(\frac{1 + \tau_3}{2} \right) V. \quad (\text{B.8.27})$$

B.8.5. Conclusions

A self-consistent treatment of self-gravitating system of degenerate neutrons, protons and electrons in beta equilibrium is presented in the framework of general relativity including the Coulomb and hadronic interaction. We obtained the generalized particle Fermi energies from the Dirac equations for nucleons and electrons.

Then, we used the generalized Fermi energies to obtain the modified beta equilibrium condition for the particle species. Finally, we outlined how from the Einstein-Maxwell-Dirac equations, the electron equilibrium condition and the beta equilibrium condition, it follows the constancy of the generalized Fermi energy of each particle specie including the contribution of all fields.

B.9. A self-consistent general relativistic solution for a self-gravitating system of degenerate neutrons, protons and electrons in beta equilibrium

B.9.1. Introduction

In nearly all of the scientific literature on neutron stars it is assumed that the condition of local charge neutrality applies identically to all points of the equilibrium configuration. The corresponding solutions of the Einstein equations for a non-rotating neutron star, following the work of Tolman (1939) and the work of Oppenheimer and Volkoff (1939), have been systematically applied Haensel et al. (2007). We prove that this approach is conceptually inconsistent and violates the equations of motion of the system on the microphysical scale. We also give the new set of Einstein-Maxwell equations and general relativistic Thomas-Fermi equations substituting the TOV equations and give the methodology of their integration in the simplest, complete and nontrivial case. The correct solution necessitates violation of local charge neutrality. In a set of interesting papers (see Glendenning (1992); Glendenning and Pei (1995); Christiansen and Glendenning (1997); Glendenning and Schaffner-Bielich (1999); Christiansen et al. (2000)) Glendenning has relaxed the local charge neutrality condition for the description of the mixed phases in hybrid stars. In such configurations the global charge neutrality condition, as opposed to the local one, is applied to the limited regions where mixed phases occur while in the pure phases the local charge neutrality condition still holds. In all these works Glendenning, in conformity to the traditional approaches, assumes that “spacetime, though curved by mass-energy, is flat to a high degree over regions that are compared to interparticle distances ... We may therefore solve all problems of the structure and composition of matter in Minkowski spacetime and use the results in the form of the stress-energy tensor in Einstein’s equations” Glendenning (2001). We here generalize Glendenning’s results with one important difference: we are looking to a violation of the local charge neutrality condition on the entire star, still keeping its overall charge neutrality. This effect does not occur in processes occurring on typical scales of interparticle distances in the Minkowski spacetime, but it requests the global description of the equilibrium configuration. As clearly exemplified in Eq. (B.9.16) below, the local properties need the previous knowledge of the entire equilibrium configuration and therefore the description is necessarily global.

In this article we consider the description of a relativistic self-gravitating system of degenerate fermions composed of neutrons, protons and electrons in beta equilibrium: this is the simplest nontrivial system in which new elec-

hydrodynamical and general relativistic properties of the equilibrium configuration can be clearly illustrated. We focus attention upon the case in which the system is not subjected to external forces. We first prove that the condition of local charge neutrality can never be implemented since it violates necessary conditions of equilibrium at the microphysical scale. We then prove the existence of a solution with global charge neutrality by taking into account essential gravito-electrodynamical effects. First we recall the constancy of the general relativistic Fermi energies and we introduce subsequently the general relativistic Thomas-Fermi equations and the relativistic quantum statistics for the three fermion species governed by the Einstein-Maxwell equations. The solution of this system of equations presents a most formidable mathematical challenge to theoretical physics. The traditional difficulties encountered in proving the existence and unicity of the solution of the Thomas-Fermi equation are here enhanced by the necessity of solving the general relativistic Thomas-Fermi equation coupled with the Einstein-Maxwell system of equations. We were helped in solving this problem by the recent progress made in the analysis of the relativistic Thomas-Fermi equations in the simplified case of massive nuclear density cores with constant proton density Popov et al. (2010). We present the general solution for the equilibrium configuration, from the center of the star all the way to the border, giving the details of the gravitational field, of the electro-dynamical field as well as of the conserved quantities.

We illustrate such a solution by selecting a central density $\rho(0) = 4\rho_0$, where $\rho_0 \simeq 2.7 \times 10^{14} \text{ g cm}^{-3}$ is the nuclear density. We point out the existence near the boundary of the core in the equilibrium configuration of three different radii, in decreasing order: R_e corresponding to the vanishing of the Fermi momentum of the electron component; $P_e^F = 0$, R_p corresponding to the vanishing of the Fermi momentum of the proton component; $P_p^F = 0$ and R_n corresponding to the radius at which the Fermi momentum of neutrons vanishes: $P_n^F = 0$. We then give explicit expressions for the proton versus electron density ratio and the proton versus neutron density ratio for any value of the radial coordinate as well as for the electric potential at the center of the configuration. A novel situation occurs: the determination of these quantities needs prior knowledge of the global electro-dynamical and gravitational potential as well as of the radii R_n , R_p and R_e ! This is a necessary outcome of the self-consistent solution for the eigenfunction of the general relativistic Thomas-Fermi equation in the Einstein-Maxwell background. As expected from the considerations in Popov et al. (2010), the electric potential at the center of the configuration fulfills $eV(0) \simeq m_\pi c^2$ and the gravitational potential $1 - e^{\nu(0)/2} \simeq m_\pi/m_p$. The implementation of the constancy of the general relativistic Fermi energy and the consequent system of equations illustrated here in the simplest possible example admitting a rigorous solution will necessarily apply in the case of additional particle species and of the in-

clusion of nuclear interactions and/or external forces as well.

B.9.2. Einstein-Maxwell, general relativistic Thomas-Fermi equations and boundary conditions

We consider the equilibrium configurations of a degenerate gas of neutrons, protons and electrons with total matter energy density and total matter pressure (we use hereafter units with $\hbar = c = 1$)

$$\mathcal{E} = \sum_{i=n,p,e} \mathcal{E}_i = \sum_{i=n,p,e} \frac{2}{(2\pi)^3} \int_0^{P_i^F} \sqrt{p^2 + m_i^2} 4\pi p^2 dp, \quad (\text{B.9.1})$$

$$P = \sum_{i=n,p,e} P_i = \sum_{i=n,p,e} \frac{1}{3} \frac{2}{(2\pi)^3} \int_0^{P_i^F} \frac{p^2}{\sqrt{p^2 + m_i^2}} 4\pi p^2 dp, \quad (\text{B.9.2})$$

that satisfy the condition of beta equilibrium

$$\mu_n = \mu_p + \mu_e, \quad (\text{B.9.3})$$

where P_i^F is the Fermi momentum and $\mu_i = \partial\mathcal{E}/\partial n_i = \sqrt{(P_i^F)^2 + m_i^2}$ is the free-chemical potential of particle species of number density $n_i = \frac{(P_i^F)^3}{3\pi^2}$. In addition, we introduce the extension to general relativity of the Thomas-Fermi equilibrium condition on the generalized Fermi energy E_e^F of the electron component

$$E_e^F = e^{v/2} \mu_e - m_e - eV = \text{constant}, \quad (\text{B.9.4})$$

where e is the fundamental charge, V is the Coulomb potential of the configuration and we have introduced the metric

$$g_{\alpha\beta} = \text{diag}(e^{v(r)}, -e^{\lambda(r)}, -r^2, -r^2 \sin^2 \theta), \quad (\text{B.9.5})$$

for a spherically symmetric non-rotating neutron star. The metric function λ is related to the mass $M(r)$ and the electric field $E(r) = -e^{-(v+\lambda)/2} V'$ through $e^{-\lambda} = 1 - 2GM(r)/r + Gr^2 E^2(r)$. Thus the equations for the neutron star equilibrium configuration consist of the following Einstein-Maxwell

equations and general relativistic Thomas-Fermi equation

$$M' = 4\pi r^2 \mathcal{E} - 4\pi r^3 e^{-\nu/2} \hat{V}' (n_p - n_e), \quad (\text{B.9.6})$$

$$\frac{\nu'}{r} + \frac{1 - e^\lambda}{r^2} = 8\pi G e^\lambda \left[P - \frac{e^{-(\nu+\lambda)}}{8\pi\alpha} (\hat{V}')^2 \right], \quad (\text{B.9.7})$$

$$P' + \frac{\nu'}{2} (\mathcal{E} + P) = -(P^{\text{em}})' - \frac{4P^{\text{em}}}{r}, \quad (\text{B.9.8})$$

$$\hat{V}'' + \frac{2}{r} \hat{V}' \left[1 - \frac{r(\nu' + \lambda')}{4} \right] = -4\pi\alpha e^{\nu/2} e^\lambda \left\{ n_p - \frac{e^{-3\nu/2}}{3\pi^2} [\hat{V}^2 + 2m_e \hat{V} - m_e^2 (e^\nu - 1)]^{3/2} \right\}, \quad (\text{B.9.9})$$

where a prime stands for radial derivative, α denotes the fine structure constant, $\hat{V} = E_e^F + eV$ and $P^{\text{em}} = -E^2/(8\pi)$.

It can be demonstrated that the assumption of the equilibrium condition (B.9.4) together with the beta equilibrium condition (B.5.5) and the hydrostatic equilibrium (B.9.8) is enough to guarantee the constancy of the generalized Fermi energy

$$E_i^F = e^{\nu/2} \mu_i - m_i + q_i V, \quad i = n, p, e, \quad (\text{B.9.10})$$

for all particle species separately. Here q_i denotes the particle unit charge of the i -species. Indeed, as shown by Olson and Bailyn (1975, 1978), when the fermion nature of the constituents and their degeneracy is taken into account, in the configuration of minimum energy the generalized Fermi energies E_i^F defined by (B.9.10) must be constant over the entire configuration. These minimum energy conditions generalize the equilibrium conditions of Klein (1949) and of Kodama and Yamada (1972) to the case of degenerate multi-component fluids with particle species with non-zero unit charge.

If one were to assume, as often done in literature, the local charge neutrality condition $n_e(r) = n_p(r)$ instead of assuming the equilibrium condition (B.9.4), this would lead to $V = 0$ identically (since there will be no electric fields generated by the neutral matter distribution) implying via Eqs. (B.9.3) and (B.9.8)

$$E_e^F + E_p^F = e^{\nu/2} (\mu_e + \mu_p) - (m_e + m_p) = E_n^F + m_n - (m_e + m_p) = \text{constant}. \quad (\text{B.9.11})$$

Thus the neutron Fermi energy would be constant throughout the configuration as well as the sum of the proton and electron Fermi energies but not the individual Fermi energies of each component. In Fig. B.25 we show the results of the Einstein equations for a selected value of the central density of a system of degenerate neutrons, protons, and electrons in beta equilibrium under the constraint of local charge neutrality. In particular, we have

plotted the Fermi energy of the particle species in units of the pion mass. It can be seen that indeed the Fermi energies of the protons and electrons are not constant throughout the configuration which would lead to microscopic instability. This proves the impossibility of having a self-consistent configuration fulfilling the condition of local charge neutrality for our system. This result is complementary to the conclusion of Eq. (4.6) of Olson and Bailyn (1975) who found that, at zero temperature, only a dust solution with zero particle kinetic energy can satisfy the condition of local charge neutrality and such a configuration is clearly unacceptable for an equilibrium state of a self-gravitating system.

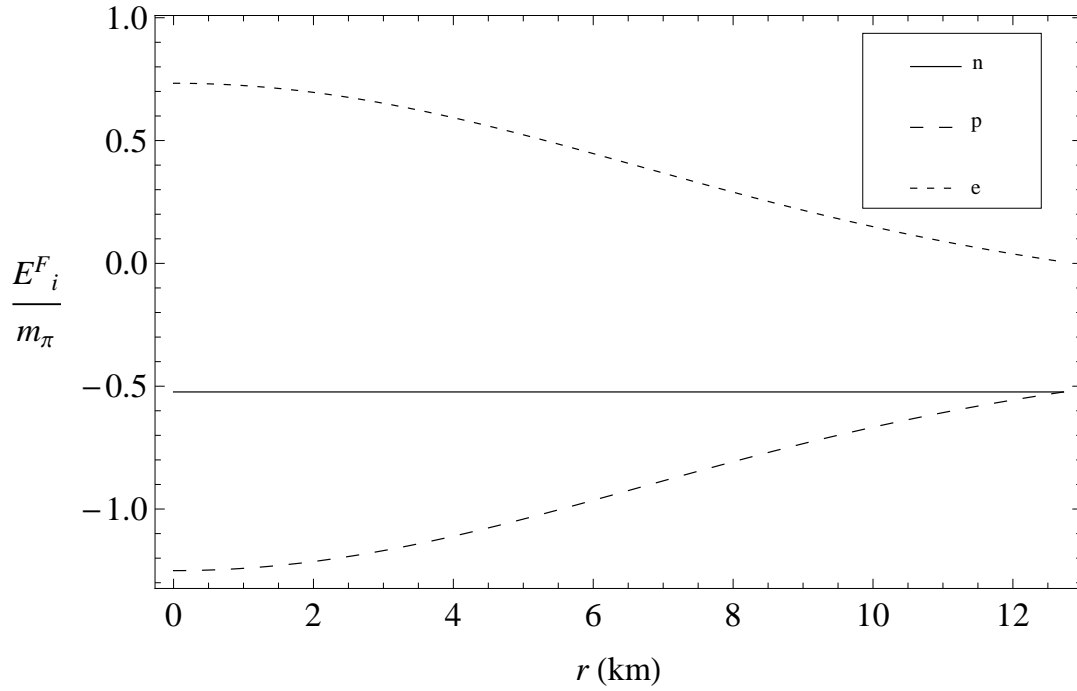


Figure B.25.: Fermi energies for neutrons, protons and electrons in units of the pion mass for a locally neutral configuration with central density $\rho(0) = 4\rho_0$, where $\rho_0 = 2.7 \times 10^{14} \text{ g cm}^{-3}$ denotes the nuclear density.

We turn now to describe the equilibrium configurations fulfilling only global charge neutrality. We solve self-consistently Eq. (B.9.6) and (B.9.7) for the metric, Eq. (B.9.8) for the hydrostatic equilibrium of the three degenerate fermions and, in addition, we impose Eq. (B.9.3) for the beta equilibrium. The crucial equation relating the proton and the electron distributions is then given by the general relativistic Thomas-Fermi equation (B.9.9). The boundary conditions are: for Eq. (B.9.6) the regularity at the origin: $M(0) = 0$, for Eq. (B.9.8) a given value of the central density, and for Eq. (B.9.9) the regularity at the origin $n_e(0) = n_p(0)$, and a second condition at infinity which results in an eigenvalue problem determined by imposing the global charge

neutrality conditions

$$\hat{V}(R_e) = E_e^F, \quad \hat{V}'(R_e) = 0, \quad (\text{B.9.12})$$

at the radius R_e of the electron distribution defined for a configuration not subject to external pressure by

$$P_e^F(R_e) = 0, \quad (\text{B.9.13})$$

from which follows

$$E_e^F = m_e e^{v(R_e)/2} - m_e = m_e \sqrt{1 - \frac{2GM(R_e)}{R_e}} - m_e. \quad (\text{B.9.14})$$

Then the eigenvalue problem consists in determining the gravitational potential and the Coulomb potential at the center of the configuration that satisfy the conditions (B.9.12)–(B.9.14) at the boundary.

B.9.3. Numerical integration of the equilibrium equations

The solution for the density, the gravitational potential and electric potential are shown in Fig. (B.26) for a configuration with central density $\rho(0) = 4\rho_0$. In order to compare our results with those obtained in the case of massive nuclear density cores Popov et al. (2010) as well as to analyze the gravito-electrodynamical stability of the configuration we have plotted the electric potential in units of the pion mass and the gravitational potential in units of the pion-to-proton mass ratio. One particular interesting new feature is the approach to the boundary of the configuration: three different radii are present corresponding to distinct radii at which the individual particle Fermi pressures vanish. The radius R_e for the electron component corresponding to $P_e^F(R_e) = 0$, the radius R_p for the proton component corresponding to $P_p^F(R_p) = 0$ and the radius R_n for the neutron component corresponding to $P_n^F(R_n) = 0$.

The smallest radius R_n is due to the threshold energy for beta decay which occurs at a density $\sim 10^7 \text{ g cm}^{-3}$. The radius R_p is larger than R_n because the proton mass is slightly smaller than the neutron mass. Instead, $R_e > R_p$ due to a combined effect of the difference between the proton and electron masses and the implementation of the global charge neutrality condition through the Thomas-Fermi equilibrium conditions.

For the configuration of Fig. B.26 we found $R_n \simeq 12.735 \text{ km}$, $R_p \simeq 12.863 \text{ km}$ and $R_e \simeq R_p + 10^3 \lambda_e$ where $\lambda_e = 1/m_e$ denotes the electron Compton wavelength. We find that the electron component follows closely the proton component up to the radius R_p and neutralizes the configuration at R_e without having a net charge, contrary to the results e.g of Olson and Baily (1978).

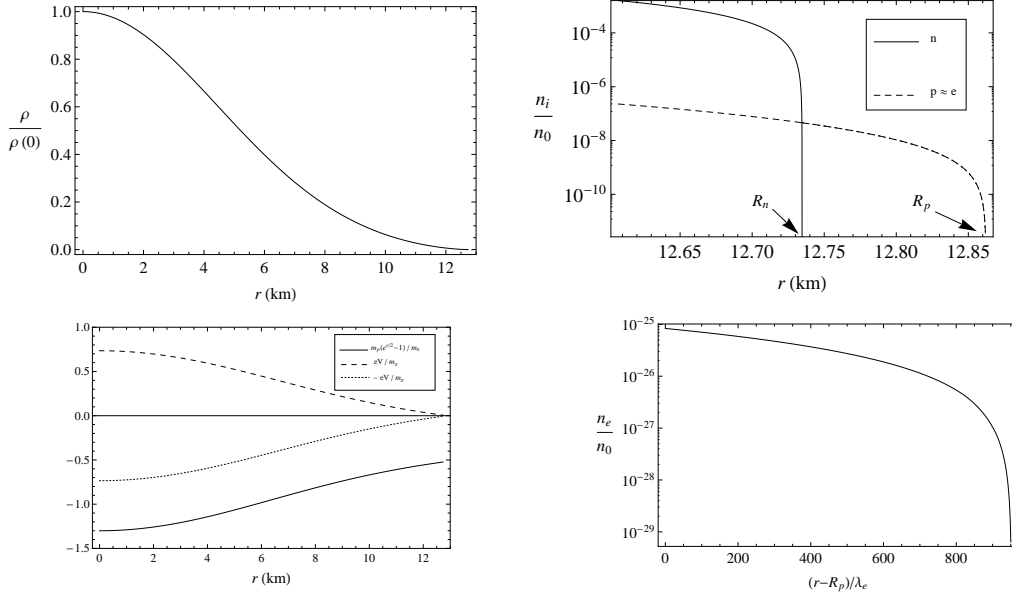


Figure B.26.: Upper left panel: energy density normalized to the central density $\rho(0) = 4\rho_0$ where $\rho_0 \simeq 2.7 \times 10^{14} \text{ g cm}^{-3}$ denotes the nuclear density. Bottom left panel: proton and electron Coulomb potential in units of the pion mass eV/m_π and $-eV/m_\pi$ respectively and the proton gravitational potential in units of the pion mass $m_p(e^{V/2} - 1)/m_\pi$. Upper right panel: neutron (solid curve) and proton (dashed curve) number density approaching the boundary of the configuration in units of the nuclear number density $n_0 \simeq \rho_0/m_n$. Bottom right panel: electron number density for $r \geq R_p$ in units of the nuclear number density n_0 .

It can be seen from Fig. B.26 that the negative proton gravitational potential energy is indeed always larger than the positive proton electric potential energy. Therefore the configuration is stable against Coulomb repulsion. This confirms the results of Eqs. (18) and (24) in Popov et al. (2010).

From Eq. (B.9.10) and the relation between Fermi momentum and the particle density $P_i^F = (3\pi^2 n_i)^{1/3}$, we obtain the proton-to-electron and proton-to-neutron ratio for any value of the radial coordinate

$$\frac{n_p(r)}{n_e(r)} = \left[\frac{f^2(r)\mu_e^2(r) - m_p^2}{\mu_e^2(r) - m_e^2} \right]^{3/2}, \quad \frac{n_p(r)}{n_n(r)} = \left[\frac{g^2(r)\mu_n^2(r) - m_p^2}{\mu_n^2(r) - m_n^2} \right]^{3/2}, \quad (\text{B.9.15})$$

where $f(r) = (E_p^F + m_p - eV)/(E_e^F + m_e + eV)$, $g(r) = (E_p^F + m_p - eV)/(E_n^F +$

m_n) and the constant values of the generalized Fermi energies are given by

$$E_n^F = m_n e^{\nu(R_n)/2} - m_n, \quad (\text{B.9.16})$$

$$E_p^F = m_p e^{\nu(R_p)/2} - m_p + eV(R_p), \quad (\text{B.9.17})$$

$$E_e^F = m_e e^{\nu(R_e)/2} - m_e. \quad (\text{B.9.18})$$

A novel situation occurs: the determination of the quantities in Eqs. (B.9.15) and (B.9.16) necessarily require the prior knowledge of the global electro-dynamical and gravitational potential from the center of the configuration all the way out to the boundary defined by the radii R_e , R_p and R_n ! This necessity is an outcome of the solution for the eigenfunction of the general relativistic Thomas-Fermi equation (B.9.9).

From the regularity condition at the center of the star $n_e(0) = n_p(0)$ together with Eq. (B.9.15) we obtain the Coulomb potential at the center of the configuration

$$eV(0) = \frac{(m_p - m_e)}{2} \left[1 + \left(\frac{E_p^F - E_e^F}{m_p - m_e} \right) - \left(\frac{m_p + m_e}{E_n^F + m_n} \right) e^{\nu(0)} \right], \quad (\text{B.9.19})$$

which after some algebraic manipulation and defining the central density in units of the nuclear density $\eta = \rho(0)/\rho_0$ can be estimated as

$$\begin{aligned} eV(0) &\simeq \frac{1}{2} \left[m_p e^{\nu(R_p)/2} - m_e e^{\nu(R_e)/2} - \frac{m_n e^{\nu(R_n)/2}}{1 + (P_n^F(0)/m_n)^2} \right] \\ &\simeq \frac{1}{2} \left[\frac{(3\pi^2\eta/2)^{2/3} m_p}{(3\pi^2\eta/2)^{2/3} m_\pi + m_n^2/m_\pi} \right] m_\pi, \end{aligned} \quad (\text{B.9.20})$$

where we have approximated the gravitational potential at the boundary as $e^{\nu(R_e)/2} \simeq e^{\nu(R_p)/2} \simeq e^{\nu(R_n)/2} \simeq 1$. Then for configurations with central densities larger than the nuclear density we necessarily have $eV(0) \gtrsim 0.35m_\pi$. In particular, for the configuration we have exemplified with $\eta = 4$ in Fig. B.26, from the above expression (B.9.20) we obtain $eV(0) \simeq 0.85m_\pi$. This value of the central potential agrees with the one obtained in the simplified case of massive nuclear density cores with constant proton density Popov et al. (2010).

B.9.4. Conclusions

In conclusion, we have proved in the first part of this article that the treatments generally used in textbooks of neutron stars adopting the condition of local charge neutrality (see e.g. Haensel et al. (2007)) are not consistent with the Einstein equations and with the equations of motion of the parti-

cles (see Fig. B.25). The only self-consistent solution of neutron star structure for degenerate neutrons, protons and electrons in beta equilibrium is the one presented here.

Although the mass-radius relation in the simple example considered here in our new treatment, differs slightly from the one of the traditional approaches, the difference in electrodynamic structure is clearly very large. As is well-known these effects can lead to important astrophysical consequences on the physics of the gravitational collapse of a neutron star to a black hole Ruffini et al. (2010).

Having established in the simplest possible example the new set of Einstein-Maxwell and general relativistic Thomas-Fermi equations, we can proceed to their implementation when strong interactions are present. The contribution of the hadronic fields to the energy-momentum tensor, to the four-vector current and consequently to the Einstein-Maxwell equations have to be taken into account. Such more general case preserves the r -independence of the generalized Fermi energy of the electrons, requires the fulfillment of the general relativistic Thomas-Fermi equation and confirms all the gravito-electrodynamical effects here introduced Rueda et al. (2010c); Pugliese et al. (2010). The fluid of neutrons, protons and electrons in this more general case does not extend all the way to the neutron star surface but is confined to the neutron star core surrounded by the neutron star crust.

A recent specific example presented in Rueda et al. (2010c) shows how the correct boundary conditions derived from our treatment leads to new family of neutron stars with crusts of smaller mass and smaller thickness, and consequently to neutron stars with alternative mass-radius relations. This result follows from enforcing in the core-crust transition surface the continuity of the generalized Fermi energy of the electrons. Such a continuity in turn leads to a discontinuity in the pressure and density, which have been assumed continuous in the core-crust transition in the current literature. The order of magnitude of such a difference in the crust mass can be as large as $\Delta M_{\text{crust}} \sim 10^{-5}-10^{-4}M_{\odot} \sim 10^{48}-10^{49}$ erg. There are on going discussions on the uniqueness of such solutions.

It is appropriate to mention that all the above considerations can be straightforwardly applied in the Newtonian formalism by taking the first-order series-expansion for small gravitational field of the general relativistic formulas. However, the challenge has been to find the consistent general relativistic treatment presented here. Such a treatment is mandatory in view of the large discrepancies encountered in the gravitational Thomas-Fermi systems in the Newtonian regime.

The considerations have been formulated for configurations at zero temperature. It is worth to recall that temperatures of the order of $\sim 10^6$ K expected to exist in old neutron stars would not affect the considerations here introduced. For neutron stars the Fermi temperature is $T^F \sim 10^{13}$ K.

Bibliography

- AKSENOV, A.G., RUFFINI, R. AND VERESHCHAGIN, G.V.
«Thermalization of Nonequilibrium Electron-Positron-Photon Plasmas».
Physical Review Letters, **99(12)**, pp. 125003–+ (2007).
- ALCOCK, C., FARHI, E. AND OLINTO, A.
«Strange stars».
Astrophysical Journal, **310**, pp. 261–272 (1986).
- ALFORD, M., RAJAGOPAL, K., REDDY, S. AND WILCZEK, F.
«Minimal color-flavor-locked-nuclear interface».
Physical Review D, **64(7)**, pp. 074017–+ (2001).
- ARNETT, D.
private communication (2010).
- BAYM, G., BETHE, H.A. AND PETHICK, C.J.
«Neutron star matter».
Nuclear Physics A, **175**, pp. 225–271 (1971a).
- BAYM, G., PETHICK, C. AND SUTHERLAND, P.
«The Ground State of Matter at High Densities: Equation of State and Stellar Models».
Astrophysical Journal, **170**, pp. 299–+ (1971b).
- BERTONE, G. AND RUFFINI, R.
«Equilibrium configurations of relativistic white dwarfs».
Nuovo Cimento B Serie, **115**, pp. 935–+ (2000).
- BETHE, H.A., BORNER, G. AND SATO, K.
«Nuclei in Neutron Matter».
Astronomy & Astrophysics, **7**, pp. 279–+ (1970).
- BOCCALETTI, D. AND RUFFINI, R.
Fermi and Astrophysics (World Scientific, Singapore, 2010).
- BOGUTA, J. AND BODMER, A.R.
«Relativistic calculation of nuclear matter and the nuclear surface».
Nuclear Physics A, **292**, pp. 413–428 (1977).

- BÜRVENICH, T.J., MISHUSTIN, I.N. AND GREINER, W.
«Nuclei embedded in an electron gas».
Physical Review C, **76(3)**, pp. 034310–+ (2007).
- C. DE WITT, B. S. DE WITT (ed.).
R. Ruffini: “On the energetics of Black Holes” in *Black Holes-Les astres occlus* (1972).
- CAMERON, A.G.W.
«Neutron Stars».
Annual Review of Astronomy and Astrophysics, **8**, pp. 179–+ (1970).
- CASE, K.M.
«Singular Potentials».
Physical Review, **80**, pp. 797–806 (1950).
- CHABRIER, G. AND POTEKHIN, A.Y.
«Equation of state of fully ionized electron-ion plasmas».
Physical Review E, **58**, pp. 4941–4949 (1998).
- CHANDRASEKHAR, S.
«The highly collapsed configurations of a stellar mass».
Monthly Notices of the Royal Astronomical Society, **91**, pp. 456–466 (1931a).
- CHANDRASEKHAR, S.
«The Maximum Mass of Ideal White Dwarfs».
Astrophysical Journal, **74**, pp. 81–+ (1931b).
- CHANDRASEKHAR, S.
«The highly collapsed configurations of a stellar mass (Second paper)».
Monthly Notices of the Royal Astronomical Society, **95**, pp. 207–225 (1935).
- CHANDRASEKHAR, S.
An introduction to the study of stellar structure (1939).
- CHANDRASEKHAR, S.
The mathematical theory of black holes (1992).
- CHERUBINI, C., GERALICO, A., J. A. RUEDA, H. AND RUFFINI, R.
« $e^- - e^+$ pair creation by vacuum polarization around electromagnetic black holes».
Physical Review D, **79(12)**, pp. 124002–+ (2009).
- CHRISTIANSEN, M.B. AND GLENDENNING, N.K.
«Finite size effects and the mixed quark-hadron phase in neutron stars».
Physical Review C, **56**, pp. 2858–2864 (1997).

- CHRISTIANSEN, M.B., GLENDENNING, N.K. AND SCHAFFNER-BIELICH, J.
«Surface tension between a kaon condensate and the normal nuclear matter phase».
Physical Review C, **62(2)**, pp. 025804–+ (2000).
- CIUFOLINI, I. AND RUFFINI, R.
«Equilibrium configurations of neutron stars and the parametrized post-Newtonian metric theories of gravitation».
Astrophysical Journal, **275**, pp. 867–877 (1983).
- COSTA, E., FRONTERA, F., HEISE, J., FEROCI, M., IN'T ZAND, J., FIORE, F., CINTI, M.N., DAL FIUME, D., NICASTRO, L., ORLANDINI, M. ET AL.
«Discovery of an X-ray afterglow associated with the γ -ray burst of 28 February 1997».
Nature, **387**, pp. 783–785 (1997).
- DAMOUR, T. AND RUFFINI, R.
«Quantum Electrodynamical Effects in Kerr-Newmann Geometries».
Physical Review Letters, **35**, pp. 463–466 (1975).
- DARWIN, C.G.
«The Wave Equations of the Electron».
Royal Society of London Proceedings Series A, **118**, pp. 654–680 (1928).
- DIRAC, P.A.M.
«The Quantum Theory of the Electron».
Royal Society of London Proceedings Series A, **117**, pp. 610–624 (1928a).
- DIRAC, P.A.M.
«The Quantum Theory of the Electron. Part II».
Royal Society of London Proceedings Series A, **118**, pp. 351–361 (1928b).
- DIRAC, P.A.M.
Proc. Cambridge Phil. Soc., **26**, pp. 376–+ (1930).
- DIRAC, P.A.M.
Principles of Quantum Mechanics (1958).
- DOUCHIN, F. AND HAENSEL, P.
«A unified equation of state of dense matter and neutron star structure».
Astronomy & Astrophysics, **380**, pp. 151–167 (2001).
- DUERR, H.
«Relativistic Effects in Nuclear Forces».
Physical Review, **103**, pp. 469–480 (1956).

EDDINGTON, SIR, A.S.

«On "relativistic degeneracy,"».

Monthly Notices of the Royal Astronomical Society, **95**, pp. 194–206 (1935).

EMDEN, R.

Gaskugeln Anwendungen der Mechanischen Wärmetheorie auf Kosmologische und Meteorologische Probleme (Leipzig, Teubner, Berlin, 1907).

FERMI, E.

«Un Metodo Statistico per la Determinazione di alcune Priopriet dell'Atomo».

Rend. Accad. Naz. Lincei, **6**, pp. 602–+ (1927).

FERMI, E. (ed.).

Nuclear physics (1950).

FERREIRINHO, J., RUFFINI, R. AND STELLA, L.

«On the relativistic Thomas-Fermi model».

Physics Letters B, **91**, pp. 314–316 (1980).

FEYNMAN, R.P., METROPOLIS, N. AND TELLER, E.

«Equations of State of Elements Based on the Generalized Fermi-Thomas Theory».

Physical Review, **75**, pp. 1561–1573 (1949).

FOWLER, R.H.

«On dense matter».

Monthly Notices of the Royal Astronomical Society, **87**, pp. 114–122 (1926).

FREIRE, P.C.C., RANSOM, S.M., BÉGIN, S., STAIRS, I.H., HESSELS, J.W.T., FREY, L.H. AND CAMILO, F.

«Eight New Millisecond Pulsars in NGC 6440 and NGC 6441».

Astrophysical Journal, **675**, pp. 670–682 (2008).

FRENKEL, Y.I.

Zeit. fur Phys., **50**, p. 234 (1928).

GAMOW, G.

Constitution of Atomic Nuclei and Radioactivity (1931).

GIACCONI, R. AND RUFFINI, R. (eds.).

S. Chandrasekhar: "Why are the stars as they are ?" in *Physics and astrophysics of neutron stars and black holes* (1978).

GIBBONS, G.W. AND HAWKING, S.W.

«Action integrals and partition functions in quantum gravity».

Physical Review D, **15**, pp. 2752–2756 (1977).

- GINZBURG, V.L.
«The Magnetic Fields of Collapsing Masses and the Nature of Superstars». *Soviet Physics Doklady*, **9**, pp. 329–+ (1964).
- GLENDENNING, N.K.
«First-order phase transitions with more than one conserved charge: Consequences for neutron stars». *Physical Review D*, **46**, pp. 1274–1287 (1992).
- GLENDENNING, N.K.
«Phase transitions and crystalline structures in neutron star cores». *Physics Reports*, **342**, pp. 393–447 (2001).
- GLENDENNING, N.K. AND PEI, S.
«Crystalline structure of the mixed confined-deconfined phase in neutron stars». *Physical Review C*, **52**, pp. 2250–2253 (1995).
- GLENDENNING, N.K. AND SCHAFFNER-BIELICH, J.
«First order kaon condensate». *Physical Review C*, **60(2)**, pp. 025803–+ (1999).
- GOMBÁS, P.
Die Statistische Theorie des Atoms und Ihre Anwendungen (1949).
- GORDON, W.
«Über den Stoß zweier Punktladungen nach der Wellenmechanik». *Zeitschrift für Physik*, **48**, pp. 180–191 (1928).
- GREENBERG, J.S. AND GREINER, W.
«Search for the sparking of the vacuum». *Physics Today*, **35**, pp. 24–35 (1982).
- GURSKY, H. AND RUFFINI, R. (eds.).
Neutron stars, black holes and binary X-ray sources; Proceedings of the Annual Meeting, San Francisco, Calif., February 28, 1974, volume 48 of *Astrophysics and Space Science Library* (1975).
- H. GURSKY, R. RUFFINI, & L. STELLA (ed.).
R. Ruffini: “On the critical mass: the case of white dwarfs” in *Exploring the universe: a Festschrift in honor of Riccardo Giacconi* (2000).
- H. KLEINERT, R. T. JANTZEN, R. RUFFINI (ed.).
R. Ruffini et al.: “On Gamma-Ray Bursts” in *Proceedings of the Eleventh Marcel Grossmann Meeting on General Relativity* (2008).

- HAENSEL, P., POTEKHIN, A.Y. AND YAKOVLEV, D.G. (eds.).
Neutron Stars 1 : Equation of State and Structure, volume 326 of *Astrophysics and Space Science Library* (2007).
- HAENSEL, P. AND ZDUNIK, J.L.
«Equation of state and structure of the crust of an accreting neutron star».
Astronomy & Astrophysics, **229**, pp. 117–122 (1990a).
- HAENSEL, P. AND ZDUNIK, J.L.
«Non-equilibrium processes in the crust of an accreting neutron star».
Astronomy & Astrophysics, **227**, pp. 431–436 (1990b).
- HAENSEL, P. AND ZDUNIK, J.L.
«Models of crustal heating in accreting neutron stars».
Astronomy & Astrophysics, **480**, pp. 459–464 (2008).
- HAMADA, T. AND SALPETER, E.E.
«Models for Zero-Temperature Stars.»
Astrophysical Journal, **134**, pp. 683–+ (1961).
- HARRISON, B.K., THORNE, K.S., WAKANO, M. AND WHEELER, J.A.
Gravitation Theory and Gravitational Collapse (1965).
- HARRISON, B.K., WAKANO, M. AND WHEELER, J.A.
Onzieme Conseil de Physique de Solvay (1958).
- HAWKING, S.W.
«Black hole explosions?»
Nature, **248**, pp. 30–31 (1974).
- HAWKING, S.W.
«Particle creation by black holes».
Communications in Mathematical Physics, **43**, pp. 199–220 (1975).
- HEILBRON, J.L.
«The Origins of the Exclusion Principle».
Historical Studies in the Physical Sciences, **13**, pp. 261–310 (1983).
- HEISENBERG, W. AND EULER, H.
«Folgerungen aus der Diracschen Theorie des Positrons».
Zeitschrift fur Physik, **98**, pp. 714–732 (1936).
- HO, W.C.G. AND HEINKE, C.O.
«A neutron star with a carbon atmosphere in the Cassiopeia A supernova remnant».
Nature, **462**, pp. 71–73 (2009).

- HOYLE, F. AND FOWLER, W.A.
«Nucleosynthesis in Supernovae.»
Astrophysical Journal, **132**, pp. 565–+ (1960).
- HUND, F.
Erg. d. exacten Natwis., **15**, p. 189 (1936).
- ITOH, N.
«Hydrostatic Equilibrium of Hypothetical Quark Stars.»
Progress of Theoretical Physics, **44**, pp. 291–292 (1970).
- KETTNER, C., WEBER, F., WEIGEL, M.K. AND GLENDENNING, N.K.
«Structure and stability of strange and charm stars at finite temperatures.»
Physical Review D, **51**, pp. 1440–1457 (1995).
- KLEIN, O.
«On the Thermodynamical Equilibrium of Fluids in Gravitational Fields.»
Reviews of Modern Physics, **21**, pp. 531–533 (1949).
- KLEINERT, H., RUFFINI, R. AND XUE, S.
«Electron-positron pair production in space- or time-dependent electric fields.»
Physical Review D, **78(2)**, pp. 025011–+ (2008).
- KODAMA, T. AND YAMADA, M.
«Theory of Superdense Stars.»
Progress of Theoretical Physics, **47**, pp. 444–459 (1972).
- LANDAU, L.D.
«On the theory of stars.»
Phys. Z. Sowjetunion, **1**, pp. 285–288 (1932).
- LANDAU, L.D.
Nature, **19**, p. 333 (1938).
- LANDAU, L.D. AND LIFSHITZ, E.M.
Statistical physics. Part1 (Pergamon Press, Oxford, 1980).
- LEE, T.D.
«Abnormal nuclear states and vacuum excitation.»
Reviews of Modern Physics, **47**, pp. 267–275 (1975).
- LEE, T.D. AND MARGULIES, M.
«Interaction of a dense fermion medium with a scalar-meson field.»
Physical Review D, **11**, pp. 1591–1610 (1975).

- LEE, T.D. AND PANG, Y.
«Fermion soliton stars and black holes».
Physical Review D, **35**, pp. 3678–3694 (1987).
- LEE, T.D. AND WICK, G.C.
«Vacuum stability and vacuum excitation in a spin-0 field theory».
Physical Review D, **9**, pp. 2291–2316 (1974).
- LIEB, E.H.
«Thomas-fermi and related theories of atoms and molecules».
Reviews of Modern Physics, **53**, pp. 603–641 (1981).
- LIEB, E.H. AND SIMON, B.
«Thomas-Fermi Theory Revisited».
Physical Review Letters, **31**, pp. 681–683 (1973).
- LUNDQVIST, S. AND MARCH, N.H.
Theory of the Inhomogeneous Electro Gas (1983).
- MANCHESTER, R.N. AND TAYLOR, J.H.
Pulsars. (1977).
- MARCH, N.H.
«The Thomas-Fermi approximation in quantum mechanics».
Advances in Physics, **6**, pp. 1–101 (1957).
- MARSH, J.S.
«Magnetic and electric fields of rotating charge distributions».
American Journal of Physics, **50**, pp. 51–53 (1982).
- MEZZACAPPA, A.
«Open Issues in Core Collapse Supernova Theory: An Overview».
In A. Mezzacappa & G. M. Fuller (ed.), *Open Issues in Core Collapse Supernova Theory*, pp. 3–+ (2005).
- MIGDAL, A.B., POPOV, V.S. AND VOSKRESENSKIĬ, D.N.
«The vacuum charge distribution near super-charged nuclei».
Soviet Journal of Experimental and Theoretical Physics, **45**, pp. 436–+ (1977).
- MIGDAL, A.B., VOSKRESENSKIĬ, D.N. AND POPOV, V.S.
«Distribution of vacuum charge near supercharged nuclei».
Soviet Journal of Experimental and Theoretical Physics Letters, **24**, pp. 163–+ (1976).
- MILNE, E.A.
«The analysis of stellar structure».
Monthly Notices of the Royal Astronomical Society, **91**, pp. 4–55 (1930).

- MÜLLER, B., PEITZ, H., RAFELSKI, J. AND GREINER, W.
«Solution of the Dirac Equation for Strong External Fields».
Physical Review Letters, **28**, pp. 1235–1238 (1972).
- MÜLLER, B. AND RAFELSKI, J.
«Stabilization of the Charged Vacuum Created by Very Strong Electrical Fields in Nuclear Matter».
Physical Review Letters, **34**, pp. 349–352 (1975).
- NAUENBERG, M.
«Edmund C. Stoner and the Discovery of the Maximum Mass of White Dwarfs».
Journal for the History of Astronomy, **39**, pp. 297–312 (2008).
- OLSON, E. AND BAILYN, M.
«Internal structure of multicomponent static spherical gravitating fluids».
Physical Review D, **12**, pp. 3030–3036 (1975).
- OLSON, E. AND BAILYN, M.
«Charge effects in a static, spherically symmetric, gravitating fluid».
Physical Review D, **13**, pp. 2204–2211 (1976).
- OLSON, E. AND BAILYN, M.
«Internal structure of multicomponent fluids».
Physical Review D, **18**, pp. 2175–2179 (1978).
- OPPENHEIMER, J.R. AND VOLKOFF, G.M.
«On Massive Neutron Cores».
Physical Review, **55**, pp. 374–381 (1939).
- PAGLIAROLI, G., VISSANI, F., COCCIA, E. AND FULGIONE, W.
«Neutrinos from Supernovae as a Trigger for Gravitational Wave Search».
Physical Review Letters, **103(3)**, pp. 031102–+ (2009a).
- PAGLIAROLI, G., VISSANI, F., COSTANTINI, M.L. AND IANNI, A.
«Improved analysis of SN1987A antineutrino events».
Astroparticle Physics, **31**, pp. 163–176 (2009b).
- PATRICELLI, B., ROTONDO, M. AND RUFFINI, R.
«On the Charge to Mass Ratio of Neutron Cores and Heavy Nuclei».
In C. L. Bianco & S.-S. Xue (ed.), *Relativistic Astrophysics*, volume 966 of *American Institute of Physics Conference Series*, pp. 143–146 (2008).
- PAVLOV, G.G. AND LUNA, G.J.M.
«A Dedicated Chandra ACIS Observation of the Central Compact Object in the Cassiopeia A Supernova Remnant».
Astrophysical Journal, **703**, pp. 910–921 (2009).

- PERLMUTTER, S., ALDERING, G., GOLDHABER, G., KNOP, R.A., NUGENT, P., CASTRO, P.G., DEUSTUA, S., FABBRO, S., GOOBAR, A., GROOM, D.E. ET AL.
«Measurements of Omega and Lambda from 42 High-Redshift Supernovae».
Astrophysical Journal, **517**, pp. 565–586 (1999).
- PHILLIPS, M.M.
«The absolute magnitudes of Type IA supernovae».
Astrophys. J. Lett., **413**, pp. L105–L108 (1993).
- PIEPER, W. AND GREINER, W.
«Interior electron shells in superheavy nuclei».
Zeitschrift fur Physik, **218**, pp. 327–340 (1969).
- POPOV, V., ROTONDO, M., RUFFINI, R. AND XUE, S.
«On the relativistic and electrodynamical stability of massive nuclear density cores».
Submitted to Physical Review C (2010).
- POPOV, V.S.
«Electron Energy Levels at $Z \approx 137$ ».
Soviet Journal of Experimental and Theoretical Physics Letters, **11**, pp. 162–+ (1970).
- POPOV, V.S.
«On the Properties of the Discrete Spectrum for Z Close to 137».
Soviet Journal of Experimental and Theoretical Physics, **33**, pp. 665–+ (1971a).
- POPOV, V.S.
«Position Production in a Coulomb Field with $Z \approx 137$ ».
Soviet Journal of Experimental and Theoretical Physics, **32**, pp. 526–+ (1971b).
- POTEKHIN, A.Y., CHABRIER, G. AND ROGERS, F.J.
«Equation of state of classical Coulomb plasma mixtures».
Physical Review E, **79(1)**, pp. 016411–+ (2009).
- PREPARATA, G., RUFFINI, R. AND XUE, S.
«The dyadosphere of black holes and gamma-ray bursts».
Astronomy & Astrophysics, **338**, pp. L87–L90 (1998).
- PUGLIESE, D., RUEDA, J.A., RUFFINI, R. AND XUE, S.S.
to be submitted to Physical Review D (2010).
- RAFELSKI, J., FULCHER, L.P. AND KLEIN, A.
«Fermions and bosons interacting with arbitrarily strong external fields».
Physics Reports, **38**, pp. 227–361 (1978).

- REISENEGGER, A.
«Chemical Equilibrium and Stable Stratification of a Multicomponent Fluid: Thermodynamics and Application to Neutron Stars».
Astrophysical Journal, **550**, pp. 860–862 (2001).
- REISENEGGER, A.
«Magnetic field evolution in neutron stars».
Astronomische Nachrichten, **328**, pp. 1173–+ (2007).
- REISENEGGER, A., BENGURIA, R., PRIETO, J.P., ARAYA, P.A. AND LAI, D.
«Hall drift of axisymmetric magnetic fields in solid neutron-star matter».
Astronomy & Astrophysics, **472**, pp. 233–240 (2007).
- RIESS, A.G., FILIPPENKO, A.V., CHALLIS, P., CLOCCHIATTI, A., DIERCKS, A., GARNAVICH, P.M., GILLILAND, R.L., HOGAN, C.J., JHA, S., KIRSHNER, R.P. ET AL.
«Observational Evidence from Supernovae for an Accelerating Universe and a Cosmological Constant».
Astronomical Journal, **116**, pp. 1009–1038 (1998).
- RIESS, A.G., STROLGER, L., TONRY, J., CASERTANO, S., FERGUSON, H.C., MOBASHER, B., CHALLIS, P., FILIPPENKO, A.V., JHA, S., LI, W. ET AL.
«Type Ia Supernova Discoveries at $z < 1$ from the Hubble Space Telescope: Evidence for Past Deceleration and Constraints on Dark Energy Evolution».
Astrophysical Journal, **607**, pp. 665–687 (2004).
- RING, P.
«Relativistic mean field theory in finite nuclei».
Progress in Particle and Nuclear Physics, **37**, pp. 193–263 (1996).
- ROTONDO, M., RUEDA, J.A., RUFFINI, R. AND XUE, S.
«On the relativistic Thomas-Fermi treatment of compressed atoms and compressed nuclear matter cores of stellar dimensions».
Submitted to Physical Review C (2009).
- RUDERMAN, M.
«Pulsars: Structure and Dynamics».
Annual Review of Astronomy and Astrophysics, **10**, pp. 427–+ (1972).
- RUDERMAN, M.
«Spin-Driven Changes in Neutron Star Magnetic Fields».
Journal of Astrophysics and Astronomy, **16**, pp. 207–+ (1995).
- RUEDA, J.A., ROTONDO, M., RUFFINI, R. AND XUE, S.S.
«A self-consistent general relativistic solution for a self-gravitating system of degenerate neutrons, protons and electrons in beta equilibrium».

- Submitted to *Physical Review Letters* (2010a).
- RUEDA, J.A., ROTONDO, M., RUFFINI, R. AND XUE, S.S.
in preparation (2010b).
- RUEDA, J.A., RUFFINI, R. AND XUE, S.
«On the self-consistent general relativistic equilibrium equations of neutron stars».
Submitted to Physical Review Letters (2010c).
- RUEDA, J.A., RUFFINI, R. AND XUE, S.
«The relativistic Feynman-Metropolis-Teller theory for white-dwarfs in general relativity».
Submitted to Physical Review D (2010d).
- RUFFINI, R.
«R. Ruffini: “Beyond the Critical Mass: The Dyadosphere of Black Holes” in Black Holes and High Energy Astrophysics».
In H. Sato & N. Sugiyama (ed.), *Frontiers Science Series 23: Black Holes and High Energy Astrophysics*, pp. 167–+ (1998).
- RUFFINI, R., BERNARDINI, M.G., BIANCO, C.L., CAITO, L., CHARDONNET, P., DAINOTTI, M.G., FRASCHETTI, F., GUIDA, R., ROTONDO, M., VERESHCHAGIN, G. ET AL.
«The Blackholic energy and the canonical Gamma-Ray Burst».
In M. Novello & S. E. Perez Bergliaffa (ed.), *XIIIth Brazilian School of Cosmology and Gravitation*, volume 910 of *American Institute of Physics Conference Series*, pp. 55–217 (2007a).
- RUFFINI, R. AND BONAZZOLA, S.
«Systems of Self-Gravitating Particles in General Relativity and the Concept of an Equation of State».
Physical Review, **187**, pp. 1767–1783 (1969).
- RUFFINI, R., ROTONDO, M. AND XUE, S.
«Electrodynamics for Nuclear Matter in Bulk».
International Journal of Modern Physics D, **16**, pp. 1–9 (2007b).
- RUFFINI, R. AND STELLA, L.
«Some comments on the relativistic Thomas-Fermi model and the Vallarta-Rosen equation».
Physics Letters B, **102**, pp. 442–444 (1981).
- RUFFINI, R., VERESHCHAGIN, G. AND XUE, S.
«Electron-positron pairs in physics and astrophysics: From heavy nuclei to black holes».
Physics Reports, **487**, pp. 1–140 (2010).

- RUFFINI, R. AND WHEELER, J.A.
«Introducing the black hole.»
Physics Today, **24**, pp. 30–36 (1971).
- SALPETER, E.E.
«Energy and Pressure of a Zero-Temperature Plasma.»
Astrophysical Journal, **134**, pp. 669–+ (1961).
- SAUTER, F.
«Über das Verhalten eines Elektrons im homogenen elektrischen Feld nach der relativistischen Theorie Diracs.»
Zeitschrift für Physik, **69**, pp. 742–764 (1931).
- SCHWINGER, J.
«On Gauge Invariance and Vacuum Polarization.»
Physical Review, **82**, pp. 664–679 (1951).
- SCHWINGER, J.
«The Theory of Quantized Fields. V.»
Physical Review, **93**, pp. 615–628 (1954a).
- SCHWINGER, J.
«The Theory of Quantized Fields. VI.»
Physical Review, **94**, pp. 1362–1384 (1954b).
- SEGRÉ, E.
Nuclei and Particles (1977).
- SHAPIRO, S.L. AND TEUKOLSKY, S.A.
Black holes, white dwarfs, and neutron stars: The physics of compact objects (1983).
- SHKLOVSKII, I.S.
Supernovae (1968).
- SLATER, J.C. AND KRUTTER, H.M.
«The Thomas-Fermi Method for Metals.»
Phys. Rev., **47**, pp. 559–+ (1935).
- SOMMERFELD, A.
«Asymptotische Integration der Differentialgleichung des Thomas-Fermischen Atoms.»
Zeitschrift für Physik, **78**, pp. 283–308 (1932).
- SPRUCH, L.
«Pedagogic notes on Thomas-Fermi theory (and on some improvements): atoms, stars, and the stability of bulk matter.»
Reviews of Modern Physics, **63**, pp. 151–210 (1991).

SPRUIT, H.C.

«Dynamo action by differential rotation in a stably stratified stellar interior».

Astronomy & Astrophysics, **381**, pp. 923–932 (2002).

STONER, E.C.

«The Distribution of Electrons among Atomic Levels».

Philosophical Magazine (Series 6), **48**, pp. 719–736 (1924).

STONER, E.C.

«The limiting density of White Dwarfs».

Philosophical Magazine (Series 7), **7**, pp. 63–70 (1929).

TAYLER, R.J.

«The adiabatic stability of stars containing magnetic fields-I. Toroidal fields».

Monthly Notices of the Royal Astronomical Society, **161**, pp. 365–+ (1973).

THOMAS, L.H.

«The calculation of atomic fields».

Proc. Cambridge Phil. Soc., **23**, pp. 542–+ (1927).

THOMPSON, C. AND DUNCAN, R.C.

«Neutron star dynamos and the origins of pulsar magnetism».

Astrophysical Journal, **408**, pp. 194–217 (1993).

THOMPSON, C. AND DUNCAN, R.C.

«The soft gamma repeaters as very strongly magnetized neutron stars - I. Radiative mechanism for outbursts».

Monthly Notices of the Royal Astronomical Society, **275**, pp. 255–300 (1995).

THOMPSON, C. AND DUNCAN, R.C.

«The Soft Gamma Repeater as Very Strongly Magnetized Neutron Stars. II. Quiescent Neutrino, X-Ray, and Alfvén Wave Emission».

Astrophysical Journal, **473**, pp. 322–+ (1996).

TOLMAN, R.C.

«Static Solutions of Einstein's Field Equations for Spheres of Fluid».

Physical Review, **55**, pp. 364–373 (1939).

USOV, V.V.

«Bare Quark Matter Surfaces of Strange Stars and e^+e^- Emission».

Physical Review Letters, **80**, pp. 230–233 (1998).

VALLARTA, M.S. AND ROSEN, N.

«The Relativistic Thomas-Fermi Atom».

Physical Review, **41**, pp. 708–712 (1932).

- WALECKA, J.D.
«A theory of highly condensed matter.»
Annals of Physics, **83**, pp. 491–529 (1974).
- WALI, K.C.
«Chandrasekhar vs. Eddington—an unanticipated confrontation».
Physics Today, **35**, pp. 33–42 (1982).
- WEART, S.
Interview with Chandrasekhar, Niels Bohr Library, American Institute of Physics (1977).
- WERNER, F.G. AND WHEELER, J.A.
«Superheavy Nuclei».
Physical Review, **109**, pp. 126–144 (1958).
- WIGNER, E. AND SEITZ, F.
«On the Constitution of Metallic Sodium».
Physical Review, **43**, pp. 804–810 (1933).
- WIGNER, E. AND SEITZ, F.
«On the Constitution of Metallic Sodium. II».
Physical Review, **46**, pp. 509–524 (1934).
- WITTEN, E.
«Cosmic separation of phases».
Physical Review D, **30**, pp. 272–285 (1984).
- WOLTJER, L.
«X-Rays and Type i Supernova Remnants.»
Astrophysical Journal, **140**, pp. 1309–1313 (1964).
- ZEL'DOVICH, I.B.
«Nuclear Reactions in Super-Dense Cold Hydrogen».
Soviet Journal of Experimental and Theoretical Physics, **6**, pp. 760–+ (1958).
- ZELDOVICH, Y.B. AND POPOV, V.S.
«Reviews of Topical Problems: Electronic Structure of Superheavy Atoms».
Soviet Physics Uspekhi, **14**, pp. 673–694 (1972).